Abstract

A Genetics-First Approach to the Identification of Behavioral and Neural Correlates of Sensory Processing in Autism Spectrum Disorder

Introduction: Single-locus forms of autism spectrum disorder (ASD) offer opportunities to explore gene-specific neural and behavioral responses. The current study evaluates Phelan-McDermid syndrome (PMS), ADNP, and FOXP1 syndromes. **Methods:** Linear modeling examined group differences for children with idiopathic ASD (iASD), ADNP, FOXP1, PMS, and controls. Study 1 participants completed the Sensory Assessment for Neurodevelopmental Disorders (SAND) and the Short Sensory Profile (SSP). In Study 2, contrast-reversing checkerboards elicited transient visual evoked potentials (tVEPs) under standard (60-s) and short-duration (2-s) conditions. Group differences in amplitude, latency, magnitude-squared coherence (MSC), and power were explored. **Results:** Study 1, significant differences were found for the SAND, $F(32, 1120.00) = 12.85$, $p < .001$. Distinct sensory profiles emerged for PMS and ADNP: PMS was strongly characterized by greater hyporeactivity, and ADNP was characterized by greater tactile, auditory seeking and tactile hyporeactivity. Study 2, controls exhibited larger amplitudes than iASD and single-locus groups. FOXP1 exhibited significantly later P_{100} latencies compared to other groups (p's < .001). Frequency-domain analysis indicated group differences in MSC, $F(9, 891.75) = 9.74$, $p < .001$, and total power, $F(9, 889.54) = 2.79$, $p = .003$. The iASD, ADNP, and FOXP1 groups exhibited lower MSC values and total power for high frequency bands. Age demonstrated differential effects across groups. Behavioral sensory processing abnormalities

correlated with weaker tVEPs. **Conclusions:** Distinct sensory phenotypes in PMS and ADNP and impaired glutamatergic signaling in iASD/single-locus cases were found, as were relationships between behavioral and electrophysiological measures. VEPs may yield objective, clinically-meaningful biomarkers of ASD.

A Genetics-First Approach to the Identification of Behavioral and Neural Correlates of Sensory Processing in Autism Spectrum Disorder

by

Stacey Lurie, M.A.

Submitted in partial fulfillment of the requirements

For the degree of

Doctor of Philosophy in Clinical Psychology

in the Ferkauf Graduate School of Psychology

Yeshiva University

New York

January 2020

The committee for this doctoral dissertation consists of:

Vance Zemon, Ph.D., Chairperson, Ferkauf Graduate School of Psychology, Yeshiva University

Paige Siper, Ph.D., Seaver Autism Center for Research and Treatment, Icahn School of Medicine at Mount Sinai

James Gordon, Ph.D., Hunter College, City University of New York

Acknowledgements

I first and foremost would like to thank Vance, without whom none of this would be possible. Your knowledge, patience, guidance, and wholehearted belief in me has made this project thorough and exciting. I always will fondly recall how you warmly welcomed me into your home, fed me chocolate, and explored copious amounts of data by my side. I also must express my heartfelt gratitude to Paige. Throughout my clinical career thus far, you have served not only as a research mentor, but also as a supervisor and trusted friend. You introduced me to this exciting field of research, and have continuously pushed me to be the absolute best I can be. I truly cannot thank you enough for your endless support, mentorship, and compassion. I would also like to thank Jim for serving as a member of my committee, and for always making himself available to me should I need it.

Having served as a research coordinator, I know that none of this research would happen without the hard work of the research coordinators at the Seaver Autism Center. I would especially like to thank them for their organization, warmth, and diligence.

I am sincerely grateful for the unending support I have received from my family. Phone calls, dinners, and trips into Brooklyn did not go unnoticed, and I will forever be in your debt for all you have provided for me through graduate school and my life. Drew, you have repeatedly believed in my ability to accomplish all my goals, lovingly compelled me to engage in self-care, and given me unconditional love and encouragement. For you, I am immensely thankful.

And last but certainly not least, I would like to thank the children and their families who participated in this study. I dedicate this dissertation to them, and to all children who struggle with mental health problems and developmental disabilities.

Table of Contents

List of Tables

List of Figures

List of Appendices

Chapter I: Introduction

Autism spectrum disorder (ASD), defined by deficits in social communication and interaction as well as the presence of repetitive and restricted behaviors and interests (American Psychiatric Association, 2013), affects one in 59 children in the United States, regardless of age, race, ethnicity, and socioeconomic background (Baio et al., 2018). The clinical presentation of the disorder is highly heterogeneous, such that individuals with ASD exhibit a wide variability in diagnostic (social communication and interaction, repetitive behaviors/interests), developmental (cognition, language, motor, adaptive behavior), and other psychiatric symptoms. It is this heterogeneity that has hindered the development of objective diagnostic measures, reliable biomarkers, and efficacious treatments.

In recent years, there have been significant advances in understanding the genetic etiology of ASD and intellectual disability (ID): around 1,000 ASD genes have been identified, accounting for 10-20% of ASD cases (Geschwind, 2011). Various causes of ASD and ID appear to converge on common underlying molecular pathways, including those that control synaptic function, cellular signaling during development, transcriptional regulation, and chromatin remodeling (De Rubeis et al., 2014; Krumm, O'Roak, Shendure, & Eichler, 2014; Sakai et al., 2011). With the intent of parsing the heterogeneity of ASD with no known genetic cause (herein referred to as idiopathic ASD, or iASD) and validating the presence for discrete clinical subtypes, studying forms of ASD and intellectual disability in which a genetic cause can be identified (herein referred to as single-locus ASD) offers a unique opportunity to constrain phenotypic presentation to groups where the neuropathology is

better understood. Ongoing studies at the Seaver Autism Center at the Icahn School of Medicine at Mount Sinai are examining underlying and overlapping molecular pathways of developmental disability through thorough genotypic, molecular, and phenotypic assessment of three of the most common single-locus forms of ASD**:** Phelan-McDermid syndrome (PMS), forkhead-box protein P1 (FOXP1) syndrome, and activity-dependent neuroprotective protein (ADNP) syndrome. The current study seeks further these efforts by assessing in depth the sensory domain of the aforementioned single-locus causes of ASD using observational, parent-report, and electrophysiological methods. The current study is particularly interested in the sensory domain, as it constitutes a core feature of ASD (American Psychiatric Association, 2013), has a significant impact on daily functioning (Hannant, Tavassoli, & Cassidy, 2016), and is hypothesized to contribute to the non-social (restricted interests and repetitive behaviors) and social (coordinating eye contact with speech and gesture) patterns of behavioral characteristics of ASD (Wiggins, Robins, Bakeman, & Adamson, 2009). Sensory reactivity also represents a novel area to target in the context of clinical trials.

In the current study, sensory reactivity was carefully assessed in a sample of children with PMS, FOXP1 syndrome, and ADNP syndrome, as well as individuals with iASD and TD controls using both a novel, clinician-administered observational assessment and corresponding caregiver interview known as the Sensory Assessment for Neurodevelopmental Disorders (SAND) (Siper, Kolevzon, Wang, Buxbaum, & Tavassoli, 2017), as well as the Sensory Profile (Dunn & Westman, 1997) and Short Sensory Profile (Dunn, 1999). Visual evoked potentials (VEPs) were also collected to examine electrophysiological markers of sensory reactivity—specifically measures of excitation and

inhibition in the brain. VEPs provide a noninvasive, objective and reliable technique to rapidly assess underlying neural mechanisms, and it may yield an electrophysiological biomarker. The long-term goal of the proposed research is to develop reliable and objective biomarkers of ASD that further our understanding of underlying brain mechanisms and brain-behavior relationships, ultimately aiding with diagnosis, predicting targeted treatments (i.e., personalized medicine), and evaluating treatment efficacy.

Background and Significance

Autism spectrum disorder and intellectual disability. Autism spectrum disorder (ASD) is a neurodevelopmental disorder characterized by persistent and global deficits in social communication and social interaction, and the manifestation of restricted, repetitive, and stereotyped patterns of behavior (American Psychiatric Association, 2013). Social communicative and interaction deficits of ASD are commonly observed as deficits in: social-emotional reciprocity, nonverbal communicative behaviors used in social interactions—namely abnormal eye contact, poor use of gestures, lack of facial expression, and the inability to integrate multiple modes of communication—and developing, maintaining, and/or understanding social relationships (American Psychiatric Association, 2013). The restricted, repetitive patterns of behavior, interests, or activities common in ASD include: stereotyped or repetitive motor movements, use of objects, or speech; insistence on sameness, inflexible adherence to routines, or ritualized patterns of verbal/nonverbal behavior; and restricted, fixated interests that are abnormal in intensity or focus (American Psychiatric Association, 2013). Of particular importance for the current study, the DSM-5 also includes hyper- or hyporeactivity to sensory input, or sensory seeking behaviors (interest

in sensory aspects of environment) as a core feature of ASD within the restricted and repetitive behavior domain (American Psychiatric Association, 2013).

ASD is highly comorbid with intellectual disability (ID), a neurodevelopmental disorder with onset during childhood that includes both intellectual and adaptive functioning deficits in conceptual, social, and practical domains (American Psychiatric Association, 2013). About 40% of ID cases are diagnosed with comorbid ASD (American Psychiatric Association, 2013).

While ASD is diagnostically conceptualized as a single disorder, a main characteristic feature is its phenotypic heterogeneity: individuals with ASD present with varying profiles of communication and socialization skills; sensory preferences, aversions, and general profiles; repetitive behaviors and restricted interests; developmental course; language and adaptive functioning skills; and comorbid psychiatric (i.e., ID, attention deficit/hyperactivity disorder), medical (i.e., gastrointestinal problems), and neurological conditions (i.e., epilepsy). It is this phenotypic variability that hampers the development of diagnostic tools and treatments for ASD.

Prevalence. ASD affects one in 59 children in the United States (Baio et al., 2018). The disorder is consistently reported as being more common in males, with the male-to-female ratio generally reported as ~4:1 (Baio, 2012; Blumberg et al., 2013; Christensen et al., 2016; Fombonne, 2009). This ratio increases to 7:1 in high functioning individuals and decreases to 2:1 in individuals with moderate to severe ID (Baio, 2012; Blumberg et al., 2013; Fombonne, 2009), indicating that the overall diagnostic discrepancy between sexes is driven by affected individuals without ID (White et al., 2017). While a valid, reliable, and

stable diagnosis of ASD can be made at age two, most children go undiagnosed until age four (Christensen et al., 2016; Kleinman et al., 2008).

Heritability and genetic heterogeneity of ASD. ASD has more recently been conceptualized as a collection of various neurodevelopmental disorders with a strong, intricate genetic component (Fakhoury, 2018). Evidence from twin and sibling studies suggests a high concordance rate of about 88-90% in monozygotic twins, 31% in dizygotic twins, and 18.7% in siblings (Bailey et al., 1995; Ozonoff et al., 2011; Ritvo, Freeman, Mason-Brothers, Mo, & Ritvo, 1985; Rosenberg et al., 2009), demonstrably suggesting the high heritability of the disorder.

Like the phenotypic presentation of the disorder, the genetic etiology of ASD is also highly heterogeneous. Several linkage studies, chromosomal microarray analyses, whole exome sequencing, and genome-wide association studies have implicated chromosomal abnormalities, *de novo* copy number variations, and single nucleotide polymorphisms in the risk and development of ASD (Fakhoury, 2018). Large-scale sequencing studies of children with ASD and their parents has enabled the detection of about 1,000 ASD genes, thereby accounting for 10-20% of ASD cases (Geschwind, 2011). Recent exome- and genome-wide sequencing studies have revealed that myriad genetic causes of ASD and ID appear to converge on common underlying molecular pathways, namely those that control synaptic function, cellular signaling during development, transcriptional regulation, and chromatin remodeling (De Rubeis et al., 2014; Krumm et al., 2014; Sakai et al., 2011).

Studying single-locus forms of ASD and ID, in which a genetic component can be identified, offers a unique opportunity to confine variability in ASD symptomatology using a

subset of individuals in which the neuropathology is better understood and can more readily be targeted for assessment and treatment.

Single-locus causes of ASD. In contrast to idiopathic autism (iASD), or ASD without an identifiable genetic cause, syndromic ASD is utilized to describe cases of ASD with an identifiable Mendelian condition or single-locus-caused genetic syndrome. The current study evaluated three single-locus causes of ASD, in which there are identifiable causes for the phenotypic pattern of symptoms: Phelan-McDermid syndrome, FOXP1 syndrome, and ADNP syndrome.

***Phelan-McDermid syndrome*.** Phelan-McDermid syndrome (PMS; OMIM 606232) is a single-locus form of ASD which results from the loss of one functional copy (haploinsufficiency) of the *SHANK3* gene due to 22q13.3 deletions or point mutations, and accounts for 0.5 to 2% of ASD cases (Bonaglia et al., 2007; Cooper et al., 2011; Durand et al., 2007; Gauthier et al., 2009; Leblond et al., 2014; Marshall et al., 2008; Moessner et al., 2007). *SHANK3* codes for a scaffolding protein in NMDA, AMPA, and mGlu glutamate synapses (Boeckers, 2006; Bozdagi et al., 2010; Durand et al., 2012; Ehlers, 1999; Yang et al., 2012), and studies in animal and human neuronal models of *Shank3*-deficiency confirm glutamatergic dysfunction (Bozdagi, Tavassoli, & Buxbaum, 2013; Shcheglovitov et al., 2013; Yang et al., 2012). Clinically, PMS is characterized by ID, ASD features, hypotonia, delayed or absent speech, and sleep impairments (Soorya et al., 2013). Neurologically, individuals with PMS present with seizures, abnormal visual tracking, gait disturbance, fine motor coordination deficits, and several EEG and MRI abnormalities (Frank et al., 2017; Soorya et al., 2013). Individuals with PMS also exhibit several hallmark dysmorphic features, and are often diagnosed with recurrent upper respiratory infections and GERD,

among others (Soorya et al., 2013). Researchers have also uncovered a clear genotypic-phenotypic link in PMS: larger mutations are shown to be correlated with increased levels of dysmorphic features, medical comorbidities, and ASD-related impairments (Soorya et al., 2013).

FOXP1 syndrome. FOXP1 syndrome results from haploinsufficiency of the forkhead-box protein P1 (*FOXP1*) gene due to heterozygous deletions or mutations in 3p14.1 (Banham et al., 2001; Hamdan et al., 2010; Le Fevre et al., 2013; Siper, De Rubeis, et al., 2017; Srivastava et al., 2014). Genotypically, the syndrome may result from *de novo* (meaning spontaneous or uninherited) missense, frame-shift, nonsense, and splice-site mutations that may cause loss-of-function or gain-of-function of the protein; this genotypic variability is crucial when considering any potential phenotypic heterogeneity (Siper, De Rubeis, et al., 2017). *FOXP1* is a transcription factor crucial to neuronal cell migration and differentiation during early development (Ferland, Cherry, Preware, Morrisey, & Walsh, 2003; Li et al., 2015). *FOXP1* is expressed in the γ-aminobutyric acid (GABA)-ergic medium spiny neurons of the striatum (a brain region critical for language production and comprehension), pyramidal neurons in the neocortex, and the CA1/CA2 hippocampal subfields (Ferland et al., 2003; Fröhlich, Rafiullah, Schmitt, Abele, & Rappold, 2017; Hisaoka, Nakamura, Senba, & Morikawa, 2010; Tamura, Morikawa, Iwanishi, Hisaoka, & Senba, 2004; Teramitsu, Kudo, London, Geschwind, & White, 2004). Studies in brain-specific FOXP1-deficient mice show deficits in ultrasonic vocalization, striatal morphological defects, and social and cognitive deficits—namely, hyperactivity, increased anxiety, communication impairments, decreased sociability, and significant deficits in learning and memory tasks (Araujo et al., 2015; Araujo et al., 2017; Bacon et al., 2015;

Fröhlich et al., 2017). Recent research has found significantly elevated mRNA levels of *FOXP1* in individuals with ASD as compared to TD controls (Chien et al., 2013). Studies characterizing the phenotype of individuals with FOXP1 syndrome found that while many patients display several ASD-related behaviors, not all meet full diagnostic criteria (Siper, De Rubeis, et al., 2017). Many individuals with the syndrome have delayed motor milestones and language development, with greater impairments in receptive language than expressive language (Siper, De Rubeis, et al., 2017). FOXP1 syndrome is also characterized by other comorbid psychiatric traits—such as obsessive-compulsive traits, attention deficits, anxiety, and oppositional traits—as well as several medical features and comorbidities, namely non-specific structural brain abnormalities, dysmorphic features, gastrointestinal problems, sleep disturbance, and sinopulmonary infections (Siper, De Rubeis, et al., 2017).

ADNP syndrome. ADNP syndrome (OMIM 615873) accounts for about 0.17% of all ASD cases and results from a heterozygous mutation in the *activity-dependent neuroprotective protein* (ADNP) gene, 20q13.13 (Helsmoortel et al., 2014). *ADNP* has been identified as a regulator of synaptic transmission, namely axonal transport (Amram et al., 2016) and dendritic spine plasticity (Oz et al., 2014). More specifically, translational models of *Adnp*-deficiency in mice results in slower axonal transport related to impaired hippocampal expression of the voltage-dependent calcium channel (Cacnb1), serotonin transporter (Slc6a4), and autophagy regulator BECN1 (Beclin1) genes (Amram et al., 2016; Oz et al., 2014). *ADNP* is also implicated in chromatin remodeling (Mandel & Gozes, 2007); embryonic brain and organ development, specifically neural tube closure (Mandel, Rechavi, & Gozes, 2007; Pinhasov et al., 2003); and neuronal cell differentiation and maturation (Mandel, Spivak-Pohis, & Gozes, 2008). Clinically,

individuals with ADNP syndrome present with ASD, mild-to-severe ID, motor delays, speech delays, and sleep problems, as well as several dysmorphic features (i.e., prominent forehead, high hairline, eversion or notch of the eyelid, broad nasal bridge, thin upper lip and smooth/long philtrum) (Helsmoortel et al., 2014; Van Dijck, Helsmoortel, Vandeweyer, & Kooy, 2016; Van Dijck et al., 2018). Neurologically, hypotonia, structural brain abnormalities, and seizures are common (Van Dijck et al., 2016; Van Dijck et al., 2018). Typical medical features include visual problems (i.e., strabismus, cerebral visual impairment, hypermetropia), gastrointestinal problems (most common of which are GERD and constipation), ear problems (i.e., narrow hearing canal, frequent otitis media, and hearing tubes), cardiac problems, and joint hypermobility, among others (Helsmoortel et al., 2014; Van Dijck et al., 2016; Van Dijck et al., 2018). ADNP syndrome is also characterized by several comorbid psychiatric problems, including ADHD, obsessive-compulsive behaviors, and aggressive behaviors and temper tantrums (Van Dijck et al., 2018).

Excitatory and Inhibitory Imbalance as a Relevant Theoretical Framework of Neural Underpinnings of ASD. To date, imbalances of excitatory and inhibitory activity have been hypothesized as a comprehensive, circuit-based alteration of neural activity in various neurodevelopmental disorders, including ASD. In general, neural activity relies on a balance between excitatory and inhibitory activity, predominantly driven by glutamatergic and GABAergic synaptic activity, respectively. Excitation triggers neuron firing, whereas inhibition discontinues or prevents neuronal response. Therefore, balance of excitatory (E) and inhibitory (I) activity is crucial for neural transmission and synchrony. When E/I activity is balanced, neurons are excitable in response to incoming input, and are also well tuned and

capable of filtering out irrelevant input (Foss-Feig et al., 2017). Additionally, neural circuits are well-organized, differentiated, and capable of signal transmission and synchrony (Foss-Feig et al., 2017). When the E/I ratio is elevated, which can occur secondary to increased excitation and/or decreased inhibition, neural circuits at baseline may exhibit high levels of random firing and proneness to seizure-like activity (Foss-Feig et al., 2017). Also, evoked responses to incoming stimuli may be exaggerated, and neural circuits are poorly tuned and may respond to inappropriate stimuli (Foss-Feig et al., 2017). Behaviorally, responses to basic sensory information may be exaggerated and complex behavior is likely impaired (Foss-Feig et al., 2017). Reduced E/I ratio, resulting from adaptive levels of excitation and excessive levels of inhibition, results in reduced baseline neural activity, as well as blunted responses to evoked stimulation (Foss-Feig et al., 2017).

Rubenstein and Merzenich (2003) were among the first to attribute the core symptoms in ASD to an imbalance of E/I activity. Authors suggest that the E/I ratio is increased in ASD, attributed to increased excitation and/or decreased inhibition. Coghlan et al. (2012) enumerated evidence from genetic, epigenetic, animal models, and post-mortem studies in humans which point to deficits in GABA in ASD. However, results from various electrophysiological and neuroimaging studies have been mixed with respect to the specificity of this E/I ratio. One study using EEG in the visual domain uncovered weaker steady-state gamma frequency range (30-90 Hz) responses to contextual modulation in participants with ASD as compared to TD controls; given that gamma oscillations are dependent on GABAergic signaling, this atypical response in ASD is suggestive of elevated E/I ratio (Snijders, Milivojevic, & Kemner, 2013). Conversely, parallel studies using EEG found that peak-gamma frequency, which provides an indication of neural inhibition, was

reduced in the visual cortex for individuals with ASD and neurotypical controls with higher autistic traits; authors thus argue that these responses are suggestive of increased occipital GABAergic inhibition, and thus reduced E/I ratios, in ASD (Dickinson, Bruyns-Haylett, Jones, & Milne, 2015; Dickinson, Bruyns-Haylett, Smith, Jones, & Milne, 2016). Similarly, MEG studies measuring somatosensory cortical response to the stimulation of adjacent fingers (a phenomenon controlled by cortical inhibition) using a passive tactile stimulation task revealed hypoconnectivity and enhanced inhibition in the somatosensory cortex in ASD, suggestive of reduced E/I ratio (Coskun, Loveland, Pearson, Papanicolaou, & Sheth, 2013a, 2013b). Foss-Feig et al. (2017) conducted a comprehensive review of multi-modal neuroimaging assessment of this E/I imbalance in ASD, which included fMRI, MRS, EEG and MEG studies, and found that various neural circuits, cell and receptor types, and developmental timeframes are implicated in E/I alterations seen in the disorder. Consequently, the heterogeneity of the ASD phenotype is likely attributed to specific alterations in each of these implicated domains. Authors also uncovered that correlations between neural measures and clinical symptom severity were frequently reported, thus suggesting that the E/I imbalances reported may affect the ASD clinical phenotype in a graded fashion.

Sensory symptoms in ASD. One of the major changes to the DSM-5 criteria for ASD was the inclusion of sensory symptoms into the restricted and repetitive behavior domain. Per the DSM-5, individuals with ASD may present with sensory hyperreactivity, hyporeactivity, or unusual sensory interest or sensory seeking behaviors (American Psychiatric Association, 2013). Hyperreactivity is often characterized as an “adverse response to sensory stimuli”; anecdotally, hyperreactivity symptoms often present as

covering one's ears or being upset by daily/benign sounds, or extreme discomfort for certain textures (American Psychiatric Association, 2013). Hyporeactivity is described as an "indifference" to sensory stimuli, and frequently presents as high pain threshold and often bumping into objects without care (American Psychiatric Association, 2013). Unusual sensory interests or sensory seeking behaviors frequently are characterized by a ''fascination with stimuli'' and behaviorally present as finger-flicking in front of one's eyes, peering at objects, holding objects up to one's ears, or repeatedly touching or rubbing objects (American Psychiatric Association, 2013).

Parents of children with ASD report vision and hearing problems among the first areas of concern, both of which are often noticeable prior to their child's first birthday (Bolton, Golding, Emond, & Steer, 2012; Kozlowski, Matson, Horovitz, Worley, & Neal, 2011). Sensory symptoms are consistently reported as among the most impairing on daily functioning (Hannant et al., 2016). Moreover, increased symptom severity in children with ASD is related to higher levels of anxiety, increased functional difficulties (specifically verbal communication and maladaptive behaviors), and increased levels of parental stress (Ausderau et al., 2016; Lane, Young, Baker, & Angley, 2010; Uljarević, Lane, Kelly, & Leekam, 2016). Importantly, sensory symptoms are among the first areas assessed and treated in early intervention (i.e., with occupational therapy).

Assessing sensory symptomatology. Until recently, few advances have been made in diagnostic processes to comprehensively assess sensory symptomatology. Our gold-standard diagnostic evaluations, comprised of the Autism Diagnostic Observation Schedule (ADOS-2) (Lord et al., 2012) and Autism Diagnostic Interview (ADI-R) (Lord, Rutter, & Le Couteur, 1994), comprehensively assess social communication deficits and restricted and repetitive

behaviors and interests; however, they are lacking in their characterization of the sensory domain. Cognitive and adaptive functioning assessments are also remiss in characterizing sensory symptoms, despite the fact they often impact cognitive performance and daily functioning.

Our extant sensory measures, which include both questionnaires and observational tools, are comprehensive and inexpensive to administer; however, they rely on parent-report or require significant language skills, and are therefore subject to bias and low generalizability. Tavassoli et al. (2016) comprehensively reviewed several of these existing measures in her study validating the Sensory Processing Scale Assessment, which include: the Short Sensory Profile (Dunn, 1999), Sensory Processing Over-responsivity (SenSOR) Scales—both a caregiver interview and assessment (Schoen, Miller, & Green, 2008; Schoen, Miller, & Sullivan, 2014), Sensory Experiences Questionnaire (Baranek, David, Poe, Stone, & Watson, 2006), the Sensory Questionnaire (Boyd & Baranek, 2005; Boyd, McBee, Holtzclaw, Baranek, & Bodfish, 2009), the Sensory Integration and Praxis Tests (SIPT) (Ayres, 1989) the Sensory Processing Assessment for Young Children (SPA) (Baranek, 1999; Patten, Ausderau, Watson, & Baranek, 2013), and the Tactile Defensiveness and Discrimination Test—Revised (TDDT-R) (Baranek, 2010).

The Sensory Profile and Short Sensory Profile. The Sensory Profile (Dunn & Westman, 1997) is a 125-item parent report form that investigates daily life sensory experiences in children. Caregivers are asked to rate the frequency, from 1 (always: when presented with the opportunity your child always responds in this manner, or 100% of the time) to 5 (never: when presented with the opportunity your child never responds in this manner, or 0% of the time), with which their child performs certain behaviors. Behaviors fall into three sections:

sensory processing, modulation, and behavior and emotional responses. Within the sensory processing section, questions are further subdivided into six subsections based on sensory modality (i.e., auditory processing, visual processing, vestibular processing, touch processing, multisensory processing, and oral sensory processing). Modulation is subdivided into five subsections reflecting combinations of sensory input that affect daily functioning (i.e., sensory processing related to endurance/tone, modulation related to body position and movement, modulation of movement reflecting activity level, modulation of sensory input affecting emotional responses, and modulation of visual input affecting emotional responses and activity level). The behavior and emotional responses portion of the questionnaire are divided into three subsections that reflect emotional and behavioral responses that may result from sensory processing difficulties (i.e., emotional/social responses, behavioral outcomes of sensory processing, and items indicating thresholds for response). The Sensory Profile has moderate test-retest reliability across factor (ICC = .69-.88) and section (ICC = .50-.87) scores, as well as high internal consistency across factor scores (α's = .82-.93) and moderate internal consistency across section scores (α's = .67-.93) (Ohl et al., 2012).

The Short Sensory Profile (SSP) (Dunn, 1999), derived from the Sensory Profile, consists of 38 items in which parents are asked to rate frequency of their child's behavior on a 5-point Likert scale from 1 (always) to 5 (never), with higher scores indicating typical/normal behavior. The SSP has seven subscales: Tactile Sensitivity, Taste/Smell Sensitivity, Movement Sensitivity, Underresponsive/Seeks Sensation, Auditory Filtering, Low Energy/Weak, and Visual/Auditory Sensitivity. Relevant to the current study, scores for Short Sensory Profile domains can be obtained from the full form, which allows for additional analysis. The SSP has high internal reliability (α's = .90-.95) (Dunn, 1999) and

reliably differentiates sensory symptomatology in typically-developing (TD) controls and ASD groups (Leekam, Nieto, Libby, Wing, & Gould, 2007; Wiggins et al., 2009).

The Sensory Assessment of Neurodevelopmental Disorders. To address the aforementioned pitfalls of our existing sensory assessments, Siper, Kolevzon, et al. (2017) developed and validated a novel clinician-administered observational assessment and caregiver interview—the Sensory Assessment of Neurodevelopmental Disorders (SAND)—to measure sensory symptoms in individuals of all ages and levels of verbal ability. The SAND captures sensory symptoms based on the DSM-5 criteria for ASD—namely hyperreactivity, hyporeactivity, and sensory seeking—across visual, auditory, and tactile domains.

The clinician-administered observation portion of the assessment is comprised of one-to-two minutes of unstructured play with standardized materials/toys to acclimate the child to the testing environment and observe any behaviors that may not arise during more structured interactions to follow. The unstructured play is followed by standardized presentation of 15 sensory stimuli/toys, with five toys per sensory modality (e.g., flashlight and moving disc for visual, musical toy and buzzer for auditory, and vibrating toy, weighted stuffed animal, and heated/cold toys for tactile, etc.). The assessment concludes with one-to-two minutes of unstructured play. Participants' behavioral responses are rated by a reliable and trained examiner on an algorithm that provides scores for each sensory modality (visual, tactile, auditory) and by DSM-5 symptom domain (hyper-reactivity, hypo-reactivity, seeking). Scores are based on a summary of all behaviors observed throughout the assessment, and are dichotomous, 0 (not present) and 1 (present). Severity scores, 1 (mild) and 2 (moderate-to-severe) were also coded within each domain if a behavior was coded as present.

The corresponding clinician-administered caregiver interview is comprised of 36-items in which caregivers reported whether (1) or not (0) their child exhibits a given sensory behavior. Again, severity scores were given, 1 (mild) and 2 (moderate-to-severe), if behaviors were reported as present within a given domain.

The SAND provides an overall score, based on summing observed and reported scores across domains and modalities, scores for each sensory domain (visual, auditory, and tactile), scores for each DSM-5 sensory symptom subtype (hyperreactivity, hyporeactivity, and sensory seeking). Domain scores range from 0 to 30, and total SAND scores range from 0 to 90, with higher scores representing higher levels of sensory symptoms. In the current study, combined scores of sensory subtype and sensory domain (i.e., visual hyporeactivity, visual hyperreactivity, visual seeking, tactile hyporeactivity, etc.) were also examined.

In an initial sample of 44 children with iASD and 36 TD controls, the SAND showed high internal consistency (Cronbach's $\alpha = .90$), strong inter-rater reliability (ICC's = .87 - .91), strong test-test reliability (ICC's = .82 - .97), and good convergent validity with the Short Sensory Profile (Dunn, 1999) (SSP; $r = -.82$, $p < .001$) (Siper, Kolevzon, et al., 2017).

Sensory symptoms in iASD. Individuals with iASD exhibit a broad range of sensory symptomatology across both DSM-5 subtypes and sensory domains, and oftentimes, different sensory patterns coexist within individuals (Ausderau, Sideris, et al., 2014; Lane et al., 2010; Mieses et al., 2016; Schoen, Miller, Brett-Green, & Nielsen, 2009; Siper, Kolevzon, et al., 2017; Tavassoli et al., 2016). Researchers have attempted to parse the heterogeneity of ASD by classifying individuals into different phenotypic groups based on sensory responsivity; however, the literature is rife with disagreements on which subtypes best represent the symptomatology seen in the population, as well as which domains are most often and

severely affected. Many sensory researchers agree with the DSM-5 delineation of sensory hyperreactivity, hyporeactivity, and sensory seeking. A meta-analysis conducted by Ben-Sasson et al. (2009) found that across studies utilizing parent-report/proxy measures, individuals with iASD exhibited significantly higher levels of sensory symptoms as compared to controls, the greatest of which was under-responsivity, followed by over-responsivity and sensory seeking; however, authors found that the magnitude of differences between subtypes in ASD was highly variable across studies and was moderated by several demographic variables (i.e., chronological age, autism symptom severity, and type of control group used as comparison). A national survey of sensory symptoms measured using the Sensory Experience Questionnaire (Baranek et al., 2006), Ausderau, Sideris, et al. (2014) found four distinct behavioral categories or sensory response patterns: hyporesponsiveness; hyperresponsiveness; sensory interests, repetitions and seeking behaviors; and a new fourth subcategory termed enhanced perception. Authors further characterized these sensory behaviors into discrete, homogenous subtypes using latent profile transition analysis: Mild (few sensory behaviors), Sensitive-Distressed (experiencing more hyperreactive and enhanced perception behaviors), Attenuated-Preoccupied (more hyporeactive and seeking behaviors), and Extreme Mixed (high incidence of all four sensory behavior patterns) (Ausderau, Furlong, et al., 2014; Ausderau, Sideris, et al., 2014). Using the Short Sensory Profile (Dunn, 1999), Lane et. al. (2014; 2010) similarly identified four distinct sensory subtypes which differ based on severity and the affected domains: sensory adaptive (no clinically significant sensory symptoms), taste/smell sensitive (severe levels of taste/smell sensitivity and clinically significant levels of auditory filtering difficulties and under-responsive/seeking behaviors), postural inattentive (severe low energy/weak symptoms and

clinically significant concerns in auditory filtering and under-responsive/seeks sensation), and generalized sensory difference (all domains severely affected). A study conducted by Tavassoli et al. (2016) assessing sensory symptomatology in high functioning children with iASD using an observational measure similarly found that different sensory modalities more commonly fell within different sensory subtypes: in the vision domain, the most common sensory subtype was sensory seeking, whereas auditory and tactile domains were more often hyperreactive.

While these studies offer interesting insights into the heterogeneous nature of sensory symptomatology in iASD, they offer little in the way of understanding etiology and providing targeted efficacious treatment. The current study seeks to instead parse the diverse presentation of sensory symptoms in iASD in single-locus causes of ASD where pathophysiology and etiology are better understood.

Sensory symptoms in single-locus causes of ASD. Conversely to what is observed in iASD, individuals with single-locus causes of ASD reportedly exhibit more homogenous sensory profiles that are unique to each syndrome. In both human and mouse models of Fragile X syndrome (FXS)—a single-locus cause of ASD caused by the trinucleotide CGG expansion of the fragile X mental retardation (FMR1) gene resulting in the loss of the fragile X mental retardation protein (FMRP) and subsequent neuronal hyperexcitability (Bear, Huber, & Warren, 2004)–individuals exhibit higher levels of sensory hyperresponsivity (Chen & Toth, 2001; Miller et al., 1999), with severity of hyperresponsivity increasing with age (Baranek et al., 2008). Individuals with PMS reportedly have increased pain tolerance, as well as unusual sensory interests and sensitivities (Soorya et al., 2013). When sensory symptoms are assessed using the Short Sensory Profile (SSP) (Dunn, 1999), individuals with

PMS reportedly have fewer sensory reactivity symptoms in the domains of taste/smell sensitivity, visual/auditory sensitivity, and auditory sensitivity, and increased low-energy/weak symptoms as compared to individuals with iASD (Mieses et al., 2016). In FOXP1 syndrome, parents report definite sensory differences, many of which relate to sensory seeking and hyporeactivity (Siper, De Rubeis, et al., 2017). Per parent report, individuals with ADNP syndrome frequently present with insensitivity to pain and sensory processing disorder (Van Dijck et al., 2018).

The Visual System. The human visual system is a complex system comprised of an optical component and neural component. Neural signals are first generated in photoreceptors—rods and cones—in the retina, the photosensitive tissue located in the back of the eye, and transmitted to the brain via the optic nerve. The retina contains three main layers, each of which shares synapses with the adjacent layer: the photoreceptive layer, the bipolar cell layer, and the ganglion cell layer. Light passes through these three translucent layers and is detected by the rods and cones. Through the process of phototransduction, photoreceptor cells convert the light energy impinging upon them into an electrochemical response. This electrochemical cascade travels from photoreceptor cells to the adjacent bipolar cells, then generates action potentials in the ganglion cells. The axons of the retinal ganglion cells form the optic nerve (Carlson, 2010; Widmaier, Raff, & Strang, 2006).

The visual pathway continues from the optic nerve to the lateral geniculate nucleus (LGN) in the thalamus, which contains six layers: the four dorsal layers are parvocellular (P), the two ventral layers are magnocellular (M), and the intermediary layers, border regions are koniocellular (K). The P layers of the LGN receive input from midget retinal ganglion cells, which have responsivity to high contrast stimuli (Carlson, 2010; Kaplan, 1991, 2003; Kaplan

& Shapley, 1986; Zemon & Gordon, 2006). The M layers of the LGN receive input from parasol retinal ganglion cells, which have high sensitivity to low contrast stimuli (Carlson, 2010; Kaplan, 1991, 2003; Kaplan & Shapley, 1986; Zemon & Gordon, 2006). Next, information travels from the LGN to the striate cortex, or the primary visual cortex (V1); more specifically, information from the M layers of the LGN travel to layer 4Cα, and from the P layers to 4Cβ (Carlson, 2010; Kaplan, 2003). From V1, information travels to extrastriate cortical areas, including V2, V3, V4, V5, etc., as well as subcortical areas, namely the LGN, pons, superior colliculus, pulvinar, and claustrum (Carlson, 2010). Importantly, the division of the magnocellular and parvocellular streams continues through to these extrastriate areas (Tootell & Nasr, 2017).

Visual Evoked Potentials. While behavioral measures allow us to comprehensively assess behavioral clinical symptomatology, objective measures of underlying neural activity are crucial to better understand the syndromes to be studied in the current study. Visual evoked potentials (VEPs) provide a rapid, noninvasive, objective, reliable technique to assess the functional integrity of the visual pathway (Zemon, Kaplan, & Ratliff, 1986). VEPs reflect the sum of excitatory and inhibitory postsynaptic potentials occurring on the apical dendrites of the pyramidal cells located in the outermost layers of V1 (Creutzfeldt & Kuhnt, 1973; Purpura, 1959; Zemon et al., 1986). The apical dendrites serve as the main generator of the VEP response (Zemon et al., 1986). The VEP is recorded from the surface of the scalp over V1 and is extracted from the ongoing electroencephalogram (EEG) via signal averaging. Unlike fMRI and other brain scanning techniques, which capture brain responses on the order of seconds, VEPs reflect real-time brain processes which occur on the order of milliseconds. Moreover, unlike traditional event-related potentials (ERPs)—in which the neural generators

of the response are not well understood—the specific neural contributors of the VEP response are well-characterized. Using specific, varied stimuli, VEPs can assess various excitatory and inhibitory subsystems in the brain, including magnocellular and parvocellular pathways, ON and OFF pathways, shunting inhibition, neural noise (response variability), direct-through excitatory pathways, long-range and short-range lateral inhibitory pathways, and spatial processing (Ratliff & Zemon, 1982; Zemon & Gordon, 2006; Zemon, Gordon, & Welch, 1988; Zemon et al., 1986; Zemon & Ratliff, 1982, 1984).

VEPs have been utilized clinically in glaucoma (Celesia, 1982; Greenstein, Seliger, Zemon, & Ritch, 1998; Towle, Moskowitz, Sokol, & Schwartz, 1983; Zemon et al., 2008), optic nerve diseases (Celesia & Kaufman, 1985), amblyopia (Levi & Manny, 1986; Regan, 1977; Sokol, 1983), multiple sclerosis (Bodis-Wollner, Hendley, Mylin, & Thornton, 1979; Ghilardi et al., 1991; Hennerici, Wenzel, & Freund, 1977; Regan, Milner, & Heron, 1977), Parkinson's (Bhaskar, Vanchilingam, Bhaskar, Devaprabhu, & Ganesan, 1986; Bodis-Wollner & Yahr, 1978), migraines (Coppola et al., 2013), and epilepsy (Conte & Victor, 2009). Extensive VEP research has also been conducted in patients with schizophrenia (Butler et al., 2001; Butler et al., 2005; Kim, Wylie, Pasternak, Butler, & Javitt, 2006; Kim, Zemon, Saperstein, Butler, & Javitt, 2005; Schechter et al., 2005), a psychiatric disorder with known symptomatic and genetic overlaps with ASD (Konstantareas & Hewitt, 2001; Stefansson et al., 2014).

***Transient and steady-state VEPs*.** Transient and steady-state VEPs are classified based on the modulation of the stimulus frequency and the resultant elicited response**.** The transient VEP (tVEP) is elicited by modulating the luminance or contrast of a stimulus at low frequencies (i.e., less than 4 Hz). Moreover, these stimulus changes occur abruptly (e.g.,

using a square-wave signal), allowing the response to settle between changes. The resulting characteristic tVEP response, typically represented in the time domain as amplitude versus time, appears as a series of positive and negative deflections within the record's first few hundred milliseconds. Analysis of tVEPs involves examining selected peaks and troughs in the response, and measuring amplitude and time to peak (latency) for each point of interest. Steady-state VEPs (ssVEPs) are produced by a light stimulus that is modulated sinusoidally at a higher frequency (i.e., equal to or greater than 4 Hz). In ssVEPs, the frequent stimulus changes create responses that overlap and generate on oscillatory waveform. Steady-state VEPs are frequently analyzed via examining amplitude and phase data of individual frequency components. The current study utilized tVEPs.

Transient VEPs to contrast-reversing checkerboard. Transient VEPs are typically elicited by checkboard patterns whose light and dark elements, often set to high contrast (85-100%), are reversed at the onset of the stimulus cycle and again halfway through the cycle. This rather conventional VEP stimulus produces a characteristic transient waveform with a positive peak at approximately 60 ms ($P_{60,}$ P_0), reflecting activation of V1 from the lateral geniculate nucleus; a subsequent negative trough at approximately 75 ms (N_{75}, N_1), reflecting depolarization and glutamatergic postsynaptic activity in the superficial layers of V1; and a positive peak at 100 ms (P_{100}, P_1), reflecting hyperpolarization and GABAergic postsynaptic activity in the superficial layers of V1 (Zemon, Kaplan, & Ratliff, 1980) (Figure 1).

Development of tVEP waveforms. Contrast-reversing checkerboards have been used to elicit tVEPs throughout the lifespan, including in early infancy. In neonates, P_{100} latency occurs around 260 ms, and decreases significantly within the first weeks of life (McCulloch, Orbach, & Skarf, 1999). Researchers have repeatedly indicated that latencies of tVEP

components, particularly the easily-identifiable P_{100}, decrease with increasing age until age 55; specifically, P_{100} latency decreases rapidly up to 1 year of age, and then slowly from 1 to 6 years of age (Creel, 2013; Moskowitz & Sokol, 1983; Sokol & Jones, 1979; Zemon et al., 1995). However, Zemon et al. (1995) found the the latency of the initial P_{60} positive wave increased with increasing age. McCulloch et al. (1999) found that the most rapid maturation of P_{100} latency occurs between 6 to 9 weeks of age depending on the stimulus size. Additional evidence exists that complex changes in the electrophysiological response continue well into adolescence. Using flash VEPs, Dustman and Beck (1966) found that amplitude of the VEP response rapidly increases throughout young childhood until it reached a maximum between ages 5-6 years, with means of amplitudes about twice as large as those in some older adults. Authors also observed a rapid decline in amplitude in children's responses between ages 7 and 14, followed by an increase in amplitude between ages 14 and 16, with amplitudes stabilizing thereafter. In pattern VEPs, Spekreijse (1978) similarly found maturational changes in the VEP response until age 10, and specifying that this maturation of the response occurs in two stages: Stage 1, which occurs from birth until about 8 months of age, is characterized by changes in peak amplitude versus check size as a function of VEP acuity changes; and Stage 2, which extends from eight months of age until age 16, is characterized by modifications of the positive-negative-positive form of the VEP response (specifically with only a positive peak observed at a latency of 150 ms before age four, with the negative peak increasing until about age 16) (De Vries-Khoe & Spekreijse, 1982). By age 55, tVEP waveforms become significantly more variable, and there is attenuation in amplitude and slowing of the P_{100} component (Creel, 2013). Reproducible tVEP waveforms

to large pattern element, contrast-reversing stimuli are present even by three weeks of age (McCulloch et al., 1999), and appear adult-like by age four (Moskowitz & Sokol, 1983).

VEPs in iASD. VEPs have been utilized to understand the underlying pathophysiology in iASD. Results from our groups' research using a contrast-reversing checkerboard indicate that children with iASD have significantly weaker P_{60}-N_{75} and N_{75}–P_{100} amplitudes than their TD counterparts, which reflect initial glutamatergic and GABAergic activity in the cortex, respectively (Siper et al., 2016). Moreover, iASD participants showed significantly reduced responses in the frequency domain for frequency bands that encompass both low and high gamma-wave activity (Siper et al., 2016). In studies utilizing bright and dark isolated-check patterns which tap into ON- and OFF-cell activity, results indicated that children with iASD exhibit significantly weaker signal-to-noise ratios for the dark check condition at low contrasts (i.e., 4% and 8% depth of modulation (DOM)). Children with iASD also displayed significantly greater within-individual response variability (neural noise) as compared to TD controls for the dark check condition at low contrasts (i.e., 1%, 2% and 4% DOM); moreover, the level of neural noise remained constant across DOMs in the iASD group, whereas for the controls, the noise levels were lower at lower contrasts and higher at higher contrasts. Together, these results suggest magnocellular pathway deficits and increased neural noise in iASD (Weinger, Zemon, Soorya, & Gordon, 2014; Zweifach, 2016). With respect to lateral inhibitory interactions as measured by VEPs, research in adults with iASD found no significant differences in amplitude and latency of short- or long-range inhibitory responses (Censi, Simard, Mottron, Saint-Amour, & Bertone, 2014). Dickinson, Gomez, Jones, Zemon, and Milne (2018) similarly found no group-level differences in short- and long-range lateral inhibitory interactions between adults with iASD

and TD controls; yet, exploratory results indicated that ASD symptom severity was related to increased short-range lateral inhibition, suggesting that different VEP responses may be related to different phenotypic/behavioral presentations. A recent unpublished study by the current author found that in a sample of children with iASD and TD controls, children with iASD exhibited deficits in long-range lateral inhibitory interactions as well as increased levels of neural noise as compared to TD controls (Lurie, 2018).

VEPs in single-locus causes of ASD. Of particular relevance to the current study, VEPs have additionally been studied in single-locus causes of ASD. Knoth, Vannasing, Major, Michaud, and Lippe (2014) analyzed VEPs using a contrast-reversing checkerboard in adults with FXS and unaffected controls. Patients with FXS exhibited significantly increased amplitudes at N_{70} and N_2 as compared to chronologically-age-matched controls, which may be indicative of impairments in GABAergic inhibition in the cortex. Our groups' preliminary, unpublished VEP research in FXS shows enhancement in P_{60}-N_{75} amplitude relative to N_{75}-P_{100} amplitude, suggestive of relatively greater excitatory activity—which is consistent with the neuronal excitability and exaggerated long-term depression dependent on metabotropic glutamate receptors (mGluR) seen in translational models of the syndrome (Bear et al., 2004). Varcin et al. (2015) conducted a study assessing VEPs in infants with and without tuberous sclerosis complex (TSC). TSC is another single-locus cause of ASD caused by loss of function mutations in the TSC1 or TSC2 genes, thereby leading to hyperactivation of the mTOR pathway (key for cell proliferation and synaptic plasticity during neuronal development) (Varcin et al., 2015). Authors found no significant differences in latency or amplitude between groups (Varcin et al., 2015). In a study assessing VEPs in young females with Rett syndrome (LeBlanc et al., 2015)—another single-locus form of ASD caused by *de*

novo mutations of the MECP2 gene (Amir et al., 1999)—females with Rett syndrome displayed significantly weaker N_{75}-P_{100} and P_{100}-N_{135} amplitudes as compared to TD controls, as well as slow recovery from the P_{100} peak. Authors hypothesized that these weaker responses likely result from decreased excitation and increased inhibition, as evidenced in mouse and human models of the syndrome. A recent study conducted by Siper et al. (2019) examined tVEPs used in the current study in children with PMS. Results indicated that children in the PMS group exhibited significantly weaker P_{60}-N_{75} and N_{75}-P_{100} amplitudes as compared to their unaffected siblings and TD controls. While the PMS and iASD groups did not differ significantly with respect to P_{60}-N_{75} and N_{75}-P_{100} amplitudes, the examination of the waveforms elucidated complete absence or significant diminishment of the P_{60}-N_{75} amplitude for children with PMS with deletions in SHANK3, reflective of deficits in glutamatergic activity. Moreover, children in the PMS group displayed weaker beta- and gamma-band activity as compared to TD controls and their unaffected siblings.

Together, these results suggest that each syndrome exhibits a unique VEP profile that is often related to the neural pathophysiology exhibited in translational models of the syndrome. The proposed study seeks to continue along this line of research by studying VEPs and behavioral sensory responsivity in PMS, FOXP1 syndrome, and ADNP syndrome.

Relationships between VEPs and behavioral measures of sensory symptoms. To establish the clinical relevance of electrophysiological biomarkers, it is crucial to understand the relationships between these markers and clinical behavioral phenotypes. Recent research using our group's methodology has elucidated a link between ssVEP responses and ASD symptomatology, such that ASD symptom severity is related to increased short-range lateral inhibition (Dickinson et al., 2018). Unfortunately, general ASD symptomatology is not a

specific enough measure to examine clinical correlates of electrophysiological markers in both single-locus and idiopathic ASD populations, as social communication deficits (a hallmark feature of ASD) are less prominent in single-locus cases of ASD than in iASD (Bishop et al., 2017). As previously mentioned, sensory reactivity symptoms are present across iASD and single-locus causes of ASD; the sensory domain therefore represents a more promising clinical behavioral correlate for electrophysiological markers. Recent research from our group supports the rationale of a relationship between VEP response and behavioral sensory reactivity (Siper et al., 2019). Authors found significant correlations between VEP measures in the time (P_{60}-N_{75} and N_{75}-P_{100} amplitudes) and frequency (MSC Bands 2, 3, and 4) domains and SAND and SSP scores, which are based on both parent-report and clinician-observed outcomes. Specifically, SSP and SAND scores indicative of greater sensory processing-related difficulties were related to smaller amplitudes. Moreover, SAND hyporeactivity and SSP low energy/weak and underresponsiveness domain scores were significantly associated with all relevant peaks and troughs of the VEP response, with reduced amplitudes corresponding to greater sensory hyporesponsiveness on both measures. The current study will expand upon Siper et al.'s (2019) previous work by examining the link between VEPs and behavioral sensory symptoms in two additional single-locus causes of ASD.

Rationale

The sensory literature in iASD is varied with respect to subtypes and affected domains, and researchers unanimously agree that sensory phenotypes are highly heterogeneous in iASD, with various domains being affected in different ways. Sensory symptomatology in single-locus causes of ASD is more homogenous and distinctive to each

syndrome. As previously mentioned, individuals with FXS exhibit higher levels of sensory hyperresponsivity (Chen & Toth, 2001; Miller et al., 1999), and individuals with PMS exhibit significantly greater sensory hyporesponsivity (Mieses et al., 2016; Soorya et al., 2013). Moreover, preliminary unpublished work using the SAND in a sample of children with PMS (n = 27), iASD (n = 60), and TD (n = 35) controls revealed that TD controls scored significantly lower on the measure as compared to the iASD and PMS groups, indicative of significantly fewer sensory symptoms. While there was no difference in total sensory symptoms between iASD and PMS groups, results revealed a unique PMS sensory profile: children in the PMS group had significantly greater visual, auditory, and tactile sensory hyporeactivity as compared to both iASD and TD groups. The iASD group exhibited significantly greater hyperreactivity and seeking behaviors as compared to PMS and TD groups. Furthermore, our results suggest that approximately 30% of children with iASD display SAND hyporeactivity scores within one standard deviation of the PMS mean, reflecting “PMS-like” sensory reactivity. The current study will therefore examine behavioral sensory symptomatology in iASD, PMS, and TD controls, as well as two under-researched syndromes: FOXP1 syndrome and ADNP syndrome.

The aforementioned mechanistic E/I hypothesis of ASD holds clinical promise, as glutamatergic and GABAergic activity can serve as biomarkers of ASD pathology. VEPs are uniquely qualified to assess the E/I imbalance hypothesis in ASD, as glutamatergic and GABAergic interactions formulate the electrogenesis of the VEP. As previously mentioned, our group’s previously published work suggests that children with iASD have significantly weaker P_{60}-N_{75} and N_{75}–P_{100} amplitudes than TD controls, suggestive of reductions in initial glutamatergic and resultant GABAergic activity in the cortex (Siper et al., 2016).

Additionally, research utilizing VEPs in several single-locus causes of ASD—namely FXS and Rett syndrome—suggests that each syndrome exhibits a unique electrophysiological response that can be best explained by the underlying pathophysiology of the syndrome. Our group's findings in PMS support this rationale through providing evidence of a unique VEP signature in PMS, demonstrative of deficits in glutamatergic activity (Siper et al., 2019). Siper et al.'s (2019) VEP results in PMS are consistent with the Seaver Autism Center's work with animal models demonstrating glutamatergic system dysfunction due to the adverse effects of *SHANK3* deficiency (Bozdagi et al., 2010; Bozdagi et al., 2013) and from VEP data in *Shank3*-deficient mice. The current study seeks to expand upon the existing single-locus ASD literature by examining VEPs in children with FOXP1 and ADNP syndrome, and exploring the underlying pathophysiology using a promising sensory-related electrophysiological technique.

The current study aims to comprehensively assess sensory symptomatology in three single-locus causes of ASD using both behavioral and electrophysiological measures, with the long-term goal of parsing the heterogeneity of iASD to better inform etiology of behavior, and identify and utilize novel, targeted treatment. By broadening our understanding of sensory phenotypes in single-locus forms of ASD, we expect to uncover subsets of individuals with iASD who display similar profiles. While the iASD VEP and sensory behavior literature is beginning to provide novel insights into underlying physiology, a more targeted approach using genetically-defined subtypes will allow more targeted analysis. Moreover, our preliminary results suggest our methods may be useful for objective patient stratification, translational biomarkers, novel outcome measures and, ultimately personalized treatment approaches.

Innovation

While there have been significant advances in gene discovery related to ASD in the past several years, little has been done to utilize the information we have gathered in single-locus causes of ASD to inform our understanding of iASD. This is the first known study to comprehensively assess sensory symptoms in three single-locus causes of ASD. The current study is innovative because it is among the first to take a genetics-first approach to inform behavioral and electrophysiological marker discovery in iASD, as well as identify relationships between clinical outcomes (i.e., measures of sensory symptomatology) and biological variables (i.e., glutamatergic and GABAergic activity as measured by VEPs). Ultimately, results can be translated to establish biomarkers and clinical outcome measures in individuals with iASD who show similar profiles in the absence of an identifiable genetic cause. The electrophysiological methods used in the current study can be directly translated to animal models for preclinical drug efficacy research. In the long-term, the proposed methodology can be utilized to stratify iASD patients with the intent to provide more targeted therapeutics. The current project is methodologically innovative because it utilized short-duration stimuli that measure underlying neural mechanisms that mature early in life, which have shown to be feasible to use in individuals at varying levels of functional and verbal ability. Moreover, the current project utilized a novel behavioral measure that can be used with children of varying levels of cognitive ability and developmental level to assess sensory symptomatology. The current project is also innovative because it seeks to examine the relationship between behavioral and electrophysiological assessments of sensory reactivity, thereby continuing to substantiate the clinical relevance of these electrophysiological

measures and bolstering their candidacy as a meaningful biomarker in ASD and related disorders.

Aims and Hypotheses

Aim 1: Characterize sensory behavior in individuals with single-locus causes of ASD (i.e., PMS, FOXP1 syndrome, and ADNP syndrome) relative to individuals with iASD and TD controls.

Hypothesis 1a: **It is expected that the TD controls will exhibit fewer sensory reactivity symptoms than iASD and single-locus ASD groups across sensory subtype, sensory domain, and combined measures of sensory domain and subtype as measured by the Sensory Assessment of Neurodevelopmental Disorders (SAND), as well as on all subscales on the Short Sensory Profile (SSP).** This hypothesis is consistent with previous literature using the SAND and SSP, in which iASD groups exhibited significantly more sensory symptoms than TD controls (Siper, Kolevzon, et al., 2017).

Hypothesis 1b: **It is hypothesized that the PMS group will exhibit significantly more visual, tactile, and auditory hyporeactivity symptoms than iASD, ADNP, FOXP1, and TD groups**, which is consistent with previous studies in PMS (Mieses et al., 2016; Soorya et al., 2013).

Hypothesis 1c: **While this is the first study to examine sensory symptoms in ADNP and FOXP1 syndrome, we expect that each syndrome group will exhibit a unique sensory profile as compared to TD, iASD, and other single-locus groups**. Previous literature indicated other single-locus causes of ASD exhibit unique sensory phenotypes when compared to iASD—namely increased hyperresponsivity in FXS, (Baranek et al., 2008; Chen & Toth, 2001; Miller et al., 1999) and increased hyporesponsivity in PMS

(Mieses et al., 2016; Soorya et al., 2013). Therefore, we hypothesize that the ADNP and FOXP1 groups will individually exhibit significantly more sensory symptoms in either visual hyperreactivity, visual hyporeactivity, visual sensory seeking, auditory hyperreactivity, auditory hyporeactivity, auditory sensory seeking, tactile hyperreactivity, tactile hyporeactivity, and tactile sensory seeking, as well as on subscales of the SSP, when compared to TD, iASD, and other single-locus groups.

Aim 2: Identify electrophysiological markers of sensory reactivity using tVEPs in individuals with ADNP and FOXP1 syndrome relative to individuals with iASD and TD controls.

Hypothesis 2a: **It is expected that TD controls will exhibit significantly larger amplitudes, MSC values, and greater power than iASD, ADNP, and FOXP1 groups. We do not expect there to be significant differences in latency between groups.** Previous findings show that iASD and PMS groups exhibit reduced amplitudes and MSC values than do TD controls, but similar latencies (Siper et al., 2019; Siper et al., 2016). However, previous studies did not examine estimates of response power in the frequency domain. This is also the first study to examine tVEP responses in ADNP and FOXP1 groups.

Hypothesis 2b**: We expect children with FOXP1 syndrome and ADNP syndrome to exhibit unique VEP signatures that will inform our understanding of underlying biology.** Previous studies using VEPs in single-locus causes of ASD have found that results are consistent with known translational research underlying neuropathophysiology. Specifically, patients with FXS exhibited significantly increased amplitudes at N_{70} and N_2 as compared to chronologically-age-matched controls, indicative of impairments in GABAergic inhibition and increased excitation in the cortex, which are consistent with translational

models of the syndrome (Knoth et al., 2014). A study using VEPs in Rett syndrome found significantly weaker N_{75}-P_{100} and P_{100}-N_{135} amplitudes as compared to TD controls, as well as slow recovery from the P_{100} peak, indicative of decreased excitation and increased inhibition, which was consistent with mouse and human models of the syndrome (LeBlanc et al., 2015). A recent study using VEPs in PMS indicated that children with PMS exhibited significantly weaker P_{60}-N_{75} and N_{75}-P_{100} amplitudes as compared to their unaffected siblings and TD controls, as well as an absence or significant diminishment of the P_{60}-N_{75} amplitude for children with PMS with deletions in SHANK3, reflective of deficits in glutamatergic activity, which is consistent with translational models of the syndrome.

Exploratory Aim: Examine the relationship between underlying neuropathophysiology and behavioral clinical outcomes.

Exploratory Hypothesis: **We expect VEPs will correlate with the SAND and SSP.** Previous studies conducted by our group have found that tVEPs correlate significantly with measures of behavioral sensory reactivity (Siper et al., 2019).

Chapter II: Methods

Study 1

Participants

One hundred and forty children participated in the current study. A final sample of 30 individuals with PMS (13 males, 17 females, M_{age} = 6.67 years, *SD* = 2.66), 15 with FOXP1 syndrome (5 males, 10 females, M_{age} = 7.37 years, *SD* =3.05), 16 with ADNP syndrome (11 males, 5 females, M_{age} = 6.96 years, *SD* = 3.33), 55 with iASD (46 males, 9 females, M_{age} = 6.26 years, *SD = 2.18*), and 24 typically-developing (TD) controls (13 males, 11 females, M_{age} = 6.54 years, *SD* = 3.00) were included in this study. Participant characteristics are summarized in Table 1.

PMS, FOXP1, ADNP, and iASD participants were assessed for ASD status using the Autism Diagnostic Observation Schedule, Second Edition (ADOS-2) (Lord et al., 2012), Autism Diagnostic Interview-Revised (ADI-R) (Lord et al., 1994), and DSM-5 criteria (American Psychiatric Association, 2013). ASD diagnosis was established according to consensus diagnosis among clinicians at the Seaver Autism Center at the Icahn School of Medicine at Mount Sinai based on the aforementioned gold-standard measures.

The current study was conducted at the Seaver Autism Center at the Icahn School of Medicine at Mount Sinai. Informed consent was obtained from participants' legal guardians and assent was obtained from participants when appropriate. This study was approved by the institutional review board at the Icahn School of Medicine at Mount Sinai and at Albert

Einstein College of Medicine. All study materials were de-identified; participant data were instead labeled using unique study identification numbers.

Eligibility and exclusion criteria. PMS, FOXP1 syndrome, and ADNP syndrome were confirmed using either chromosomal microarray, Sanger sequencing, or whole exome sequencing, as appropriate. The iASD sample also received chromosomal microarray to confirm idiopathic status. For individuals in the iASD group, eligibility was determined based on presence of ASD diagnosis through consensus diagnosis described above. The presence of comorbid psychiatric and medical (e.g., seizures, cerebral visual impairment) conditions were carefully assessed in all participants during clinical interview, but were not exclusionary. For the TD group, exclusion criteria included history of ASD or developmental disorders in the self or family members, as determined by intake.

Measures

Gold-Standard Assessments. For single-locus and iASD groups, ASD diagnosis was assessed using the Autism Diagnostic Observation Schedule, Second Edition (ADOS-2) (Lord et al., 2012), Autism Diagnostic Interview-Revised (ADI-R) (Lord et al., 1994), and DSM-5 criteria (American Psychiatric Association, 2013). Cognitive functioning was assessed using the Mullen Scales of Early Learning (Mullen, 1995), the Differential Ability Scales, 2nd Edition (DAS-II) (Elliott, 2007), the Wechsler Intelligence Scale for Children, Fifth Edition (WISC-V) (Wechsler, 2014), the Wechsler Abbreviated Intelligence Scale, Second Edition (WASI-II) (Wechsler, 2011), the Wechsler Preschool and Primary Scale of Intelligence, Fourth Edition (WPPSI-IV) (Wechsler, 2012), or the Stanford Binet Intelligence Scales, Fifth Edition (SB-5) (Roid, 2003). Adaptive functioning was assessed using the

Vineland Adaptive Behavior Scales, Survey Interview, Second Edition (Sparrow, Cicchetti, & D.A., 2005) or Third Edition (Sparrow, Cicchetti, & Saulnier, 2016).

Sensory Assessments. Sensory symptomatology was evaluated using the Sensory Assessment for Neurodevelopmental Disorders (SAND) (Siper, Kolevzon, et al., 2017) and the Sensory Profile (Dunn & Westman, 1997). Scores from the Sensory Profile were then converted to obtain scores for the Short Sensory Profile (Dunn, 1999)

Power Analysis

G*power 3.1 (Faul, Erdfelder, Lang, & Buchner, 2007) was used for a priori power analyses. A large effect size ($f^2 = 0.35$) (Cohen, 1988) was used for the current analyses, as the long-term goal of the current proposal is to establish biomarkers to aid in diagnosis and treatment efficacy, which will require large effects. For Aim 1, using a MANOVA special effects and interactions model with five categories of group and nine outcome variables, a sample size of 55 will yield 80% power at the α level of .05 to detect differences among groups on the SAND combined sensory subtype and domain measures. The current study exceeds this sample size estimate.

Statistical Analyses

All statistical analyses were run using SPSS version 26. Demographic comparisons for sex and age were analyzed using chi-square and between-groups ANOVAs, respectively. A one-way between groups analysis of variance (ANOVA) was conducted to explore diagnostic group differences in SAND total score between groups. To test hypotheses for Aim 1, a series of multivariate analysis of variance (MANOVAs) were used to assess diagnostic group differences in SAND measures separately for sensory subtype (i.e., hyperreactivity, hyporeactivity, sensory seeking), sensory domain (i.e., visual, auditory,

tactile), and combined domain and subtype (visual hyperreactivity, visual hyporeactivity, visual sensory seeking, auditory hyperreactivity, auditory hyporeactivity, auditory sensory seeking, tactile hyperactivity, tactile hyporeactivity, and tactile sensory seeking) separately comparing each single-locus group to TD and iASD groups, as well as comparing all five groups to each other. Each MANOVA was followed up with a discriminant analysis. Multivariate statistics were also conducted on the SSP to examine group differences on subscales measured therein. For SSP analyses, MANOVAs were followed up with pairwise comparisons using Bonferroni correction.

Linear mixed effects models (LMM) were used to determine if data were correlated within an individual, and to examine group differences in SAND combined domain and subtype scores. LMM facilitates the analysis of multiple data points within an individual participant. LMM also concurrently models discrete and continuous variables, as well as the covariance structure, which thus permits violations of sphericity and homogeneity of variance.

In the LMM of these data, participants were treated as a random effect to assess the variance components and within- and between-groups differences using intraclass correlation coefficients (ICCs). An ICC greater than .05 indicated that there is significant correlation of data within an individual, thus necessitating modeling of the covariance structure of the data and use of LMM. In Model 1, the null model, only participant was treated as a random effect, without any fixed effects. In Model 2, diagnostic group was added to the model as a fixed effect. In Model 3, SAND subscale (i.e., combined sensory domain and subtype scores) was added as a fixed effect. In Model 4, a two-way interaction of Diagnosis x SAND subscale was added. The fit of each model was examined using chi-square likelihood ratio tests.

Improvements between models was assessed using the difference in -2 log likelihood (-2LL) between models, with chi-square degrees of freedom equal to the difference in parameters between models. Larger decreases in -2LL values (or smaller -2LL values) are indicative of improvements to the model. Post hoc t-tests were used when LMM revealed significant main effects and interactions.

Study 2

Participants

One hundred and fifty children participated in the current study. Five participants (two in the ADNP group, three in the FOXP1 group) were removed due to nonsignificant responses, as measured by MSC. A final sample of nine children with FOXP1 syndrome (two males, M = 8.75 years, SD = 2.71), 12 with ADNP syndrome (8 males, M = 7.04 years, SD = 3.44), 79 with iASD (70 males, M = 6.72 years, SD = 2.59), and 45 TD controls (25 males, M = 6.69 years, SD = 2.67) were included in this study. Participant characteristics are summarized in Table 8.

FOXP1, ADNP, and iASD participants were assessed for ASD status using the Autism Diagnostic Observation Schedule, Second Edition (ADOS-2) (Lord et al., 2012), Autism Diagnostic Interview-Revised (ADI-R) (Lord et al., 1994), and DSM-5 criteria (American Psychiatric Association, 2013). ASD diagnosis was established according to consensus diagnosis among clinicians at the Seaver Autism Center at the Icahn School of Medicine at Mount Sinai based on the aforementioned gold-standard measures.

The current study was conducted at the Seaver Autism Center at the Icahn School of Medicine at Mount Sinai. Informed consent was obtained from participants' legal guardians and assent was obtained from participants when appropriate. The study was approved by the

institutional review board at the Icahn School of Medicine at Mount Sinai and at Albert Einstein College of Medicine. All study materials were de-identified; participant data were instead labeled using unique study identification numbers.

Eligibility and exclusion criteria. FOXP1 and ADNP syndromes were confirmed using either chromosomal microarray, Sanger sequencing, or whole exome sequencing, as appropriate. The iASD sample also received chromosomal microarray to confirm idiopathic status. For individuals in the iASD group, eligibility was determined based on presence of ASD diagnosis through consensus diagnosis described above. The presence of comorbid psychiatric and medical (e.g., seizures, cerebral visual impairment) conditions were carefully assessed in all participants during clinical interview, but were not exclusionary. For the typically developing group, exclusion criteria included history of ASD or developmental disorders in the self or family members, as determined by intake.

Measures

Gold-Standard Assessments. For single-locus and iASD groups, ASD diagnosis was assessed using the Autism Diagnostic Observation Schedule, Second Edition (ADOS-2) (Lord et al., 2012), Autism Diagnostic Interview-Revised (ADI-R) (Lord et al., 1994), and DSM-5 criteria (American Psychiatric Association, 2013). Cognitive functioning was assessed using the Mullen Scales of Early Learning (Mullen, 1995), the Differential Ability Scales, 2nd Edition (DAS-II) (Elliott, 2007), the Wechsler Intelligence Scale for Children, Fifth Edition (WISC-V) (Wechsler, 2014), the Wechsler Abbreviated Intelligence Scale, Second Edition (WASI-II) (Wechsler, 2011), the Wechsler Preschool and Primary Scale of Intelligence, Fourth Edition (WPPSI-IV) (Wechsler, 2012), or the Stanford Binet Intelligence Scales, Fifth Edition (SB-5) (Roid, 2003). Adaptive functioning was assessed using the

Vineland Adaptive Behavior Scales, Survey Interview, Second Edition (Sparrow et al., 2005) or Third Edition (Sparrow et al., 2016).

VEP Recording. A Neucodia system (Verisci Corp., USA) was used for data collection. Three electrodes were placed on the midline of the scalp based on the International 10-20 system, with the active electrode over the occipital cortex (Oz), the reference electrode at the vertex (Cz), and the ground electrode over the parietal cortex (Pz) (Klem, Lüders, Jasper, & Elger, 1999). Gaze fixation was monitored using built-in eye tracking. Behavioral supports (e.g., visual schedule, 1:1 research assistant support) were utilized as needed. All EEGs were recorded synchronized to the display frame rate. The raw EEG was amplified with a gain of 20,000, filtered with a bandpass of 0.5 to 100 Hz, and digitized at four samples per frame (600 samples per second). The Neucodia system provided automated noise detection in the EEG recording for 60 Hz noise, drift, or saturation, and automatically rejected EEG epochs with artifacts (e.g., potential spikes or drifts). The Neucodia system's multivariate outlier analysis detected and rejected extreme values in a set of responses relative to other responses, based on a statistical significance criterion value of .05. If artifacts or outliers are detected and then deleted, the examiner is prompted to repeat the run until 10 valid runs are collected.

VEP Stimulus Conditions. The stimuli were presented using a cathode-ray tube (CRT) display with stimulus field size subtending a 10° x 10° of visual angle. Background luminance was ~50 cd/m^2. Contrast-reversing checkerboards (a standard 61-s condition, with 60-s of EEG epoch and 1-s of adaptation, and a short-duration, 10 3-s run condition, with ~1-s adaption and 2-s EEG epoch), consisting of 32 x 32 checks that are contrast-reversed with a

1 Hz square-wave modulation (100% contrast) to elicit a transient VEP (tVEP; Figure 1) were used.

Procedures

Three surface electrodes were placed on the scalp using water-soluble electrode paste. Participants sat in a comfortable chair at a viewing distance of 114 cm in a dimly lit room. Participants were instructed to fixate on a crosshair at the center of the display screen. Fixation was closely monitored using an infrared camera. A research coordinator was also present to aid with behavior management and ensure gaze fixation. Parents were occasionally present during the procedure, and participants occasionally sat on their parent's lap. Participants were tested binocularly for both conditions.

Statistical Analyses

For each participant, the vector-mean of 10 runs for the short-duration condition was used for analysis. To extract harmonic frequency components of the response, a discrete Fourier transform was applied to EEG data. Waveforms were reconstructed using even harmonics 2-84 Hz (minus the 60 Hz component). For tVEPs, amplitudes (μV) were measured peak-to-trough (P_{60}-N_{75}, N_{75}-P_{100}) and latency (ms) was measured by time to peak (P_{60}, N_{75}, P_{100}). Frequency domain analyses were conducted using power and a magnitude-squared coherence (MSC) statistic (Zemon & Gordon, 2018; Zemon et al., 2009). MSC measures the ratio of signal power to signal-plus-noise power for a given frequency component of a response. A pure signal (response) produces a value of 1 and no signal (noise) produces a value of 0.1 (bias level); therefore, higher MSC values reflect stronger and more consistent (coherent) activity for a given frequency band (Zemon & Gordon, 2018; Zemon et al., 2009). Four distinct frequency bands were assessed: Band 1, 6–12 Hz; Band 2,

14–28 Hz; Band 3, 30–40 Hz; Band 4, 42–48 Hz (Zemon & Gordon, 2018). These bands were obtained using principal components analysis and represent distinct neural mechanisms. Power bands (μV^2/band) were obtained by calculating the squared vector-mean amplitude for each frequency component of a given MSC band and summing those values, yielding four discrete power bands; Power Band 3 serves as an objective measure of excitatory input to the cortex (Zemon & Gordon, 2018). Intraclass correlation coefficients (ICC) were analyzed to test for agreement between short and standard stimulus conditions.

SPSS version 26 was used for all statistical analyses. Demographic comparisons for sex and age were analyzed using chi-square and between-groups ANOVAs, respectively. Linear mixed effects models (LMM) were used to determine if data were correlated within an individual using intraclass correlation coefficients (ICC), and to examine group differences in each critical tVEP measure for both standard and short-duration stimulus conditions: amplitude, latency, MSC, and the square root of power. As stated in Study 1, LMM facilitates the analysis of multiple data points within an individual participant. LMM also concurrently models discrete and continuous variables, as well as the covariance structure, which allows for violations of homogeneity of variance and sphericity.

In the LMMs of these data, participants were treated as a random effect to assess the variance components and within- and between-groups differences using intraclass correlation coefficients (ICCs). ICCs greater than .05 indicated that there is significant correlation of data within an individual, thus necessitating modeling of the covariance structure of the data and use of LMM. Model 1, the null model, only participant was treated as a random effect, without any fixed effects. In Model 2, group was added to the model as a fixed effect. In Model 3, stimulus condition type (i.e., standard or short condition) was added to the model as

a fixed effect. In Model 4 for the LMM of amplitude, peak to trough measurements of amplitude (i.e., P_{60}-$N_{75,}$ N_{75}-P_{100}) were added as a fixed effect. In Model 4 for the LMM of latency, time to peak measurements were added as a fixed effect. In Model 4 for the LMMs for MSC and power (square root of power), band number (i.e., Band 1, 2, 3, 4) was added as a fixed effect. In Model 5 for all LMMs, two- and three-way interactions were added to the model as fixed effects. Improvements between models was assessed using the difference in -2 log likelihood (-2LL) between models, with chi-square degrees of freedom equal to the difference in parameters between models. Larger decreases in -2LL values (or smaller -2LL values) are indicative of improvements to the model. Post hoc *t*-tests were used when LMM revealed significant main effects and interactions.

To explore the relationship between behavioral measures of sensory reactivity and the electrophysiological measures (Exploratory Aim), Pearson *r* correlations were conducted for children who participated in both Study 1 and Study 2 (i.e., completed both the tVEP and SAND).

Chapter III: Results

Study 1

Group Demographics

Results from one-way ANOVA indicated no significant difference between groups for age, $F(4,135) = .62$, $p = .65$. Results from chi-square analyses indicated a significant difference between groups for sex, $\chi^2(4, N = 140) = 21.68$, $p < .001$, $\phi = .394$. The iASD group was comprised of significantly more males than females, the ADNP group was comprised of more males than females, and the FOXP1 group was comprised of significantly more females than males. This unequal sex distribution in the iASD sample is representative of the higher male-to-female sex-ratio in the general population of those with ASD, in which the male-to-female ratio is ~4:1 (Baio, 2012; Blumberg et al., 2013; Christensen et al., 2016; Fombonne, 2009). See Table 1 for additional demographic information. Verbal and nonverbal IQ data were missing from one child in the TD group, one child in the iASD group, and one child in the PMS group. Vineland Adaptive Behavior Scale Adaptive Behavior Composite scores were missing from eight children in the iASD group and six children in the PMS group. ADOS-2 total scores were missing from two children in the iASD group and one child in the PMS group, and ADOS-2 comparison scores were missing for four children in the iASD group, one child in the FOXP1 group, and three children in the PMS group. ADI-R scores were missing from 11 children in the iASD group, two children in the ADNP group, one child in the FOXP1 group, and five children in the PMS group.

SAND: TD, iASD, and ADNP groups

Group statistics are displayed in Table 2. A one-way between-groups analysis of variance (ANOVA) was conducted to explore group differences in SAND total score between TD, iASD, and ADNP groups (see Figure 2). Groups differed significantly on SAND total scores, $F(2, 92) = 76.61$, $p < .001$. Post hoc comparisons using Bonferroni correction and visual inspection of Figure 2 indicated that the TD group exhibited lower scores, and therefore fewer sensory symptoms, on the SAND as a whole as compared to iASD and ADNP groups (p's < .001). There were no significant differences between iASD and ADNP groups on SAND total score ($p = .07$).

A series of multivariate analyses of variance (MANOVAs) were used to assess diagnostic group differences in SAND measures among TD, iASD, ADNP groups, separately for sensory subtype (i.e., hyperreactivity, hyporeactivity, sensory seeking), sensory domain (i.e., visual, auditory, tactile), and combined domain and subtype (visual hyperreactivity, visual hyporeactivity, visual sensory seeking, auditory hyperreactivity, auditory hyporeactivity, auditory sensory seeking, tactile hyperactivity, tactile hyporeactivity, and tactile sensory seeking). There were no significant effects of age or sex on any variables, and therefore they were not included as covariates in subsequent analyses.

Sensory Subtype. Visual inspection of 95% CIs in Figure 3 indicates that the TD group exhibits fewer hyperreactivity, hyporeactivity, and sensory seeking scores than iASD and ADNP groups; additionally, iASD and ADNP groups exhibit similar scores for hyperreactivity and hyporeactivity, but the ADNP group exhibits more sensory seeking behaviors than TD and iASD groups. There was a significant multivariate difference among groups for sensory subtype, $F(6, 182) = 16.07$, $p < .001$, Pillai's trace $V = .693$. Post hoc

univariate analyses demonstrated an effect for group for hyperreactivity, $F(2, 92) = 14.05$, $p < .001$, hyporeactivity, $F(2, 92) = 15.27$, $p < .001$, and sensory seeking, $F(2, 92) = 49.23$, $p < .001$, subscales.

The MANOVA was followed up with a discriminant analysis, which revealed two distinct discriminant functions. The first explained 93.6% of the variance, canonical $R = .77$, and the second explained only 6.4% of the variance, canonical $R = .31$. In combination, these discriminant functions significant differentiated groups, Wilk's Lambda $\Lambda = .36$, $\chi^2(6) = 92.15$, $p < .001$. Removing the first function, the second function still significantly differentiated groups, Wilk's Lambda $\Lambda = .91$, $\chi^2(2) = 8.89$, $p = .012$. Correlations between outcomes and the discriminant functions revealed that sensory seeking loaded highly onto the first function ($r = .83$); hyporeactivity ($r = .47$) and hyperreactivity ($r = .40$) loaded moderately. Hyperreactivity loaded highly onto the second function ($r = .84$); seeking loaded moderately onto this function ($r = -.54$). The discriminant function plot (Figure 6) showed that the first function discriminated between TD, iASD, and ADNP groups, and the second function differentiated the ADNP group from the iASD and TD groups. See Appendix A for structure matrix and functions at group centroids. Thus, this analysis indicates that sensory seeking significantly differentiates all three groups, whereas hyperreactivity is important for differentiating the iASD group from ADNP and TD groups. Overall, 77.9% of the original grouped cases were correctly classified using these two functions: 100% of the TD cases and 80% of the iASD were correctly classified, but only 37.5% of ADNP cases were correctly classified. This result indicates that these functions are best at classifying the TD children, but they slightly more errors when classifying iASD children. The functions incorrectly classified 56.3% ADNP children into the iASD group.

Sensory Domain. Visual inspection of 95% CIs in Figure 4 indicate that the TD group exhibits lower SAND scores across visual, tactile, and auditory domains than iASD and ADNP groups; additionally, while iASD and ADNP groups do not differ in visual and auditory symptoms, the ADNP group exhibits more tactile symptoms than the iASD group. A significant multivariate difference among TD, iASD, and ADNP groups was observed for sensory domain, $F(6, 182) = 21.61$, $p < .001$, Pillai's trace $V = .832$. Post hoc univariate analyses demonstrated an effect for group for visual, $F(2, 92) = 39.64$, $p < .001$, auditory, $F(2, 92) = 30.76$, $p < .001$, and tactile domain, $F(2, 92) = 57.32$, $p < .001$, subscales.

The MANOVA was followed up with a discriminant analysis, which revealed two distinct discriminant functions. The first explained 84.0% of the variance, canonical $R = .78$, whereas the second explained only 16.0% of the variance, canonical $R = .48$. In combination, these discriminant functions significantly differentiated between groups, Wilk's Lambda $\Lambda = .31$, $\chi^2(6) = 108.01$, $p < .001$. Removing the first function, the second function still significantly differentiated between groups, Wilk's Lambda $\Lambda = .77$, $\chi^2(2) = 23.36$, $p < .001$. Correlations between outcomes and the discriminant functions revealed that tactile ($r = .88$), visual ($r = .73$) and auditory symptoms ($r = .62$) loaded moderately to highly onto the first function; whereas tactile ($r = -.40$), visual ($r = .38$) and auditory symptoms ($r = .55$) loaded moderately onto the second function. The discriminant function plot (Figure 7) showed that both the first and second functions discriminated between TD, iASD, and ADNP groups. See Appendix A for structure matrix and functions at group centroids. Overall, 82.1% of the original grouped cases were correctly classified using these two functions; 100% of the TD cases, 81.8% of the iASD cases, and 56.3% of ADNP cases were correctly classified.

Sensory Domain and Subtype. Visual inspection of 95% CIs in Figure 5 indicate that the TD group exhibits lower SAND scores on all nine subscales when compared to iASD and ADNP groups; moreover, the ADNP group demonstrates more sensory symptoms than the iASD group on tactile hyporeactivity, tactile seeking, and auditory seeking, and the iASD group demonstrates more sensory symptoms than the ADNP group in auditory hyperreactivity. When assessing measures of combined sensory domain and subtype, there was a significant multivariate difference among TD, iASD, and ADNP groups, $F(18, 170) = 13.18$, $p < .001$, Pillai's trace $V = 1.165$. Post hoc univariate analyses demonstrated an effect for group for visual sensory seeking, $F(2, 92) = 28.25$, $p < .001$, visual hyporeactivity, $F(2, 92) = 12.88$, $p < .001$, tactile hyperreactivity, $F(2, 92) = 3.39$, $p = .04$, tactile hyporeactivity, $F(2, 92) = 27.11$, $p < .001$, tactile sensory seeking ($F(2, 92) = 34.45$, $p < .001$), auditory hyperreactivity, $F(2, 92) = 26.34$, $p < .001$, and auditory sensory seeking, $F(2, 92) = 25.89$, $p < .001$. A trend was found for visual hyperreactivity, $F(2, 92) = 3.00$, $p = .06$, and no significant difference between groups was observed for auditory hyporeactivity $F(2, 92) = 2.31$, $p = .11$.

The MANOVA was followed up with a discriminant analysis, which revealed two distinct discriminant functions. The first explained 68.5% of the variance, canonical $R = .82$, whereas the second explained 31.5% of the variance, canonical $R = .70$. In combination, these discriminant functions significantly differentiated between groups, Wilk's Lambda $\Lambda = .17$, $\chi^2(18) = 158.26$, $p < .001$. Removing the first function, the second function still significantly differentiated between groups, Wilk's Lambda $\Lambda = .51$, $\chi^2(8) = 59.15$, $p < .001$. Combined sensory and domain measures loaded weakly to moderately onto the first function, with tactile seeking ($r = .59$) loading the strongest, followed by visual seeking ($r = .52$), tactile

hyporeactivity (r = .52), and auditory seeking (r = .51). Outcome variables loaded weakly to moderately onto the second function, with auditory hyperreactivity (r = .61) loading strongest. See Table 3 for the structure matrix with all variable loadings. The discriminant function plot (Figure 8) showed that both the first and second functions discriminated between TD, iASD, and ADNP groups. See Appendix A for functions at group centroids. Overall, 88.4% of the original grouped cases were correctly classified using these two functions; 100% of the TD cases, 85.5% of the iASD cases, and 81.3% of ADNP cases were correctly classified. This suggests that these combined sensory subtype and domain variables best predicted group membership when comparing TD, iASD, and ADNP groups; moreover, tactile seeking, visual seeking, auditory seeking, auditory hyperreactivity and tactile hyporeactivity most strongly discriminating among groups.

Short Sensory Profile: TD, iASD, and ADNP groups

Of the children who completed the SAND, a total of 82 children had a parent-completed Short Sensory Profile (SSP): 22 TD, 44 iASD, and 16 ADNP children. Group statistics are displayed in Table 2. A MANOVA was used to assess diagnostic group differences on subscales of the SSP. There was a significant multivariate difference among groups, $F(14, 148) = 8.63$, $p < .001$, Pillai's trace $V = .90$. Post hoc univariate analyses demonstrated an effect for group on all subscales of the SSP: Tactile Sensitivity, $F(2, 79) = 6.94$, $p = .002$, Taste/Smell Sensitivity, $F(2, 79) = 9.13$, $p < .001$, Movement Sensitivity, $F(2, 79) = 6.27$, $p = .003$, Underresponsive/Seeks Sensation, $F(2, 79) = 45.97$, $p < .001$, Auditory Filtering, $F(2, 79) = 34.36$, $p < .001$, Low Energy/Weak, $F(2, 79) = 19.18$, $p < .001$, and Visual/Auditory Sensitivity, $F(2, 79) = 18.85$, $p < .001$.

Post hoc pairwise comparisons using Bonferroni correction revealed that the iASD group had lower scores on the SSP, indicative of more sensory reactivity symptoms, than the TD group on Tactile Sensitivity ($p = .004$), Taste/Smell Sensitivity ($p < .001$), Underresponsive/Seeks Sensation ($p < .001$), Auditory Filtering ($p < .001$), Low Energy/Weak ($p < .001$), and Visual/Auditory Sensitivity ($p < .001$). There was no significant difference between iASD and TD groups on the Movement Sensitivity subscale ($p = .12$). The ADNP group similarly exhibited significantly lower scores than the TD group on Tactile Sensitivity ($p = .007$), Underresponsive/Seeks Sensation ($p < .001$), Auditory Filtering ($p < .001$), Low Energy/Weak ($p < .001$), Visual/Auditory Sensitivity ($p < .001$), and Movement Sensitivity ($p = .002$), and a trend towards lower scores on Taste/Smell Sensitivity ($p = .06$). The iASD and ADNP group had similar sensory reactivity symptoms on the Tactile Sensitivity ($p = 1.00$), Taste/Smell Sensitivity ($p = .75$), Movement Sensitivity ($p = .12$), Auditory Filtering ($p = .68$) and Visual/Auditory Sensitivity ($p = 1.00$) subscales. In contrast, the ADNP group exhibited significantly lower scores than the iASD group on the Low Energy/Weak ($p = .04$) subscale, indicative of greater sensory hyporeactivity. Consistent with SAND results, the ADNP group also exhibited significantly lower scores, and therefore more sensory seeking behaviors, on the Underresponsive/Seeks Sensation ($p < .001$) subscale when compared to the iASD group.

SAND: TD, iASD, and FOXP1 groups

Group statistics for the SAND are displayed in Table 2. A one-way between-groups ANOVA was conducted to explore group differences in SAND total score between TD, iASD, and FOXP1 groups (see Figure 2). Groups differed significantly on SAND total scores, $F(2, 91) = 62.51$, $p < .001$. Post hoc comparisons using Bonferroni correction

indicated that the TD group exhibited lower scores, and therefore fewer sensory symptoms, on the SAND as a whole as compared to iASD and FOXP1 groups (p's < .001). There were no significant differences between iASD and FOXP1 groups on the SAND total scores (p = 1.00).

A series of MANOVAs were used to assess group differences in SAND measures among TD, iASD, and FOXP1 groups, separately for sensory subtype (i.e., hyperreactivity, hyporeactivity, sensory seeking), sensory domain (i.e., visual, auditory, tactile), and combined domain and subtype (visual hyperreactivity, visual hyporeactivity, visual sensory seeking, auditory hyperreactivity, auditory hyporeactivity, auditory sensory seeking, tactile hyperactivity, tactile hyporeactivity, and tactile sensory seeking). There were no significant effects of age or sex on any variables, and therefore they were not included as covariates in subsequent analyses.

Sensory Subtype. Visual inspection of 95% CIs in Figure 3 indicate that the TD group exhibits lower SAND scores than iASD and FOXP1 groups for hyperreactivity, hyporeactivity, and sensory seeking; in addition, the iASD and FOXP1 groups exhibit similar scores for all sensory subtypes. There was a significant multivariate difference among TD, iASD, and FOXP1 groups for sensory subtype, $F(6, 180) = 13.44$, p <.001, Pillai's trace V = .62. Post hoc univariate analyses demonstrated an effect for group for hyperreactivity, $F(2, 91) = 14.06$, $p < .001$, hyporeactivity, $F(2, 91) = 11.60$, $p < .001$, and sensory seeking, $F(2, 91) = 38.66$, $p < .001$, subscales.

The MANOVA was followed up with a discriminant analysis, which revealed two distinct discriminant functions. The first explained 95.2% of the variance, canonical R = .75, whereas the second explained only 4.8% of the variance, canonical R = .24. In combination,

these discriminant functions significant differentiated between groups, Wilk's Lambda Λ = .42, $\chi^2(6) = 79.23$, $p < .001$. Removing the first function, the second function did not significantly differentiate between groups, Wilk's Lambda $\Lambda = .94$, $\chi^2(2) = 5.54$, $p = .063$. Correlations between outcomes and the discriminant functions revealed that sensory seeking ($r = .81$) and hyporeactivity ($r = .44$) loaded strongest onto the first function, and hyperreactivity loaded most strongly and moderately onto the second function ($r = .70$). The discriminant function plot (Figure 9) revealed that the first function clearly discriminated the TD group from the iASD and FOXP1 groups; the second function slightly differentiates the iASD group and FOXP1 group. See Appendix A for the structure matrix and functions at group centroids. Overall, 77.7% of the original grouped cases were correctly classified using these two functions; 100% of the TD cases and 85.5% of the iASD cases, but only 13.3% of FOXP1 cases were correctly classified. Importantly, 80.0% of the FOXP1 cases were incorrectly classified as iASD cases. This result indicates that these functions are best at classifying the TD children, but they have significantly greater difficulty differentiating the FOXP1 children from the iASD children.

Sensory Domain. Visual inspection of 95% CIs in Figure 4 indicate that the iASD and FOXP1 group exhibit significantly higher scores on the SAND across sensory domains when compared to the TD group, but iASD and FOXP1 groups do not appear to differ largely from one another across sensory domains. The MANOVA revealed significant multivariate difference among TD, iASD, and FOXP1 groups for sensory domain, $F(6, 180) = 12.93$, $p < .001$, Pillai's trace $V = .60$. Post hoc univariate analyses demonstrated an effect for group for visual, $F(2, 91) = 34.59$, $p < .001$, auditory, $F(2, 91) = 33.38$, $p < .001$, and tactile, $F(2, 91) = 32.46$, $p < .001$, domain subscales.

The MANOVA was followed up with a discriminant analysis, which revealed two distinct discriminant functions. The first explained 95.3% of the variance, canonical $R = .74$, whereas the second explained only 4.7% of the variance, canonical $R = .24$. In combination, these discriminant functions significantly differentiated between groups, Wilk's Lambda $\Lambda = .43$, $\chi^2(6) = 76.28$, $p < .001$. Removing the first function, the second function did not significantly differentiate between groups, Wilk's Lambda $\Lambda = .94$, $\chi^2(2) = 5.22$, $p = .07$. Correlations between outcomes and the discriminant functions revealed that sensory domain strongly loaded onto the first function, with visual symptoms loading strongest ($r = .79$), followed by auditory ($r = .78$) and tactile symptoms ($r = .76$). These outcome variables had weak to moderate correlations with the second function, with tactile symptoms loading strongest ($r = .65$), but not as strongly as it did onto the first function. The discriminant function plot (Figure 10) showed that the first function discriminated the TD group from the iASD and FOXP1 groups; neither function appeared to clearly differentiate the iASD group and FOXP1 group from one another. See Appendix A for the structure matrix and functions at group centroids. Overall, 80.9% of the original grouped cases were correctly classified using these two functions; 100% of the TD cases, 92.7% of the iASD cases, and 6.7% of the FOXP1 cases were correctly classified. Importantly, 86.7% of the FOXP1 cases were classified as iASD cases.

Sensory Domain and Subtype. Visual inspection of 95% CIs in Figure 5 indicate that the iASD and FOXP1 groups exhibit higher SAND scores than the TD group for visual hyporeactivity, visual seeking, tactile hyporeactivity, tactile seeking, auditory hyperreactivity, and auditory seeking. The iASD group also exhibits higher SAND scores than the TD group for visual hyperreactivity. FOXP1 and iASD groups display overlapping

CIs for all SAND subscales of combined sensory domain and subtype. The MANOVA revealed a significant multivariate difference among TD, iASD, and FOXP1 groups for combined measures of sensory subtype and domain, $F(18, 168) = 6.11$, $p < .001$, Pillai's trace $V = .79$. Post hoc univariate analyses demonstrated an effect for group for visual hyperreactivity, $F(2, 91) = 3.82$, $p = .03$, visual hyporeactivity, $F(2, 91) = 11.02$, $p < .001$, visual sensory seeking, $F(2, 91) = 26.33$, $p < .001$, tactile hyporeactivity, $F(2, 91) = 12.14$, $p < .001$, tactile seeking, $F(2, 91) = 23.40$, $p < .001$, auditory hyperreactvity, $F(2, 91) = 24.58$, $p < .001$, and auditory sensory seeking, $F(2, 91) = 17.50$, $p < .001$. No significant differences were seen between groups for measures of auditory hyporeactivity, $F(2, 91) = 1.70$, $p = .17$, and tactile hyperreactivity, $F(2, 91) = 2.79$, $p = .08$.

The MANOVA was followed up with a discriminant analysis, which revealed two distinct discriminant functions. The first explained 92.3% of the variance, canonical $R = .81$, whereas the second explained only 7.7% of the variance, canonical $R = .37$. In combination, these discriminant functions significantly differentiated between groups, Wilk's Lambda $\Lambda = .30$, $\chi^2(18) = 105.20$, $p < .001$. Removing the first function, the second function did not significantly differentiate between groups, Wilk's Lambda $\Lambda = .87$, $\chi^2(8) = 12.79$, $p = .12$. Correlations between outcomes and the discriminant functions revealed weak to moderate correlations, with visual seeking loading strongest onto the first function ($r = .55$), followed by auditory hyperreactivity ($r = .52$), and auditory seeking ($r = .44$). Visual hyperreactivity ($r = .49$) loaded strongest onto the second function ($r = .44$), followed by auditory hyporeactivity ($r = .40$). The discriminant function plot (Figure 11) showed that the first function clearly discriminated the TD group from the iASD and FOXP1 groups, and the section function slightly discriminated the FOXP1 group from the iASD and TD groups. See

Appendix A for the structure matrix and functions at group centroids. Overall, 83.0% of the original grouped cases were correctly classified using these two functions; 100% of the TD cases and 87.3% of the iASD cases were correctly classified, but only 40.0% of the FOXP1 cases were correctly classified. Instead, 60.0% of the FOXP1 cases were classified as iASD.

Short Sensory Profile: TD, iASD, and FOXP1 groups

Of the children who completed the SAND, a total of 79 children had a parent-completed Short Sensory Profile (SSP): 22 TD children, 44 with iASD, and 13 with FOXP1. Group statistics are displayed in Table 2. Results from the MANOVA indicated a significant difference among TD, iASD, and FOXP1 groups on the SSP, $F(14, 142) = 7.28$, $p < .001$, Pillai's Trace $V = .84$. Post hoc univariate analyses demonstrated an effect of group for Tactile Sensitivity, $F(2, 76) = 10.82$, $p < .001$, Taste/Smell Sensitivity, $F(2, 76) = 10.74$, $p < .001$, Underresponsive/Seeks Sensation, $F(2, 76) = 38.84$, $p < .001$, Auditory Filtering, $F(2, 76) = 33.24$, $p < .001$, Low Energy/Weak, $F(2, 76) = 10.83$, $p < .001$, and Visual/Auditory Sensitivity, $F(2, 76) = 16.55$, $p < .001$. There were no significant differences between groups on the Movement Sensitivity subscale, $F(2, 76) = 2.68$, $p = .08$.

Post hoc analyses using Bonferroni correction indicate that the TD group exhibited higher scores, and therefore fewer sensory symptoms, than the iASD and FOXP1 group on the Tactile Sensitivity ($p = .005$, $p < .001$, respectively), Underresponsive/Seeks Sensation (p's $< .001$), Auditory Filtering (p's $< .001$), Low Energy/Weak ($p < .001$, $p = .002$, respectively), and Visual/Auditory Sensitivity (p's $< .001$) subscales. The TD group also exhibited lower scores on the Taste/Smell Sensitivity subscale than the iASD group ($p < .001$), but not the FOXP1 group ($p = .39$). The FOXP1 group did not exhibit significantly different scores than the iASD group for any SSP subscales (p's $> .08$).

SAND: TD, iASD, and PMS groups

Group statistics for the SAND are displayed in Table 2. A one-way between-groups ANOVA was conducted to explore diagnostic group differences in SAND total scores between TD, iASD, and PMS groups (see Figure 2). Groups differed significantly on SAND total scores, $F(2, 106) = 57.26$, $p < .001$. Post hoc comparisons using Bonferroni correction indicated that the TD group exhibited lower scores, and therefore fewer sensory symptoms, on the SAND as a whole as compared to iASD and PMS groups (p's < .001). There were no significant differences between iASD and PMS groups on the SAND total scores ($p = 1.00$).

A series of MANOVAs were used to assess group differences in SAND measures among TD, iASD, and PMS groups, separately for sensory subtype (i.e., hyperreactivity, hyporeactivity, sensory seeking), sensory domain (i.e., visual, auditory, tactile), and combined domain and subtype (visual hyperreactivity, visual hyporeactivity, visual sensory seeking, auditory hyperreactivity, auditory hyporeactivity, auditory sensory seeking, tactile hyperactivity, tactile hyporeactivity, and tactile sensory seeking). There were no significant effects of age or sex on any variables, and therefore they were not included as covariates in subsequent analyses.

Sensory Subtype. Visual inspection of 95% CIs in Figure 3 indicate that the iASD group exhibits greater hyperreactivity scores than the TD and PMS groups; in addition, the iASD and PMS groups exhibit greater hyporeactivity and seeking scores than the TD group, with the PMS group also exhibiting higher scores than the iASD group for hyporeactivity on the SAND. Results from one MANOVA revealed a significant multivariate difference among TD, iASD, and PMS groups for sensory subtype, $F(6, 210) = 35.96$, $p < .001$, Pillai's trace $V = 1.01$. Post hoc univariate analyses demonstrated an effect for group for hyperreactivity,

$F(2, 106) = 19.42$, $p < .001$, hyporeactvity, $F(2, 106) = 55.58$, $p < .001$, and sensory seeking subscales, $F(2, 106) = 33.52$, $p < .001$.

The MANOVA was followed up with a discriminant analysis, which revealed two distinct discriminant functions. The first explained 53.5% of the variance, canonical $R = .72$, and the second explained 46.5% of the variance, canonical $R = .70$. In combination, these discriminant functions significantly differentiated between groups, Wilk's Lambda $\Lambda = .24$, $\chi^2(6) = 148.57$, $p < .001$. Removing the first function, the second function still significantly differentiated between groups, Wilk's Lambda $\Lambda = .51$, $\chi^2(2) = 70.50$, $p < .001$. Correlations between outcomes and the discriminant functions revealed that hyporeactivity loaded highly onto the first function ($r = .80$); sensory seeking ($r = -.30$) and hyperreactivity ($r = -.38$) loaded moderately. Seeking loaded highly onto the second function ($r = .75$), followed by hyporeactivity ($r = .60$) and hyperreactivity ($r = .47$). The discriminant function plot (Figure 12) showed that the first function, predominantly hyporeactivity, significantly differentiated the PMS group from the TD and iASD groups, and the second function, which was predominantly sensory seeking, significantly differentiated the TD group from the iASD and PMS groups. See Appendix A for the structure matrix and functions at group centroids. Overall, 84.4% of the original grouped cases were correctly classified using these two functions; 100% of the TD cases, 80.0% of the iASD cases, and 80.0% of the PMS cases were correctly classified.

Sensory Domain. Visual inspection of 95% CIs in Figure 4 indicate that the iASD and PMS groups exhibit similar scores on the SAND for all sensory domains, and both groups exhibit higher scores than the TD group across domains. A significant multivariate difference among TD, iASD, and PMS groups was found for sensory domain, $F(6, 210) =$

12.26, p <.001 , Pillai's trace V = .52. Post hoc univariate analyses demonstrated an effect for group for visual, $F(2, 106) = 35.14$, $p < .001$, auditory, ($F(2, 106) = 30.65$, $p < .001$, and tactile domain subscales, $F(2, 106) = 30.08$, $p < .001$.

The MANOVA was followed up with a discriminant analysis, which revealed two distinct discriminant functions. The first function explained 97.3% of the variance, canonical $R = .70$, and the second explained only 2.7% of the variance, canonical $R = .16$. In combination, these two discriminant functions significantly differentiated between groups, Wilk's Lambda $\Lambda = .49$, $\chi^2(6) = 74.08$, $p < .001$. Removing the first function, the second function was no longer significant, Wilk's Lambda $\Lambda = .97$, $\chi^2(2) = 2.76$, $p = .25$. Correlations between outcomes and the discriminant functions revealed strong correlations between all sensory domain outcome measures and the first function, the strongest of which was visual symptoms ($r = .82$), followed by auditory ($r = .77$) and tactile symptoms ($r = .76$). Sensory domain measures only moderately loaded onto the second function, with tactile symptoms loading strongest ($r = .64$), followed by visual ($r = -.39$) and auditory symptoms ($r = -.12$). The discriminant function plot (Figure 13) showed that the first function differentiated TD groups from the PMS and ASD groups. See Appendix A for the structure matrix and functions at group centroids. Overall, 71.6% of the original grouped cases were correctly classified using these two functions; 100% of the TD cases and 92.7% of the iASD cases; however, only 10.0% of the PMS cases were correctly classified.

Sensory Domain and Subtype. Visual inspection of 95% CIs in Figure 5 indicates that the iASD and PMS group exhibit higher scores, indicative of more sensory reactivity symptoms, than the TD group for SAND measures of visual hyperreactivity, visual hyporeactivity, tactile hyporeactivity, auditory hyporeactivity, and auditory seeking. The

iASD group exhibits higher scores than both PMS and TD groups for visual seeking, tactile hyperreactivity, auditory hyperreactivity. The PMS group exhibits higher scores than both iASD and TD groups for visual, tactile, and auditory hyporeactivity. A MANOVA assessing combined measures of sensory subtype in each domain revealed a significant multivariate difference among groups, $F(18, 198) = 14.50$, $p < .001$, Pillai's trace $V = 1.14$. Post hoc univariate analyses demonstrated an effect for group for visual hyperreactivity, $F(2, 106) = 3.25$, $p = .043$, visual hyporeactivity, $F(2, 106) = 43.25$, $p < .001$, visual sensory seeking, $F(2, 106) = 37.57$, $p < .001$, tactile hyperreactivity, $F(2, 106) = 4.42$, $p = .01$, tactile hyporeactivity, $F(2, 106) = 28.85$, $p < .001$, tactile sensory seeking, $F(2, 106) = 16.31$, $p < .001$, auditory hyperreactivity, $F(2, 106) = 32.51$, $p < .001$, auditory hyporeactivity, $F(2, 106) = 36.75$, $p < .001$, and auditory sensory seeking, $F(2, 106) = 13.69$, $p < .001$.

Post hoc discriminant analysis revealed two distinct discriminant functions. The first function explained 57.8% of the variance of the sample, canonical $R = .78$, and the second explained 42.2% of the variance, canonical $R = .73$. When combined, these two discriminant functions significantly differentiated between groups, Wilk's Lambda $\Lambda = .19$, $\chi^2(18) = 173.35$, $p < .001$. Removing the first function, the second function remained significant, Wilk's Lambda $\Lambda = .47$, $\chi^2(8) = 77.09$, $p < .001$. Correlations between outcomes and the discriminant functions revealed weak to moderate loadings onto the first function, with visual seeking symptoms loading strongest ($r = .68$), followed by auditory hyperreactivity ($r = .63$) and auditory seeking ($r = .39$). Weak to strong correlations were observed between outcome measures and the second function, with visual hyporeactivity loading strongest ($r = .85$), followed by auditory hyporeactivity ($r = .72$) and tactile hyporeactivity ($r = .69$). Analysis of the discriminant function plot (Figure 14) revealed that the first and second functions

discriminated all three groups from each other. See Appendix A for the structure matrix and functions at group centroids. Overall, 85.3% of the original grouped cases were correctly classified using these two functions; 100% of the TD cases, 85.5% of the iASD cases, and 73.3% of the PMS cases were correctly classified. These results suggest that visual, auditory, and tactile hyporeactivity symptoms are among the strongest to differentiate between all three groups, whereas visual and auditory seeking symptoms and auditory hyperreactivity symptoms best differentiate the iASD group from other groups.

Short Sensory Profile: TD, iASD, and PMS groups

Group differences on the Short Sensory Profile were not analyzed as part of the current study, as they were previously reported in (Mieses et al., 2016).

SAND: TD, iASD, ADNP, FOXP1 and PMS groups

A one-way between-groups ANOVA was conducted to explore group differences in SAND total score between TD, iASD, ADNP, FOXP1, and PMS groups. Groups differed significantly on SAND total score, $F(4, 135) = 32.93$, $p < .001$. Post hoc comparisons using Bonferroni correction indicated that the TD group exhibited lower scores, and therefore fewer sensory symptoms, on the SAND as a whole as compared to iASD, ADNP, FOXP1, and PMS groups (p's < .001). There were no significant differences between iASD and single-locus groups on SAND total scores (ADNP: $p = .38$; FOXP1: $p = 1.00$; PMS, $p = 1.00$). Single-locus groups also did not significantly differ from each other on SAND total score (p's > .22).

A series of MANOVAs were used to assess group differences in SAND measures among TD, iASD, ADNP, FOXP1, and PMS groups, separately for sensory subtype (i.e., hyperreactivity, hyporeactivity, sensory seeking), sensory domain (i.e., visual, auditory,

tactile), and combined domain and subtype (visual hyperreactivity, visual hyporeactivity, visual sensory seeking, auditory hyperreactivity, auditory hyporeactivity, auditory sensory seeking, tactile hyperactivity, tactile hyporeactivity, and tactile sensory seeking). There were no significant effects of age or sex on any variables, and therefore they were not included as covariates in subsequent analyses.

Sensory Subtype. Visual inspection of Figure 3 indicates that the TD group exhibits lower SAND scores for all sensory subtypes when compared to iASD and single-locus groups. The PMS group exhibits higher hyporeactivity scores than all other groups, and the ADNP group exhibits higher sensory seeking scores than iASD and PMS groups, but not than the FOXP1 group. A significant multivariate difference among groups was observed for sensory subtype, $F(12, 405) = 19.19$, $p < .001$, Pillai's trace $V = 1.09$. Post hoc univariate analyses demonstrated an effect for group for hyperreactivity, $F(4, 135) = 10.41$, $p < .001$, hyporeactivity, $F(4, 135) = 30.47$, $p < .001$, and sensory seeking, $F(4, 135) = 29.28$, $p < .001$.

The MANOVA was followed up with a discriminant analysis, which revealed three distinct discriminant functions. The first function explained 56.0% of the variance of the sample, canonical $R = .74$, the second explained 39.8% of the variance, canonical $R = .68$, and the third function explained only 4.2% of the variance, canonical $R = .29$. When combined, these three discriminant functions significantly differentiated between groups, Wilk's Lambda $\Lambda = .23$, $\chi^2(12) = 201.21$, $p < .001$. Removing the first function, the second and third functions remained significant, Wilk's Lambda $\Lambda = .50$, $\chi^2(6) = 94.75$, $p < .001$. When both the first and second functions were removed, the third function still significantly differentiated between groups, Wilk's Lambda $\Lambda = .92$, $\chi^2(2) = 11.55$, $p = .003$. Correlations between outcomes and the discriminant functions revealed sensory seeking loaded strongest

onto the first function (r = .71), and weaker onto the second function (r = .53) and third function (r = -.46). Hyporeactivity loaded strongest onto the second function (r = .92), and less strongly onto the first (r = -.38) and third (r = -.01) functions. Hyperreactivity loaded strongest onto the third function (r = .89), and weaker onto the first (r = .42) and second (r = .17) functions. See Table 4a for the structure matrix and Table 4b functions at group centroids. Visual inspection of the discriminant plots (Figure 15) indicates that that Function 1 (mostly sensory seeking) and Function 2 (mostly hyporeactivity) clearly discriminate the TD group and the PMS group from each other (Function 2), and from the FOXP1, ADNP, and iASD groups (Function 1). Overall, 67.9% of the original grouped cases were correctly classified using these three functions; 95.8% of the TD cases, 72.7% of the iASD cases, 80.0% of the PMS cases, 37.5% of the ADNP cases, and 13.3% of the FOXP1 cases were correctly classified. Results thus indicate that that Function 1 separates PMS from the other iASD and single-locus groups, and Function 2 best separates the TD group from all other groups. Function 3, largely characterized by hyperreactivity, discriminates the iASD group from both ADNP and FOXP1 groups.

Sensory Domain. Visual inspection of Figure 4 indicates that iASD, ADNP, FOXP1, and PMS groups exhibit more sensory symptoms than the TD group for visual, auditory, and tactile domains; additionally, the ADNP group exhibits higher total tactile scores than the other ASD groups. There was a significant multivariate difference among groups for sensory domain, $F(12, 405) = 9.20$, $p < .001$, Pillai's trace $V = .643$. Post hoc univariate analyses demonstrated an effect for group for visual, $F(4, 135) = 17.20$, $p < .001$, tactile, $F(4, 135) = 26.85$, $p < .001$, and auditory domains, $F(4, 135) = 16.57$, $p < .001$.

Post hoc tests with a discriminant analysis revealed three distinct discriminant functions. The first function explained 83.4% of the variance of the sample, canonical R = .70, the second explained 16.3% of the variance, canonical R = .39, and the third function explained only 0.4% of the variance, canonical R = .06. When combined, these three discriminant functions significantly differentiated between groups, Wilk's Lambda Λ = .43, $\chi^2(12) = 112.59$, $p < .001$. Removing the first function, the second and third functions remained significant, Wilk's Lambda Λ = .84, $\chi^2(6) = 23.21$, $p = .001$. When both the first and second functions were removed, the third function did not significantly differentiate between groups, Wilk's Lambda Λ = 1.00, $\chi^2(2) = .53$, $p = .77$. Correlations between outcomes and the discriminant functions revealed that all symptoms in all sensory modalities loaded strongly onto the first function: tactile symptoms loaded strongest (r = .90), followed by visual (r = .72) and auditory symptoms (r = .68). These variables loaded weakly to moderately on the second and third functions. See Table 5a for the structure matrix and Table 5b functions at group centroids. Visual inspection of the discriminant plots (Figure 16) indicates that the first function clearly discriminates the TD group from the iASD and single-locus groups. Overall, only 57.1% of the original grouped cases were correctly classified using these three functions; 100.0% of the TD cases, 83.6% of the iASD cases, 56.3% of the ADNP cases, 0.0% of the FOXP1 cases, and 3.3% of the PMS cases were correctly classified.

Sensory Domain and Subtype. A significant multivariate difference among groups was observed for combined measures of sensory domain and subtype, $F(36, 520) = 8.37$, $p < .001$, Pillai's trace V = 1.47. Post hoc univariate analyses demonstrated an effect for group for visual hyporeactivity, $F(4, 135) = 19.14$, $p < .001$, visual seeking, $F(4, 135) = 19.98$, $p <$

.001, tactile hyperreactivity, $F(4, 135) = 2.89$, $p = .03$, tactile hyporeactivity, $F(4, 135) = 17.45$, $p < .001$, tactile seeking, $F(4, 135) = 19.04$, $p < .001$, auditory hyperreactivity, $F(4, 135) = 17.74$, $p < .001$, auditory hyporeactivity, $F(4, 135) = 26.39$, $p < .001$, and auditory seeking, $F(4, 135) = 16.49$, $p < .001$; but not for visual hyperreactivity, $F(4, 135) = 1.98$, $p = .10$.

The MANOVA was followed up with a discriminant analysis, which revealed four distinct discriminant functions. The first function explained 52.2% of the variance of the sample, canonical $R = .79$, the second explained 29.5% of the variance, canonical $R = .69$, the third function explained 17.5% of the variance, canonical $R = .59$, and the fourth function explained 0.8% of the variance, canonical $R = .15$. When combined, these four discriminant functions significantly differentiated between groups, Wilk's Lambda $\Lambda = .13$, $\chi^2(36) = 272.28$, $p < .001$. Removing the first function, the remaining three functions continued to significantly differentiate between groups, Wilk's Lambda $\Lambda = .33$, $\chi^2(24) = 145.67$, $p < .001$. Removing the first and second functions, the remaining third and fourth functions still significantly differentiated between groups, Wilk's Lambda $\Lambda = .63$, $\chi^2(14) = 60.16$, $p < .001$. After removing the first three functions, the fourth function was no longer significant, Wilk's Lambda $\Lambda = .98$, $\chi^2(6) = 3.19$, $p = .78$. Correlations between outcomes and the discriminant functions revealed that visual seeking loaded strongest and moderately onto the first function ($r = .59$), and auditory seeking ($r = .50$), tactile seeking ($r = .46$), and auditory hyperreactivity ($r = .43$) loaded moderately onto the first function. Visual hyporeactivity ($r = .77$), tactile hyporeactivity ($r = .74$), auditory hyporeactivity ($r = .68$), and tactile seeking ($r = .47$) loaded most strongly and moderately onto the second function. Auditory hyperreactivity loaded strongest and moderately onto the third function ($r = .65$). Visual hyperreactivity ($r =$

.84) and tactile hyperreactivity (r = .52) loaded strongest onto the fourth function. See Table 6a for the structure matrix and Table 6b functions at group centroids. Visual inspection of the discriminant function plot (Figure 17) suggests that the first function, characterized by visual and auditory seeking, most strongly differentiates the TD and PMS group from the iASD, FOXP1, and ADNP groups. The second function, characterized by tactile seeking and visual, auditory, and tactile hyporeactivity, differentiates the PMS and TD groups from each other, but does not clearly distinguish the ADNP, FOXP1, and iASD groups, nor the ADNP group from the PMS group. Function 3, largely auditory hyperreactivity, differentiates the ADNP group from all other groups, particularly the iASD group. Overall, 75.0% of the original grouped cases were correctly classified using these four functions; 100.0% of the TD cases, 76.4% of iASD cases, 81.3% of the ADNP cases, 13.3% of the FOXP1 cases, and 80.0% of the PMS cases were correctly classified.

Linear mixed effects modeling (LMM) with SAND combined domain and subtype scores as the outcome variable were also conducted with group (TD, iASD, ADNP, FOXP1, and PMS) as a fixed effect; estimates of fixed effects are reported in Table 7. In Model 1, with participant as a random intercept and no fixed effects (i.e., null model), the individual accounted for a significant portion of the variance in SAND scores with an ICC of .13, indicating correlated data within individuals. In Model 2, group was added as a fixed effect factor, which significantly improved the model fit (Δ-2LL = 95.34, Δdf = 4, $p < .001$) and was a significant predictor of aggregate SAND scores, $F(4, 140.00) = 34.15$, $p < .001$. Pairwise comparisons indicate that the TD group exhibited significantly lower scores on the SAND than iASD, ADNP, FOXP1, and PMS groups (p's < .001); additionally, the ADNP group exhibited significantly higher scores than the iASD group (p = .03), and the PMS

group exhibited significantly lower scores than the iASD group (p = .02). In Model 3, SAND subscale was added as a fixed factor, which improved the model fit (Δ-2LL = 224.76, Δdf = 8, p < .001), and significantly explained variance in aggregate SAND scores, F(8, 1120.00) = 31.11, p < .001, while group remained significant (p < .001). In Model 4, the two-way interaction of Diagnosis x SAND subscale was added to the model, and significantly improved the model fit (Δ-2LL = 350.30, Δdf = 32, p < .001). Tests of fixed effects indicated that the Group x SAND subscale interaction explained variance in SAND scores, F(32, 1120.00) = 12.85, p < .001, while group and SAND subscale remained significant main effects (p's < .001). Inspection of means and 95% confidence intervals (Figure 5) indicates that the iASD and FOXP1 groups exhibit higher scores on auditory hyperreactivity than the ADNP and TD groups. The PMS group exhibits significantly greater auditory hyporeactivity than all other groups. The ADNP group exhibits significantly greater scores on auditory seeking than TD, iASD, and PMS groups, but not significantly greater than the FOXP1 group. All ASD groups did not significantly differ on tactile hyperreactivity symptoms, but the TD group exhibited the lowest scores. The ADNP and PMS groups exhibited significantly greater tactile hyporeactivity symptoms than the TD and iASD groups; the FOXP1 group only exhibited significantly greater scores than the TD group, but not compared to the other ASD groups. The ADNP group exhibited significantly higher tactile seeking scores than the TD, iASD, and PMS groups, but not than the FOXP1 group. The PMS group exhibited greater tactile seeking scores than the TD group, but not than the iASD group; the PMS group also exhibited lower tactile seeking scores than the FOXP1 group. All groups exhibited similar scores on measures of visual hyperreactivity. While all ASD groups exhibited significantly greater visual hyporeactivity scores than the TD group, the PMS

group exhibited significantly greater scores on this scale than the iASD, ADNP, and FOXP1 groups. The iASD, ADNP, and FOXP1 groups exhibited significantly greater scores on visual seeking than TD and PMS groups, but did not significantly differ from one another.

Study 2

Group Demographics

Results from a one-way ANOVA indicated no significant differences among groups for age, $F(3, 141) = 1.63$, $p = .19$. Results from chi-square analyses indicated a significant difference among groups for sex, $\chi^2(3, N = 145) = 28.32$, $p < .001$). The iASD group was comprised of more males than females, the ADNP group was comprised of more males than females, and the FOXP1 group was comprised of significantly more females than males. As previously mentioned, this unequal sex distribution of our iASD sample is representative of the higher male-to-female sex-ratio in the general population of those with ASD (Baio, 2012; Blumberg et al., 2013; Christensen et al., 2016; Fombonne, 2009). See Table 8 for additional demographic information. Verbal and nonverbal IQ data were missing from twelve children in the TD group and three children in the iASD group. Vineland Adaptive Behavior Scale Adaptive Behavior Composite scores were missing from sixteen children in the iASD group. ADOS-2 scores were missing from five children in the iASD group. Several children in both the FOXP1 and ADNP groups had parent-reported vision problems. In the FOXP1 group, six children had reported vision problems, including amblyopia, strabismus, and esotropia. In the ADNP group, six children had reported vision problems, which included strabismus, amblyopia, and cortical visual impairment.

tVEP Results: Amplitude, Latency, MSC, and Power

The standard condition was successfully obtained from 88.89% of the TD group (*n* = 40), 83.54% of the iASD group (*n* = 66), 66.67% of the ADNP group (*n* = 8), and 100% of the FOXP1 group (*n* = 9), as compared to 95.56% of the TD group (*n* = 43), 93.67% of the iASD group (*n* = 74), 91.67% of the ADNP group (*n* = 11), and 77.78% of the FOXP1 group (*n* = 7) for the short condition. Two participants in the ADNP group did not complete the standard condition. Data for two participants in the ADNP group for the standard condition and two participants in the FOXP1 group for the short condition were removed secondary to non-significant responses, meaning that their mean MSC values did not exceed the critical MSC value for the .05 significance level for any MSC Band, as is standard practice for the Seaver Autism Center VEP studies. Information was not available to discern whether these non-significant responses occurred because of performance/behaviors or organic responses. This therefore could bias results, reducing any changes that may be present between TD and ASD groups, and may not be truly representative of the population. Linear mixed effects modeling (LMM) with amplitude, latency, MSC, and square root of power as the outcome variables were conducted.

ADNP Group Analyses. The tVEP superimposed individual waveforms, MSC data, and power data (herein, power refers to square root of power throughout unless otherwise specified) were visually inspected for each participant in the ADNP group, and are depicted in Figures 18a-d. Data were inspected for the group as a whole, and separately for individuals with (*n* = 6) and without (*n* = 6) any reported vision problems. Amplitudes and power were larger in the short condition as compared to the standard condition. Waveforms were more prominent (i.e., peaks and troughs were more visible) for children in the ADNP group without as compared to those with reported vision problems. MSC values were higher in the

short condition as compared to the standard condition for a majority of the ADNP group, and especially for participants ADNP2 (age 10 years) and ADNP10 (5 years). MSCs were similar between children in the ADNP group with and without vision problems. In the ADNP group without reported vision problems, participant ADNP2 exhibited strong late activity, as evidenced by a pronounced P_{180} peak; this participant also had strong activity in Power Band 1, and MSC Bands 1 through 3. Another participant without reported vision problems, ADNP1 (age 2 years), exhibited a large N_{75}–P_{100} amplitude for the short condition, as well as strong responses in the frequency domain for MSC Bands 2 and 3. Another child, participant ADNP6 (age 4 years), exhibited a later $P_{100,}$ which occurred at about 135 ms; moreover, this participant exhibited weak coherent activity in all MSC bands, but relatively greater activity in Power Band 1. For the children in the ADNP group with reported vision problems, participant ADNP10 (age 5 years) exhibited a double P_{100} peak with nearly identical amplitudes several milliseconds apart in both the short and standard stimulus conditions; moreover, ADNP10 exhibited a later N_{135} wave. Several participants' waveforms line up with one another (i.e., ADNP7 and ADNP8 at N_{75} and P_{100}-N_{135}; and ADNP9 and ADNP11 at N_{75}), especially for the short condition, suggesting greater response consistency.

FOXP1 Group Analyses. The tVEP superimposed waveforms, MSC data, and power data were visually inspected for each individual participant in the FOXP1 group, and are depicted in Figures 18e-h. Data were inspected for the group as a whole, and separately for individuals with (n = 3) and without any reported vision problems (n = 6). For participants in the FOXP1 group without any reported vision problems, one individual, FOX2 (age 5 years), exhibited a large negative wave, indicative of strong excitatory input into the cortex, as well as a prominent second positive peak at 200 ms. Participant FOX1 (age

11 years) exhibited a shorter P_{100} peak, as well as lack of a prominent N_{75} for both short and standard conditions. A third child without vision problems, participant FOX3 (age 7 years), exhibited relatively smaller P_{60} and N_{75} peaks, indicative of weak excitatory input to the cortex, and a subsequent broadened P_{100} peak. Inspection of MSC and power bands for the participants without reported vision problems are characterized by more low frequency activity, as indicated by larger responses in Bands 1 and 2. For the children in the FOXP1 group with reported visual problems, waveforms generally appear broadened and dispersed, especially for the P_{100} peak, which occurred between 125 ms and 150 ms for four individuals for the standard condition. Participant FOX6 (age 10 years) exhibits a positive peak at P_{100} that is sustained, suggesting tonic rather than phasic inhibition.

Amplitude. Group statistics for amplitudes are in depicted in Table 9a. Box plots with medians and interquartile ranges can be seen in Figure 19, which demonstrate outliers and extreme values in each group. Clustered bar graphs with 95% confidence intervals can also be found in Appendix C. Results from these univariate statistics and visual inspection of Figure 19 indicate that P_{60}-N_{75} and N_{75}-P_{100} amplitudes are larger in the short condition as compared to the standard condition. Moreover, the TD group exhibits larger P_{60}-N_{75} and N_{75}-P_{100} amplitudes than do iASD, ADNP, and FOXP1 groups for both standard and short conditions. As expected, P_{60}-N_{75} amplitudes were smaller than N_{75}-P_{100} amplitudes in both conditions. While the ADNP and FOXP1 groups exhibit smaller P_{60}-N_{75} and N_{75}-P_{100} amplitudes in the standard condition as compared to TD and iASD groups, the iASD, ADNP, and FOXP1 groups exhibit similar P_{60}-N_{75} and N_{75}-P_{100} amplitudes in the short condition.

Linear mixed effects modeling (LMM) for amplitude as the outcome variable was conducted with group (TD, iASD, ADNP, and FOXP1) as a fixed effect; estimates of fixed

effects are reported in Table 12. In Model 1, with participant as a random effect and no fixed effects (i.e., null model), participant accounted for a significant portion of the variance in amplitude with an ICC of .42, indicating highly correlated data within individuals. In Model 2, group was added as a fixed effect, which significantly improved the model fit (Δ-2LL = 26.46, Δ*df* = 3, $p < .001$) and predicted aggregate effects of amplitude, $F(3, 148.09) = 9.63$, $p < .001$. The TD group exhibited significantly larger amplitudes overall, as revealed by pairwise comparisons between groups (*p*'s < .01). In Model 3, stimulus condition (i.e., short versus standard condition) was added to the model as a fixed effect, which significantly improved the model fit (Δ-2LL = 28.89, Δ*df* = 1, $p < .001$). The addition of stimulus condition also significantly explained variance for aggregates of amplitude, $F(1, 397.75) = 30.33$, $p < .001$. The short condition exhibited significantly larger responses than did the standard condition ($p < .001$). In Model 4, peak-to-trough measures of amplitude (P_{60}–N_{75} and N_{75}–P_{100}; herein termed 'amplitude type') were added to the model as a fixed effect, which significantly improved the model fit (Δ-2LL = 284.04, Δ*df* = 1, $p < .001$) and significantly explained variance in aggregate measures of amplitude, $F(1, 358.67) = 433.90$, $p < .001$). As expected, P_{60}–N_{75} amplitudes were significantly smaller than N_{75}–P_{100} amplitudes, $b = -11.60$, $t(358.67) = -20.83$, $p < .001$. In Model 5, fixed effects of two- and three-way interactions were added to the model, but did not significantly improve the model fit (Δ-2LL = 15.53, Δ*df* = 10, $p = .11$). Only the Group x Stimulus Condition interaction marginally explained the variance in amplitude, $F(3, 382.87) = 3.09$, $p = .03$. Though interpreted with caution, main effects for group, $F(3, 145.07) = 10.04$, $p < .001$, stimulus condition, $F(1, 384.34) = 51.39$, $p < .001$, and amplitude type, $F(1, 359.12) = .49$, $p < .001$, also significantly explained variance in amplitude. Pairwise comparisons and inspection of

the data in Figure 19 reveal that all groups exhibited significantly larger amplitudes in the short condition as compared to the standard condition (p's < .001), and that P_{60}–N_{75} amplitudes were significantly smaller than N_{75}–P_{100} amplitudes when collapsed across condition and group (p's < .001). Importantly, pairwise comparisons and Figure 19 indicate that the TD group exhibits larger total amplitudes for combined conditions as compared to all other groups (p's ≤ .009); the ASD groups did not differ from one another in overall amplitude for combined conditions.

Developmental (age) effects on measures of amplitude were observed, and slopes differed across the groups. Bivariate scatter plots by group and affiliated linear regression parameters are located in Appendix B. The effects of age on amplitude were explored statistically using linear mixed effects modeling. As significant differences in amplitude were observed between stimulus conditions, LMM analyses were conducted after splitting the dataset by condition to examine short and standard conditions separately. In Model 1 (i.e., the null model), participant was treated as a random effect without any fixed effects. In Model 1, participant accounted for a significant portion of the variance in amplitude with an ICC of .31 for the standard condition and an ICC of .37 for the short condition, indicating highly correlated data within individuals. In Model 2, group was added to the model as a fixed effect. In Model 3, peak-to-trough measures of amplitude (P_{60}-N_{75} and N_{75}-P_{100}; amplitude type) were added as a fixed effect. In Model 3, two-way Group x Amplitude Type interactions were added as fixed effects. In Model 4, age was added as a fixed effect and covariate. In Model 5, all two- and three-way interactions were added to the model as fixed effects. The results from this model are discussed below.

In Model 5, participant continued to account for a significant portion of the variance in amplitude for the standard condition, Var(u_{0j}) = 57.52, Var(ε_{ij}) = 28.17, p's < .001, and short condition Var(u_{0j}) = 92.64, Var(ε_{ij}) = 29.67, p's < .001. For the standard condition, amplitude type significantly predicted amplitudes, $F(1, 120.21) = 7.65$, $p = .007$, as did the Group x Amplitude Type interaction, $F(3, 120.16) = 4.08$, $p = .008$, and the Group x Amplitude Type x Age interaction, $F(3, 120.45) = 3.72$, $p = .013$. However, group did not significantly predict amplitudes $F(3, 120.83) = .70$, $p = .55$; nor did age, $F(1, 121.36) = .62$, $p = .43$, Group x Age interaction, $F(3, 121.13) = .75$, $p = .53$, nor Amplitude Type x Age, $F(1, 120.68) = .03$, $p = .87$. For the short condition, amplitude type significantly predicted amplitudes, $F(1, 142.05) = 38.04$, $p < .001$, as did the Group x Amplitude Type interaction, $F(3, 130.71) = 3.84$, $p = .01$, the Amplitude Type x Age interaction, $F(1, 138.65) = 13.57$, $p < .001$, and the Group x Amplitude Type x Age interaction, $F(3, 120.25) = 3.56$, $p = .02$. Together, results indicate that age has a differential effect for each diagnostic group for each condition, such that the changes in amplitude with age for each diagnostic group in each condition were statistically significant.

Latency. Group statistics for latency are depicted in Table 9b. Box plots with medians and interquartile ranges can be seen in Figure 19, which demonstrate outliers and extreme values in each group. Clustered bar graphs with 95% confidence intervals can also be found in Appendix C. Results from these univariate statistics and visual inspection of Figure 20 indicate that all groups exhibit similar P_{60} and N_{75} latencies for both standard and short duration conditions. The TD and iASD groups exhibit similar P_{100} latencies for both standard and short conditions. The ADNP group exhibits earlier P_{100} latencies for the standard condition and later latencies for the short condition as compared to iASD and TD

groups. The FOXP1 group exhibits later P_{100} latencies than all other groups for the short and standard condition, but P_{100} latencies are significantly later in the standard condition as compared to the short condition.

Linear mixed effects modeling (LMM) for latency as the outcome variable was conducted with group (TD, iASD, ADNP, and FOXP1) as fixed effects. In Model 1, with participant as a random intercept and no fixed effects (i.e., null model), Model 2, in which group was added as a fixed factor, and Model 3, in which stimulus condition was added as a fixed factor, a positive definite Hessian matrix could not be obtained. Because of this problematic result, ICCs could not be calculated. When time-to-peak latency measure (P_{60}, $N_{75,}$ and P_{100}; herein referred to as 'time point') was added to the model as a fixed effect in Model 4, a positive definite Hessian matrix was obtained. In Model 5, all two- and three-way interactions were added to the model as fixed effects. Results from Model 5 are reported below.

In Model 5, participant accounted for a significant portion of the variance in latency, $\text{Var}(u_{0j}) = 12.07$, $\text{Var}(\varepsilon_{ij}) = 27.05$, p's < .001. Group, $F(3, 135.61) = 11.08$, $p < .001$, significantly explained variance in latency; pairwise comparisons indicated that the FOXP1 group exhibited significantly later aggregate latencies than TD, iASD, and ADNP groups (p's < .001). Time point also significantly explained variance in latency, $F(2, 602.29) = 2938.12$, $p < .001$, with all time points significantly differing from one another, as expected. The main effect for stimulus condition did not adequately explain variance in latency, $F(1, 677.03) = 1.90$, $p = .17$. All two-way interactions significantly explained variance in latency: Group x Stimulus Condition, $F(3, 673.21) = 4.72$, $p = .003$; Group x Time Point, $F(6, 601.93) = 11.26$, $p < .001$; and Stimulus Condition x Time Point, $F(2, 602.98) = 8.49$, $p < .001$.

Importantly, the three-way Group x Stimulus Condition x Time Point interaction significantly explained variance in aggregate latency, $F(6, 602.37) = 3.64$, $p = .001$. As depicted in Figure 20, all groups exhibited similar values for P_{60} and N_{75} latencies; however, the FOXP1 group exhibited significantly longer P_{100} latencies as compared to the TD, iASD, and ADNP groups for the standard condition, but not the short condition. These results are consistent with broadened waveforms seen in individual waveform inspection (Figure 18e-h), in which children with FOXP1 syndrome exhibited broadened P_{100} waveforms.

Developmental (age) effects on measures of latency were observed, and slopes differed across the groups. Bivariate scatter plots by group and affiliated linear regression parameters are located in Appendix B.

The effects of age on latency were also explored statistically using linear mixed effects modeling. As significant differences in latency were observed between conditions, LMM was conducted after splitting the dataset by condition to examine short and standard conditions separately. Again, the Hessian matrix was not positive definite until time point and the Group x Time Point interaction was added to the model in Model 3. In Model 1 (i.e., the null model), participant was treated as a random effect without any fixed effects; ICCs were unable to be calculated as a result of the non-positive-definite Hessian matrix. In Model 2, group was added to the model as a fixed effect. In Model 3, time point and the Group x Time Point interaction were added as fixed effects. In Model 4, age was added as a fixed effect and covariate. In Model 5, all two- and three-way interactions were added to the model as fixed effects. The results from this model are discussed below.

In Model 5, participant continued to account for a significant portion of the variance in latency for the standard condition, $\text{Var}(u_{0j}) = 7.72$, $p = .002$, $\text{Var}(\varepsilon_{ij}) = 30.83$, $p < .001$, and

short condition Var(u_{0j}) = 10.48, $p < .001$, Var(ε_{ij}) = 23.23, $p < .001$. For the standard condition, group, $F(3, 118.24) = 4.62$, $p = .004$, time point, $F(2, 238.78) = 180.03$, $p < .001$, and the Group x Time Point interaction, $F(6, 238.71) = 3.63$, $p = .002$, significantly explained variance in latencies. Pairwise comparisons in the standard condition indicate that the FOXP1 group exhibited significantly longer latencies for aggregated time points when compared to all other group (p's < .001). As depicted in Figure 20, the FOXP1 group exhibited significantly longer latencies for P_{100} in the standard condition as compared to all other groups. Age significantly explained variance in latency for the standard condition: the Time Point x Age interaction significantly explained variance in latencies, $F(2, 239.34 = 3.39$, $p = .035$, as did the Group x Time Point, x Age interaction, $F(6, 239.10) = 2.54$, $p = .02$. Age, $F(1, 118.90) = 2.55$, $p = .11$, and the Group x Age interaction, $F(3, 118.63) = .80$, $p = .50$, did not significantly explain variance in latencies. Together, these results suggest that age has a differential effect for each diagnostic group in the standard condition, such that the changes in latency with age for each diagnostic group in each condition were statistically significant.

In Model 5, for the short condition, only Time Point, $F(2, 283.82) = 160.63$, $p < .001$, Age, $F(1, 163.41) = 5.85$, $p = .017$, and the Time Point x Age interaction, $F(2, 279.40) = 3.90$, $p = .02$, significantly explained variance in latency. All latencies generally appear to decrease with increasing age in the short condition. Group did not explain variance in latencies in the short condition, $F(3, 148.34) = 1.55$, $p = .20$, nor did the interactions of Group x Time Point, $F(6, 268.78) = 1.46$, $p = .19$. As previously mentioned, Figure 20 shows that there are no large differences between groups for P_{60}, N_{75}, and P_{100} latencies in the short condition. The Group x Age interaction, $F(3, 145.75) = .81$, $p = .49$, and Group x Time Point

x Age interaction, $F(6, 268.21) = .93$, $p = .48$, also did not significantly explain variance in latencies in the short condition.

These differences in the Group x Time Point and the Group x Time Point x Age interactions between the short and standard conditions again suggest that the standard and short stimulus conditions differentially affect the groups in the current study, and have different developmental trajectories in each group.

MSC. Group statistics for MSC are depicted in Table 10. Box plots with medians and interquartile ranges can be seen in Figure 21, which demonstrate outliers and extreme values in each group. Clustered bar graphs with 95% confidence intervals can also be found in Appendix C. Results from these univariate statistics and visual inspection of Figure 21 indicate that for the standard condition, the TD group exhibits larger MSC values than the iASD, ADNP, and FOXP1 groups for Bands 2, 3, and 4. While the TD and iASD groups exhibit similar values for Band 1 in the standard condition, they exhibit larger MSC values than the FOXP1 and ADNP groups for Band 1, with greater variability in Band 1 for the ADNP group than the FOXP1 group. ADNP and FOXP1 groups also exhibited smaller MSC values than the iASD group for Bands 2 and 3 for the standard condition. In the short condition, visual inspection of Figure 21 indicates that the TD, iASD, and ADNP groups exhibit similar median values for Band 1; while the FOXP1 group exhibits smaller median values in this band, there is large interquartile range overlap with the other three groups. Additionally, the TD group exhibited larger MSC values than the iASD, ADNP, and FOXP1 groups in Bands 2, 3, and 4. The ADNP and FOXP1 groups exhibited smaller MSC values than the iASD group in Bands 2 and 3 for the short condition.

Linear mixed effects modeling for MSC as the outcome variable was conducted with group (TD, iASD, ADNP, and FOXP1) as a fixed effect; estimates of fixed effects are reported in Table 13. In Model 1 with participant as a random intercept and no fixed effects (i.e., null model), participant accounted for a significant portion of the variance in MSC, with an ICC of .31, indicative of highly correlated data within individuals. In Model 2, group was added as a fixed effect, which significantly improved the model fit (Δ-2LL = 40.15, Δdf = 3, $p < .001$) and predicted aggregate effects of MSC, $F(3, 144.95) = 15.29$, $p < .001$. Pairwise comparisons revealed significantly larger aggregate MSC values in the TD group as compared to all other groups (p's < .001); the FOXP1 group also exhibited significantly smaller MSC values than the iASD group ($p = .046$). In Model 3, stimulus condition (i.e., short versus standard condition) was added to the model as a fixed effect. This addition also improved the model fit (Δ-2LL = 40.47, $\Delta df = 1$, $p < .001$) and significantly explained variance in MSC, $F(1, 959.53) = 41.28$, $p < .001$. Group also remained significant F(3, 146.48) = 15.63, $p < .001$. Pairwise comparisons indicate that larger MSC values were observed in the standard condition as compared to the short condition ($p < .001$). In Model 4, MSC band (i.e., Bands 1, 2, 3, 4) was added to the model as a fixed effect, and significantly improved the model fit (Δ-2LL = 466.43, $\Delta df = 3$, $p < .001$). The addition of MSC band also significantly explained variance in aggregate measures of MSC, $F(3, 892.02) = 204.22$, $p < .001$. Pairwise comparisons revealed that all MSC bands significantly differed from one another (p's < .001), with Band 2 exhibiting largest MSC values, followed by Band 1, then Band 3, and Band 4 exhibiting the smallest values. In Model 5, all two-way and three-way interactions were added to the model as fixed effects. This addition improved the model fit (Δ-2LL = 123.66, $\Delta df = 24$, $p < .001$). The Stimulus Condition x MSC Band interaction did

not significantly explain variance in MSC values, $F(3, 891.75) = .27$, $p = .85$, indicating that each MSC values did not differentially vary across bands between conditions. The Group x Stimulus Condition interaction significantly explained variance in MSC values, $F(3, 950.32) = 9.35$, $p < .001$. As depicted in Figure 21 and Table 10, the TD and iASD groups exhibited larger MSC values in the standard condition as compared to the short condition, while the ADNP and FOXP1 groups exhibited larger MSC values in the short condition as compared to the standard condition. The Group x MSC Band interaction significantly explained variance in MSC values, $F(9, 891.75) = 9.74$, $p < .001$. As seen in Figure 21 and Table 10, the TD group exhibited larger MSC values than iASD, ADNP, and FOXP1 groups for Bands 2, 3, and 4; moreover, the ADNP and FOXP1 groups also exhibited smaller MSC values than the iASD group for Bands 2 and 3. iASD and single-locus groups did not differ significantly in MSC Bands 1 and 4. Group The three-way interaction between Group x Stimulus Condition x MSC Band did not significantly explain variance of aggregate MSC values observed in this sample, $F(9, 891.75) = .80$, $p = .62$.

Developmental (age) effects on MSC values were observed, and slopes differed across the groups. Bivariate scatter plots by group and affiliated linear regression parameters are located in Appendix B.

The effects of age on MSC were also explored statistically using LMM. As significant differences in MSC values were observed between conditions, LMM was conducted after splitting the dataset by stimulus condition to examine short and standard conditions separately. In Model 1 (i.e., the null model), participant was treated as a random effect without any fixed effects, and participant accounted for a significant portion of the variance in MSC with an ICC of .38 for the standard condition and an ICC of .19 for the

short condition, indicating highly correlated data within individuals. In Model 2, group was added to the model as a fixed effect. In Model 3, MSC band was added as a fixed effect. In Model 4, the Group x MSC Band interaction was added as a fixed effect. In Model 5, age was added as a fixed effect and covariate. In Model 6, all two- and three-way interactions were added to the model as fixed effects. The results from this model are discussed below.

In Model 6, participant explained a significant portion of the variance in MSC for the standard condition, Var(u_{0j}) = .01, Var(ε_{ij}) = .01, *p*'s < .001, and short condition Var (u_{0j}) = .005, Var(ε_{ij}) = .008, *p*'s < .001. For the standard condition, MSC band, $F(3, 369.00) = 6.45$, $p < .001$, age, $F(1, 123.00) = 4.23$, $p = .04$, and the Group x MSC Band x Age interaction significantly explained variance in MSCs, $F(9, 369.00) = 2.96$, $p = .002$. The following fixed effects did not significantly predict MSCs in the standard condition: group, $F(3, 123.00) = 1.63$, $p = .19$; Group x MSC Band, $F(9, 369.00) = .93$, $p = .50$; Group x Age, $F(3, 123.00) = .99$, $p = .40$; and MSC Band x Age, $F(3, 369.00) = 1.62$, $p = .19$. Results therefore suggest that age has a differential effect on MSC for each group in the standard condition, such that the changes in MSC with increasing age for each group were statistically significant. For the short condition, only MSC band significantly explained variance in MSCs, $F(3, 408.00) = 9.21$, $p < .001$. Pairwise comparisons indicate that all MSC bands were significantly different from one another in the short condition (*p*'s < .028), with Band 2 exhibiting the largest MSC values, followed by Band 1, Band 3, and Band 4. No other main effects or interactions significantly explained variance in MSC values in the short condition, including: group, $F(3, 126.00) = .24$, $p = .87$; age, $F(1, 136.00) = 2.63$, $p = .12$; Group x MSC Band, $F(9, 408.00) = .55$, $p = .84$; Group x Age, $F(3, 136.00) = .87$, $p = .46$; MSC Band x Age, $F(3, 408.00) = .52$,

p = .67; and Group x MSC Band x Age, $F(9, 408.00) = 1.30$, p = .23. Thus, MSC bands do not significantly differ by age nor group in the short condition.

Power. Box plots with medians and interquartile ranges can be seen in Figure 22, which demonstrate outliers and extreme values in each group. Group statistics in power are depicted in Table 11. Clustered bar graphs with 95% confidence intervals can also be found in Appendix C. Results from these univariate statistics and visual inspection of Figure 22 indicate that for the standard and short conditions, power decreases from Band 1 through Band 4 for each group. Larger power values are seen in the short condition as compared to the standard condition. Moreover, the TD group exhibits greater power for Bands 1, 2, and 3 than iASD, ADNP, and FOXP1 groups for the standard condition, and Bands 2 and 3 for the short condition. The TD and ADNP groups exhibit greater power in Band 1 than the iASD and FOXP1 groups in the short condition, although there is an extreme value in the ADNP group that may be driving these power values. Groups do not differ largely in Power Band 4 in the short and standard conditions. The ADNP and FOXP1 groups exhibit smaller power values than the iASD group for Band 2 in the standard condition. ADNP and FOXP1 groups do not differ greatly from each other in power values (with the exception of Band 1 on the short condition, mentioned above).

Linear mixed effects modeling with power as the outcome variable was conducted with group (TD, iASD, ADNP, and FOXP1) as a fixed effect; estimates of fixed effects are reported in Table 14. In Model 1, with participant as a random intercept and no fixed effects (i.e., null model), participant accounted for a significant portion of the variance in power with an ICC of .02, indicating weakly correlated data within individuals. In Model 2, group was added as a fixed effect, which significantly improved the model fit (Δ-2LL = 12.48, Δdf = 3,

p = .006) and was a significant predictor of aggregate measures of power, F(3, 152.08) = 4.34, p = .006. Post hoc pairwise comparisons indicated that the TD group exhibited significantly greater power than did the iASD group (p = .001) and the FOXP1 group (p = .03), but not the ADNP group (p = .60). In Model 3, stimulus condition (i.e., standard versus short condition) was added as a fixed effect, which significantly improved the model fit (Δ-2LL = 11.30, Δdf = 1, p < .001) and accounted for significant variance in power, F(1, 995.02) = 11.39, p = .001, while group remained significant (p = .006). Pairwise comparisons indicated that significantly weaker power was observed in the standard condition as compared to the short condition, b = -.48, t(995.02) = -3.38, p = .001. In Model 4, power band (i.e., Band 1, 2, 3, 4) was added to the model as a fixed effect, which also significantly improved the model fit (Δ-2LL = 1134.88, Δdf = 3, p < .001), and significantly explained variance in power, F(3, 889.93) = 763.06, p = .001. As expected, pairwise comparisons indicated that all power bands significantly differed from one another (p's < .001), with Band 1 exhibiting greatest power, followed by Bands 2, 3, and 4. In Model 5, two- and three-way interactions were added to the model as fixed effects. The addition of these interactions significantly improved the model fit (Δ-2LL = 59.43, Δdf = 24, p < .001). The Group x Stimulus Condition interaction did not significantly explain variance in power, F(3, 970.03) = 2.14, p = .09. The Group x Power Band interaction significantly explained variance in power, F(9, 889.54) = 2.79, p = .003. As seen in Figure 22 and Table 11, the TD group exhibited significantly greater power for Bands 1, 2, and 3 when compared to iASD, ADNP, and FOXP1 groups, and ADNP and FOXP1 groups exhibited lower power values than the iASD group for Band 2. The Stimulus Condition x Power Band interaction was also significant, F(3, 889.54) = 8.07, p < .001. As seen in Table 11, larger responses for each band

were observed in the short condition as compared to the standard condition. The Group x Stimulus Condition x Power Band interaction did not significantly explain the variance in power, $F(9, 889.54) = .63$, $p = .78$.

Developmental (age) effects on measures of power were observed, and slopes differed across the groups. Bivariate scatter plots by group and affiliated linear regression parameters are located in Appendix B.

To statistically examine these changes in power with age for each diagnostic group, age was added as a covariate and fixed factor in Model 6 (continued from the LMM described above), and all two-, three-, and four-way interactions were added to the model as fixed effects for Model 7. In Model 7, the individual continued to account for a significant portion of the variance in power, $\text{Var}(u_{0j}) = .54$, $\text{Var}(\varepsilon_{ij}) = 1.32$, p's $< .001$. The additions of the interactions to the model did not significantly improve the model fit (Δ-2LL = 38.73, $\Delta df = 31$, $p = .16$). The Group x Stimulus Condition x Power Band x Age interaction did not significantly explain variance in power, $F(9, 888.66) = .23$, $p = .99$. The three-way interactions of Stimulus Condition x Power Band x Age, $F(3, 888.66) = .50$ $p = .68$, Group x Stimulus Condition x Age, $F(3, 950.06) = .47$, $p = .71$, and Group x Power Band x Age, $F(9, 888.66) = 1.62$, $p = .11$, did not significantly explain variance in power. The Group x Age interaction did not significantly explain variance in power, $F(3, 145.20) = .60$, $p = .62$. The two-way interaction between Power Band x Age significantly explained variance in power, $F(3, 888.66) = 3.10$, $p = .03$. Thus, each power band differentially changes with increasing age in all groups.

Agreement between standard and short conditions. ICCs for amplitude, latency, MSC, and power were analyzed to assess the absolute and relative agreement between

stimulus conditions. Overall, estimates of relative agreement between conditions were larger than were those for absolute agreement. When measuring absolute agreement, there was moderate reliability between short and standard conditions for measures of amplitude: estimates for P_{60}-N_{75} amplitude was .75 with a 95% CI [.36, .88], and for N_{75}-P_{100} amplitude was .62 with a 95% CI [.35, .77]. Estimates of relative agreement were higher, estimates for P_{60}-N_{75} amplitude was .83 with a 95% CI [.76, .88], and for N_{75}-P_{100} amplitude was .69 with a 95% CI [.57, .78]. Estimates of reliability between conditions for P_{60} latency were poor, with estimates of absolute and relative agreement both equaling .26 with a 95% CI [.07, .43]. Estimates of absolute agreement were stronger for N_{75} latency (ICC = .73, 95% CI [.63, .81]) and P_{100} latency (ICC = .66, 95% CI [.54, .75]), with moderate agreement between the two stimulus conditions; estimates of relative agreement were similar for N_{75} latency (ICC = .74, 95% CI [.64, .81]) and P_{100} latency (ICC = .67, 95% CI [.55, .76]). Absolute agreement ICC for MSC Band 1 was .32 with a 95% CI [.12, .49], for MSC Band 2 it was .58 with a 95% CI [.39, .71], for MSC Band 3 it was .70 with a 95% CI [.54, .80], and for MSC Band 4 it was .61 with a 95% CI [.47, .76]; relative agreement ICC for MSC Band 1 was .37, with a 95% CI [.20, .51], for MSC Band 2 it was .62 with a 95% CI [.49, .72], for MSC Band 3 it was .74 with a 95% CI [.64, .81], and for MSC Band 4 it was .63 with a 95% CI [.51, .73]. Estimates of absolute agreement were moderate for Power Band 1 (ICC = .54, 95% CI [.35, .68]) and Power Band 2 (ICC = .64, 95% CI [.45, .76]), but were weaker for Power Band 3 (ICC = .48, 95% CI [.32, .62]) and Power Band 4 (ICC = .15, 95% CI [-.03, .32]). Estimates of relative agreement similarly fell in the moderate range for Power Band 1 (ICC = .59, 95% CI [.45, .70]), Power Band 2 (ICC = .68, 95% CI [.57, .77]), and Power Band 3 (ICC = .51, 95% CI [.36, .63]), but were weaker for Power Band 4 (ICC = .15, 95% CI [-.03, .32]).

Associations of time-domain and frequency-domain measures of magnitude. To explore replicability of findings from Zemon and Gordon (2018), in which N_{75}-P_{100} amplitude correlated strongest with power in Frequency Band 2, Figure 23 depicts grouped scatter plots of N_{75}-P_{100} amplitude versus power in Band 2 for the short and standard conditions; see Table 15 for affiliated linear regression parameters. These plots demonstrate that power of Band 2 yields accurate, objective estimates of N_{75}-P_{100} amplitude with about 76% to 77% of the variance explained by the linear relation when looking at all groups together for both conditions. When looking at each group separately, Power Band 2 yields accurate estimates of N_{75}-P_{100} amplitude with about 72% of the variance explained in the standard condition and 76% of the variance explained in the short condition for the TD group. For the iASD group, Power Band 2 generated accurate estimates of N_{75}-P_{100} amplitude with about 76% of the variance explained in the standard condition and 72% of the variance explained in the short condition. In the ADNP group, Power Band 2 exhibited greater prediction of N_{75}-P_{100} amplitude in the short condition, with about 71% of the variance explained, as compared to the standard condition, with only about 29% of the variance explained. Power Band 2 generated the most accurate estimates of N_{75}-P_{100} amplitude in the FOXP1 condition, with about 86% of the variance explained in the standard condition and 88% of the variance explained in the short condition.

Correlations with behavioral measures of sensory reactivity

One hundred children in Study 2 who underwent the VEP also participated in Study 1. Correlations are summarized in Tables 16-18.

Results generally indicate that higher SAND scores across the various subscales, indicative of greater sensory processing abnormalities, are correlated with smaller

amplitudes, lower MSC values, and weaker power. Specifically, SAND total score correlates significantly and negatively with tVEP amplitude (*p*'s < .05), MSC Bands 2, 3, and 4 (*p*'s < .01), and several power bands for short and standard conditions. SAND visual domain scores also correlate significantly and negatively with tVEP measures in the time and frequency domains. SAND hyperreactivity does not correlate significantly with any tVEP measures; however, SAND hyporeactivity and sensory seeking exhibit moderate negative correlations with several tVEP measures in time and frequency domains. Visual hyporeactivity exhibits relatively strong significant negative correlations with several tVEP measures in both time and frequency domains, as does visual seeking, tactile hyporeactivity, auditory hyperreactivity, and auditory seeking. Tactile hyperreactivity and tactile seeking only exhibit significant negative correlations with tVEP MSC values. Visual hyperreactivity exhibits a significant positive relation with Power Band 4.

Results from bivariate correlations between the SP/SSP and tVEPs generally indicate lower scores on these SSP subscales, indicative of more sensory symptoms, correlate with smaller amplitudes, lower MSC values, and weaker power. SP visual domain scores exhibit significant positive correlations with several tVEP measures in the frequency domain, but not the time domain. Underresponsive/Seeks Sensation exhibits moderate-to-strong significant positive correlations with almost all tVEP measures (*r*'s .32-.56). Tactile Sensitivity, Auditory Filtering, Low Energy/Weak, and Visual Auditory Sensitivity also exhibit significant moderate positive correlations with several tVEP measures in the time and frequency domains. Taste/Smell sensitivity only exhibit a weak correlation with MSC Band 2 in the standard condition. The Movement Sensitivity subscale has significant moderate

positive correlations with MSC Bands 2 and 3 in the standard condition, and a significant moderate negative correlation with Power Band 4 in the standard condition.

Chapter IV: Discussion

The goals of this study were to investigate behavioral and electrophysiological sensory responsivity in children with iASD and three single-locus causes of ASD—ADNP syndrome, FOXP1 syndrome, and PMS—using the SAND, SSP, and tVEP. Relationships between behavioral and electrophysiological measures were then explored to examine the clinical utility and relevance of the electrophysiological methods. This is the first known study to examine behavioral and electrophysiological correlates of sensory reactivity in ADNP syndrome and FOXP1 syndrome, and it seeks to build upon ground-breaking sensory research in PMS conducted by investigators at the Seaver Autism Center. Participants in Study 1 underwent assessments of sensory reactivity using the clinician-administered SAND and parent-report SSP. Multivariate statistics were utilized to assess group differences in sensory subtype (i.e., hyperreactivity, hyporeactivity, and sensory seeking), sensory domain (i.e., visual, tactile, and auditory), and combined measures of sensory domain and subtype (i.e., visual hyperreactivity, visual hyporeactivity, visual seeking, tactile hyperreactivity, tactile hyporeactivity, tactile seeking, auditory hyperreactivity, auditory hyporeactivity, and auditory seeking). Multivariate statistics were also applied to the SSP data to examine group differences on SSP subscales. Each syndrome group was compared individually to iASD and TD groups, and then all groups were analyzed together. For the SAND analyses, MANOVAs were followed up with discriminant function analyses; for SSP analyses, MANOVAs were followed up with pairwise comparisons using Bonferroni correction. Linear mixed effects modeling (LMM) was also applied to account for the intercorrelated data within individuals.

Models were built hierarchically to take relevant factors into account. Participants in Study 2 included TD children, as well as those with iASD, ADNP syndrome, and FOXP1 syndrome. VEPs were collected using two contrast-reversing checkerboard stimulus conditions that varied in duration (i.e., short versus standard), which provide objective methods of examining excitatory and inhibitory neurophysiological activity in the cortex. Group differences in amplitude, latency, MSC, and power were analyzed using linear mixed effects modeling. Developmental effects of age on tVEP measures were also considered and analyzed using these statistical techniques.

Interpretation

<u>Aim 1</u>: Characterize sensory behavior in individuals with single-locus causes of ASD (i.e., PMS, FOXP1 syndrome, and ADNP syndrome) relative to individuals with iASD and TD controls. When comparing ADNP, iASD and TD groups on the SAND as a whole, the TD group exhibited significantly lower scores, indicative of fewer sensory symptoms; moreover, these significantly lower scores in the TD group emerged across analyses of the various SAND subscales. The ADNP and iASD group exhibited similar total scores on the SAND. Additionally, the ADNP and iASD groups exhibited similar scores on total sensory hyperreactivity and hyporeactivity subscales, but the ADNP group exhibited significantly more sensory seeking symptoms than both iASD and TD groups. The ADNP group also exhibited significantly more symptoms in the tactile domain as compared to both iASD and TD groups, although domain alone was not sufficient in correctly discriminating between groups. These symptom differences in the ADNP group appear to be driven by significantly greater tactile, visual, and auditory sensory seeking symptoms, as well as tactile hyporeactivity symptoms, which together statistically discriminated the ADNP group from

iASD and TD groups. Moreover, the ADNP group exhibited significantly lower auditory hyperreactivity scores than the iASD group, which significantly differentiated the two groups from one another. Consistent with these findings, the ADNP group exhibited significantly lower scores, indicative of greater sensory symptoms, than both TD and iASD groups on subscales of the Short Sensory Profile (SSP) that measure sensory hyporeactivty and seeking behaviors (i.e., Low Energy/Weak and Underresponsive/Seeks Sensation subscales).

When comparing FOXP1, iASD, and TD groups on the SAND across all sensory subtype, sensory domain, and combined subtype and domain scores, the TD group exhibited significantly lower scores than iASD and FOXP1 groups; however, the FOXP1 and iASD groups did not exhibit distinct sensory phenotypes on these scales. Similar results were found using the SSP, such that the FOXP1 group did not exhibit significantly different scores than the iASD group across all subscales, but both groups exhibited greater sensory symptoms than the TD group. Results overwhelmingly suggest that behavioral symptoms, as measured by the SAND and SSP, do not adequately distinguish children with FOXP1 from those with iASD.

Analyses assessing PMS, iASD, and TD groups again suggested the TD group exhibited fewer sensory symptoms on both the SAND total scores and all subscale scores than the PMS and iASD groups. While PMS and iASD groups exhibited similar total scores on the SAND, the PMS group exhibited a unique sensory profile characterized by greater hyporeactivity symptoms across visual, auditory, and tactile domains, as evidenced by significantly greater total hyporeactivity scores, as well as visual hyporeactivity, auditory hyporeactivity, and tactile hyporeactivity scores on the SAND when compared to iASD and TD groups. This PMS sensory phenotype that is predominated by hyporeactivity symptoms

is consistent with previously reported research using additional sensory measures, including the SSP (Mieses et al., 2016; Soorya et al., 2013). Again, the iASD group phenotype, which distinguished the group from PMS and TD groups, was characterized by auditory hyperreactivity, as well as visual seeking symptoms.

Analyses also compared all five groups to further examine the distinct nature of these behavioral phenotypes. Analysis of sensory subtypes as measured by the SAND indicated that the iASD, ADNP, and FOXP1 groups exhibited significantly greater hyperreactivity symptoms when compared to TD and PMS groups. Moreover, these elevated hyperreactivity symptoms also differentiated the iASD group from ADNP and FOXP1 groups. Consistent with earlier analyses, the PMS group exhibited significantly greater sensory hyporeactivity symptoms than all other groups, solidifying this hyporeactive phenotype as a distinct and unique marker of PMS. Regarding sensory seeking scores, the ADNP group exhibited the highest scores on this scale, which were significantly greater than TD, iASD, and PMS groups; the FOXP1 group exhibited intermediate scores between iASD and ADNP groups for sensory seeking behaviors. Analysis of SAND sensory domain total scores revealed the TD group exhibited fewer sensory symptoms across domains when compared to the iASD and single-locus groups, and that the iASD and single-locus groups did not differ from one another with respect to symptoms in the visual and auditory domains. However, the ADNP group exhibited more symptoms in the tactile domain than did TD, iASD, and PMS groups.

Evaluation of combined sensory subtype and domain scores using both multivariate and LMM analyses indicated that all groups differed significantly from one another on the combined SAND subscales. Results show that the TD group yielded the lowest scores on all SAND subscales as compared to the iASD and single-locus groups. Consistent with previous

analyses in the current study, the PMS group exhibited significantly greater scores and thus more symptoms on visual and auditory hyporeactivity subscales when compared to all other groups. The PMS group similarly had greater tactile hyporeactivity symptoms than iASD, TD, and FOXP1 groups, but the ADNP group exhibited similarly elevated tactile hyporeactivity scores. Moreover, while iASD, FOXP1, and ADNP groups appear to exhibit elevated levels of sensory seeking symptoms across sensory domains when compared to TD and PMS groups, the ADNP group emerged as having significantly greater auditory and tactile seeking symptoms when compared to the iASD group, with the FOXP1 group exhibiting intermediate levels of symptoms between the two groups on these subscales. Importantly, the iASD group exhibited greater auditory hyperreactivity symptoms than do the TD, PMS, and ADNP groups.

Overall, results support Hypothesis 1a, which posited that TD groups would exhibit fewer sensory symptoms than iASD and single-locus ASD groups. Results also support Hypothesis 1b, as the PMS group exhibited a distinct hyporeactivity sensory phenotype as measured by the SAND, which is consistent with previous literature (Mieses et al., 2016; Soorya et al., 2013). Additionally, consistent with Hypothesis 1c, a unique sensory phenotype emerged for the ADNP group, pointing to sensory seeking behaviors across visual, auditory, and tactile domains, as well as tactile hyporeactivity as key markers of behavioral sensory dysfunction in the syndrome. Also, the iASD group was characterized by a hyperreactivity phenotype, driven by scores in the auditory hyperreactivity domain. However, the FOXP1 group exhibited sensory profiles on the SAND that overlapped with iASD, ADNP, and PMS groups, suggesting more heterogeneity in the sensory phenotype.

<u>Aim 2</u>: Identify electrophysiological markers of sensory reactivity using tVEPs in individuals with single-locus causes of ASD relative to individuals with idiopathic ASD, and TD controls. In general, ADNP and FOXP1 groups exhibited the tri-part waveform typically seen for contrast-reversing tVEPs. Results from analyses of amplitude indicate that the iASD and single-locus ASD groups exhibit significantly smaller P_{60}-N_{75} and N_{75}-P_{100} amplitudes than the TD group, which reflect primarily excitatory and inhibitory activity, respectively; however, the iASD, ADNP, and FOXP1 groups did not differ significantly in amplitudes for these critical peaks and troughs. These results are consistent with previous studies in iASD and PMS groups using the methods applied in the current study (Siper et al., 2019; Siper et al., 2016). The results also suggest that the reduced P_{60}-N_{75} amplitudes found in iASD, ADNP, and FOXP1 groups reflect weaker excitatory input to the cortex, and result in subsequent reductions of the N_{75}-P_{100} amplitudes.

The TD, iASD, ADNP, and FOXP1 groups exhibited similar latencies for P_{60} and N_{75} time points for standard and short conditions. However, the FOXP1 group exhibited later P_{100} latencies as compared to the TD, iASD, and ADNP groups for both the short and standard conditions, with significantly later P_{100} latencies in the standard condition. These later P_{100} latencies were apparent in the broadened waveforms seen in this group, which were observed for both children with and without visual problems. Previous literature using these stimulus conditions and electrophysiological techniques posit that the continuous, repeated stimulation inherent in the standard condition may cause an adaptation effect in the visual system, resulting in later latencies even in typically-developing adults (Zemon & Gordon, 2018). This adaptation effect was replicated in our study, as all groups exhibited shorter peak times in the

short condition versus the standard condition, especially for the P_{100} component; yet, this adaptation effect was highly evident in the FOXP1 group.

There are two possible explanations for these late P_{100} latencies and increased adaptation effects in the FOXP1 group. First, late P_{100} latency has repeatedly been found in individuals with amblyopia (Sokol, 1983), which was a common characteristic in several FOXP1 participants with parent-reported visual problems. Seminal research conducted by Duffy, Burchfiel, and Conway (1976) suggests that having an amblyopic condition can alter the GABAergic inhibitory activity in the cortex; specifically, authors found that while cells in the amblyopic eye were initially unresponsive to stimulation, blocking GABAergic activity in the cortex using bicuculline released the neurons that were originally GABAergically inhibited to give a response from the amblyopic eye. While amblyopia may explain some of the broadened waveforms seen in the FOXP1 group, there was one child in the group without any reported vision problems who also exhibited late P_{100} latency and a dispersed waveform; additionally, several children in the ADNP group also had amblyopia and associate visual problems, but did not exhibit these late latencies. Therefore, amblyopia alone is not sufficient to explain the pronounced adaptation effects and late latencies. Second, the prominent adaptation in the P_{100} component of the tVEP, known to reflect GABA-mediated cortical inhibition, may in fact be due to deficits in initial excitatory activation, as previously mentioned in analyses of amplitude. Translational research of FOXP1 syndrome has found that the Foxp1 gene is expressed in the glutamate projection neurons in cortical layers III (a key cortical layer in the generation of the tVEP signal), IV, V and VI, but not in the cortical GABAergic interneurons (Ferland et al., 2003; Hisaoka et al., 2010). Diminished activity in ionotropic glutamate receptors—also known to be affected in PMS (Bozdagi et al., 2010;

Yang et al., 2012)—would affect fast-acting high frequency excitatory activity, and the subsequent resultant cortical inhibition. Therefore, reduced initial glutamatergic excitatory activity in the cortex would produce broadened waveforms and later P_{100} latencies observed in our FOXP1 sample. Furthermore, previous work using ssVEPs with migraine patients found abnormalities in GABA-mediated short-range lateral interactions in response to repeated stimulation, which authors hypothesized was dependent upon initial levels of cortical activation (Coppola et al., 2013). Considering the FOXP1 group exhibited significantly later latencies at the inhibitory P_{100} component in response to repeated stimulation, it is possible that the FOXP1 group exhibits similar impairments in initial cortical activation and resultant GABAergic inhibitory activity.

Importantly, the iASD, ADNP, and FOXP1 groups exhibited lower MSC values than did the TD group for MSC Bands 2, 3, and 4 for both stimulus conditions, which is consistent with previous work in iASD and PMS (Siper et al., 2019; Siper et al., 2016). In addition, the FOXP1 and ADNP groups exhibited even lower MSC values than the iASD group in Bands 2 and 3. The observed deficits in these bands again point to reduced fast-acting, high frequency excitatory activity in iASD and single-locus ASDs. Consistent with abnormal inhibitory activity observed in the time-domain (i.e., increased P_{100} latency), the FOXP1 group also exhibited lower values than TD and iASD groups in Band 1 for the standard condition, which reflects deficits in later cortical inhibitory activity.

For tVEP power, the TD group exhibited significantly greater power in Bands 1, 2, and 3 when compared to iASD and single-locus ASD groups, and ADNP and FOXP1 groups exhibited lower power values than the iASD group for Band 2 in the standard condition. Research conducted by Zemon and Gordon (2018) posits that power in Bands 2 and 3 are

related to high frequency early excitatory activity, and power in Band 1 is correlated with late, low frequency inhibitory activity. Thus, results from analyses of total power are consistent with time-domain and MSC results in the current study suggestive of weaker initial glutamatergic excitatory activity and consequent diminutions in GABAergic inhibition.

Taken together, results from Study 2 using tVEPs support Hypothesis 2a, such that the TD group exhibited significantly larger amplitudes, greater MSC values, and power than did iASD and single-locus groups. Individuals with iASD exhibited similar tVEP responses to ADNP and FOXP1 groups. Supportive of Hypothesis 2b, a unique VEP marker of pathophysiology may have been identified for individuals with FOXP1 syndrome, characterized by significantly later P_{100} latency and broadened waveforms at the P_{100} peak.

Furthermore, results from the current study overwhelmingly suggest that both iASD and single-locus groups exhibit deficits in initial excitatory cortical activity, which results in diminished subsequent GABAergic inhibitory activity. While results regarding the direction and specificity of E/I imbalance in ASD are mixed (Dickinson, Jones, & Milne, 2016; Foss-Feig et al., 2017), some translational models of ASD have indicated that reduced excitatory synaptic transmission (specifically a reduced NMDA/AMPA ratio at corticostriatal synapses) may be responsible for repetitive behaviors (Blundell et al., 2010), such as sensory reactivity. Additionally, studies in humans have found reduced glutamate and glutamine (Glx) levels in individuals with ASD in cortical white matter (Corrigan et al., 2013) and grey matter of the occipital cortex (DeVito et al., 2007). Moreover, studies using ssVEPs indicate that both short- and long-range lateral inhibition in the cortex is intact in iASD, and comparable to TD individuals (Dickinson et al., 2018; Lurie, 2018). It is imperative that future studies examine

initial glutamatergic and GABAergic activity separately using more targeted VEP stimulus conditions in these single-locus groups.

Developmental effects. Results from the current study emphasize the importance of examining developmental trajectories of tVEP components in iASD and single-locus causes of ASD. These results from the current study indicate that age has a differential effect on amplitude, latency, and MSC for each group. Additionally, results indicate that total power and latencies in the short condition generally decrease with increasing age. When examining the effects of age on amplitude, TD children exhibit increases in amplitude for the P_{60}-N_{75}, which is characteristic of children ages 6 and younger, whereas P_{60}-N_{75} amplitude decreases with increasing age for the single-locus groups, which is characteristic of children ages 7 to 14 (Dustman & Beck, 1966). All groups exhibited age-expected decreases in the N_{75}-P_{100} amplitude. Regarding latency, the P_{60} component increased with increasing age for the TD group, as expected (Zemon et al., 1995), and is relatively unchanged with increasing age for iASD, ADNP, and FOXP1 groups in the standard condition, but increases with increasing age for the FOXP1 group in the short condition. All groups generally exhibited expected decreased latencies for increasing age for the N_{75} component. For the P_{100} component, all groups exhibited expected decreases in latency with increasing age for the short condition, but in the standard condition, only iASD, TD, and FOXP1 groups exhibited the expected developmental decreases in latency, while the ADNP group increased in latency.

Effects of stimulus condition. Results from the current study repeatedly found significant differences between stimulus conditions for all outcome variables. Specifically, stronger amplitudes, greater power, and slightly earlier latencies (for all groups) were observed in the short condition as compared to the standard condition. As previously

mentioned, these findings are due to adaptation effects resulting from repeated stimulation in the standard condition (Zemon & Gordon, 2018). Additionally, higher MSC values were seen in the standard condition as compared to the short condition. One possible reason is that there are three-times the amount of data collected in the standard condition. Another potential explanation is that in the standard condition responses are not truly independent (as they are in the short condition); the responses are therefore intercorrelated because of continuous epochs of the EEG, which will thus enhance estimates of MSC values. Overall, consistent with Zemon and Gordon (2018), the short condition likely represents more accurate estimates of responses under normal viewing conditions. Even with these significant differences in tVEP components between conditions, there was substantial agreement between short and standard conditions. Importantly, the strong correlations between conditions replicate previous findings in TD, iASD, and PMS populations (Siper et al., 2019; Siper et al., 2016; Zemon & Gordon, 2018).

Novel frequency domain measures. Results from the current study also replicated findings from Zemon and Gordon (2018) such that a strong linear relationship was observed between N_{75}-P_{100} amplitude and square root of power in Band 2 for both standard and short conditions, with about 76% of the variance explained by the linear relation for the entire study sample, and an average (between short and standard conditions) of 74% explained for the TD group, 74% for the iASD group, 87% explained for the FOXP1 group, and 50% explained for the ADNP group. Results therefore suggest that even in children with abnormal neurodevelopment, the square root of power in Band 2 can yield objective, reliable estimates of N_{75}-P_{100} amplitude.

<u>Exploratory Aim:</u> Examine the relationship between underlying neuropathophysiology and behavioral clinical outcomes. Consistent with previous work (Simmons et al., 2009; Siper et al., 2019), the current study revealed a significant relationship between behavioral sensory reactivity and low-level visual processing as measured by VEP. More specifically, the current study identified significant correlations between VEP responses in both time and frequency domains and two distinct measures of sensory reactivity based on parent-report and clinician-observation. Across sensory measures, scores indicative of greater sensory processing abnormalities were correlated with smaller amplitudes, weaker MSC values, and reduced power in tVEPs.

Clinical Implications

The prevalence of ASD worldwide has increased over the past 15 years, such that it affects one in every 59 children (Baio et al., 2018). Individuals with ASD experience deficits in social communication and restricted and repetitive behaviors, as well as several comorbid neurological, medical, and psychiatric comorbidities. The economic costs of ASD in the U.S. have been estimated to be between $11.5 billion – $60.9 billion, which cover costs of medical care, special education, residential and supportive care, and lost parental and individual income (Buescher, Cidav, Knapp, & Mandell, 2014; Lavelle et al., 2014); moreover, a delay in a diagnosis of ASD is found to be associated with higher costs for individuals, families, and communities (Horlin, Falkmer, Parsons, Albrecht, & Falkmer, 2014). Early diagnosis and access to appropriate early interventions are associated with improved long-term outcomes for children and families (Orinstein et al., 2014). While diagnostic assessments and genetic testing have developed highly over the past decade to improve the ability to diagnose ASD and associated disorders early in childhood, and the

ability to develop objective diagnostic tools and efficacious treatments has been hampered by the heterogeneity of the disorder.

Characterization of Sensory Phenotypes. The current study is in line with a new wave conceptualization of ASD symptomatology, which postulates that sensory symptoms are core, primary symptoms in ASD neurobiology and phenotype (Robertson & Baron-Cohen, 2017). Variations in sensory reactivity in ASD are apparent early in development, and sensory symptoms often emerge prior to social communicative and other symptoms in the restricted and repetitive behavior (RRB) domain (Bolton et al., 2012; Kozlowski et al., 2011). These early sensory symptoms are also predictive of diagnostic status, social-communication deficits, and RRBs (Boyd et al., 2010; Turner-Brown, Baranek, Reznick, Watson, & Crais, 2013), and are related to impairments in daily functioning, increased anxiety, increased functional difficulties, and increased levels of parental stress (Ausderau et al., 2016; Hannant et al., 2016; Lane et al., 2010; Uljarević et al., 2016).

Consideration of specificities in sensory reactivity abnormalities (in conjunction with developmental, adaptive, and social communicative symptoms) is crucial to aid with treatment planning, as targeted treatments can hopefully reduce some of the associated difficulties mentioned above. For example, patients who are sensory seeking, such as those with ADNP syndrome, would greatly benefit from sensory input provided by occupational therapists to help them cope with potential feelings of anxiety or increase their ability to attend to other tasks. Furthermore, sensory techniques for hyporesponsivity, which was prevalent for children with PMS, can be integrated into school and family rituals to increase a child’s engagement and enjoyment in the activity or task at hand.

Our current gold-standard diagnostic assessments offer little in the characterization of the sensory phenotype, and are therefore ineffective to aid with this crucial component of intervention planning for patients. Other existing sensory assessments rely solely on patient or parent report, and therefore are either prone to bias by parent perception of their child's behaviors, or require sufficient patient verbal skills. Results from the current study demonstrate the continued feasibility of the SAND for individuals with iASD, as well as individuals with single-locus ASD—who often present with limited cognitive abilities. Thus, not only does this study demonstrate the continued importance of combining information for assessment from multiple sources (Kim & Lord, 2012; Risi et al., 2006), but also highlights the accessibility of the SAND due to its ability to be used with populations of varying verbal ability.

As neural sensory processing in the brain is well understood and has been evolutionarily conserved, sensory symptoms are a critical tool for translational research to better understand alterations of neural circuitry in ASD (Robertson & Baron-Cohen, 2017). Various *de novo* mutations to genes implicated in ASD, such as those which cause the single-locus conditions examined in the current study (i.e., *Shank3*, *Adnp*, and *Foxp1*), are known to converge on overlapping pathways implicated in synaptic transmission and plasticity, and early brain development (De Rubeis et al., 2014), and therefore likely affect global processes such as sensation and perception (Robertson & Baron-Cohen, 2017). Thus, gaining in-depth understandings of sensory phenotypes and processing in ADNP syndrome, FOXP1 syndrome, and PMS can help gain insight into the underlying neural dysfunction in ASD.

Biomarkers for ASD. Current clinical care, diagnostic assessments, and evaluation of treatment efficacy in ASD rely on subjective report and behavioral observations; however,

the heterogeneity of symptoms inherent to the disorder has impeded the success of clinical trials and outcome research. Researchers have thus increased efforts to search for reliable biomarkers, objective indicators of ASD symptomatology, ASD risk, and changes over time in response to treatment/intervention (McPartland, 2017). The ultimate goal is for biomarkers to be utilized in conjunction with current diagnostic tools to uncover underlying neuropathophysiology and eventually provide tailor targeted, personalized treatments based on these neural underpinnings. However, three overarching barriers have emerged that have impeded the development of "clinically practicable" biomarkers (i.e., markers that are applicable in clinical settings) in ASD thus far: 1) the heterogeneity of the disorder, 2) human development and the changes in symptoms over time, and 3) logistical considerations such as applicability, robustness to variations in behavior during acquisition of the marker itself, accessibility, and economy (McPartland, 2017).

Objective measures of sensory processing, and VEPs in particular, have emerged as a strong biomarker candidate, as VEPs have the ability to address these aforementioned barriers to biomarker discovery. First and foremost, VEPs offer an objective and reliable technique to elucidate underlying E/I imbalance in ASD, as the various VEP components are known to be generated by excitatory and inhibitory postsynaptic potentials in the cortex. VEPs have also been shown to be clinically relevant, as evidenced by significant correlations to behavioral aspects of the clinical phenotype, namely sensory reactivity and ASD general symptoms severity (Dickinson et al., 2018; Siper et al., 2019). Conclusions from the current study and our group's previous work have repeatedly shown that VEPs objectively differentiate individuals with iASD from TD controls (Siper et al., 2015; Siper et al., 2019; Weinger et al., 2014; Zweifach, 2016). Additionally, the current study and previous work by

Siper et al. (2019) demonstrate that VEPs can reliably parse the heterogeneity in ASD, as single-locus causes of ASD such as PMS and FOXP1 syndrome exhibit unique VEP profiles, and several iASD individuals display overlapping neural profiles with these single-locus groups. In addition, age-dependent developmental changes in VEPs are well documented (Creel, 2013; Dustman & Beck, 1966; McCulloch et al., 1999; Moskowitz & Sokol, 1983; Sokol & Jones, 1979; Spekreijse, 1978; Zemon et al., 1995), and age norms can feasibly be established in each laboratory (or groups of labs in a consortium utilizing the exact same VEP techniques), thereby taking developmental changes in the disorder into account. Finally, VEPs have repeatedly been shown to be feasible in infants, children, and adults with varying levels of cognitive ability and ASD symptomatology, and are therefore highly applicable. VEPs are also robust to variations in behavior and arousal, as they rely on low-level processes; in addition, certain behaviors, such as not looking at the stimuli or movement, can easily be monitored and remedied during the VEP procedure, and potential confounds, like vision problems, can easily be examined and accounted for. Moreover, VEPs are also highly accessible, as a Current Procedural Terminology (CPT) code for the VEP already exists and VEPs are already utilized in several physicians' practices. Additionally, as compared to neuroimaging and other costly techniques, VEPs are cost-effective and economical.

Utility of different tVEP components in clinical research. Importantly, the various components of the tVEP can serve different roles as biomarkers. Results from the current study and previous research indicate that amplitude and power show great inter-individual variability for participants within a diagnostic group (even a typically developing control group), and could potentially wash out differences in these variables among groups (Zemon & Gordon, 2018). The MSC statistic adjusts for these differences by normalizing the

responses obtained from individuals, and therefore may emerge as a superior measure to examine differences among groups. However, amplitude and power exhibit better agreement over time within an individual as compared to MSC (Zemon & Gordon, 2018); thus, power and amplitude may be useful and sensitive tools to examine how a particular individual changes and responds to a given treatment or intervention. Additionally, the high frequency power estimates, such as the square root of power in Frequency Bands 2 and 3, can serve as objective measures of early excitatory input to the cortex, thereby reducing any potential error that could occur when "picking off" critical time points from a tVEP waveform.

***Utility of short-duration stimuli*.** The current study bolsters the importance of the utility of the short condition for use as part of a conventional VEP stimulus battery. For most groups included in the current study, more participants were able to complete the short condition compared to the standard condition, suggesting greater feasibility in these younger and more severely affected populations. Additionally, while responses from contiguous EEG epochs in the standard condition are highly intercorrelated, responses to the short condition are independent, and thus may provide more accurate estimates of underlying neural activity under typical viewing conditions.

Study Limitations

There are several limitations in the current study. The small sample sizes, specifically in the single-locus ASD groups, represent a significant limitation. As this is a pilot exploratory study, multiple statistical tests were performed on these small samples, so there is the possibility of inflated Type I error, making some significant effects reported in the current study attributable to chance. In addition, in Study 1, several individuals across groups were missing scores for the Short Sensory Profile and Sensory Profile, limiting the study

sample size and making it difficult to meaningfully examine differences in parent-reports of behavioral sensory responsivity across groups.

The presence of visual problems in the ADNP and FOXP1 groups, though analyzed and accounted for, emerged as a significant limitation in the current study. The presence of significant visual problems makes it difficult to tease apart whether differences in tVEP responses were primarily related to visual problems or inherent to the respective genetic syndrome. Moreover, presence of visual problems was reported by parents, which may have been prone to misreporting and underreporting.

Additionally, the current study targeted a wide age range to obtain sufficient sample sizes for the single-locus ASD groups. As previously discussed, VEPs exhibit known developmental changes across the lifespan, and the current study sought to examine these developmental changes across groups. However, given the small sample sizes and the varied developmental nature of VEP components for each group, more intensive statistical techniques (i.e., using slope of outcome measure with age as a random effect in the LMM) could not be employed. Moreover, the current study exhibited significant differences in group composition based on sex, such that there were significantly more males in the iASD and ADNP groups, and more females in the FOXP1 group.

Finally, this is a cross-sectional study. Natural history studies examining these groups longitudinally would be particularly interesting in exploring developmental changes in these single-locus causes of ASD.

Future Directions

Future directions for the current project can capitalize on the study's limitations delineated above, as well as expand upon research in this area overall. Replicating the

findings for both behavioral and electrophysiological methods used in the current study in larger sample sizes would be important to assess the robustness and generalizability of these results. Ongoing studies with these populations are underway at the Seaver Autism Center to address this research need. While the current study sample included a broad age range, we anticipate that as the utilization of genetic testing as the standard of care in ASD diagnosis increases, so too will the number of individuals diagnosed with ADNP syndrome, FOXP1 syndrome, and PMS. These larger populations will then allow for examination of behavioral and electrophysiological sensory responsivity within more restricted age cohorts, as well as matching participants by age and sex. Longitudinal studies in these syndromes are also ongoing, which will increase exploration of developmental changes in these single-locus groups.

To ensure that visual abilities are better reported and tested directly, future studies could also use the spatial frequency-sweep VEP test to assess directly visual acuity in these populations, as using a Snellen chart would not be feasible given the cognitive limitations of these populations.

Future studies should also assess the utility and electrophysiological responses to additional VEP stimulus conditions, such as steady-state VEPs (ssVEPs) to isolated-check and radial pattern stimuli, which can target more specific visual processes, including direct-through excitatory pathways, long-range and short-range lateral inhibitory pathways, magnocellular and parvocellular pathways, ON and OFF pathways, shunting inhibition, neural noise (response variability), and spatial processing (Ratliff & Zemon, 1982; Zemon & Gordon, 2006; Zemon et al., 1988; Zemon et al., 1986; Zemon & Ratliff, 1982, 1984). As tVEP components rely on overlapping contributions from various neural pathways, using

these additional stimulus conditions can help tease apart the constituent pathways and mechanisms implicated in the tVEP and provide more targeted understanding of neural pathways implicated in iASD and these single-locus conditions. Recruitment at Seaver Autism Center for VEP studies using these stimulus conditions with these populations is also currently ongoing. Additionally, future studies using these tVEP techniques should examine phase data of the tVEP, as previous research (Zemon & Gordon, 2018) has uncovered that the phase of the 24^{th} harmonic frequency component can provide an objective estimate of P_{100} peak time, which would be critical for future replications of the results found in the current study.

In line with research conducted by Siper et al. (2019) examining tVEPs in children with PMS, future studies with ADNP and FOXP1 groups should explore how gene mutation type and/or deletion size are related to behavioral and electrophysiological outcomes used in the current study. This will further elucidate genotype-phenotype relationships in these disorders.

Moreover, future directions should include VEPs to measure treatment response for behavioral interventions and pharmacological treatments that specifically target glutamatergic and/or GABAergic mechanisms, or to help aid prediction of treatment response.

Conclusion

In summary, this is the first known exploratory study to deeply phenotype the sensory domain in three single-locus causes of ASD, and to provide information about underlying pathophysiology in ADNP and FOXP1 syndromes. While additional research is imperative to replicate results, the current study uncovered clear, distinct profiles of sensory reactivity in

PMS and ADNP syndrome, and demonstrated continued support for evidence of impaired glutamatergic signaling in iASD and single-locus causes of ASD, thereby elucidating the nature of the E/I imbalance in ASD. Results also demonstrated the meaningful relationship between behavioral and electrophysiological measures. The results overwhelmingly stress the utility of VEPs as a biomarker in ASD as an objective, clinically meaningful, applicable, accessible, developmentally-sensitive, and economical stratification tool, thus contributing significantly to clinical research and practice moving forward.

References

American Psychiatric Association. (2013). *Diagnostic and Statistical Manual of Mental Disorders: DSM-5*. Washington, D.C: American Psychiatric Association.

Amir, R. E., Van den Veyver, I. B., Wan, M., Tran, C. Q., Francke, U., & Zoghbi, H. Y. (1999). Rett syndrome is caused by mutations in X-linked MECP2, encoding methyl-CpG-binding protein 2. *Nat Genet, 23*(2), 185.

Amram, N., Hacohen-Kleiman, G., Sragovich, S., Malishkevich, A., Katz, J., Touloumi, O., . . . Yeheskel, A. (2016). Sexual divergence in microtubule function: the novel intranasal microtubule targeting SKIP normalizes axonal transport and enhances memory. *Molecular Psychiatry, 21*(10), 1467-1476.

Araujo, D. J., Anderson, A. G., Berto, S., Runnels, W., Harper, M., Ammanuel, S., . . . Loerwald, K. W. (2015). FoxP1 orchestration of ASD-relevant signaling pathways in the striatum. *Genes & development, 29*(20), 2081-2096.

Araujo, D. J., Toriumi, K., Escamilla, C. O., Kulkarni, A., Anderson, A. G., Harper, M., . . . Birnbaum, S. G. (2017). Foxp1 in forebrain pyramidal neurons controls gene expression required for spatial learning and synaptic plasticity. *Journal of Neuroscience, 37*(45), 10917-10931.

Ausderau, K. K., Furlong, M., Sideris, J., Bulluck, J., Little, L. M., Watson, L. R., . . . Baranek, G. T. (2014). Sensory Subtypes in Children with Autism Spectrum

Disorder: Latent Profile Transition Analysis using a National Survey of Sensory Features. *J Child Psychol Psychiatry, 55*(8), 935-944. doi:10.1111/jcpp.12219

Ausderau, K. K., Sideris, J., Furlong, M., Little, L. M., Bulluck, J., & Baranek, G. T. (2014). National Survey of Sensory Features in Children with ASD: Factor Structure of the Sensory Experience Questionnaire (3.0). *Journal of autism and developmental disorders, 44*(4), 915-925. doi:10.1007/s10803-013-1945-1

Ausderau, K. K., Sideris, J., Little, L. M., Furlong, M., Bulluck, J. C., & Baranek, G. T. (2016). Sensory subtypes and associated outcomes in children with autism spectrum disorders. *Autism Research, 9*(12), 1316-1327.

Ayres, A. J. (1989). Sensory Integration and Praxis Tests. In. Los Angeles, CA: Western Psychological Services.

Bacon, C., Schneider, M., Le Magueresse, C., Froehlich, H., Sticht, C., Gluch, C., . . . Rappold, G. (2015). Brain-specific Foxp1 deletion impairs neuronal development and causes autistic-like behaviour. *Mol Psychiatry, 20*(5), 632-639.

Bailey, A., Le Couteur, A., Gottesman, I., Bolton, P., Simonoff, E., Yuzda, E., & Rutter, M. (1995). Autism as a strongly genetic disorder: evidence from a British twin study. *Psychol Med, 25*(1), 63-77. Retrieved from http://www.ncbi.nlm.nih.gov/entrez/query.fcgi?cmd=Retrieve&db=PubMed&dopt=Citation&list_uids=7792363

Baio, J. (2012). Prevalence of Autism Spectrum Disorders: Autism and Developmental Disabilities Monitoring Network, 14 Sites, United States, 2008. Morbidity and Mortality Weekly Report. Surveillance Summaries. Volume 61, Number 3. *Centers for Disease Control and Prevention*.

Baio, J., Wiggins, L., Christensen, D. L., Maenner, M. J., Daniels, J., Warren, Z., . . . Dowling, N. F. (2018). Prevalence of Autism Spectrum Disorder Among Children Aged 8 Years — Autism and Developmental Disabilities Monitoring Network, 11 Sites, United States, 2014. *MMWR Surveill Summ, 67*(No. SS-6), 1-23. doi:http://dx.doi.org/10.15585/mmwr.ss6706a1.

Banham, A. H., Beasley, N., Campo, E., Fernandez, P. L., Fidler, C., Gatter, K., . . . Cordell, J. L. (2001). The FOXP1 winged helix transcription factor is a novel candidate tumor suppressor gene on chromosome 3p. *Cancer Research, 61*, 8820-8829.

Baranek, G. T. (1999). Sensory processing assessment for young children (SPA). *Unpublished manuscript, University of North Carolina at Chapel Hill*.

Baranek, G. T. (2010). Tactile defensiveness and discrimination test–revised (TDDT-R). *Unpublished manuscript*.

Baranek, G. T., David, F. J., Poe, M. D., Stone, W. L., & Watson, L. R. (2006). Sensory Experiences Questionnaire: discriminating sensory features in young children with autism, developmental delays, and typical development. *Journal of Child Psychology and Psychiatry*, *47*(6), 591-601.

Baranek, G. T., Roberts, J. E., David, F. J., Sideris, J., Mirrett, P. L., Hatton, D. D., & Bailey, D. B., Jr. (2008). Developmental trajectories and correlates of sensory processing in young boys with fragile X syndrome. *Phys Occup Ther Pediatr, 28*(1), 79-98.

Bear, M. F., Huber, K. M., & Warren, S. T. (2004). The mGluR theory of fragile X mental retardation. *Trends in Neurosciences, 27*(7), 370-377.

Ben-Sasson, A., Hen, L., Fluss, R., Cermak, S. A., Engel-Yeger, B., & Gal, E. (2009). A meta-analysis of sensory modulation symptoms in individuals with autism spectrum disorders. *J Autism Dev Disord, 39*(1), 1-11.

Bhaskar, P., Vanchilingam, S., Bhaskar, E. A., Devaprabhu, A., & Ganesan, R. (1986). Effect of L-dopa on visual evoked potential in patients with Parkinson's disease. *Neurology, 36*(8), 1119-1119.

Bishop, S. L., Farmer, C., Bal, V., Robinson, E. B., Willsey, A. J., Werling, D. M., . . . Thurm, A. (2017). Identification of developmental and behavioral markers associated with genetic abnormalities in autism spectrum disorder. *American Journal of Psychiatry, 174*(6), 576-585.

Blumberg, S. J., Bramlett, M. D., Kogan, M. D., Schieve, L. A., Jones, J. R., & Lu, M. C. (2013). *Changes in prevalence of parent-reported autism spectrum disorder in school-aged US children: 2007 to 2011-2012*: US Department of Health and Human Services, Centers for Disease Control and Prevention, National Center for Health Statistics.

Blundell, J., Blaiss, C. A., Etherton, M. R., Espinosa, F., Tabuchi, K., Walz, C., . . . Powell, C. M. (2010). Neuroligin-1 deletion results in impaired spatial memory and increased repetitive behavior. *Journal of Neuroscience, 30*(6), 2115-2129.

Bodis-Wollner, I., & Yahr, M. D. (1978). Measurements of visual evoked potentials in Parkinson's disease. *Brain: a journal of neurology, 101*(4), 661-671.

Bodis-Wollner, I., Hendley, C. D., Mylin, L. H., & Thornton, J. (1979). Visual evoked potentials and the visuogram in multiple sclerosis. *Annals of neurology, 5*(1), 40-47.

Boeckers, T. M. (2006). The postsynaptic density. *Cell Tissue Res, 326*(2), 409-422. doi:10.1007/s00441-006-0274-5

Bolton, P. F., Golding, J., Emond, A., & Steer, C. D. (2012). Autism spectrum disorder and autistic traits in the Avon Longitudinal Study of Parents and Children: precursors and early signs. *J Am Acad Child Adolesc Psychiatry, 51*(3), 249-260.e225. doi:10.1016/j.jaac.2011.12.009

Bonaglia, M. C., Marelli, S., Gottardi, G., Zucca, C., Pramparo, T., Giorda, R., . . . Zuffardi, O. (2007). Subtelomeric trisomy 21q: a new benign chromosomal variant. *Eur J Med Genet, 50*(1), 54-59. doi:10.1016/j.ejmg.2006.07.001

Boyd, B. A., & Baranek, G. (2005). Sensory Questionnaire (SQ). *Unpublished manuscript, University of North Carolina, Chapel Hill, NC.*

Boyd, B. a., Baranek, G. T., Sideris, J., Poe, M. D., Watson, L. R., Patten, E., & Miller, H. (2010). Sensory features and repetitive behaviors in children with autism and developmental delays. *Autism Research, 3*(2), 78-87.

Boyd, B. A., McBee, M., Holtzclaw, T., Baranek, G. T., & Bodfish, J. W. (2009). Relationships among repetitive behaviors, sensory features, and executive functions in high functioning autism. *Research in Autism Spectrum Disorders, 3*(4), 959-966.

Bozdagi, O., Sakurai, T., Papapetrou, D., Wang, X., Dickstein, D. L., Takahashi, N., . . . Buxbaum, J. D. (2010). Haploinsufficiency of the autism-associated Shank3 gene leads to deficits in synaptic function, social interaction, and social communication. *Mol Autism, 1*(1), 15. doi:10.1186/2040-2392-1-15

Bozdagi, O., Tavassoli, T., & Buxbaum, J. D. (2013). Insulin-like growth factor-1 rescues synaptic and motor deficits in a mouse model of autism and developmental delay. *Mol Autism, 4*(1), 9. doi:10.1186/2040-2392-4-9

Buescher, A. V., Cidav, Z., Knapp, M., & Mandell, D. S. (2014). Costs of autism spectrum disorders in the United Kingdom and the United States. *JAMA Pediatr, 168*(8), 721-728. doi:10.1001/jamapediatrics.2014.210

Butler, P. D., Schechter, I., Zemon, V., Schwartz, S. G., Greenstein, V. C., Gordon, J., . . . Javitt, D. C. (2001). Dysfunction of early-stage visual processing in schizophrenia. *American Journal of Psychiatry, 158*(7), 1126-1133.

Butler, P. D., Zemon, V., Schechter, I., Saperstein, A. M., Hoptman, M. J., Lim, K. O., . . . Javitt, D. C. (2005). Early-stage visual processing and cortical amplification deficits in schizophrenia. *Archives of General Psychiatry, 62*(5), 495-504.

Carlson, N. R. (2010). *Physiology of Behavior* (10th ed.). Boston: Allyn & Bacon.

Celesia, G. G. (1982). STEADY-STATE AND TRANSIENT VISUAL EVOKED POTENTIALS IN CLINICAL PRACTICE. *Ann N Y Acad Sci, 388*(1), 290-305.

Celesia, G. G., & Kaufman, D. (1985). Pattern ERGs and visual evoked potentials in maculopathies and optic nerve diseases. *Investigative Ophthalmology & Visual Science, 26*(5), 726-735.

Censi, S., Simard, M., Mottron, L., Saint-Amour, D., & Bertone, A. (2014). Assessing lateral interactions within the early visual areas of adults with autism. *J Vis, 14*(10), 672-672. doi:10.1167/14.10.672

Chen, L., & Toth, M. (2001). Fragile X mice develop sensory hyperreactivity to auditory stimuli. *Neuroscience, 103*(4), 1043-1050.

Chien, W.-H., Gau, S.-F., Chen, C.-H., Tsai, W.-C., Wu, Y.-Y., Chen, P.-H., . . . Chen, C.-H. (2013). Increased gene expression of FOXP1 in patients with autism spectrum disorders. *Mol Autism, 4*(1), 23.

Christensen, D. L., Baio, J., Van Naarden Braun, K., Bilder, D., Charles, J., Constantino, J. N., . . . Yeargin-Allsopp, M. (2016). Prevalence and Characteristics of Autism Spectrum Disorder Among Children Aged 8 Years--Autism and Developmental Disabilities Monitoring Network, 11 Sites, United States, 2012. *MMWR Surveill Summ, 65*(3), 1-23. doi:10.15585/mmwr.ss6503a1

Coghlan, S., Horder, J., Inkster, B., Mendez, M. A., Murphy, D. G., & Nutt, D. J. (2012). GABA system dysfunction in autism and related disorders: from synapse to symptoms. *Neurosci Biobehav Rev, 36*(9), 2044-2055. doi:10.1016/j.neubiorev.2012.07.005

Cohen, J. E. (1988). *Statistical Power Analysis for the Behavioral Sciences*. Hillside, NJ: Lawrence Erlbaum Associates, Inc.

Conte, M. M., & Victor, J. D. (2009). VEP indices of cortical lateral interactions in epilepsy treatment. *Vision Res, 49*(9), 898-906. doi:10.1016/j.visres.2008.04.030

Cooper, G. M., Coe, B. P., Girirajan, S., Rosenfeld, J. A., Vu, T. H., Baker, C., . . . Eichler, E. E. (2011). A copy number variation morbidity map of developmental delay. *Nat Genet, 43*(9), 838-846. doi:10.1038/ng.909

Coppola, G., Parisi, V., Di Lorenzo, C., Serrao, M., Magis, D., Schoenen, J., & Pierelli, F. (2013). Lateral inhibition in visual cortex of migraine patients between attacks. *The Journal of Headache and Pain, 14*(20).

Corrigan, N. M., Shaw, D. W., Estes, A. M., Richards, T. L., Munson, J., Friedman, S. D., . . . Dager, S. R. (2013). Atypical developmental patterns of brain chemistry in children with autism spectrum disorder. *JAMA psychiatry, 70*(9), 964-974.

Coskun, M. A., Loveland, K. A., Pearson, D. A., Papanicolaou, A. C., & Sheth, B. R. (2013a). Functional assays of local connectivity in the somatosensory cortex of individuals with autism. *Autism Res, 6*(3), 190-200. doi:10.1002/aur.1276

Coskun, M. A., Loveland, K. A., Pearson, D. A., Papanicolaou, A. C., & Sheth, B. R. (2013b). Interaction of finger representations in the cortex of individuals with autism: a functional window into cortical inhibition. *Autism Res, 6*(6), 542-549. doi:10.1002/aur.1314

Creel, D. J. (2013). Visual Evoked Potentials. In H. Kolb, R. Nelson, E. Fernandez, & B. Jones (Eds.), *Webvision: The Organization of the Retina and Visual System*.

Creutzfeldt, O. D., & Kuhnt, U. (1973). Electrophysiology and topographical distribution of visual evoked potentials in animals. In *Visual Centers in the Brain* (pp. 595-646): Springer.

De Rubeis, S., He, X., Goldberg, A. P., Poultney, C. S., Samocha, K., Cicek, A. E., . . . Walker, S. (2014). Synaptic, transcriptional and chromatin genes disrupted in autism. *Nature, 515*(7526), 209.

De Vries-Khoe, L., & Spekreijse, H. (1982). Maturation of luminance and pattern EPs in man. *Doc Ophthalmol Proc Ser, 31*, 461-475.

DeVito, T. J., Drost, D. J., Neufeld, R. W., Rajakumar, N., Pavlosky, W., Williamson, P., & Nicolson, R. (2007). Evidence for cortical dysfunction in autism: a proton magnetic resonance spectroscopic imaging study. *Biological Psychiatry, 61*(4), 465-473.

Dickinson, A., Bruyns-Haylett, M., Jones, M., & Milne, E. (2015). Increased peak gamma frequency in individuals with higher levels of autistic traits. *Eur J Neurosci, 41*(8), 1095-1101. doi:10.1111/ejn.12881

Dickinson, A., Bruyns-Haylett, M., Smith, R., Jones, M., & Milne, E. (2016). Superior orientation discrimination and increased peak gamma frequency in autism spectrum conditions. *J Abnorm Psychol, 125*(3), 412-422. doi:10.1037/abn0000148

Dickinson, A., Gomez, R., Jones, M., Zemon, V., & Milne, E. (2018). Lateral inhibition in the autism spectrum: An SSVEP study of visual cortical lateral interactions. *Neuropsychologia, 111,* 369-376.

Dickinson, A., Jones, M., & Milne, E. (2016). Measuring neural excitation and inhibition in autism: different approaches, different findings and different interpretations. *Brain Res, 1648*, 277-289.

Duffy, F. H., Burchfiel, J. L., & Conway, J. L. (1976). Bicuculline reversal of deprivation amblyopia in the cat. *Nature, 260*(5548), 256-257. doi:10.1038/260256a0

Dunn, W. (1999). Short sensory profile. *San Antonio, TX: Psychological Corporation*.

Dunn, W., & Westman, K. (1997). The sensory profile: the performance of a national sample of children without disabilities. *American Journal of Occupational Therapy, 51*(1), 25-34.

Durand, C. M., Betancur, C., Boeckers, T. M., Bockmann, J., Chaste, P., Fauchereau, F., . . . Anckarsäter, H. (2007). Mutations in the gene encoding the synaptic scaffolding protein SHANK3 are associated with autism spectrum disorders. *Nature Genetics, 39*(1), 25-27.

Durand, C. M., Perroy, J., Loll, F., Perrais, D., Fagni, L., Bourgeron, T., . . . Sans, N. (2012). SHANK3 mutations identified in autism lead to modification of dendritic spine morphology via an actin-dependent mechanism. *Mol Psychiatry, 17*(1), 71-84. doi:10.1038/mp.2011.57

Dustman, R. E., & Beck, E. C. (1966). Visually evoked potentials: amplitude changes with age. *Science, 151*(3713), 1013-1015.

Ehlers, M. D. (1999). Synapse structure: Glutamate receptors connected by the shanks. *Current Biology, 9*(22), R848-R850. doi:https://doi.org/10.1016/S0960-9822(00)80043-3

Elliott, C. (2007). *Differential Ability Scales (2nd ed.)*. San Antonio, Tx: Harcourt Assessment.

Fakhoury, M. (2018). Imaging genetics in autism spectrum disorders: Linking genetics and brain imaging in the pursuit of the underlying neurobiological mechanisms. *Prog Neuropsychopharmacol Biol Psychiatry, 80*(Pt B), 101-114. doi:10.1016/j.pnpbp.2017.02.026

Faul, F., Erdfelder, E., Lang, A. G., & Buchner, A. (2007). G*Power 3: A flexible statistical power analysis program for the social, behavioral, and biomedical sciences. *Behavior Research Methods, 39*, 175-191.

Ferland, R. J., Cherry, T. J., Preware, P. O., Morrisey, E. E., & Walsh, C. A. (2003). Characterization of Foxp2 and Foxp1 mRNA and protein in the developing and mature brain. *Journal of Comparative Neurology, 460*(2), 266-279.

Fombonne, E. (2009). Epidemiology of pervasive developmental disorders. *Pediatric research, 65*(6), 591-598.

Foss-Feig, J. H., Adkinson, B. D., Ji, J. L., Yang, G., Srihari, V. H., McPartland, J. C., . . . Anticevic, A. (2017). Searching for cross-diagnostic convergence: neural mechanisms governing excitation and inhibition balance in schizophrenia and autism spectrum disorders. *Biological Psychiatry, 81*(10), 848-861.

Frank, Y., Jamison, J. M., Trelles, M. P., Siper, P. M., Tavassoli, T., Soorya, L. V., . . . Kolevzon, A. (2017). A Prospective Study of Neurological Abnormalities in Phelan-McDermid Syndrome. *Journal of Rare Disorders, 5*(1).

Fröhlich, H., Rafiullah, R., Schmitt, N., Abele, S., & Rappold, G. A. (2017). Foxp1 expression is essential for sex-specific murine neonatal ultrasonic vocalization. *Human Molecular Genetics, 26*(8), 1511-1521.

Gauthier, J., Spiegelman, D., Piton, A., Lafrenière, R. G., Laurent, S., St-Onge, J., . . . Rouleau, G. A. (2009). Novel de novo SHANK3 mutation in autistic patients. *Am J Med Genet B Neuropsychiatr Genet, 150B*(3), 421-424. doi:10.1002/ajmg.b.30822

Geschwind, D. H. (2011). Genetics of autism spectrum disorders. *Trends Cogn Sci, 15*(9), 409-416. doi:10.1016/j.tics.2011.07.003

Ghilardi, M. F., Sartucci, F., Brannan, J. R., Onofrj, M. C., Bodis-Wollner, I., Mylin, L., & Stroch, R. (1991). N70 and P100 can be independently affected in multiple sclerosis. *Electroencephalography and Clinical Neurophysiology/Evoked Potentials Section, 80*(1), 1-7.

Greenstein, V. C., Seliger, S., Zemon, V., & Ritch, R. (1998). Visual evoked potential assessment of the effects of glaucoma on visual subsystems. *Vision Research, 38*(12), 1901-1911.

Hamdan, F. F., Daoud, H., Rochefort, D., Piton, A., Gauthier, J., Langlois, M., . . . Michaud, J. L. (2010). De novo mutations in FOXP1 in cases with intellectual disability, autism, and language impairment. *Am J Hum Genet, 87*(5), 671-678. doi:10.1016/j.ajhg.2010.09.017

Hannant, P., Tavassoli, T., & Cassidy, S. (2016). The Role of Sensorimotor Difficulties in Autism Spectrum Conditions. *Frontiers in Neurology, 7*, 124. doi:10.3389/fneur.2016.00124

Helsmoortel, C., Vulto-van Silfhout, A. T., Coe, B. P., Vandeweyer, G., Rooms, L., Van Den Ende, J., . . . Vissers, L. E. (2014). A SWI/SNF-related autism syndrome caused by de novo mutations in ADNP. *Nat Genet, 46*(4), 380-384.

Hennerici, M., Wenzel, D., & Freund, H. (1977). The comparison of small-size rectangle and checkerboard stimulation for the evaluation of delayed visual evoked responses in patients suspected of multiple sclerosis. *Brain: a journal of neurology, 100*, 119.

Hisaoka, T., Nakamura, Y., Senba, E., & Morikawa, Y. (2010). The forkhead transcription factors, Foxp1 and Foxp2, identify different subpopulations of projection neurons in the mouse cerebral cortex. *Neuroscience, 166*(2), 551-563.

Horlin, C., Falkmer, M., Parsons, R., Albrecht, M. A., & Falkmer, T. (2014). The cost of autism spectrum disorders. *PLoS One, 9*(9), e106552-e106552. doi:10.1371/journal.pone.0106552

Kaplan, E. (1991). The receptive field structure of retinal ganglion cells in cat and monkey. In A. Leventhal (Ed.), *Vision and Visual Dysfunction* (pp. 10-40). Boston: CRC Press.

Kaplan, E. (2003). The M, P and K pathways in the primate visual system. *The Visual Neurosciences, 1*.

Kaplan, E., & Shapley, R. (1986). The primate retina contains two types of ganglion cells, with high and low contrast sensitivity. *Proc Natl Acad Sci U S A, 83*(8), 2755-2757.

Kim, D., Wylie, G., Pasternak, R., Butler, P. D., & Javitt, D. C. (2006). Magnocellular contributions to impaired motion processing in schizophrenia. *Schizophr Res, 82*(1), 1-8.

Kim, D., Zemon, V., Saperstein, A., Butler, P. D., & Javitt, D. C. (2005). Dysfunction of early-stage visual processing in schizophrenia: harmonic analysis. *Schizophr Res, 76*(1), 55-65. doi:10.1016/j.schres.2004.10.011

Kim, S. H., & Lord, C. (2012). Combining information from multiple sources for the diagnosis of autism spectrum disorders for toddlers and young preschoolers from 12 to 47 months of age. *J Child Psychol Psychiatry, 53*(2), 143-151. doi:10.1111/j.1469-7610.2011.02458.x

Kleinman, J. M., Ventola, P. E., Pandey, J., Verbalis, A. D., Barton, M., Hodgson, S., . . . Fein, D. (2008). Diagnostic stability in very young children with autism spectrum disorders. *J Autism Dev Disord, 38*(4), 606-615. doi:10.1007/s10803-007-0427-8

Klem, G. H., Lüders, H. O., Jasper, H. H., & Elger, C. (1999). The ten-twenty electrode system of the International Federation. . *Electroencephalogr Clin Neurophysiol,, 52*(3), 3-6.

Knoth, I. S., Vannasing, P., Major, P., Michaud, J. L., & Lippe, S. (2014). Alterations of visual and auditory evoked potentials in fragile X syndrome. *Int J Dev Neurosci, 36*, 90-97. doi:10.1016/j.ijdevneu.2014.05.003

Konstantareas, M. M., & Hewitt, T. (2001). Autistic Disorder and Schizophrenia: Diagnostic Overlaps. *J Autism Dev Disord, 31*(1), 10.

Kozlowski, A. M., Matson, J. L., Horovitz, M., Worley, J. A., & Neal, D. (2011). Parents' first concerns of their child's development in toddlers with autism spectrum disorders. *Dev Neurorehabil, 14*(2), 72-78. doi:10.3109/17518423.2010.539193

Krumm, N., O'Roak, B. J., Shendure, J., & Eichler, E. E. (2014). A de novo convergence of autism genetics and molecular neuroscience. *Trends Neurosci, 37*(2), 95-105.

Lane, A. E., Molloy, C. A., & Bishop, S. L. (2014). Classification of children with autism spectrum disorder by sensory subtype: a case for sensory-based phenotypes. *Autism Res, 7*(3), 322-333. doi:10.1002/aur.1368

Lane, A. E., Young, R. L., Baker, A. E. Z., & Angley, M. T. (2010). Sensory processing subtypes in autism: Association with adaptive behavior. *Journal of autism and developmental disorders, 40*(1), 112-122.

Lavelle, T. A., Weinstein, M. C., Newhouse, J. P., Munir, K., Kuhlthau, K. A., & Prosser, L. A. (2014). Economic burden of childhood autism spectrum disorders. *Pediatrics, 133*(3), e520-529. doi:10.1542/peds.2013-0763

Le Fevre, A. K., Taylor, S., Malek, N. H., Horn, D., Carr, C. W., Abdul-Rahman, O. A., . . . Hunter, M. F. (2013). FOXP1 mutations cause intellectual disability and a recognizable phenotype. *Am J Med Genet A, 161a*(12), 3166-3175. doi:10.1002/ajmg.a.36174

LeBlanc, J. J., DeGregorio, G., Centofante, E., Vogel-Farley, V. K., Barnes, K., Kaufmann, W. E., . . . Nelson, C. A. (2015). Visual evoked potentials detect cortical processing deficits in Rett syndrome. *Ann Neurol, 78*(5), 775-786. doi:10.1002/ana.24513

Leblond, C. S., Nava, C., Polge, A., Gauthier, J., Huguet, G., Lumbroso, S., . . . Bourgeron, T. (2014). Meta-analysis of SHANK Mutations in Autism Spectrum Disorders: A

Gradient of Severity in Cognitive Impairments. *PLoS Genet, 10*(9), e1004580. doi:10.1371/journal.pgen.1004580

Leekam, S. R., Nieto, C., Libby, S. J., Wing, L., & Gould, J. (2007). Describing the sensory abnormalities of children and adults with autism. *J Autism Dev Disord, 37*(5), 894-910. doi:10.1007/s10803-006-0218-7

Levi, D., & Manny, R. (1986). The VEP in the diagnostic evaluation of amblyopia. *Frontiers of clinical neuroscience, 3*, 437-446.

Li, X., Xiao, J., Frohlich, H., Tu, X., Li, L., Xu, Y., . . . Chen, J. G. (2015). Foxp1 regulates cortical radial migration and neuronal morphogenesis in developing cerebral cortex. *PLoS One, 10*(5), e0127671. doi:10.1371/journal.pone.0127671

Lord, C., Rutter, M., DiLavore, P. C., Risi, S., Gotham, K., & Bishop, S. (2012). *Autism diagnostic observation schedule: ADOS-2*: Western Psychological Services Los Angeles, CA.

Lord, C., Rutter, M., & Le Couteur, A. L. (1994). Autism Diagnostic Interview-Revised: A revised version of a diagnostic interview for caregivers of individuals with possible pervasive developmental disorders. *Journal of autism and developmental disorders, 24*(5), 659-685.

Lurie, S. (2018). *Assessing Lateral Interactions in Autism Spectrum Disorder using Visual Evoked Potentials*. Master's Thesis. Psychology. Ferkauf Graduate School of Psychology, Yeshiva University.

Mandel, S., & Gozes, I. (2007). Activity-dependent neuroprotective protein constitutes a novel element in the SWI/SNF chromatin remodeling complex. *J Biol Chem, 282*(47), 34448-34456. doi:10.1074/jbc.M704756200

Mandel, S., Rechavi, G., & Gozes, I. (2007). Activity-dependent neuroprotective protein (ADNP) differentially interacts with chromatin to regulate genes essential for embryogenesis. *Dev Biol, 303*(2), 814-824. doi:10.1016/j.ydbio.2006.11.039

Mandel, S., Spivak-Pohis, I., & Gozes, I. (2008). ADNP differential nucleus/cytoplasm localization in neurons suggests multiple roles in neuronal differentiation and maintenance. *J Mol Neurosci, 35*(2), 127-141. doi:10.1007/s12031-007-9013-y

Marshall, C. R., Noor, A., Vincent, J. B., Lionel, A. C., Feuk, L., Skaug, J., . . . Ren, Y. (2008). Structural variation of chromosomes in autism spectrum disorder. *The American Journal of Human Genetics, 82*(2), 477-488.

McCulloch, D. L., Orbach, H., & Skarf, B. (1999). Maturation of the pattern-reversal VEP in human infants: a theoretical framework. *Vision Res, 39*, 3673-3680.

McPartland, J. C. (2017). Developing Clinically Practicable Biomarkers for Autism Spectrum Disorder. *J Autism Dev Disord, 47*(9), 2935-2937. doi:10.1007/s10803-017-3237-7

Mieses, A., Tavassoli, T., Li, E., Soorya, L., Lurie, S., Wang, A., . . . Kolevzon, A. (2016). Brief report: sensory reactivity in children with Phelan–McDermid Syndrome. *Journal of autism and developmental disorders, 46*(7), 2508-2513.

Miller, L. J., McIntosh, D., McGrath, J., Shyu, V., Lampe, M., Taylor, A., . . . Hagerman, R. (1999). Electrodermal responses to sensory stimuli in individuals with fragile X syndrome: a preliminary report. *American Journal of Medical Genetics, 83*(4), 268-279.

Moessner, R., Marshall, C. R., Sutcliffe, J. S., Skaug, J., Pinto, D., Vincent, J., . . . Scherer, S. W. (2007). Contribution of SHANK3 mutations to autism spectrum disorder. *Am J Hum Genet, 81*(6), 1289-1297. doi:10.1086/522590

Moskowitz, A., & Sokol, S. (1983). Developmental Changes in the Human Visual System As Reflected by the Latency of the Pattern Reversal VEP. *Electroencephalography and Clinical Neurophysiology, 56.*

Mullen, E. M. (1995). *Mullen Scales of Early Learning*. Circle Pines, MN: American Guidance Services, Inc.

Ohl, A., Butler, C., Carney, C., Jarmel, E., Palmieri, M., Pottheiser, D., & Smith, T. (2012). Test-retest reliability of the sensory profile caregiver questionnaire. *Am J Occup Ther, 66*(4), 483-487. doi:10.5014/ajot.2012.003517

Orinstein, A. J., Helt, M., Troyb, E., Tyson, K. E., Barton, M. L., Eigsti, I.-M., . . . Fein, D. A. (2014). Intervention for optimal outcome in children and adolescents with a history of autism. *J Dev Behav Pediatr, 35*(4), 247-256. doi:10.1097/DBP.0000000000000037

Oz, S., Kapitansky, O., Ivashco-Pachima, Y., Malishkevich, A., Giladi, E., Skalka, N., . . . Hirsch, J. (2014). The NAP motif of activity-dependent neuroprotective protein (ADNP) regulates dendritic spines through microtubule end binding proteins. *Molecular Psychiatry, 19*(10), 1115-1124.

Ozonoff, S., Young, G. S., Carter, A., Messinger, D., Yirmiya, N., Zwaigenbaum, L., . . . Dobkins, K. (2011). Recurrence risk for autism spectrum disorders: a Baby Siblings Research Consortium study. *Pediatrics, 128*(3), e488-e495.

Patten, E., Ausderau, K. K., Watson, L. R., & Baranek, G. T. (2013). Sensory response patterns in nonverbal children with ASD. *Autism research and treatment, 2013*.

Pinhasov, A., Mandel, S., Torchinsky, A., Giladi, E., Pittel, Z., Goldsweig, A. M., . . . Gozes, I. (2003). Activity-dependent neuroprotective protein: a novel gene essential for brain formation. *Developmental Brain Research, 144*(1), 83-90. doi:https://doi.org/10.1016/S0165-3806(03)00162-7

Purpura, D. P. (1959). Nature of electrocortical potentials and synaptic organizations in cerebral and cerebellar cortex. *International review of neurobiology, 1*, 47-163.

Ratliff, F., & Zemon, V. (1982). Some new methods for the analysis of lateral interactins that influence the visual evoked potential.

Regan, D. (1977). Speedy assessment of visual acuity in amblyopia by the evoked potential method. *Ophthalmologica, 175*(3), 159-164.

Regan, D., Milner, B., & Heron, J. (1977). Slowing of visual signals in multiple sclerosis, measured psychophysically and by steady-state evoked potentials. *Visual evoked potentials in man: new developments*, 461-469.

Risi, S., Lord, C., Gotham, K., Corsello, C., Chrysler, C., Szatmari, P., . . . Pickles, A. (2006). Combining information from multiple sources in the diagnosis of autism spectrum disorders. *J Am Acad Child Adolesc Psychiatry, 45*(9), 1094-1103. doi:10.1097/01.chi.0000227880.42780.0e

Ritvo, E. R., Freeman, B., Mason-Brothers, A., Mo, A., & Ritvo, A. M. (1985). Concordance for the syndrome of autism in 40 pairs of afflicted twins. *Am J Psychiatry*.

Robertson, C. E., & Baron-Cohen, S. (2017). Sensory perception in autism. *Nature Reviews Neuroscience, 18*(11), 671-684.

Roid, G. H. (2003). *Stanford Binet intelligence scales (5th ed.)*. Itasca, IL: Riverside Publishing.

Rosenberg, R. E., Law, J. K., Yenokyan, G., McGready, J., Kaufmann, W. E., & Law, P. A. (2009). Characteristics and concordance of autism spectrum disorders among 277 twin pairs. *Arch Pediatr Adolesc Med, 163*(10), 907-914.

Rubenstein, J., & Merzenich, M. M. (2003). Model of autism: increased ratio of excitation/inhibition in key neural systems. *Genes, Brain and Behavior, 2*(5), 255-267.

Sakai, Y., Shaw, C. A., Dawson, B. C., Dugas, D. V., Al-Mohtaseb, Z., Hill, D. E., & Zoghbi, H. Y. (2011). Protein interactome reveals converging molecular pathways among autism disorders. *Sci Transl Med, 3*(86), 86ra49. doi:10.1126/scitranslmed.3002166

Schechter, I., Butler, P. D., Zemon, V. M., Revheim, N., Saperstein, A. M., Jalbrzikowski, M., . . . Javitt, D. C. (2005). Impairments in generation of early-stage transient visual evoked potentials to magno-and parvocellular-selective stimuli in schizophrenia. *Clinical Neurophysiology, 116*(9), 2204-2215.

Schoen, S. A., Miller, L. J., Brett-Green, B. A., & Nielsen, D. M. (2009). Physiological and behavioral differences in sensory processing: A comparison of children with autism spectrum disorder and sensory modulation disorder. *Frontiers in Integrative Neuroscience, 3*, 29.

Schoen, S. A., Miller, L. J., & Green, K. E. (2008). Pilot study of the sensory over-responsivity scales: Assessment and inventory. *The American Journal of Occupational Therapy, 62*(4), 393.

Schoen, S. A., Miller, L. J., & Sullivan, J. C. (2014). Measurement in sensory modulation: the sensory processing scale assessment. *Am J Occup Ther, 68*(5), 522-530. doi:10.5014/ajot.2014.012377

Shcheglovitov, A., Shcheglovitova, O., Yazawa, M., Portmann, T., Shu, R., Sebastiano, V., . . . Dolmetsch, R. E. (2013). SHANK3 and IGF1 restore synaptic deficits in neurons from 22q13 deletion syndrome patients. *Nature, 503*(7475), 267-271. doi:10.1038/nature12618

Simmons, D. R., Robertson, A. E., McKay, L. S., Toal, E., McAleer, P., & Pollick, F. E. (2009). Vision in autism spectrum disorders. *Vision Res, 49*(22), 2705-2739. doi:10.1016/j.visres.2009.08.005

Siper, P. M., De Rubeis, S., Trelles, M. D. P., Durkin, A., Di Marino, D., Muratet, F., . . . Buxbaum, J. D. (2017). Prospective investigation of FOXP1 syndrome. *Mol Autism, 8*, 57. doi:10.1186/s13229-017-0172-6

Siper, P. M., Kolevzon, A., Wang, A. T., Buxbaum, J. D., & Tavassoli, T. (2017). A clinician-administered observation and corresponding caregiver interview capturing DSM-5 sensory reactivity symptoms in children with ASD. *Autism Research*.

Siper, P. M., Lurie, S., Kolevzon, A., Zemon, V., Gordon, J., Jamison, J., . . . Buxbaum, J. D. (2015). *Transient visual evoked potentials in monogenic and idiopathic ASD*. Paper presented at the International Meeting for Autism Research Salt Lake City, UT.

Siper, P. M., Rowe, M. A., Guillory, S., Rouhandeh, A. A., George-Jones, J. L., Tavassoli, T., . . . Kolevzon, A. (2019). Visual evoked potential abnormalities in Phelan-McDermid syndrome. *Manuscript submitted for publication*.

Siper, P. M., Zemon, V., Gordon, J., George-Jones, J., Lurie, S., Zweifach, J., . . . Kolevzon, A. (2016). Rapid and Objective Assessment of Neural Function in Autism Spectrum Disorder Using Transient Visual Evoked Potentials. *PLoS One, 11*(10), e0164422. doi:10.1371/journal.pone.0164422

Snijders, T. M., Milivojevic, B., & Kemner, C. (2013). Atypical excitation-inhibition balance in autism captured by the gamma response to contextual modulation. *Neuroimage Clin, 3*, 65-72. doi:10.1016/j.nicl.2013.06.015

Sokol, S. (1983). Abnormal evoked potential latencies in amblyopia. *British Journal of Ophthalmology, 67*(5), 310-314.

Sokol, S., & Jones, K. (1979). Implicit Time of Pattern Evoked Potentials in Infancts: An Index of Maturation of Spatial Vision. *Vision Res, 19*, 747-755.

Soorya, L., Kolevzon, A., Zweifach, J., Lim, T., Dobry, Y., Schwartz, L., . . . Buxbaum, J. D. (2013). Prospective investigation of autism and genotype-phenotype correlations in 22q13 deletion syndrome and SHANK3 deficiency. *Mol Autism, 4*(1), 18. doi:10.1186/2040-2392-4-18

Sparrow, S. S., Cicchetti, D., & Saulnier, C. (2016). Vineland Adaptive Behavior Scales–Third Edition (Vineland-3). In: San Antonio, TX: Pearson.

Sparrow, S. S., Cicchetti, D. V., & D.A., B. (2005). *Vineland-II Survey Forms Manual (Vineland Adaptive Behavior Scales). Second ed*. Minneapolis, MN: AGS Publishing.

Spekreijse, H. (1978). Maturation of contrast EPs and development of visual resolution. *Archives italiennes de biologie*.

Srivastava, S., Cohen, J. S., Vernon, H., Baranano, K., McClellan, R., Jamal, L., . . . Fatemi, A. (2014). Clinical whole exome sequencing in child neurology practice. *Ann Neurol, 76*(4), 473-483. doi:10.1002/ana.24251

Stefansson, H., Meyer-Lindenberg, A., Steinberg, S., Magnusdottir, B., Morgen, K., Arnarsdottir, S., . . . Stefansson, K. (2014). CNVs conferring risk of autism or schizophrenia affect cognition in controls. *Nature, 505*(7483), 361-366. doi:10.1038/nature12818

Tamura, S., Morikawa, Y., Iwanishi, H., Hisaoka, T., & Senba, E. (2004). Foxp1 gene expression in projection neurons of the mouse striatum. *Neuroscience, 124*(2), 261-267.

Tavassoli, T., Bellesheim, K., Siper, P. M., Wang, A. T., Halpern, D., Gorenstein, M., . . . Buxbaum, J. D. (2016). Measuring sensory reactivity in autism spectrum disorder: application and simplification of a clinician-administered sensory observation scale. *J Autism Dev Disord, 46*(1), 287-293.

Teramitsu, I., Kudo, L. C., London, S. E., Geschwind, D. H., & White, S. A. (2004). Parallel FoxP1 and FoxP2 expression in songbird and human brain predicts functional interaction. *Journal of Neuroscience, 24*(13), 3152-3163.

Tootell, R. B. H., & Nasr, S. (2017). Columnar Segregation of Magnocellular and Parvocellular Streams in Human Extrastriate Cortex. *J Neurosci, 37*(33), 8014-8032. doi:10.1523/JNEUROSCI.0690-17.2017

Towle, V. L., Moskowitz, A., Sokol, S., & Schwartz, B. (1983). The visual evoked potential in glaucoma and ocular hypertension: effects of check size, field size, and stimulation rate. *Investigative Ophthalmology & Visual Science, 24*(2), 175-183.

Turner-Brown, L. M., Baranek, G. T., Reznick, J. S., Watson, L. R., & Crais, E. R. (2013). The First Year Inventory: a longitudinal follow-up of 12-month-old to 3-year-old children. *Autism, 17*(5), 527-540.

Uljarević, M., Lane, A., Kelly, A., & Leekam, S. (2016). Sensory subtypes and anxiety in older children and adolescents with autism spectrum disorder. *Autism Research, 9*(10), 1073-1078.

Van Dijck, A., Helsmoortel, C., Vandeweyer, G., & Kooy, F. (2016). ADNP-related intellectual disability and autism spectrum disorder.

Van Dijck, A., Vulto-van Silfhout, A. T., Cappuyns, E., van der Werf, I. M., Mancini, G. M., Tzschach, A., . . . Kooy, R. F. (2018). Clinical Presentation of a Complex Neurodevelopmental Disorder Caused by Mutations in ADNP. *Biol Psychiatry*. doi:10.1016/j.biopsych.2018.02.1173

Varcin, K. J., Nelson, C. A., 3rd, Ko, J., Sahin, M., Wu, J. Y., & Jeste, S. S. (2015). Visual Evoked Potentials as a Readout of Cortical Function in Infants With Tuberous Sclerosis Complex. *J Child Neurol, 31*(2), 195-202. doi:10.1177/0883073815587328

Wechsler, D. (2011). *Wechsler Abbreviated Scale of Intelligence, Second Edition*. San Antonio, TX: The Psychology Corporation.

Wechsler, D. (2012). *Wechsler preschool and primary scale of intelligence—fourth edition*. San Antonio, TX: The Psychological Corporation

Wechsler, D. (2014). *Wechsler Intelligence Scale for Children, Fifth Edition*. San Antonio, TX: NCS Pearson, Inc.: PsychCorp.

Weinger, P. M., Zemon, V., Soorya, L., & Gordon, J. (2014). Low-contrast response deficits and increased neural noise in children with autism spectrum disorder. *Neuropsychologia, 63c*, 10-18. doi:10.1016/j.neuropsychologia.2014.07.031

White, E. I., Wallace, G. L., Bascom, J., Armour, A. C., Register-Brown, K., Popal, H. S., . . . Kenworthy, L. (2017). Sex differences in parent-reported executive functioning and adaptive behavior in children and young adults with autism spectrum disorder. *Autism Research*, n/a-n/a. doi:10.1002/aur.1811

Widmaier, E. P., Raff, H., & Strang, K. T. (2006). *Vander's Human Physiology* (Eleventh ed.). Buston, MA: McGraw-Hill.

Wiggins, L. D., Robins, D. L., Bakeman, R., & Adamson, L. B. (2009). Breif Report: Sensory Abnormalities as Distinguishing Symptoms of Autism Spectrum Disorders in Young Children. *J Autism Dev Disord, 39*(7), 1087-1091. doi:10.1007/s10803-009-0711-x

Yang, M., Bozdagi, O., Scattoni, M. L., Wohr, M., Roullet, F. I., Katz, A. M., . . . Crawley, J. N. (2012). Reduced excitatory neurotransmission and mild autism-relevant phenotypes in adolescent Shank3 null mutant mice. *J Neurosci, 32*(19), 6525-6541. doi:10.1523/jneurosci.6107-11.2012

Zemon, V., Eisner, W., Gordon, J., Grose-Fifer, J., Tenedios, F., & Shoup, H. (1995). Contrast-dependent responses in the human visual system: childhood through adulthood. *International Journal of Neuroscience, 80*(1-4), 181-201.

Zemon, V., & Gordon, J. (2006). Luminance-contrast mechanisms in humans: visual evoked potentials and a nonlinear model. *Vision Research, 46*(24), 4163-4180.

Zemon, V., & Gordon, J. (2018). Quantification and Statistical Analysis of the Transient Visual Evoked Potential to a Contrast-Reversing Pattern: A Frequency-Domain Approach. *European Journal of Neuroscience, Epub*. doi:10.1111/ejn.14049

Zemon, V., Gordon, J., O'Toole, L., Monde, K., Dolzhanskaya, V., Shapovalova, V., . . . Granader, Y. (2009). Transient visual evoked potentials (tVEPs) to contrast-reversing patterns: A frequency domain analysis. *Investigative ophthalmology & visual science, 50:ARVO E-Abstract 5880*.

Zemon, V., Gordon, J., & Welch, R. (1988). Asymmetries in ON and OFF visual pathways of humans revealed using contrast-evoked cortical potentials. *Visual Neuroscience, 1*, 145-150.

Zemon, V., Kaplan, E., & Ratliff, F. (1980). Bicuculline enhances a negative component and diminishes a positive component of the visual evoked cortical potential in the cat. *Proc Natl Acad Sci U S A, 77*(12), 7476-7478.

Zemon, V., Kaplan, E., & Ratliff, F. (1986). The Role of GABA-mediated Intracortical Inhibition in the Generation of Visual Evoked Potentials. In A. R. Liss (Ed.), *Evoked Potentials* (pp. 287-295).

Zemon, V., & Ratliff, F. (1982). Visual evoked potentials: evidence for lateral interactions. *Proceedings of the National Academy of Sciences, 79*(18), 5723-5726.

Zemon, V., & Ratliff, F. (1984). Intermodulation components of the visual evoked potential: responses to lateral and superimposed stimuli. *Biol Cybern, 50*(6), 401-408.

Zemon, V., Tsai, J. C., Forbes, M., Al-Aswad, L. A., Chen, C. M., Gordon, J., . . . Jindra, L. F. (2008). Novel electrophysiological instrument for rapid and objective assessment

of magnocellular deficits associated with glaucoma. *Doc Ophthalmol, 117*(3), 233-243. doi:10.1007/s10633-008-9129-6

Zweifach, J. G. (2016). *Electrophysiological Assessment of Visual Pathways in Children with Autism Spectrum Disorder and their Unaffected Siblings: In Search of an Endophenotype (Unpublished doctoral dissertation)*. Ferkauf Graduate School of Psychology, Yeshiva University. Bronx, NY.

Table 1
Summary of Sample Demographic Characteristics – Study 1

	TD	**iASD**	**ADNP**	**FOXP1**	**PMS**
Age (years)(*M*(*SD*))	6.54 (3.00)	6.26 (2.18)	6.96 (3.33)	7.37 (3.05)	6.67 (2.66)
Sex (% female (n))	45.83 (11)	16.36 (9)	31.25 (5)	66.67 (10)	56.67 (17)
NVIQ/NVDQ *(M(SD))*	113.78 (21.09)	88.39 (27.28)	37.83 (15.11)	58.24 (19.97)	49.09 (14.02)
VIQ/VDQ *(M(SD))*	111.13 (13.05)	77.86 (25.84)	33.96 (17.47)	51.79 (22.43)	46.34 (10.17)
Vineland Adaptive Behavior Composite *(M(SD))*	--	76.70 (10.32)	51.50 (14.14)	60.33 (13.94)	59.21 (13.24)
ADOS-2 Comparison Score *(M(SD))*	--	7.69 (1.63)	5.75 (2.32)	4.79 (2.23)	6.52 (1.97)
ADOS-2 Social Affect Domain *(M(SD))*	--	11.53 (3.33)	10.50 (5.50)	6.93 (4.67)	12.63 (5.08)
ADOS-2 Repetitive, restricted behavior Domain *(M(SD))*	--	4.69 (2.04)	4.81 (1.33)	3.50 (2.62)	3.93 (1.90)

Note. All scores are standardized. *M* ≡ mean; *SD* ≡ standard deviation; NVIQ ≡ non-verbal intelligence quotient; NVDQ ≡ non-verbal developmental quotient; VIQ ≡ verbal intelligence quotient; VDQ ≡ verbal developmental quotient; ADOS-2 ≡ Autism Diagnostic Observation Scale, Second Edition; TD ≡ typically developing; iASD ≡ idiopathic autism spectrum disorder; ADNP ≡ ADNP syndrome; FOXP1 ≡ FOXP1 syndrome; PMS ≡ Phelan-McDermid syndrome

Table 2
Means and Standard Deviations of Behavioral Sensory Reactivity Measures (Study 1)

	TD	**iASD**	**ADNP**	**FOXP1**	**PMS**
SAND (*M(SD)*)					
SAND Total Score	7.50 (2.90)	28.38 (8.78)	33.44 (8.38)	28.93 (9.93)	27.33 (10.08)
Hyperreactivity	2.29 (1.63)	7.71 (5.00)	5.57 (3.08)	6.07 (3.54)	3.40 (3.46)
Hyporeactivity	1.67 (1.63)	6.73 (5.07)	8.13 (3.50)	6.20 (4.46)	15.37 (6.17)
Sensory Seeking	3.29 (2.93)	13.47 (5.85)	19.31 (6.14)	16.53 (6.30)	8.50 (5.30)
Visual Domain	1.71 (1.63)	8.76 (3.75)	9.56 (4.32)	8.53 (4.90)	7.97 (4.13)
Auditory Domain	2.50 (1.56)	9.56 (4.33)	9.06 (3.92)	9.00 (2.80)	9.10 (4.06)
Tactile Domain	3.04 (2.39)	9.62 (4.04)	14.81 (2.83)	11.40 (4.26)	10.27 (4.27)
Visual Hyperreactivity	0.25 (0.68)	1.22 (1.86)	1.19 (1.94)	0.53 (0.92)	0.80 (1.47)
Visual Hyporeactivity	0.58 (0.93)	2.82 (2.15)	3.31 (2.50)	2.60 (2.47)	5.43 (2.05)
Visual Sensory Seeking	0.96 (1.40)	4.93 (2.40)	5.06 (2.72)	5.40 (3.38)	1.73 (2.16)
Auditory Hyperreactivity	0.71 (1.12)	4.07 (2.27)	1.87 (1.93)	3.33 (1.80)	1.30 (1.95)
Auditory Hyporeactivity	0.75 (0.99)	1.47 (2.28)	0.50 (1.16)	0.67 (1.18)	5.37 (2.87)
Auditory Sensory Seeking	1.04 (1.43)	4.05 (2.74)	6.69 (2.77)	5.00 (2.00)	2.43 (2.47)
Tactile Hyperreactivity	1.33 (1.37)	2.55 (2.41)	2.94 (2.32)	2.20 (2.18)	1.33 (1.37)
Tactile Hyporeactivity	0.42 (0.83)	2.47 (2.03)	4.31 (1.14)	2.93 (2.43)	4.57 (2.54)
Tactile Sensory Seeking	1.46 (1.62)	4.80 (2.68)	7.56 (1.93)	6.27 (2.19)	4.33 (2.50)
Sensory Profile (*M(SD)*)					

SP Visual Domain (*M(SD)*)	42.89 (2.36)	34.83 (5.40)	32.06 (6.19)	34.67 (1.67)	34.73 (4.64)
Short Sensory Profile					
SSP Tactile Sensitivity	33.09 (2.56)	30.14 (3.61)	29.63 (3.59)	27.69 (4.07)	30.89 (3.51)
SSP Taste/Smell Sensitivity	18.41 (2.06)	13.25 (5.17)	14.81 (5.48)	16.08 (3.97)	18.59 (2.78)
SSP Movement Sensitivity	14.59 (1.01)	13.66 (1.67)	12.62 (2.39)	13.85 (1.86)	14.00 (1.47)
SSP Underresponsive/Seeks Sensation	31.32 (3.87)	22.83 (4.02)	19.00 (5.10)	20.38 (5.17)	20.75 (5.93)
SSP Auditory Filtering	26.59 (2.68)	18.39 (3.93)	19.75 (4.81)	19.46 (5.38)	19.85 (4.66)
SSP Low Energy/Weak	29.64 (.85)	22.91 (6.90)	18.81 (4.96)	22.46 (6.72)	18.81 (6.89)
SSP Visual/Auditory Sensitivity	23.64 (1.73)	19.09 (3.51)	18.19 (3.73)	18.31 (4.42)	21.81 (2.53)

Note. All scores presented are raw scores. *M* ≡ mean; *SD* ≡ standard deviation; SAND ≡ Sensory Assessment for Neurodevelopmental Disorders; SP ≡ Sensory Profile; SSP ≡ Short Sensory Profile; TD ≡ typically developing; iASD ≡ idiopathic autism spectrum disorder; ADNP ≡ ADNP syndrome; FOXP1 ≡ FOXP1 syndrome; PMS ≡ Phelan-McDermid syndrome

Table 3
Structure Matrix of SAND Combined Domain and Subtype Scores for TD, iASD, and ADNP Groups

SAND Scale	Function	
	1	2
Tactile seeking	.588*	-.173
Visual seeking	.519*	.236
Tactile hyporeactivity	.518*	-.176
Auditory seeking	.507*	-.165
Visual hyporeactivity	.362*	.083
Tactile hyperreactivity	.187*	.023
Visual hyperreactivity	.166*	.091
Auditory hyperreactivity	.328	.603*
Auditory hyporeactivity	.035	.223*

Note. Pooled within-groups correlations between discriminating variables and standardized canonical discriminant functions. Variables are ordered by absolute size of correlation within function. * denotes the largest absolute correlation between each variable and any discriminant function.

Table 4a

Structure Matrix of SAND Sensory Subtype Scores for TD, iASD, ADNP, FOXP1, and PMS Groups

SAND Scale	Function		
	1	2	3
Seeking	.711*	.534	-.458
Hyporeactivity	-.381	.924*	-.009
Hyperreactivity	.421	.172	.891*

Note. Pooled within-groups correlations between discriminating variables and standardized canonical discriminant functions. Variables are ordered by absolute size of correlation within function. * denotes the largest absolute correlation between each variable and any discriminant function.

Table 4b

Functions at Group Centroids of SAND Sensory Subtype Scores for TD, iASD, ADNP, FOXP1, and PMS Groups

Group	Function		
	1	2	3
TD	-.911	-1.784	-.128
iASD	.655	.025	.315
ADNP	1.212	.566	-.537
FOXP1	1.018	.047	-.326
PMS	-1.628	1.056	-.026

Note. Unstandardized canonical discriminant functions are evaluated at group means.

Table 5a

Structure Matrix of SAND Sensory Domain Scores for TD, iASD, ADNP, FOXP1, and PMS Groups

SAND Scale	Function		
	1	2	3
Total Tactile	.902*	-.419	-.107
Total Visual	.720*	.343	.603
Total Auditory	.677*	.569	-.466

Note. Pooled within-groups correlations between discriminating variables and standardized canonical discriminant functions. Variables are ordered by absolute size of correlation within function. * denotes the largest absolute correlation between each variable and any discriminant function.

Table 5b

Functions at Group Centroids of SAND Sensory Domain Scores for TD, iASD, ADNP, FOXP1, and PMS Groups

Group	Function		
	1	2	3
TD	-1.996	-.261	.013
iASD	.253	.405	.044
ADNP	1.170	-.916	.051
FOXP1	.495	-.190	-.008
PMS	.261	.050	-.113

Note. Unstandardized canonical discriminant functions are evaluated at group means.

Table 6a

Structure Matrix of SAND Combined Sensory Domain and Subtype Scores for TD, iASD, ADNP, FOXP1, and PMS Groups

SAND Scale	Function			
	1	2	3	4
Visual seeking	.590*	.085	.213	-.139
Auditory seeking	.503*	.258	-.196	.109
Visual hyporeactivity	-.082	.771*	.166	.074
Tactile hyporeactivity	.063	.744*	-.101	-.037
Auditory hyporeactivity	-.439	.678*	.315	.018
Tactile seeking	.460	.471*	-.183	-.369
Auditory hyperreactivity	.432	-.022	.645*	.132
Visual hyperreactivity	.121	.107	.117	.843*
Tactile hyperreactivity	.221	.014	.018	.522*

Note. Pooled within-groups correlations between discriminating variables and standardized canonical discriminant functions. Variables are ordered by absolute size of correlation within function. * denotes the largest absolute correlation between each variable and any discriminant function.

Table 6b

Functions at Group Centroids of SAND Combined Sensory Domain and Subtype Scores for TD, iASD, ADNP, FOXP1, and PMS Groups

	Function			
Group	1	2	3	4
TD	-1.481	-1.587	-.537	.006
iASD	.730	-.208	.676	.080
ADNP	1.533	.670	-1.585	.145
FOXP1	1.224	-.071	-.134	-.415
PMS	-1.584	1.329	.103	-.022

Note. Unstandardized canonical discriminant functions are evaluated at group means.

Table 7
Linear Mixed Effects Modeling – SAND (Study 1)

	Regression coefficients (estimates of fixed effects)			
Effect	Model 1 (null)	Model 2	Model 3	Model 4
Intercept	2.80 (0.11)***	3.04 (0.17)***	3.86 (0.25)***	1.73 (0.38)***
Main Effects				
Group	—			
TD	—	-2.20 (0.25)***	-2.20 (.25)***	-0.78 (0.57)
iASD	—	0.12 (0.21)	0.12 (0.21)	3.19 (0.47)***
ADNP	—	0.68 (0.29)*	0.68 (0.29)*	3.33 (0.64)***
FOXP1	—	0.18 (0.29)	0.18 (0.29)	3.67 (0.66)***
PMS	—	0[a]	0[a]	0[a]
SAND scale				
Auditory hyperreactivity	—	—	-1.06 (0.28)***	1.43 (0.51)
Auditory hyporeactivity	—	—	-1.64 (0.28)***	3.63 (0.51)***
Auditory seeking	—	—	-0.04 (0.28)	0.70 (0.51)
Tactile hyperreactivity	—	—	-1.54 (0.28)***	-0.37 (0.51)
Tactile hyporeactivity	—	—	-0.80 (0.28)**	2.83 (0.51)***
Tactile seeking	—	—	0.97 (0.28)***	2.60 (0.51)***
Visual hyperreactivity	—	—	-2.74 (0.28)***	-.93 (0.51)
Visual hyporeactivity	—	—	-0.60 (0.28)*	3.70 (0.51)***
Visual seeking	—	—	0[a]	0[a]
Two-way cross-level interactions				
TD x Auditory hyperreactivity	—	—	—	0.18 (0.77)
TD x Auditory hyporeactivity	—	—	—	-3.84 (0.77)***
TD x Auditory seeking	—	—	—	-0.62 (0.77)
TD x Tactile hyperreactivity	—	—	—	0.74 (0.77)
TD x Tactile hyporeactivity	—	—	—	-3.38 (0.77)***
TD x Tactile seeking	—	—	—	-2.10 (0.77)**

TD x Visual hyperreactivity	—	—	—	0.23 (0.77)
TD x Visual hyporeactivity	—	—	—	-4.08 (0.77)***
TD x Visual seeking	—	—	—	0[a]
iASD x Auditory hyperreactivity	—	—	—	-0.42 (0.63)
iASD x Auditory hyporeactivity	—	—	—	-7.09 (0.63)***
iASD x Auditory seeking	—	—	—	-1.58 (0.63)*
iASD x Tactile hyperreactivity	—	—	—	-2.02 (0.63)**
iASD x Tactile hyporeactivity	—	—	—	-5.29 (0.63)***
iASD x Tactile seeking	—	—	—	-2.73 (0.63)***
iASD x Visual hyperreactivity	—	—	—	-2.78 (0.63)***
iASD x Visual hyporeactivity	—	—	—	-5.81 (0.63)***
iASD x Visual seeking	—	—	—	0[a]
ADNP x Auditory hyperreactivity	—	—	—	-2.75 (0.86)***
ADNP x Auditory hyporeactivity	—	—	—	-8.20 (0.86)***
ADNP x Auditory seeking	—	—	—	0.93 (0.86)
ADNP x Tactile hyperreactivity	—	—	—	-1.76 (0.86)**
ADNP x Tactile hyporeactivity	—	—	—	-3.58 (0.86)***
ADNP x Tactile seeking	—	—	—	-.10 (0.86)
ADNP x Visual hyperreactivity	—	—	—	-2.94 (.86)***
ADNP x Visual hyporeactivity	—	—	—	-5.45 (.86)***
ADNP x Visual seeking	—	—	—	0[a]
FOXP1 x Auditory hyperreactivity	—	—	—	-1.63 (0.88)
FOXP1 x Auditory hyporeactivity	—	—	—	-8.34 (0.88)***
FOXP1 x Auditory seeking	—	—	—	-1.10 (0.88)
FOXP1 x Tactile hyperreactivity	—	—	—	-2.83 (0.88)***
FOXP1 x Tactile hyporeactivity	—	—	—	-5.30 (0.88)***
FOXP1 x Tactile seeking	—	—	—	-1.73 (0.88)*
FOXP1 x Visual hyperreactivity	—	—	—	-3.93 (0.88)***
FOXP1 x Visual hyporeactivity	—	—	—	-6.50 (0.88)***
FOXP1 x Visual seeking	—	—	—	0[a]

Variance components (random effects)				
Residual (σ^2)	6.52 (0.28)***	6.52 (0.28)***	5.34 (0.23)***	3.90 (0.16)***
Intercept (τ_{00})	0.97 (0.21)***	0.13 (0.11)	0.27 (0.11)*	0.43 (0.10)***
Model summary				
Deviance (-2LL)[b]	6057.76	5962.42***	5737.66***	5387.56***
Estimated parameters	3	7	15	47

Note: Standard errors for parameter estimates are listed in parentheses.
[a]The parameter is set to zero because it is redundant, cross-level interactions with redundant parameters are excluded from the table.
[b]-2LL; -2 log likelihood is a measure of how well the model fits the data. Smaller numbers are indicative of a better fit.
*p < .05. **p < .01. ***p < .001.

Table 8
Summary of Sample Demographic Characteristics – Study 2

	TD	**iASD**	**ADNP**	**FOXP1**
Age (years) (M(SD))	6.69 (2.67)	6.72 (2.58)	7.04 (3.44)	6.67 (2.71)
Sex (% female (n))	44.44 (20)	11.39 (9)	33.33 (4)	77.78 (7)
NVIQ/NVDQ *(M(SD))*	113.21 (18.37)	90.00 (29.69)	40.93 (12.69)	62.46 (17.81)
VIQ/VDQ *(M(SD))*	115.15 (13.76)	80.69 (24.61)	38.58 (16.10)	56.41 (21.63)
Vineland Adaptive Behavior Composite *(M(SD))*	--	77.19 (11.00)	54.58 (11.87)	61.67 (13.12)
ADOS-2 Comparison Score *(M(SD))*	--	7.59 (1.80)	5.25 (2.30)	4.78 (2.28)
ADOS-2 Social Affect Domain *(M(SD))*	--	11.26 (3.65)	8.92 (5.13)	6.33 (5.22)
ADOS-2 Repetitive, restricted behavior Domain *(M(SD))*	--	4.47 (2.09)	4.50 (1.24)	3.22 (1.64)

Note. All scores are standardized. *M* ≡ mean; *SD* ≡ standard deviation; NVIQ ≡ non-verbal intelligence quotient; NVDQ ≡ non-verbal developmental quotient; VIQ ≡ verbal intelligence quotient; VDQ ≡ verbal developmental quotient; ADOS-2 ≡ Autism Diagnostic Observation Scale, Second Edition; TD ≡ typically developing; iASD ≡ idiopathic autism spectrum disorder; ADNP ≡ ADNP syndrome; FOXP1 ≡ FOXP1 syndrome

Table 9a
Standard and Short Conditions – Time Domain Measures: Amplitude (Study 2)

	Standard Condition		Short Condition	
Group	P_{60}-N_{75}	N_{75}-P_{100}	P_{60}-N_{75}	N_{75}-P_{100}
TD	16.36 (9.69)	27.82 (14.72)	20.86 (11.94)	33.60 (15.37)
	[14.45 (10.47)]	[25.80 (17.10)]	[17.50 (14.40)]	[29.40 (18.09)]
iASD	9.26 (5.33)	20.71 (9.50)	11.83 (7.08)	23.97 (10.07)
	[8.90 (6.05)]	[18.30 (14.70)]	[12.20 (8.08)]	[22.97 (14.06)]
ADNP	7.63 (5.74)	12.56 (6.75)	12.24 (8.30)	23.07 (10.38)
	[5.70 (5.87)]	[12.08 (6.05)]	[10.70 (13.63)]	[22.00 (17.65)]
FOXP1	8.62 (9.25)	17.17 (9.67)	14.73 (13.82)	26.25 (26.26)
	[4.85 (7.41)]	[12.90 (12.39)]	[9.90 (16.91)]	[16.10 (7.50)]

Note. Data are presented as *M (SD)* [*Mdn (IQR)*]. TD ≡ typically developing; iASD ≡ idiopathic autism spectrum disorder; ADNP ≡ ADNP syndrome; FOXP1 ≡ FOXP1 syndrome

Table 9b
Standard and Short Conditions – Time Domain Measures: Latency (Study 2)

	Standard Condition			Short Condition		
Group	P_{60}	N_{75}	P_{100}	P_{60}	N_{75}	P_{100}
TD	50.95 (3.33)	70.15 (3.40)	100.69 (7.47)	51.18 (3.78)	69.88 (3.56)	100.78 (7.85)
	[51.00 (5.00)]	[70.00 (5.00)]	[100.00 (10.00)]	[51.00 (7.00)]	[70.00 (4.50)]	[100.00 (12.25)]
iASD	52.63 (4.94)	71.00 (3.51)	101.94 (7.73)	52.98 (4.99)	71.08 (4.58)	100.18 (7.32)
	[51.00 (6.00)]	[71.00 (5.00)]	[102.00 (10.00)]	[52.00 (5.00)]	[71.00 (5.50)]	[100.00 (10.00)]
ADNP	48.75 (3.96)	68.50 (8.67)	99.00 (9.52)	54.60 (9.34)	74.50 (8.58)	103.60 (10.10)
	[49.50 (5.75)]	[69.00 (8.00)]	[97.00 (16.00)]	[51.50 (14.75)]	[70.00 (14.00)]	[103.50 (17.50)]
FOXP1	53.13 (4.12)	77.11 (10.71)	126.33 (20.56)	53.50 (5.17)	75.86 (9.19)	110.00 (8.04)
	[53.00 (4.75)]	[78.00 (21.00)]	[131.00 (38.00)]	[53.00 (8.75)]	[78.00 (15.00)]	[113.00 (14.00)]

Note. Data are presented as *M (SD)* [*Mdn (IQR)]*. TD ≡ typically developing; iASD ≡ idiopathic autism spectrum disorder; ADNP ≡ ADNP syndrome; FOXP1 ≡ FOXP1 syndrome

Table 10
Standard and Short Conditions – Frequency Domain Measures: Magnitude Squared Coherence (MSC)(Study 2)

	Standard Condition				Short Condition			
Group	Band 1	Band 2	Band 3	Band 4	Band 1	Band 2	Band 3	Band 4
TD	0.40 (0.19) [0.38 (0.30)]	0.54 (0.22) [0.53 (0.42)]	.042 (0.22) [0.42 (0.36)]	0.24 (0.14) [0.22 (0.16)]	0.28 (0.13) [0.26 (0.21)]	0.43 (0.18) [0.45 (0.29)]	0.31 (0.15) [0.29 (0.24)]	0.17 (0.10) [0.16 (0.11)]
iASD	0.38 (0.14) [0.38 (0.18)]	0.39 (0.18) [0.38 (0.24)]	0.23 (0.14) [0.20 (0.21)]	0.13 (0.08) [0.12 (0.10)]	0.28 (0.12) [0.27 (0.18)]	0.31 (0.12) [0.29 (0.16)]	0.19 (0.10) [0.17 (0.12)]	0.12 (0.06) [0.11 (0.05)]
ADNP	0.29 (0.20) [0.22 (0.34)]	0.23 (0.09) [0.23 (0.11)]	0.16 (0.07) [0.14 (0.13)]	0.13 (0.07) [0.11 (0.09)]	0.31 (0.14) [0.26 (0.23)]	0.29 (0.17) [0.23 (0.21)]	0.17 (0.10) [0.12 (0.15)]	0.14 (0.05) [0.14 (0.08)]
FOXP1	0.24 (0.11) [0.23 (0.15)]	0.22 (0.17) [0.18 (0.17)]	0.09 (0.05) [0.14 (0.07)]	0.13 (0.04) [0.13 (0.07)]	0.26 (0.16) [0.17 (0.27)]	0.25 (0.10) [0.21 (0.11)]	0.12 (0.07) [0.11 (0.12)]	0.11 (0.04) [0.10 (0.06)]

Note. Data are presented as *M (SD)* [*Mdn (IQR)*]. TD ≡ typically developing; iASD ≡ idiopathic autism spectrum disorder; ADNP ≡ ADNP syndrome; FOXP1 ≡ FOXP1 syndrome

Table 11
Standard and Short Conditions – Frequency Domain Measures: Square Root of Power (Study 2)

	Standard Condition				Short Condition			
Group	Band 1	Band 2	Band 3	Band 4	Band 1	Band 2	Band 3	Band 4
TD	5.05 (2.84)	3.51 (1.61)	1.05 (0.63)	0.40 (0.31)	5.95 (3.07)	3.85 (1.81)	1.20 (0.63)	0.50 (0.27)
	[4.80 (3.20)]	[3.17 (2.03)]	[0.84 (0.74)]	[0.30 (0.25)]	[5.04 (3.35)]	[3.41 (1.81)]	[1.12 (0.83)]	[0.43 (0.40)]
iASD	4.18 (1.70)	2.50 (1.08)	0.67 (0.32)	0.32 (0.21)	5.04 (2.07)	2.98 (1.04)	0.87 (0.33)	0.45 (0.26)
	[3.93 (2.46)]	[2.40 (1.60)]	[0.61 (0.42)]	[0.28 (0.21)]	[4.64 (2.73)]	[2.86 (1.60)]	[0.86 (0.43)]	[0.38 (0.25)]
ADNP	3.99 (2.70)	1.32 (.59)	0.62 (0.33)	0.34 (0.14)	6.04 (3.27)	3.26 (1.58)	0.96 (0.44)	0.71 (0.38)
	[3.22 (1.89)]	[1.84 (1.17)]	[0.52 (0.29)]	[0.30 (0.18)]	[5.44 (3.44)]	[3.03 (2.58)]	[0.76 (0.41)]	[0.61 (0.26)]
FOXP1	3.52 (1.40)	1.92 (1.49)	0.53 (0.19)	0.37 (0.11)	5.62 (3.51)	3.41 (2.24)	0.72 (0.40)	0.48 (0.27)
	[3.08 (1.84)]	[1.08 (1.54)]	[0.43 (0.23)]	[0.39 (0.17)]	[4.38 (3.08)]	[2.70 (1.30)]	[0.68 (0.29)]	[0.36 (0.36)]

Note. Data are presented as *M (SD)* [*Mdn (IQR)*]. TD ≡ typically developing; iASD ≡ idiopathic autism spectrum disorder; ADNP ≡ ADNP syndrome; FOXP1 ≡ FOXP1 syndrome

Table 12
Linear Mixed Effects Modeling – Amplitude (Study 2)

	Regression coefficients (estimates of fixed effects)				
Effect	Model 1 (null)	Model 2	Model 3	Model 4	Model 5
Intercept	18.68 (0.82)***	15.73 (3.00)***	18.50 (3.07)***	23.76 (3.05)***	25.04 (3.69)***
Main Effects					
Group					
TD	—	8.84 (3.29)**	8.40 (3.31)**	8.97 (3.30)**	8.98 (4.01)*
iASD	—	.58 (3.17)	-0.04 (3.20)	0.44 (3.19)	-1.19 (3.87)
ADNP	—	-1.69 (4.06)	-2.47 (4.10)	-1.98 (4.08)	-2.00 (4.88)
FOXP1	—	0[a]	0[a]	0[a]	0[a]
Stimulus Condition	—	—			
Standard	—	—	-4.75 (.86)***	-4.92 (.59)***	-7.87 (3.15)**
Short	—	—	0[a]	0[a]	0[a]
Peak-to-Trough	—	—	—		
P_{60}-N_{75}	—	—	—	-11.60 (.56)***	-12.23 (3.43)***
N_{75}-P_{100}	—	—	—	0[a]	0[a]
Two-way cross-level interactions					0[a]
Three-way cross-level interactions					
TD x Standard x P_{60}-N_{75}	—	—	—	—	1.60 (5.85)
TD x Standard x N_{75}-P_{100}	—	—	—	—	0.83 (3.45)
TD x Short x P_{60}-N_{75}	—	—	—	—	-0.52 (3.69)
TD x Short x N_{75}-P_{100}	—	—	—	—	0[a]
iASD x Standard x P_{60}-N_{75}	—	—	—	—	4.80 (5.78)
iASD x Standard x N_{75}-P_{100}	—	—	—	—	4.02 (3.32)
iASD x Short x P_{60}-N_{75}	—	—	—	—	-.01 (3.57)
iASD x Short x N_{75}-P_{100}	—	—	—	—	0[a]
ADNP x Standard x P_{60}-N_{75}	—	—	—	—	3.31 (6.44)
ADNP x Standard x N_{75}-P_{100}	—	—	—	—	-3.99 (4.37)

ADNP x Short x P_{60}-N_{75}	—	—	—	—	1.40 (4.38)
ADNP x Short x N_{75}-P_{100}	—	—	—	—	0[a]
FOXP1 x Standard x P_{60}-N_{75}	—	—	—	—	2.74 (4.55)
FOXP1 x Standard x N_{75}-P_{100}	—	—	—	—	0[a]
FOXP1 x Short x P_{60}-N_{75}	—	—	—	—	0[a]
FOXP1 x Short x N_{75}-P_{100}	—	—	—	—	0[a]
Variance components (random effects)					
Residual (σ^2)	93.80(6.99)***	93.51 (6.94)***	85.72 (6.38)***	38.81 (2.90)***	37.13 (2.78)***
Intercept (τ_{00})	67.36(11.38)***	51.91 (9.49)***	55.52 (9.69)***	69.57 (9.66)***	70.26 (9.68)***
Model summary					
Deviance (-2LL)[b]	3874.12	3847.66***	3818.77***	3534.73***	3519.20
Estimated parameters	3	6	7	8	18

Note: Standard errors for parameter estimates are listed in parentheses.
[a]The parameter is set to zero because it is redundant, cross-level interactions with redundant parameters are excluded from the table.
[b]-2LL; -2 log likelihood is a measure of how well the model fits the data. Smaller numbers are indicative of a better fit.
*p < .05. **p < .01. ***p < .001.

Table 13
Linear Mixed Effects Modeling – MSC (Study 2)

	Regression coefficients (estimates of fixed effects)				
Effect	Model 1 (null)	Model 2	Model 3	Model 4	Model 5
Intercept	0.27 (0.01)***	0.18 (0.03)***	0.15 (0.03)***	0.02 (0.03)	0.11 (0.05)*
Main Effects					
Group					
TD	—	0.17 (0.04)***	0.18 (0.04)***	0.18 (0.04)***	0.07 (0.05)
iASD	—	0.07 (0.03)*	0.08 (0.03)*	0.08 (0.03)*	0.003 (0.05)
ADNP	—	0.03 (0.04)	0.04 (0.04)	0.04 (0.04)	0.02 (0.06)
FOXP1	—	0[a]	0[a]	0[a]	0[a]
Stimulus Condition	—	—			
Standard	—	—	0.06 (0.01)***	0.06 (0.01)***	0.02 (0.05)
Short	—	—	0[a]	0[a]	0[a]
MSC Band	—	—	—		
Band 1	—	—	—	0.17 (0.01)***	0.14 (0.05)**
Band 2	—	—	—	0.23 (0.01)***	0.13 (0.05)*
Band 3	—	—	—	0.10 (0.01)***	0.001 (0.05)
Band 4	—	—	—	0[a]	0[a]
Two-way cross-level interactions	—	—	—	—	
TD x Standard	—	—	—	—	0.03 (0.06)
TD x Short	—	—	—	—	0[a]
iASD x Standard	—	—	—	—	-0.002 (0.06)
iASD x Short	—	—	—	—	0[a]
ADNP x Standard	—	—	—	—	-0.06 (0.07)
ADNP x Short	—	—	—	—	0[a]
TD x Band 1	—	—	—	—	-0.04 (0.06)
TD x Band 2	—	—	—	—	0.13 (0.06)*
TD x Band 3	—	—	—	—	0.14 (0.06)*

TD x Band 4	—	—	—	—	0[a]
iASD x Band 1	—	—	—	—	0.02 (0.06)
iASD x Band 2	—	—	—	—	0.06 (0.06)
iASD x Band 3	—	—	—	—	0.08 (0.06)
iASD x Band 4	—	—	—	—	0[a]
ADNP x Band 1	—	—	—	—	0.03 (0.07)
ADNP x Band 2	—	—	—	—	0.02 (0.07)
ADNP x Band 3	—	—	—	—	0.03 (0.07)
ADNP x Band 4	—	—	—	—	0[a]
Standard x Band 1	—	—	—	—	-0.04 (0.07)
Standard x Band 2	—	—	—	—	-0.05 (0.07)
Standard x Band 3	—	—	—	—	-0.005 (0.07)
Standard x Band 4	—	—	—	—	0[a]
Three-way cross-level interactions	—	—	—	—	
TD x Standard x Band 1	—	—	—	—	0.09 (0.08)
TD x Standard x Band 2	—	—	—	—	0.08 (0.08)
TD x Standard x Band 3	—	—	—	—	0.04 (0.08)
TD x Standard x Band 4	—	—	—	—	0[a]
iASD x Standard x Band 1	—	—	—	—	0.12 (0.08)
iASD x Standard x Band 2	—	—	—	—	0.11 (0.08)
iASD x Standard x Band 3	—	—	—	—	0.03 (0.08)
iASD x Standard x Band 4	—	—	—	—	0[a]
ADNP x Standard x Band 1	—	—	—	—	0.03 (0.10)
ADNP x Standard x Band 2	—	—	—	—	-0.001 (0.10)
ADNP x Standard x Band 3	—	—	—	—	0.004 (0.10)
ADNP x Standard x Band 4	—	—	—	—	
Variance components (random effects)					
Residual (σ^2)	0.02 (0.001)***	0.02 (0.001)***	0.02 (0.001)***	0.01 (0.001)***	0.01 (0.001)***
Intercept (τ_{00})	0.01 (0.002)***	0.02 (0.001)***	0.01 (0.001)***	0.01 (0.001)***	0.01 (0.001)***
Model summary					

Deviance (-2LL)[b]	-841.50	-881.65***	-922.12***	-1388.55***	-1512.22***
Estimated parameters	3	6	7	10	34

Note: Standard errors for parameter estimates are listed in parentheses.
[a]The parameter is set to zero because it is redundant, cross-level interactions with redundant parameters are excluded from the table.
[b]-2LL; -2 log likelihood is a measure of how well the model fits the data. Smaller numbers are indicative of a better fit.
*$p < .05$. **$p < .01$. ***$p < .001$.

Table 14
Linear Mixed Effects Modeling – Square Root of Power (Study 2)

	Regression coefficients (estimates of fixed effects)				
Effect	Model 1 (null)	Model 2	Model 3	Model 4	Model 5
Intercept	2.32 (0.08)***	2.01 (0.29)***	2.28 (0.30)***	0.36 (0.30)	0.41 (0.51)
Main Effects					
Group					
TD	—	0.69 (0.32)*	0.65 (0.32)*	0.66 (0.32)*	0.12 (0.55)
iASD	—	0.13 (0.31)	0.08 (0.31)	0.09 (0.30)	0.03 (0.54)
ADNP	—	0.28 (0.40)	0.21 (0.40)	0.21 (0.39)	0.28 (0.66)
FOXP1	—	0[a]	0[a]	0[a]	0[a]
Stimulus Condition	—	—			
Standard	—	—	-0.48 (0.14)***	-5.26 (0.08)***	-0.04 (0.60)
Short	—	—	0[a]	0[a]	0[a]
Power Band	—	—	—		
Band 1	—	—	—	5.52 (0.11)***	5.14 (0.63)***
Band 2	—	—	—	2.61 (0.11)***	2.93 (0.63)***
Band 3	—	—	—	0.46 (0.11)***	0.24 (0.63)
Band 4	—	—	—	0[a]	0[a]
Two-way cross-level interactions	—	—	—	—	
TD x Standard	—	—	—	—	-0.18 (0.65)
TD x Short	—	—	—	—	0[a]
iASD x Standard	—	—	—	—	-0.11 (0.63)
iASD x Short	—	—	—	—	0[a]
ADNP x Standard	—	—	—	—	-0.42 (0.82)
ADNP x Short	—	—	—	—	0[a]
TD x Band 1	—	—	—	—	0.31 (0.68)
TD x Band 2	—	—	—	—	0.42 (0.68)
TD x Band 3	—	—	—	—	0.47 (0.68)

TD x Band 4	—	—	—	—	0[a]
iASD x Band 1	—	—	—	—	-0.54 (0.66)
iASD x Band 2	—	—	—	—	-0.41 (0.66)
iASD x Band 3	—	—	—	—	0.18 (0.66)
iASD x Band 4	—	—	—	—	0[a]
ADNP x Band 1	—	—	—	—	0.14 (0.80)
ADNP x Band 2	—	—	—	—	-0.38 (0.80)
ADNP x Band 3	—	—	—	—	0.01 (0.80)
ADNP x Band 4	—	—	—	—	0[a]
Standard x Band 1	—	—	—	—	-1.99 (0.84)*
Standard x Band 2	—	—	—	—	-1.38 (0.84)
Standard x Band 3	—	—	—	—	-0.08 (0.84)
Standard x Band 4	—	—	—	—	0[a]
Three-way cross-level interactions	—	—	—	—	
TD x Standard x Band 1	—	—	—	—	1.19 (0.91)
TD x Standard x Band 2	—	—	—	—	1.14 (0.91)
TD x Standard x Band 3	—	—	—	—	0.02 (0.91)
TD x Standard x Band 4	—	—	—	—	0[a]
iASD x Standard x Band 1	—	—	—	—	1.25 (0.88)
iASD x Standard x Band 2	—	—	—	—	1.03 (0.88)
iASD x Standard x Band 3	—	—	—	—	0.02 (0.88)
iASD x Standard x Band 4	—	—	—	—	0[a]
ADNP x Standard x Band 1	—	—	—	—	0.36 (1.14)
ADNP x Standard x Band 2	—	—	—	—	0.27 (1.14)
ADNP x Standard x Band 3	—	—	—	—	0.11 (1.14)
ADNP x Standard x Band 4	—	—	—	—	0[a]
Variance components (random effects)					
Residual (σ^2)	5.32 (0.25)***	5.31 (0.25)***	5.24 (0.25)***	1.47 (0.07)***	1.38 (0.07)***
Intercept (τ_{00})	0.09 (0.10)	0.02 (0.09)	0.04 (0.09)	0.53 (0.09)***	0.54 (0.09)***

Model summary					
Deviance (-2LL)[b]	4669.20	4656.72**	4645.42***	3510.54***	3451.12***
Estimated parameters	3	6	7	10	34

Note: Standard errors for parameter estimates are listed in parentheses.
[a]The parameter is set to zero because it is redundant, cross-level interactions with redundant parameters are excluded from the table.
[b]-2LL; -2 log likelihood is a measure of how well the model fits the data. Smaller numbers are indicative of a better fit.
*p < .05. **p < .01. ***p < .001.

Table 15

Linear Regression Parameters of Bivariate Correlations of N_{75}-P_{100} Amplitude and Square Root of Power Band 2

	Standard Condition	Short Condition
All Groups		
Slope	7.72	8.26
Intercept	1.11	-1.03
R^2	.76	.77
TD		
Slope	7.94	7.80
Intercept	0.44	2.05
R^2	.72	.76
iASD		
Slope	7.77	8.18
Intercept	1.08	-0.74
R^2	.76	.72
ADNP		
Slope	6.12	5.81
Intercept	1.47	2.95
R^2	.29	.71
FOXP1		
Slope	5.98	11.02
Intercept	5.66	-11.39
R^2	.86	.88

Note. Linear regression parameters associated with Figure 23 are presented.

Table 16
Pearson Correlation Coefficients of Behavioral Sensory Reactivity Measures and tVEP Amplitude

	Standard Condition		Short Condition	
	P_{60}-N_{75}	N_{75}-P_{100}	P_{60}-N_{75}	N_{75}-P_{100}
SAND Total Score	-.30*	-.23*	-.28**	-.25*
Total Visual	-.27*	-.21	-.25*	-.25*
Hyperreactivity	-.18	-.05	-.12	-.16
Hyporeactivity	-.18	-.26*	-.16	-.18
Sensory Seeking	-.24*	-.16	-.28**	-.23*
Visual Hyperreactivity	-.12	-.08	-.07	-.11
Visual Hyporeactivity	-.21*	-.21	-.15	-.15
Visual Sensory Seeking	-.27*	-.17	-.28**	-.20
Tactile Hyperreactivity	-.04	.08	.01	-.02
Tactile Hyporeactivity	-.15	-.24*	-.17	-.15
Tactile Sensory Seeking	-.15	-.09	-.20	-.14
Auditory Hyperreactivity	-.25*	-.12	-.20	-.19
Auditory Hyporeactivity	-.05	-.17	-.05	-.10
Auditory Sensory Seeking	-.26*	-.20	-.26*	-.18
SP Visual Domain	.18	.22	.20	.22
SSP Tactile Sensitivity	.15	.13	.23*	.28
SSP Taste/Smell Sensitivity	.10	.11	.19	.10
SSP Movement Sensitivity	.02	.05	.12	.11
SSP Underresponsive/Seeks Sensation	.37***	.32**	.39***	.35***
SSP Auditory Filtering	.29**	.17	.30**	.19
SSP Low Energy/Weak	.23*	.23*	.22*	.14
SSP Visual Auditory Sensitivity	.24*	.14	.24*	.17

Note. * $p < .05$ ** $p < .01$ *** $p < .001$

Table 17
Pearson Correlation Coefficients of Behavioral Sensory Reactivity Measures and tVEP MSC

	Standard Condition				Short Condition			
	MSC Band 1	MSC Band 2	MSC Band 3	MSC Band 4	MSC Band 1	MSC Band 2	MSC Band 3	MSC Band 4
SAND Total Score	-.10	-.33**	-.42***	-.41***	-.08	-.27**	-.34***	-.30**
Total Visual	-.09	-.26*	-.35***	-.38***	-.07	-0.22*	-.32***	-.27***
Hyperreactivity	.16	-.08	-.20	-.20	-.01	-.18	-.17	-.19
Hyporeactivity	-.17	-.24*	-.25*	-.32**	-.13	-.17	-.15	-.23*
Sensory Seeking	-.12	-.33**	-.39***	-.32*	-.08	-.23*	-.33***	-.19
Visual Hyperreactivity	.02	-.08	-.10	-.11	.09	-.13	-.14	-.15
Visual Hyporeactivity	-.11	-.24*	-.31**	-.40***	-.12	-.13	-.17	-.23*
Visual Sensory Seeking	-.13	-.23*	-.34***	-.29**	-.04	-.18	-.36**	-.23*
Tactile Hyperreactivity	.23*	-.01	-.15	-.05	-.01	-.11	-.12	-.04
Tactile Hyporeactivity	-.14	-.24*	-.24*	-.26*	.00	-.17	-.16	-.24*
Tactile Sensory Seeking	-.11	-.27*	-.36***	-.28*	-.03	-.18	-.30**	-.17
Auditory Hyperreactivity	.06	-.12	-.20	-.29**	-.03	-.16	-.14	-.26**
Auditory Hyporeactivity	-.16	-.09	-.04	-.10	-.19	-.08	-.03	-.07
Auditory Sensory Seeking	-.14	-.36***	-.33**	-.28**	-.08	-.21*	-.24*	-.16
SP Visual Domain	.16	.24*	.25*	.31**	.08	.29**	.27**	.33**
SSP Tactile Sensitivity	.10	.30**	.29**	.10	.11	.26**	.24*	.15
SSP Taste/Smell Sensitivity	.06	.10	.22*	.16	-.07	.13	.15	.08
SSP Movement Sensitivity	.06	.23*	.21*	.08	.02	.05	.08	.04
SSP Underresponsive/Seeks Sensation	.35***	.43***	.56***	.50***	.12	.38***	.45***	.35***
SSP Auditory Filtering	.20*	.35***	.52***	.44***	-.02	.38***	.46***	.34***
SSP Low Energy/Weak	.01	.17	.36***	.26*	-.01	.19	.30**	.21*
SSP Visual Auditory Sensitivity	.12	.33***	.44***	.31**	.09	.30**	.31**	.34***

Note. * $p < .05$ ** $p < .01$ *** $p < .001$

Table 18
Pearson Correlation Coefficients of Behavioral Sensory Reactivity Measures and tVEP Power

	Standard Condition				Short Condition			
	Power Band 1	Power Band 2	Power Band 3	Power Band 4	Power Band 1	Power Band 2	Power Band 3	Power Band 4
SAND Total Score	-.15	-.29**	-.19	.02	-.24*	-.25*	-.30**	-.03
Total Visual	.16	-.25*	-.19	.00	-.24*	-.25*	-.26*	.02
Hyperreactivity	-.03	-.15	-.13	.07	-.20	-.15	-.13	.09
Hyporeactivity	-.20	-.24*	-.05	.02	-.21*	-.22*	-.13	.03
Seeking	-.08	-.21*	-.17	.00	-.17	-.18	-.29**	-.08
Visual Hyperreactivity	-.12	-.15	-.03	.18	-.12	-.16	-.00	.20*
Visual Hyporeactivity	-.19	-.22*	-.11	-.05	-.19	-.17	-.13	.06
Visual Sensory Seeking	-.15	-.20	-.26*	-.11	-.13	-.19	-.38***	-.19
Tactile Hyperreactivity	.16	.02	-.04	.08	-.02	.01	-.10	.09
Tactile Hyporeactivity	-.13	-.24*	-.13	.00	-.10	-.17	-.12	.01
Tactile Sensory Seeking	-.06	-.12	-.08	.06	-.13	-.11	-.19	-.04
Auditory Hyperreactivity	-.13	-.23*	-.21*	-.09	-.26*	-.20	-.19	-.08
Auditory Hyporeactivity	-.15	-.11	.11	.09	-.19	-.15	-.05	-.04
Auditory Sensory Seeking	-.06	-.26*	-.16	-.00	-.11	-.17	-.24*	-.06
SP Visual Domain	.25*	.26*	.12	-.10	.24*	.26*	.22*	.19
SSP Tactile Sensitivity	.13	.19	.14	-.14	.17	.23*	.25*	.19
SSP Taste/Smell Sensitivity	.12	.08	.13	-.08	.08	.15	.12	.08
SSP Movement Sensitivity	-.02	.01	-.04	-.32**	.08	.04	.01	-.09
SSP Underresponsive/Seeks Sensation	.30**	.33***	.32**	-.04	.10*	.31**	.41***	.21*
SSP Auditory Filtering	.12	.23*	.33*	.05	.04	.20*	.36***	.14
SSP Low Energy/Weak	.11	.25*	.36***	.12	.06	.13	.29**	.02
SSP Visual Auditory Sensitivity	.12	.21*	.19	-.23*	.17	.16	.23*	.08

Note. References to power indicate are square root of power values. * $p < .05$ ** $p < .01$ *** $p < .001$

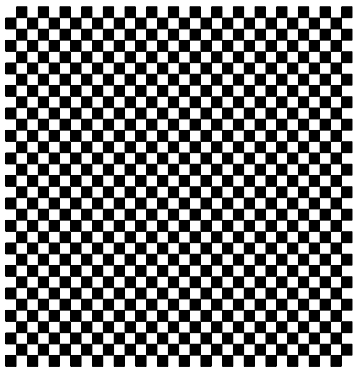

Figure 1. Contrast-reversing checkerboard stimulus pattern used to elicit tVEPs.

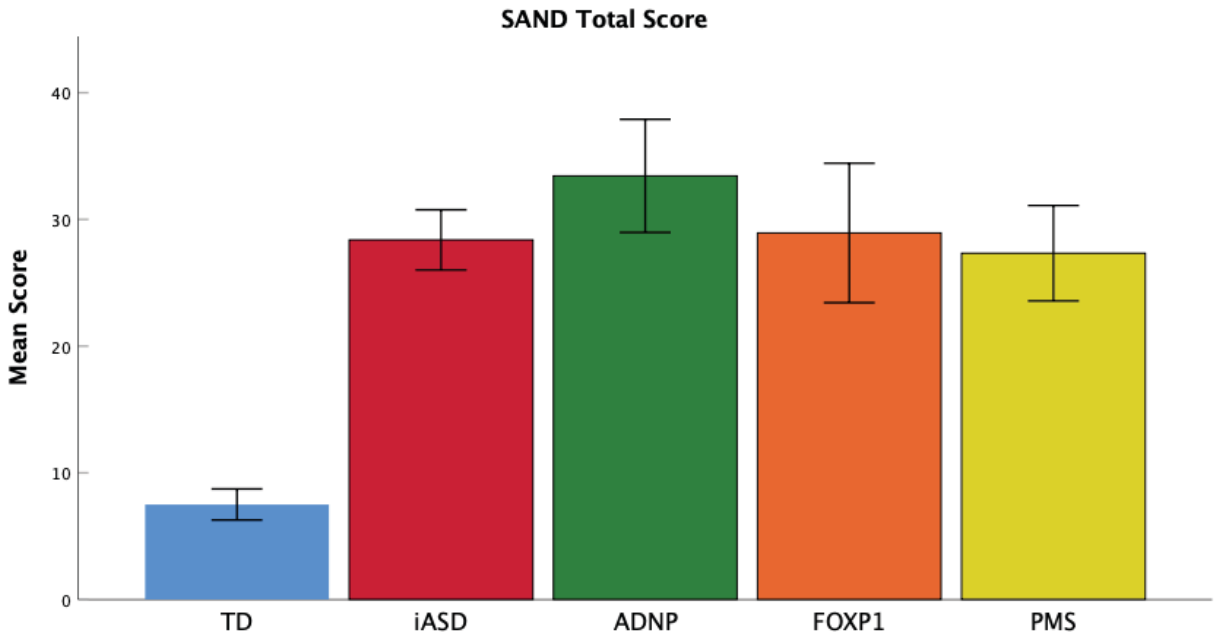

Figure 2. Mean SAND total scores for TD, iASD, ADNP, FOXP1, and PMS groups. Error bars are 95% confidence interval.

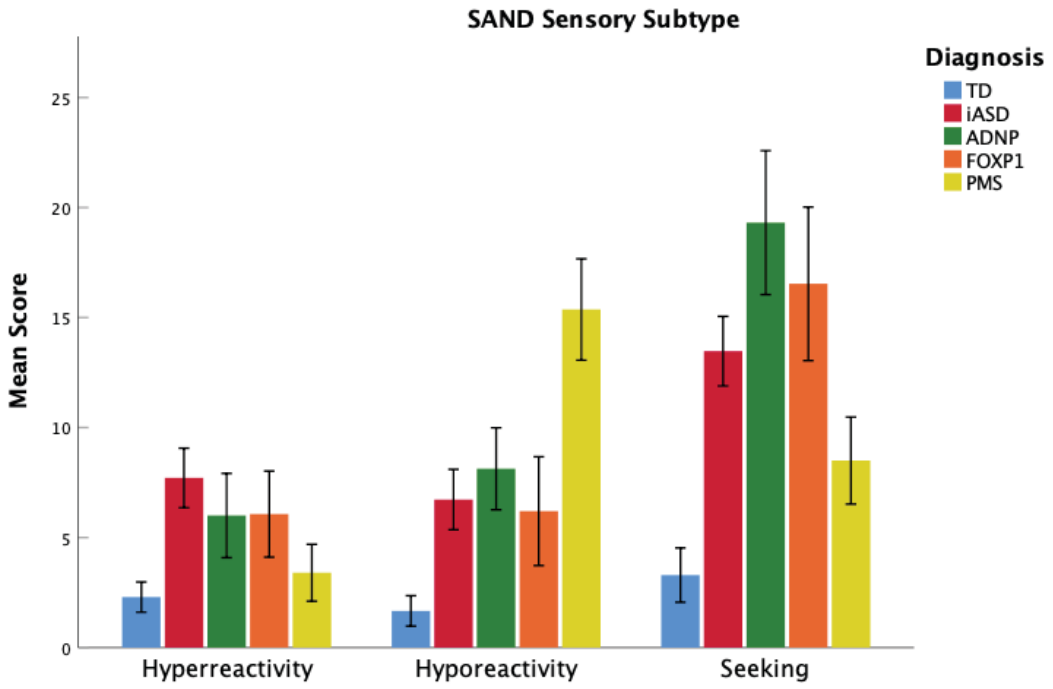

Figure 3. Mean SAND sensory subtype total scores for TD, iASD, ADNP, FOXP1, and PMS groups. Error bars are 95% confidence interval.

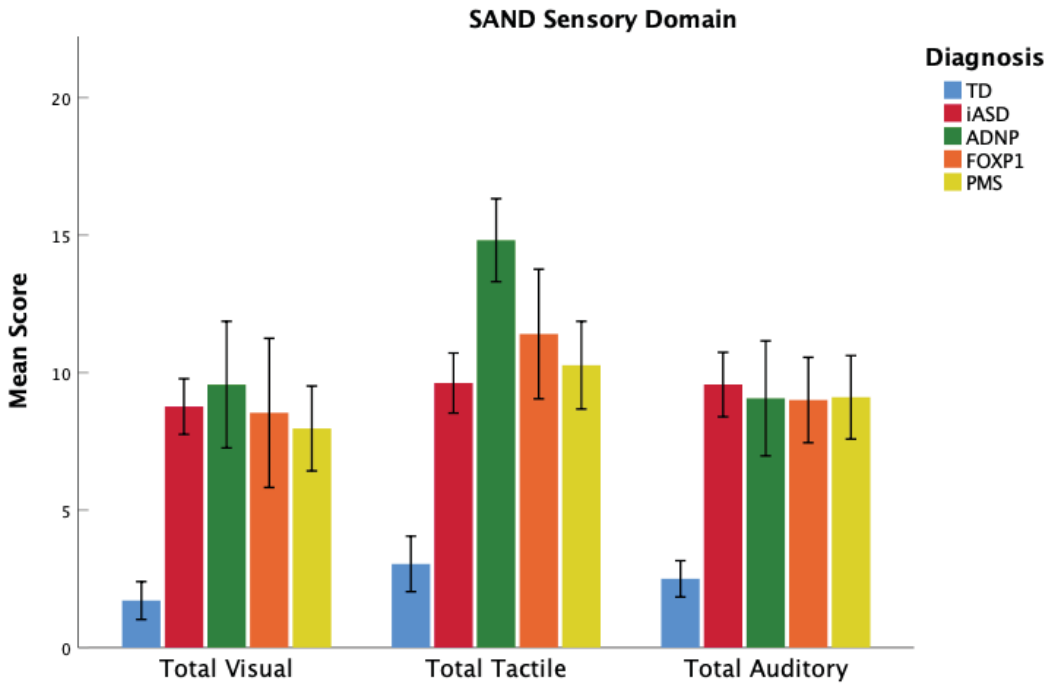

Figure 4. Mean SAND sensory domain total scores for TD, iASD, ADNP, FOXP1, and PMS groups. Error bars are 95% confidence interval.

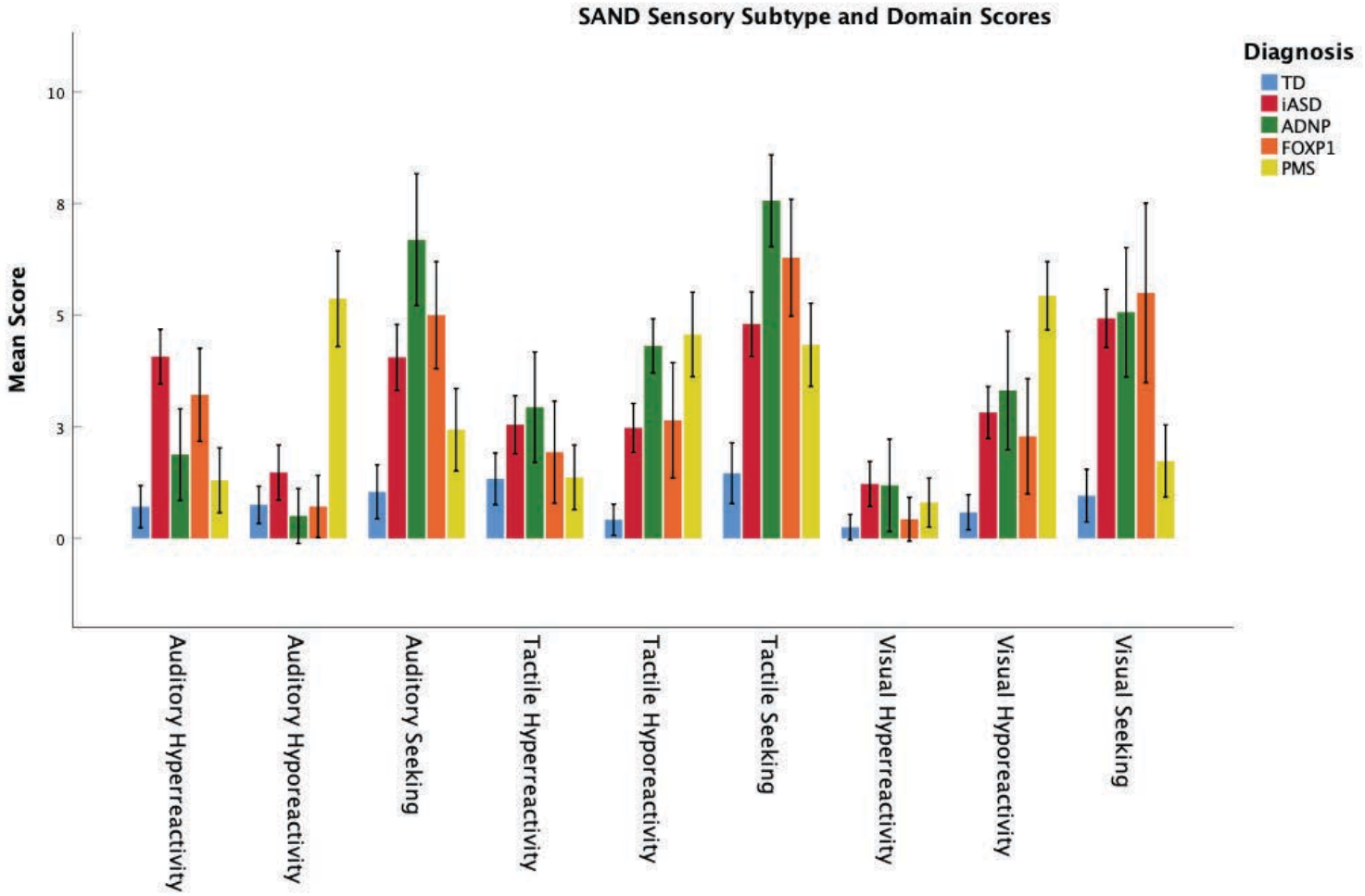

Figure 5. Mean SAND combined sensory subtype and domain scores for TD, iASD, ADNP, FOXP1, and PMS groups. Error bars are 95% confidence interval.

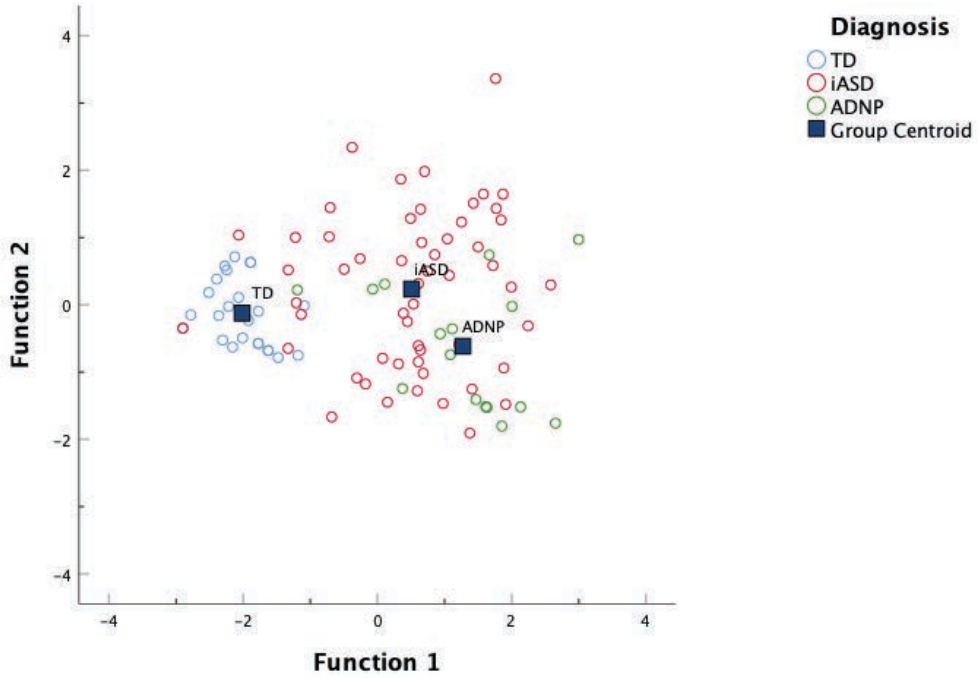

Figure 6. Canonical discriminant function plots for TD, iASD, and ADNP groups for SAND sensory subtype scores. Sensory seeking scores loaded strongly onto Function 1, and hyperreactivity scores loaded strongly onto Function 2.

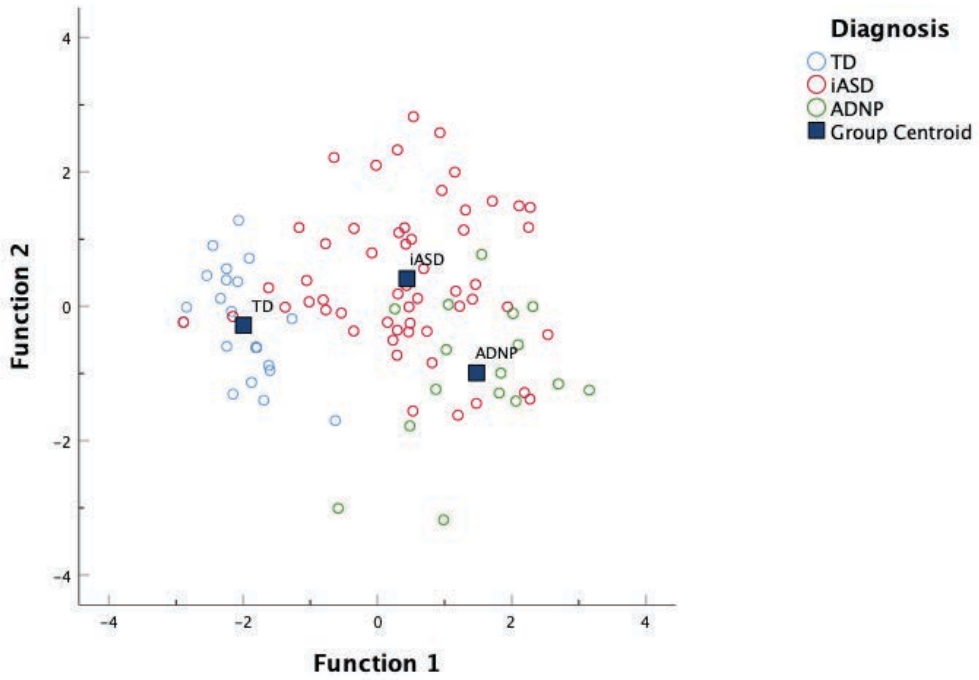

Figure 7. Canonical discriminant function plots for TD, iASD, and ADNP groups for SAND sensory domain scores. Total scores in the tactile, visual, and auditory domains loaded moderately to strongly onto Function 1. Tactile, visual, and auditory domains loaded less strongly onto Function 2.

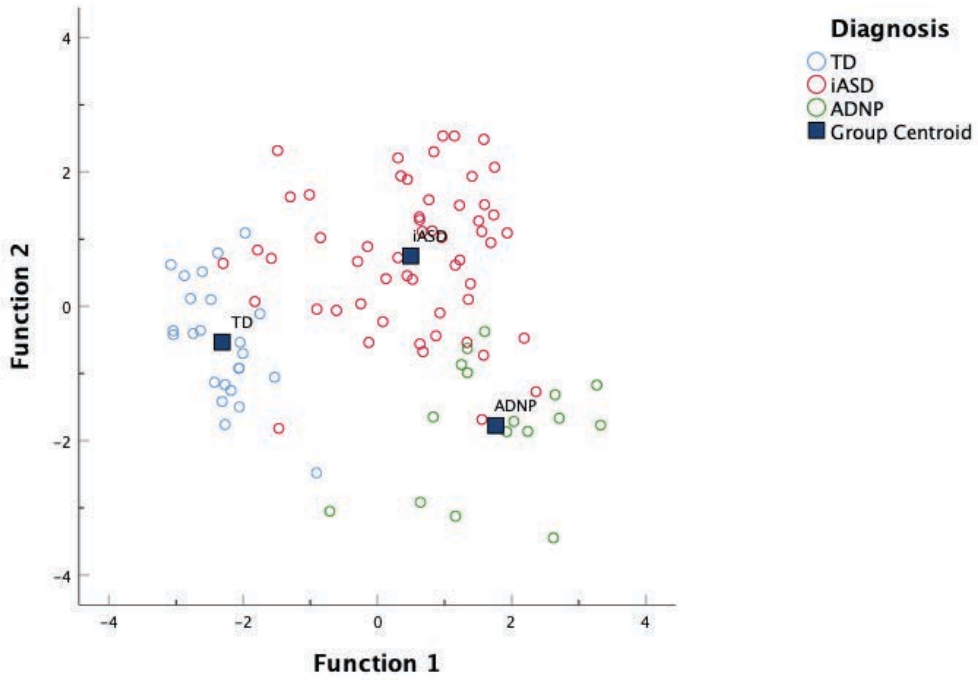

Figure 8. Canonical discriminant function plots for TD, iASD, and ADNP groups for SAND combined sensory domain and subtype scores. Tactile seeking, visual seeking, tactile hyporeactivity, and auditory seeking loaded moderately onto Function 1. Auditory hyperreactivity loaded moderately onto Function 2.

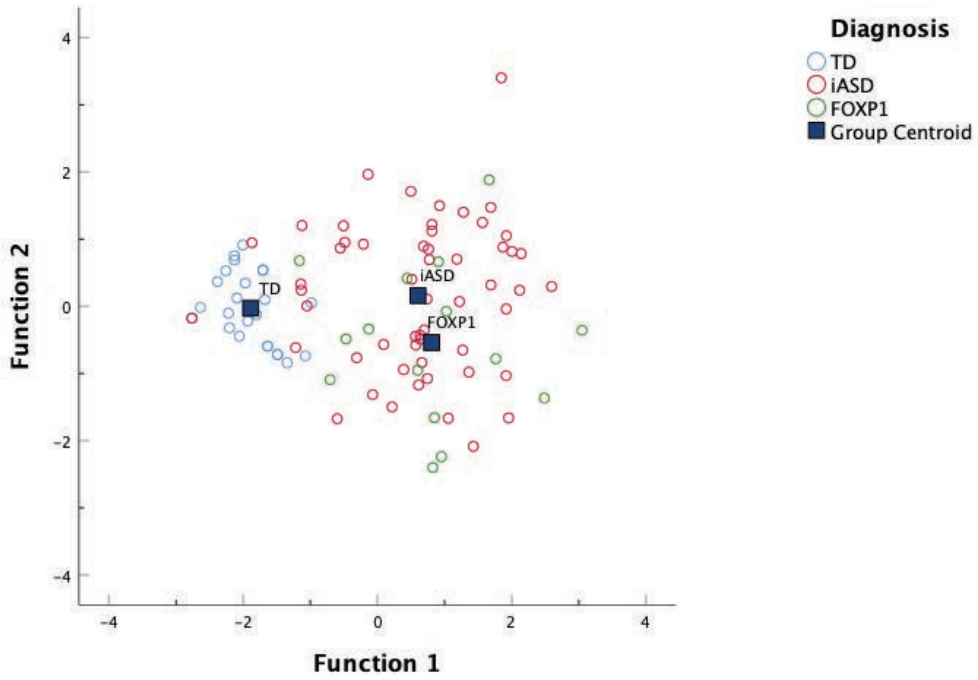

Figure 9. Canonical discriminant function plots for TD, iASD, and FOXP1 groups for SAND sensory subtype scores. Sensory seeking scores loaded strongest onto Function 1, and hyperreactivity scores loaded most strongly onto Function 2.

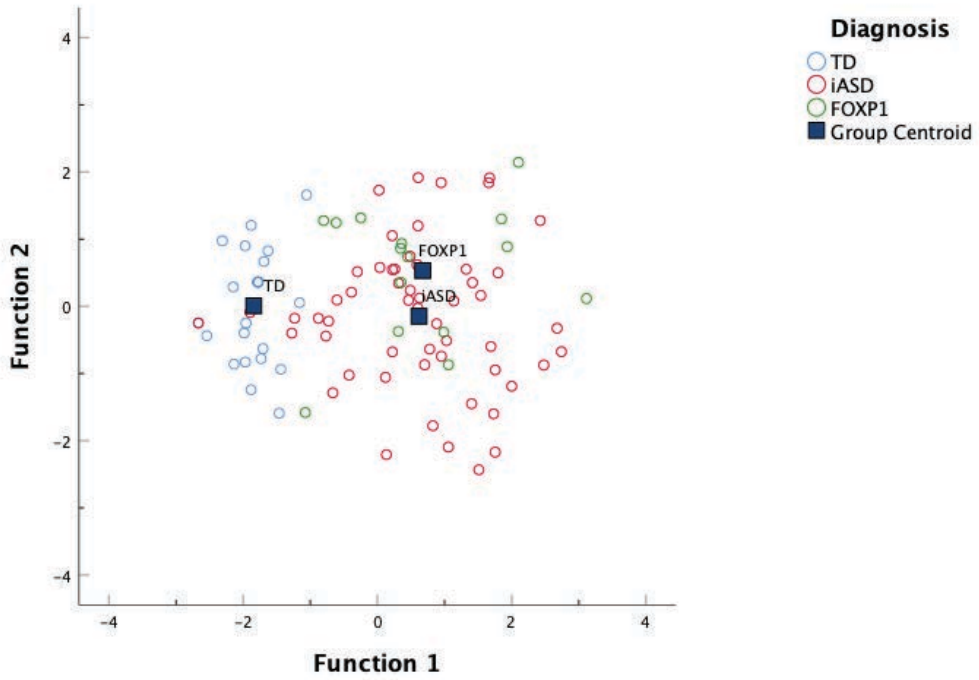

Figure 10. Canonical discriminant function plots for TD, iASD, and FOXP1 groups for SAND sensory domain scores. Total visual, auditory, tactile scores loaded strongest onto Function 1; these same scores loaded moderately onto Function 2.

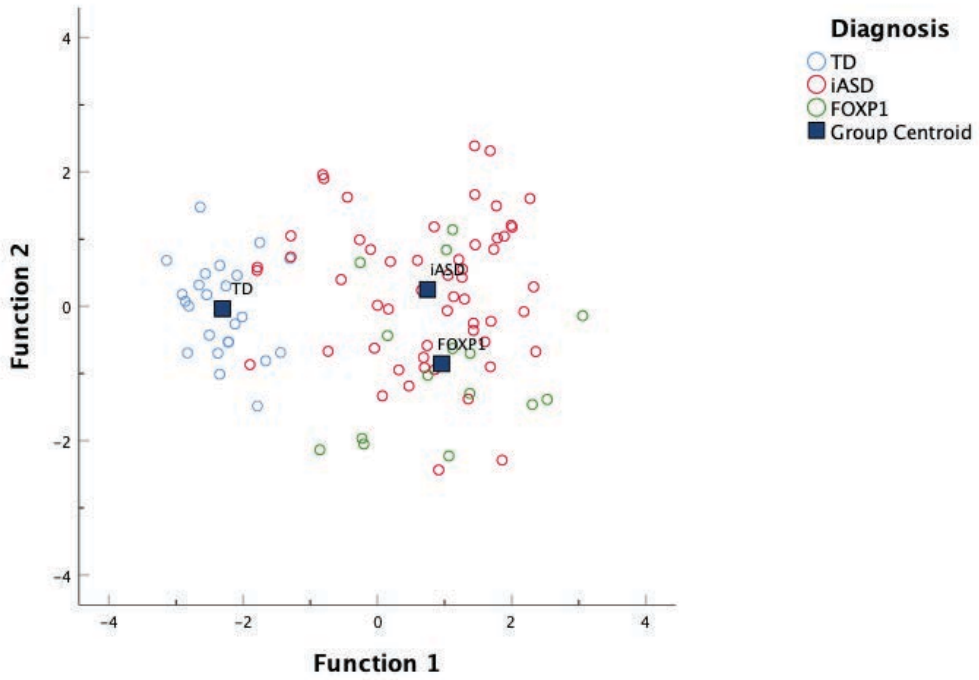

Figure 11. Canonical discriminant function plots for TD, iASD, and FOXP1 groups for SAND combined sensory subtype and domain scores. Visual sensory seeking, auditory hyperreactivity, and auditory seeking loaded moderately onto Function 1; Visual hyperreactivity and auditory hyporeactivity loaded strongest onto Function 2.

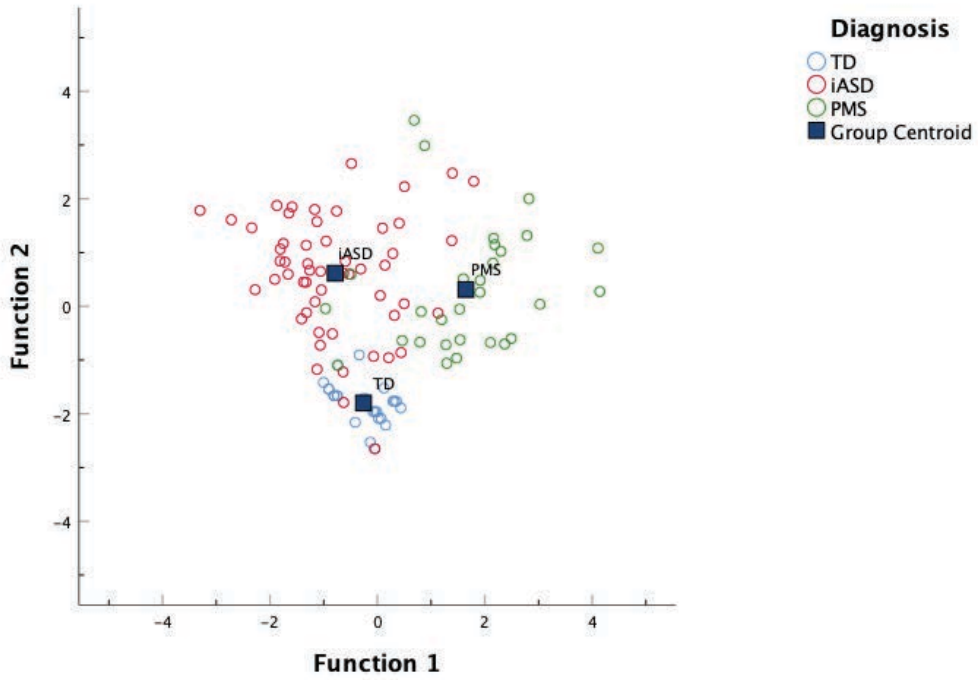

Figure 12. Canonical discriminant function plots for TD, iASD, and PMS groups for SAND sensory subtype scores. Hyporeactivity loaded highly onto Function 1. Sensory seeking and hyporeactivity loaded moderately onto Function 2.

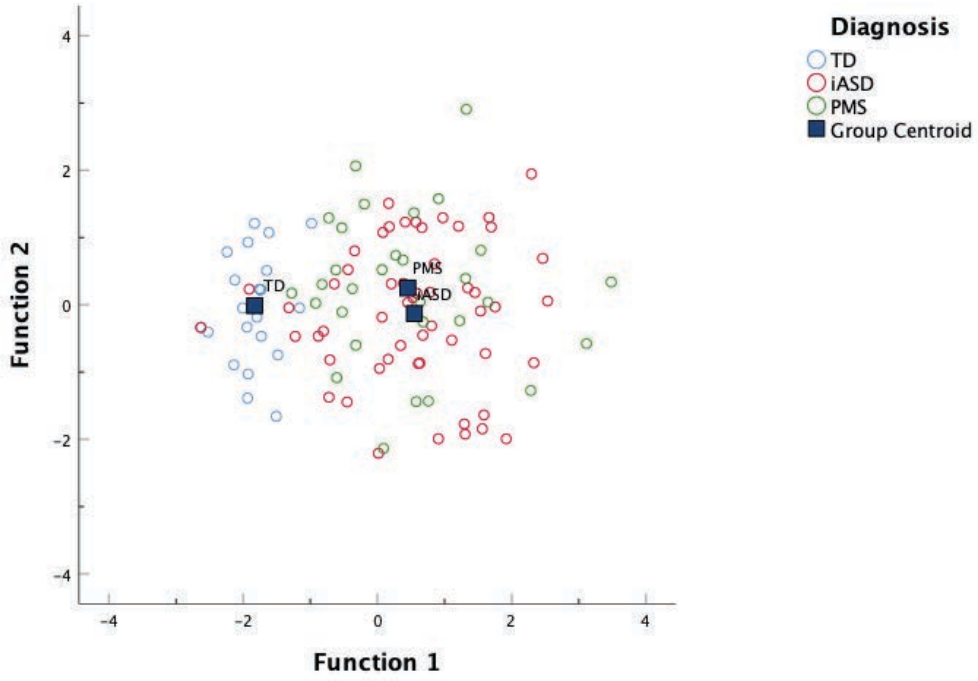

Figure 13. Canonical discriminant function plots for TD, iASD, and PMS groups for SAND sensory domain scores. Total visual, auditory, and tactile scores loaded onto Function 1. Total tactile scores loaded moderately onto Function 2.

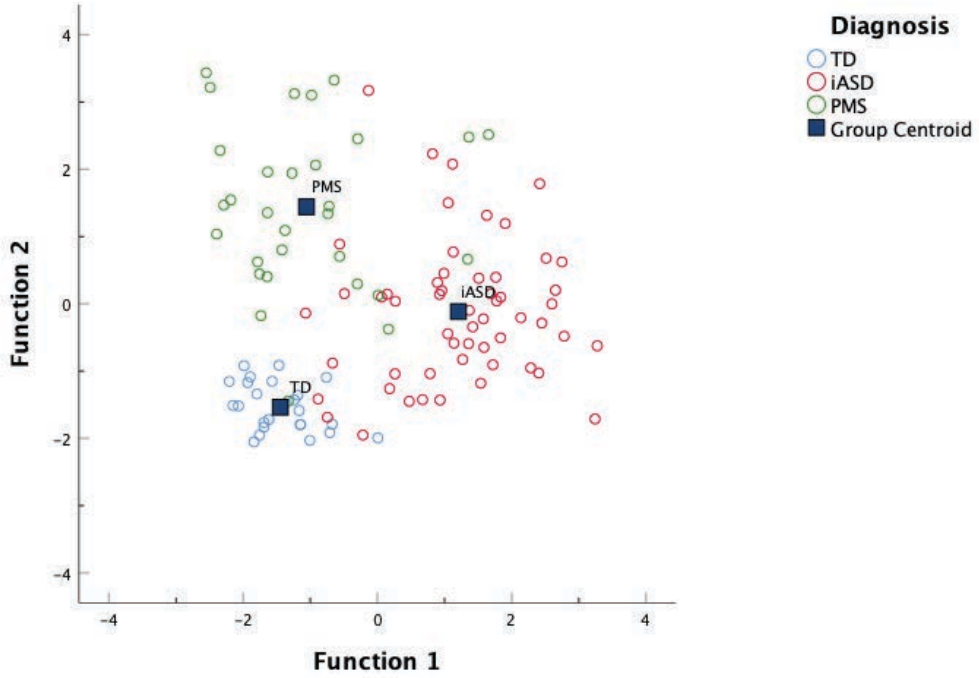

Figure 14. Canonical discriminant function plots for TD, iASD, and PMS groups for SAND combined sensory subtype and domain scores. Visual sensory seeking and auditory hyperreactivity loaded moderately and strongest onto Function 1. Visual hyporeactivity, auditory hyporeactivity, and tactile hyporeactivity loaded moderately onto Function 2.

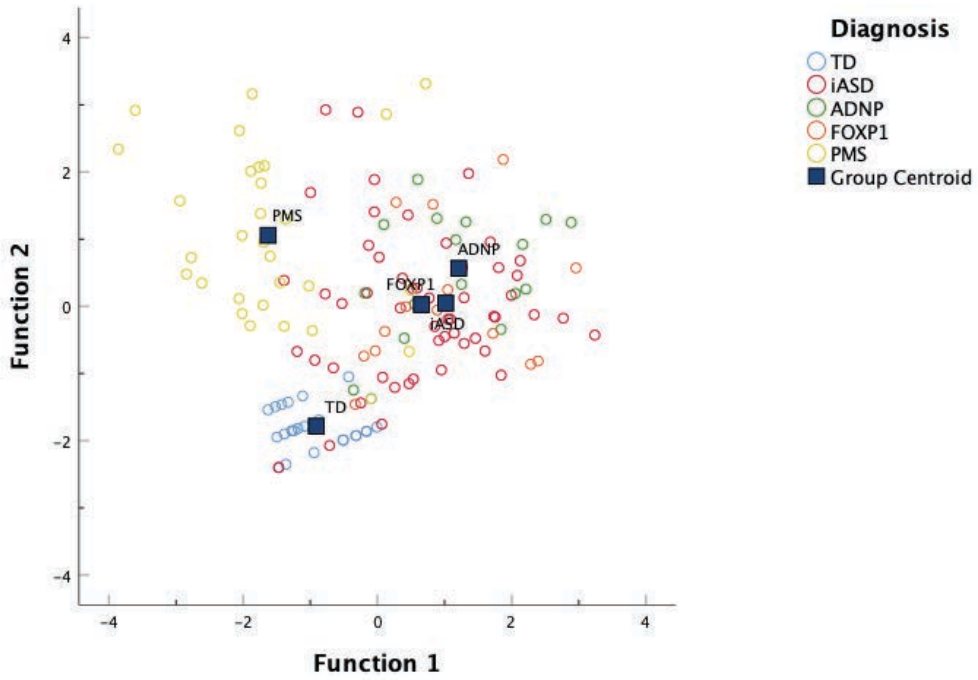

Figure 15. Canonical discriminant function plots for TD, iASD, ADNP, FOXP1, and PMS groups for SAND sensory subtype scores. Sensory seeking scores loaded most strongly onto Function 1, and hyporeactivity scores loaded most strongly onto Function 2.

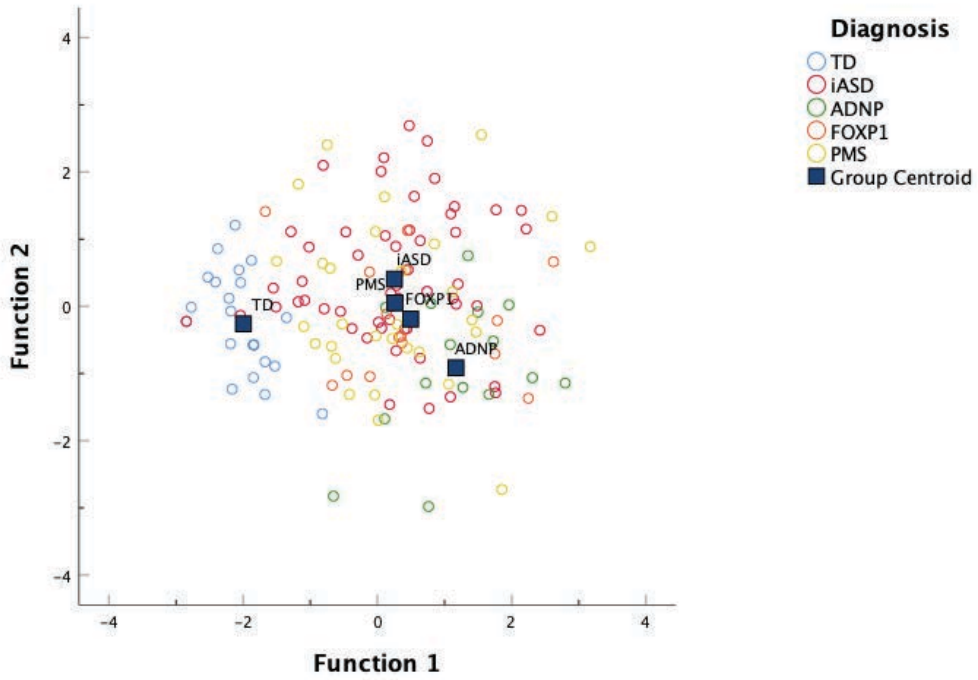

Figure 16. Canonical discriminant function plots for TD, iASD, ADNP, FOXP1, and PMS groups for SAND sensory domain scores. Total tactile, visual, and auditory scales loaded most strongly onto Function 1, and did so moderately onto Function 2.

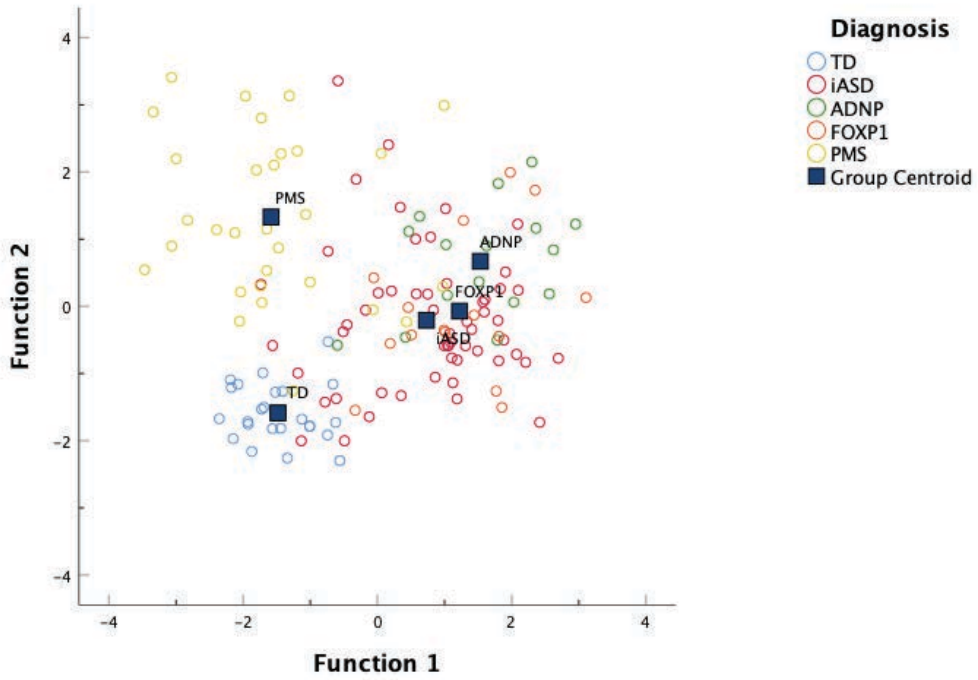

Figure 17. Canonical discriminant function plots for TD, iASD, ADNP, FOXP1, and PMS groups for SAND combined sensory subtype and domain scores. Visual sensory seeking, auditory sensory seeking, tactile sensory seeking, and auditory hyperreactivity scores loaded most strongly and moderately onto Function 1. Visual hyporeactivity, tactile hyporeactivity, auditory hyporeactivity, and tactile seeking scores loaded most strongly onto Function 2.

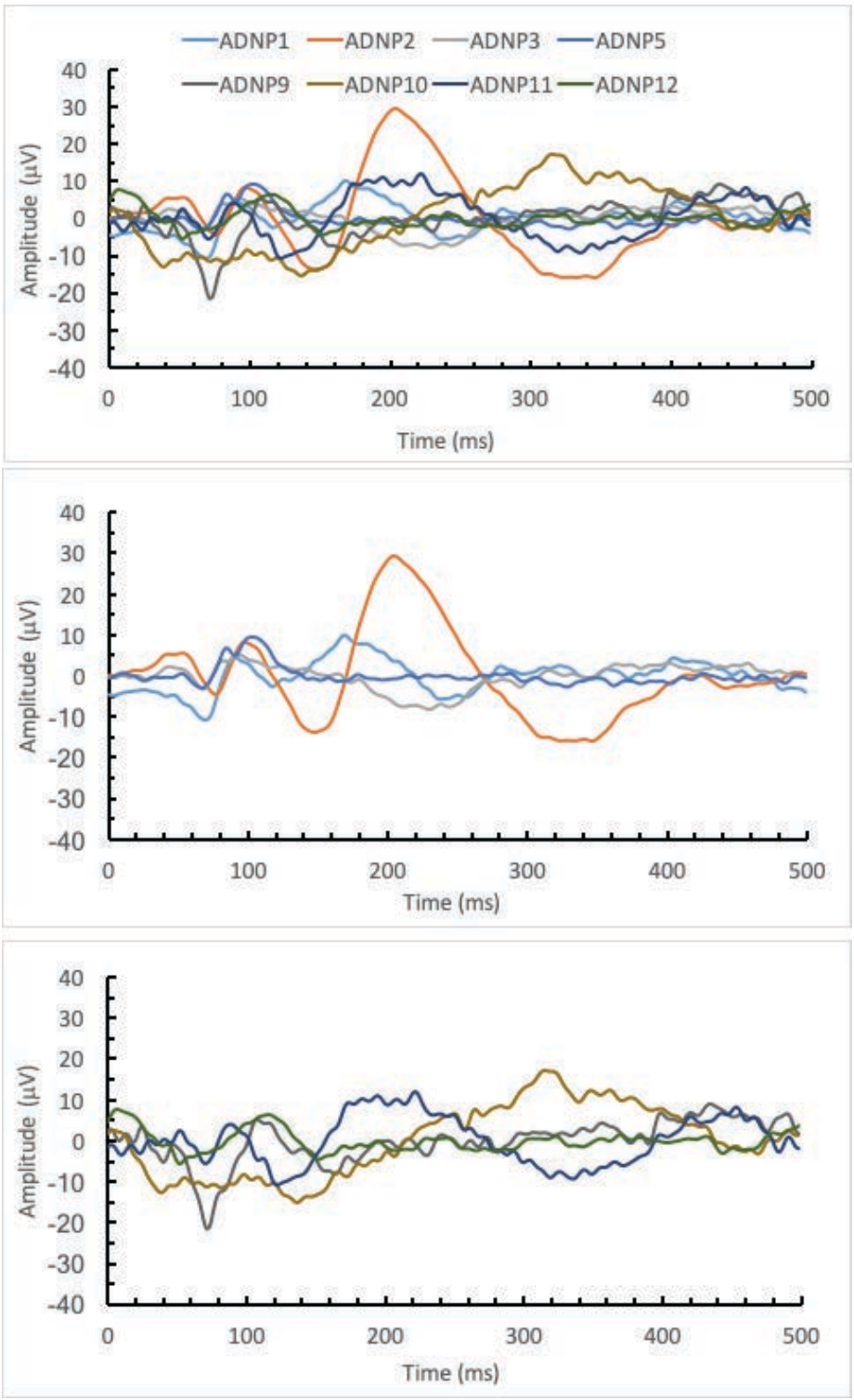

Figure 18a. Superimposed waveforms for children with ADNP syndrome for the standard condition. The first row includes all children in the ADNP group; the second row includes children without any reported vision problems, and the third row includes children with reported vision problems.

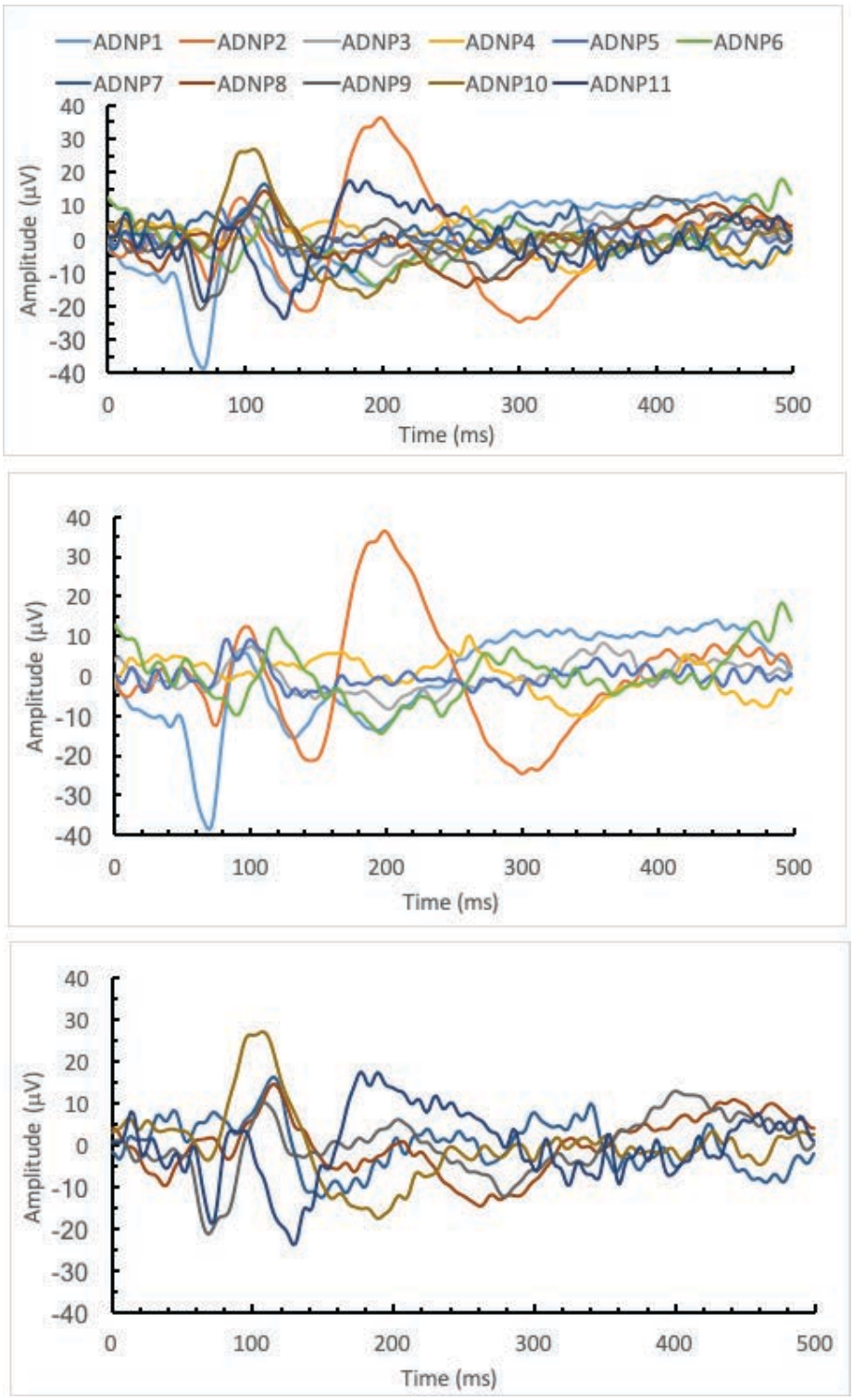

Figure 18b. Superimposed waveforms for children with ADNP syndrome for the short condition. The first row includes all children in the ADNP group; the second row includes children without any reported vision problems, and the third row includes children with reported vision problems.

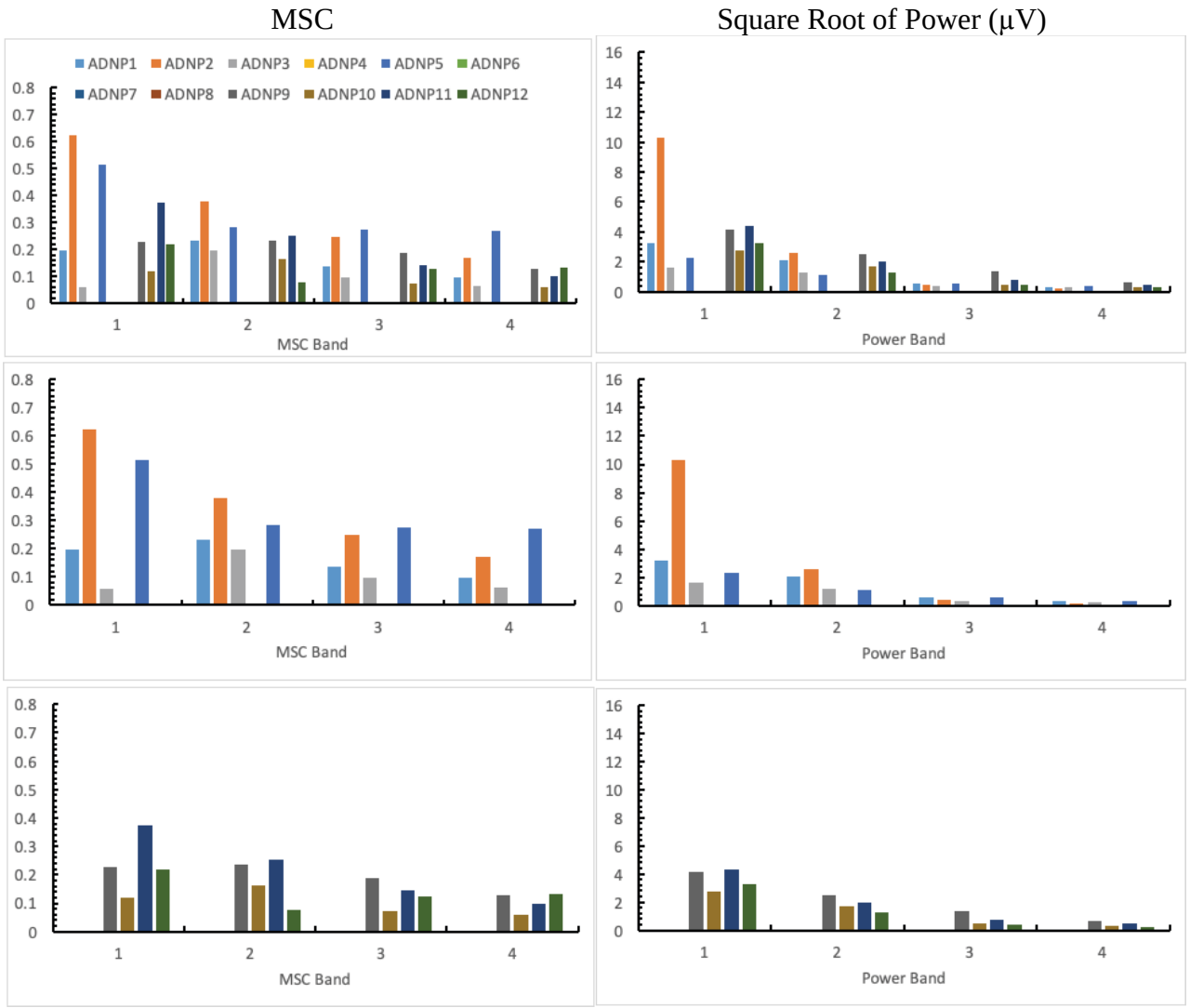

Figure 18c. MSC and square root of power values for participants in the ADNP group for the standard condition. The first row includes all children in the ADNP group; the second row includes children without any reported vision problems, and the third row includes children with reported vision problems.

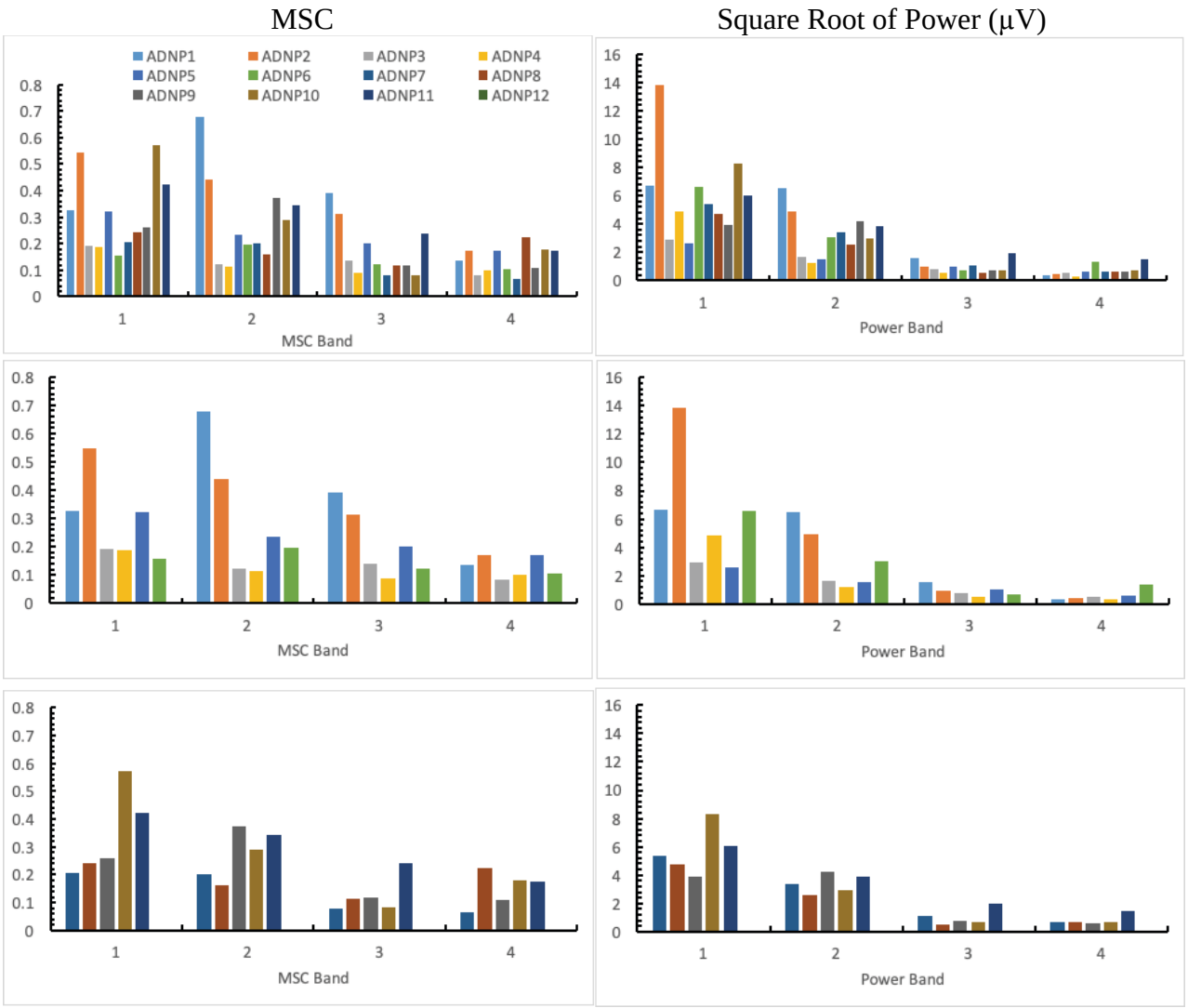

Figure 18d. MSC and power values for participants in the ADNP group for the short condition. The first row includes all children in the ADNP group; the second row includes children without any reported vision problems, and the third row includes children with reported vision problems.

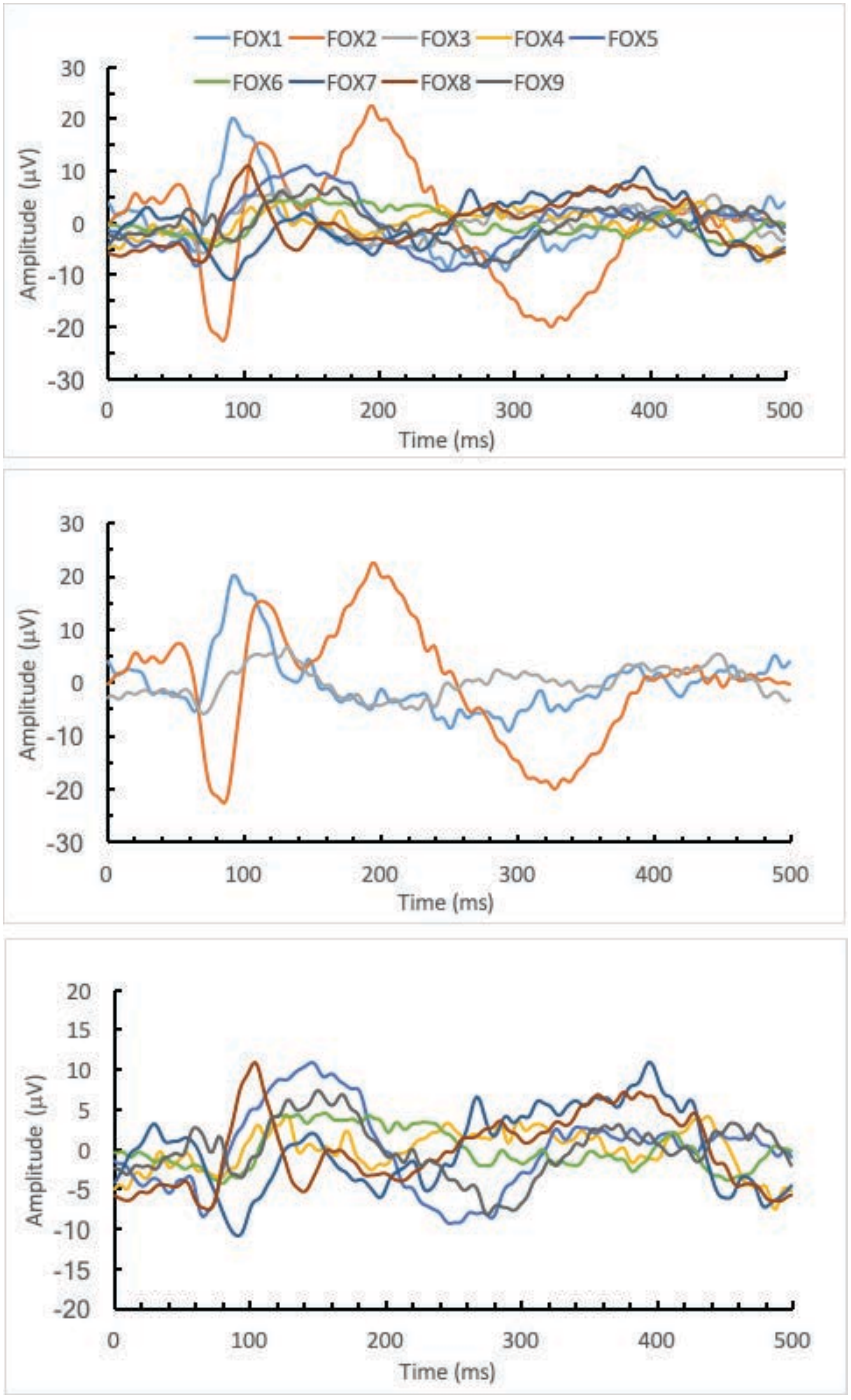

Figure 18e. Superimposed waveforms for children with FOXP1 syndrome for the standard condition. The first row includes all children in the FOXP1 group; the second row includes children without any reported vision problems, and the third row includes children with reported vision problems.

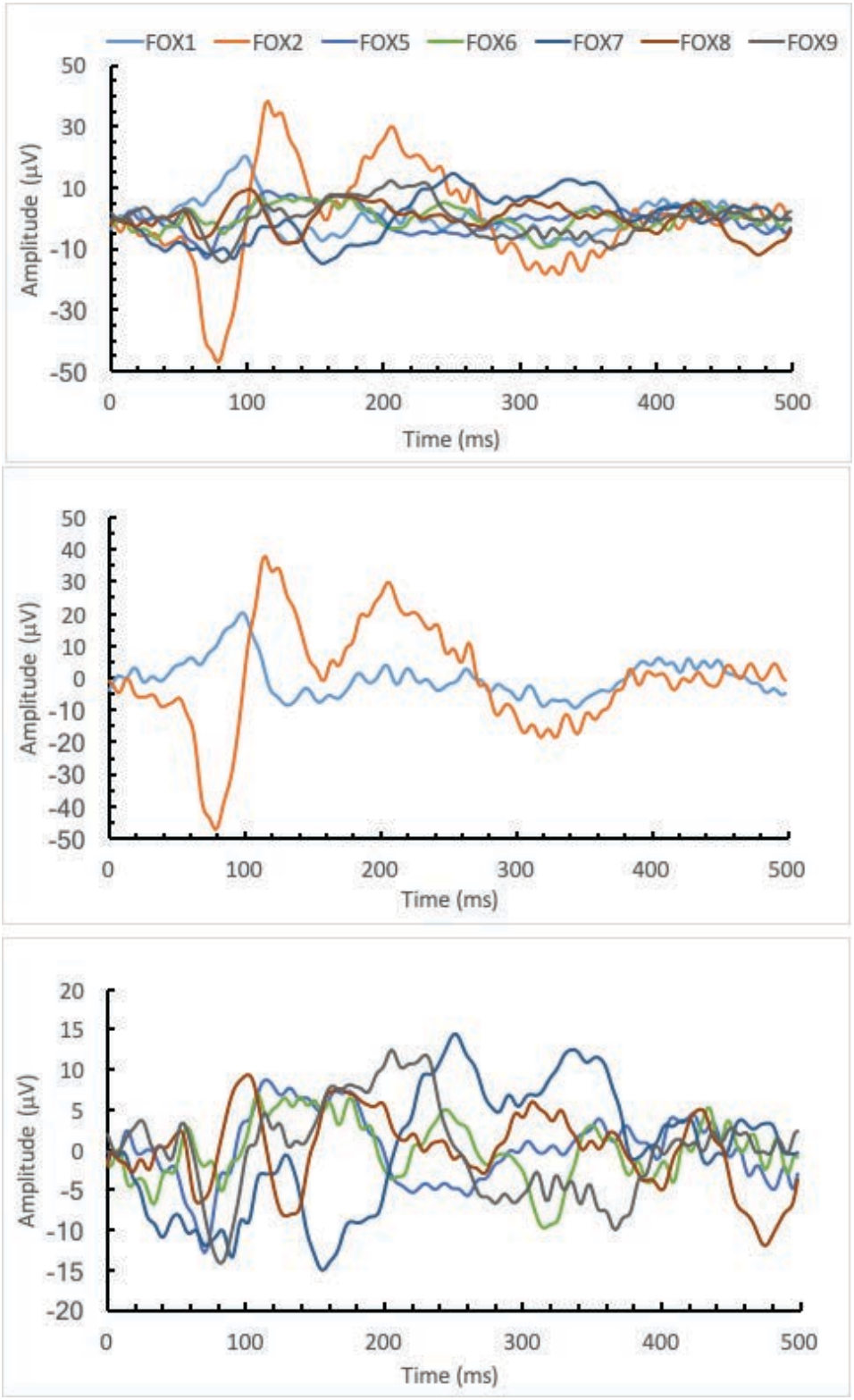

Figure 18f. Superimposed waveforms for children with FOXP1 syndrome for the short condition. The first row includes all children in the FOXP1 group; the second row includes children without any reported vision problems, and the third row includes children with reported vision problems.

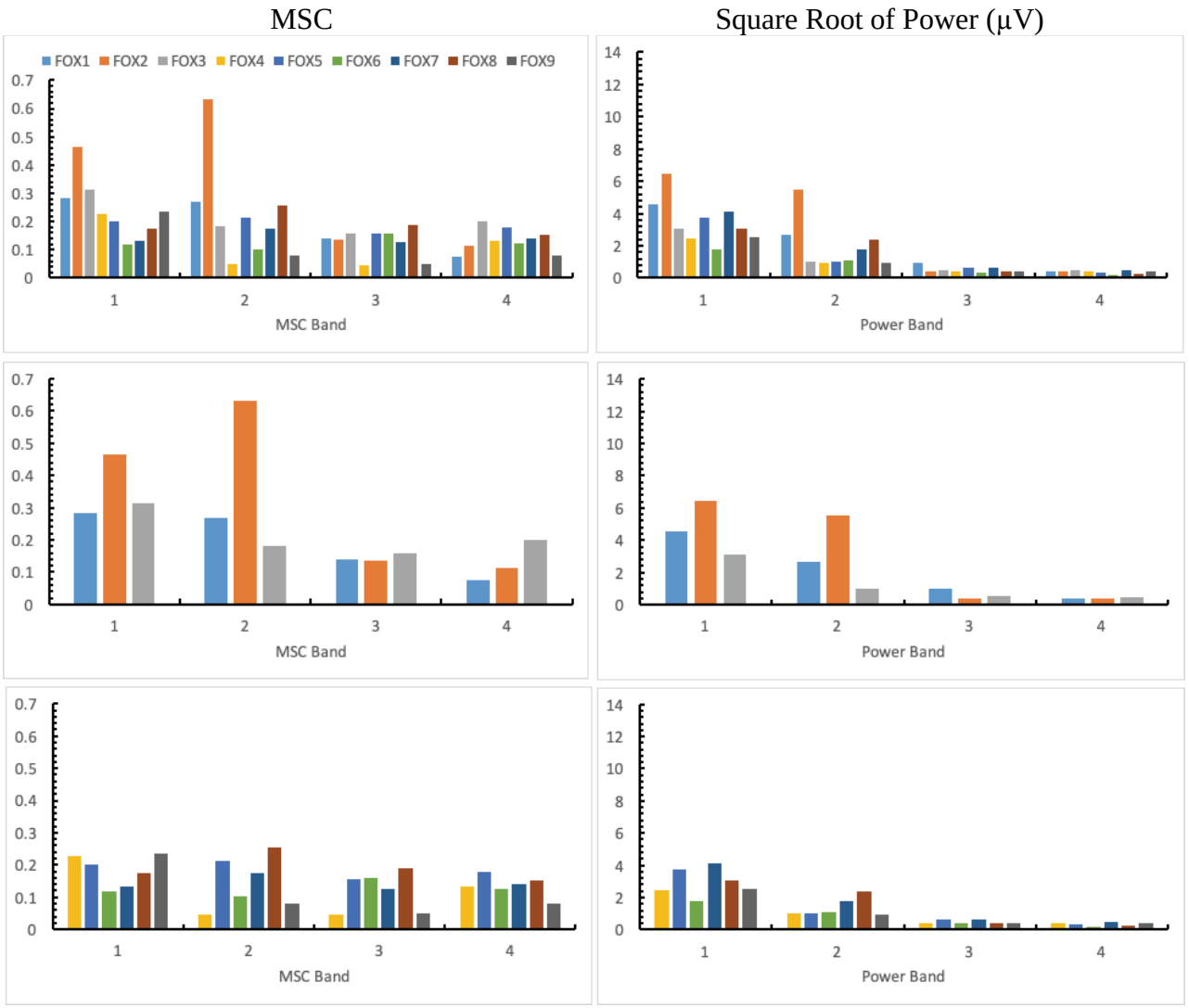

Figure 18g. MSC and square root of power values for participants in the FOXP1 group for the standard condition. The first row includes all children in the FOXP1 group; the second row includes children without any reported vision problems, and the third row includes children with reported vision problems.

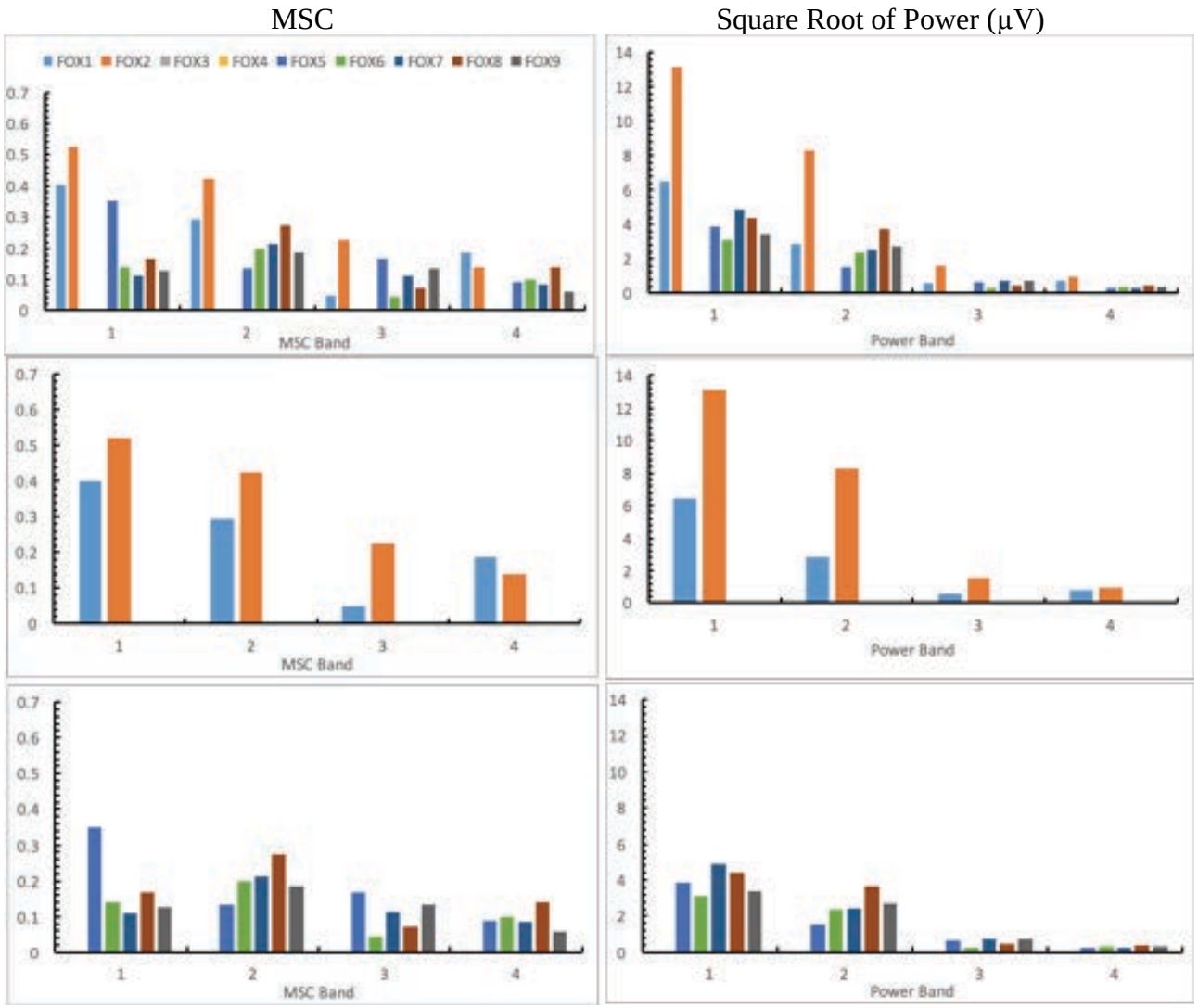

Figure 18h. MSC and square root of power values for participants in the FOXP1 group for the short condition. The first row includes all children in the FOXP1 group; the second row includes children without any reported vision problems, and the third row includes children with reported vision problems.

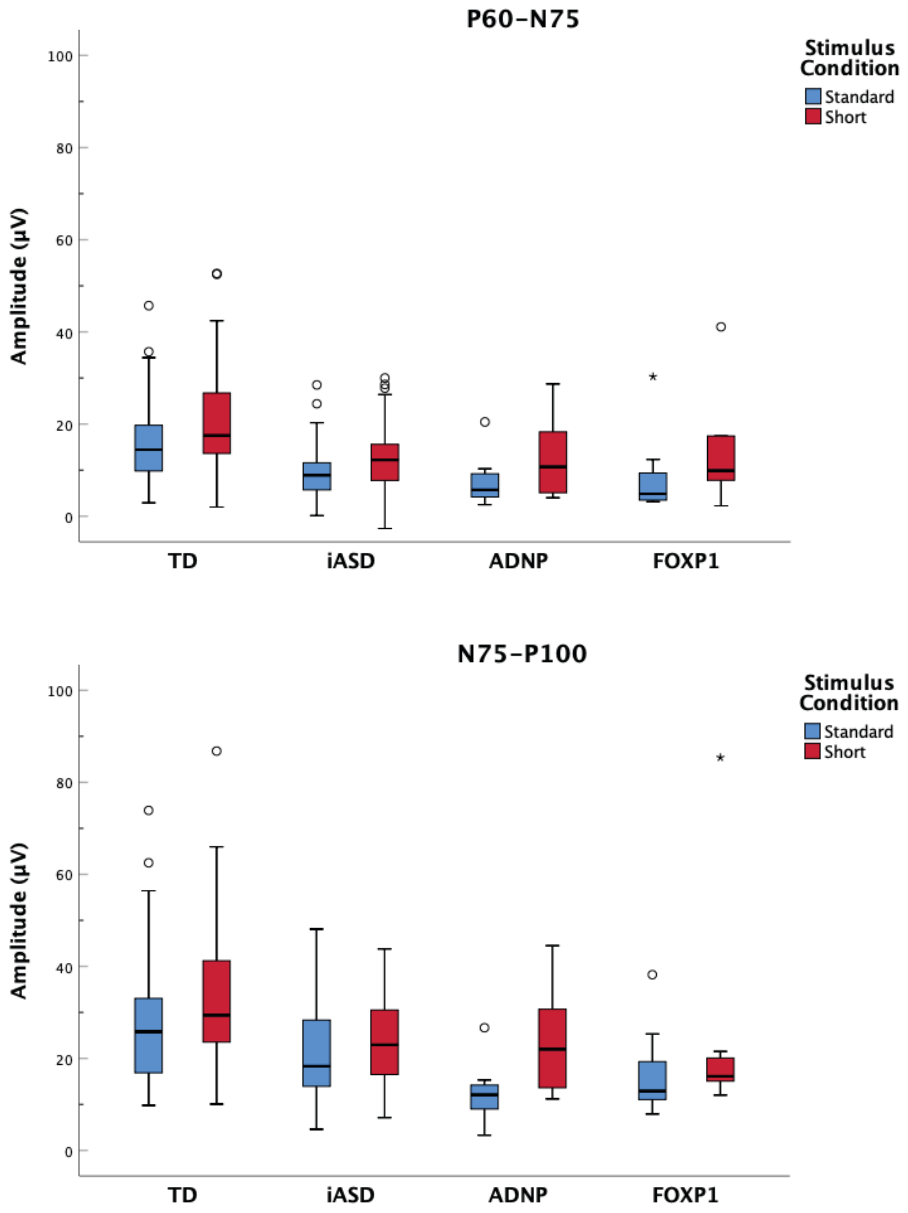

Figure 19. Box plots of amplitude for TD, iASD, ADNP, and FOXP1 groups for short and standard conditions. Each box represents 50% of the values, and the line in the middle of the box represents the median. The upper bound of the box represents the 75th percentile, and the lower bound of the box represents the 25th percentile. Whiskers represent the minimum and maximum values, excluding any outliers. Outliers, which are values that exceed 1.5 times interquartile range, are represented by open circles and extreme values, which are values 3 times outside the interquartile range, are represented by star symbols.

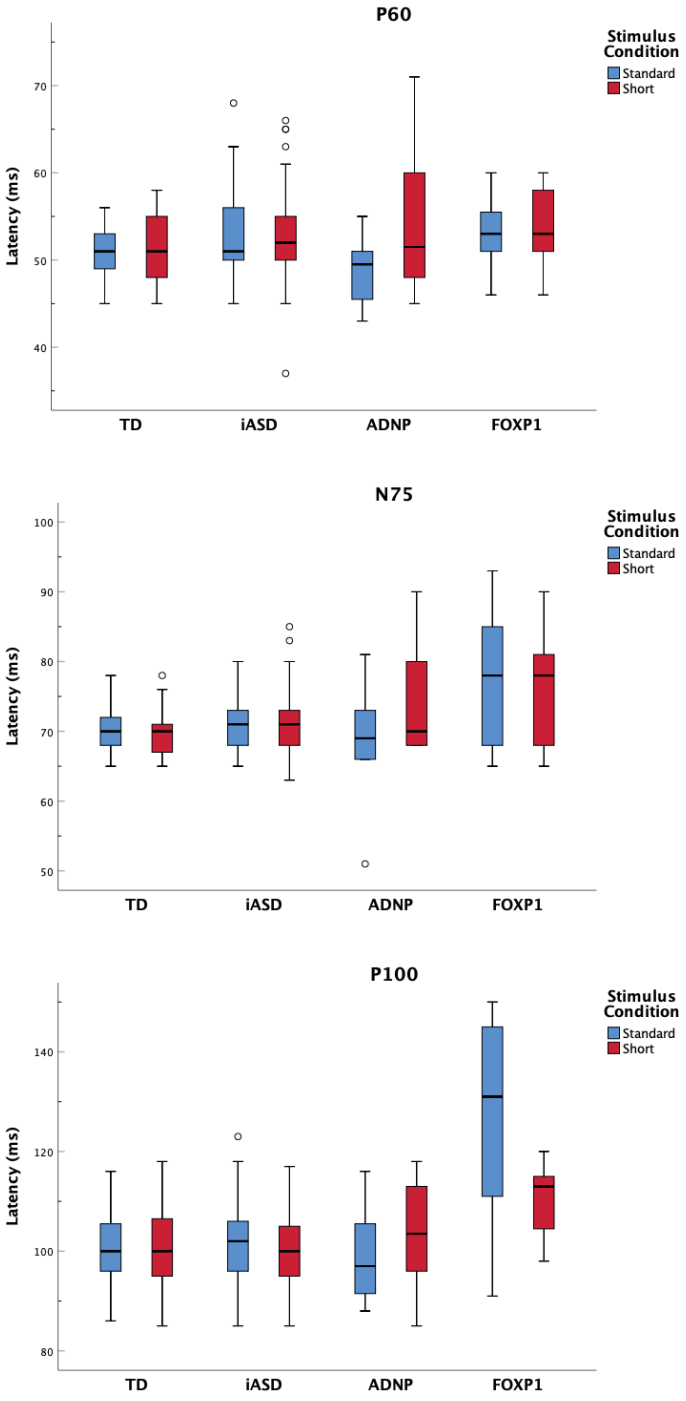

Figure 20. Box plots of P_{60}, N_{75}, and P_{100} latency for TD, iASD, ADNP, and FOXP1 groups for standard and short conditions. Each box represents 50% of the values, and the line in the middle of the box represents the median. The upper bound of the box represents the 75th percentile, and the lower bound of the box represents the 25th percentile. Whiskers represent the minimum and maximum values, excluding any outliers. Outliers, which are values that exceed 1.5 times interquartile range, are represented by open circles and extreme values, which are values 3 times outside the interquartile range, are represented by star symbols.

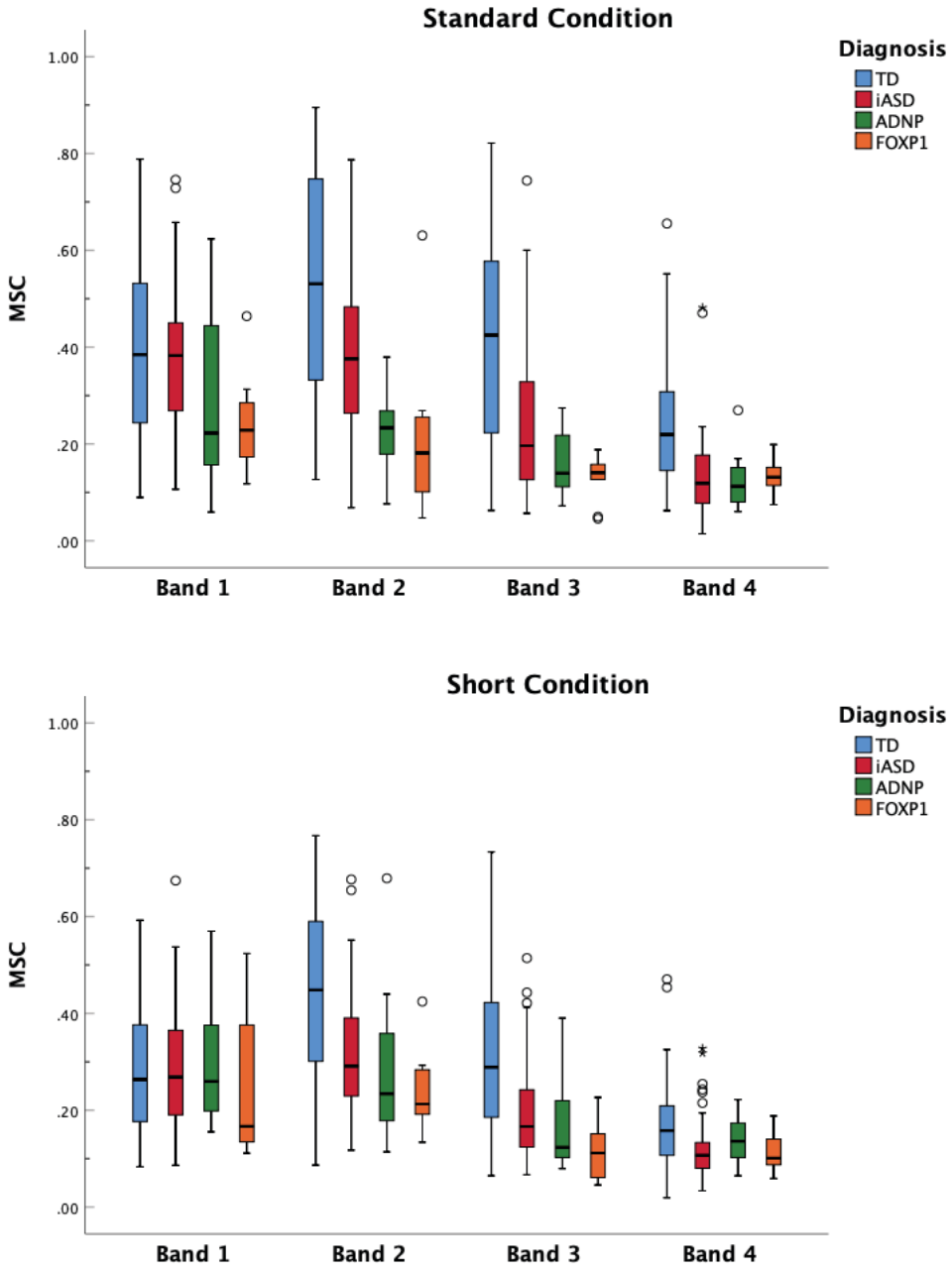

Figure 21. Box plots of MSC for TD, iASD, ADNP, and FOXP1 groups for standard (top) and short (bottom) conditions. Each box represents 50% of the values, and the line in the middle of the box represents the median. The upper bound of the box represents the 75th percentile, and the lower bound of the box represents the 25th percentile. Whiskers represent the minimum and maximum values, excluding any outliers. Outliers, which are values that exceed 1.5 times interquartile range, are represented by open circles and extreme values, which are values 3 times outside the interquartile range, are represented by star symbols.

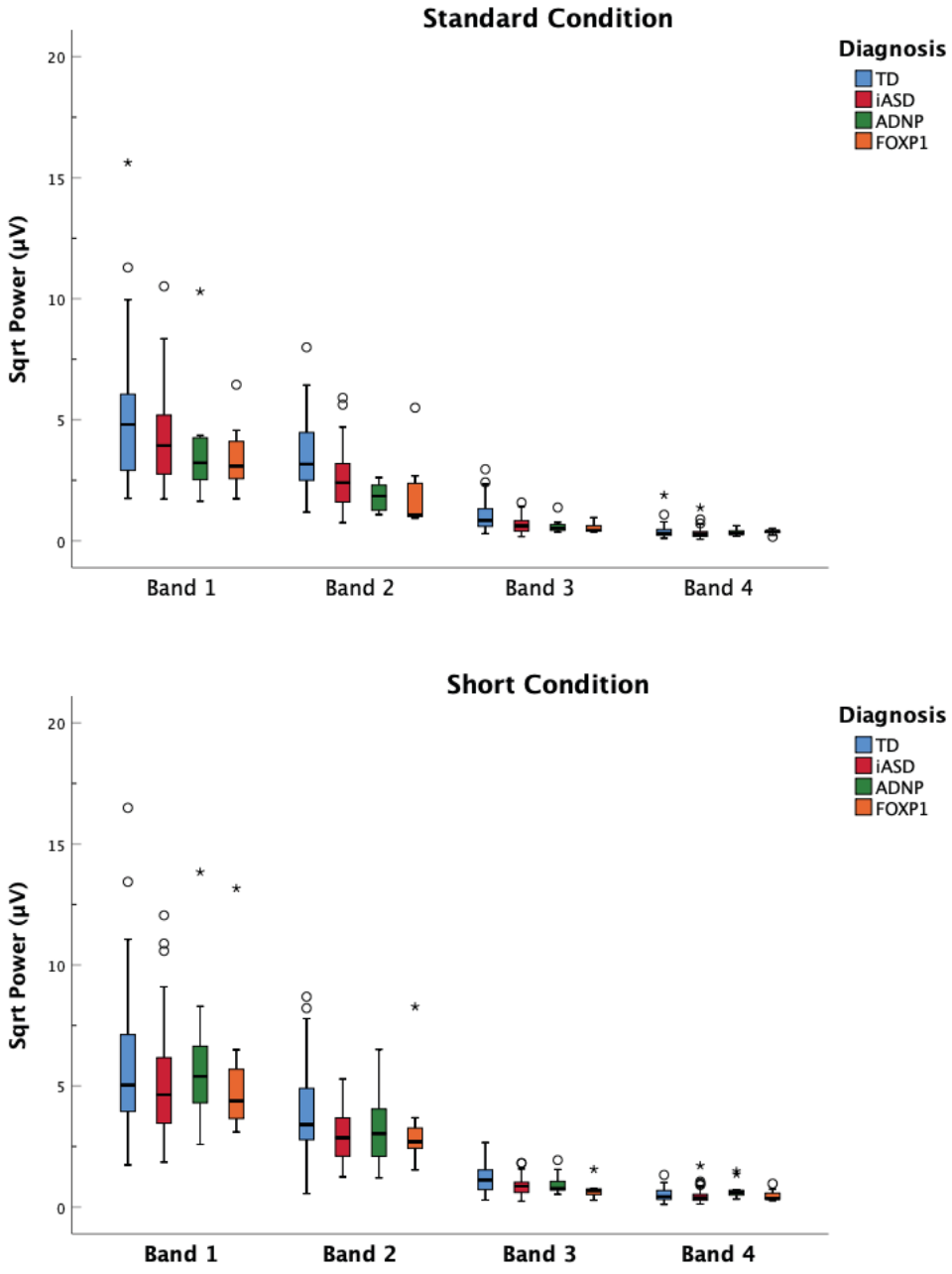

Figure 22. Box plots of square root of power for TD, iASD, ADNP, and FOXP1 groups for standard (top) and short (bottom) conditions. Each box represents 50% of the values, and the line in the middle of the box represents the median. The upper bound of the box represents the 75th percentile, and the lower bound of the box represents the 25th percentile. Whiskers represent the minimum and maximum values, excluding any outliers. Outliers, which are values that exceed 1.5 times interquartile range, are represented by open circles and extreme values, which are values 3 times outside the interquartile range, are represented by star symbol.

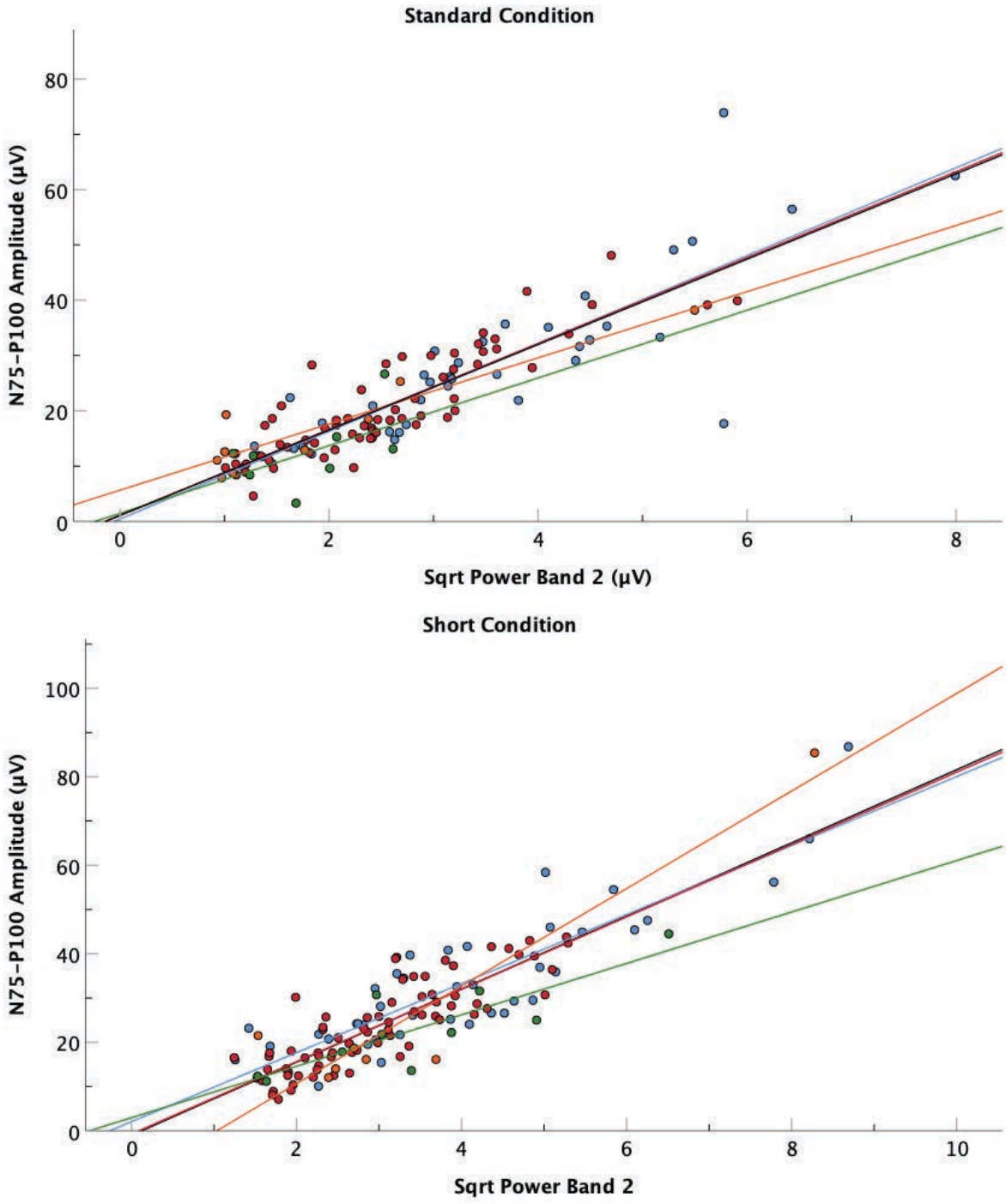

Figure 23. Grouped scatter plots of N_{75}-P_{100} amplitude versus square root of power in Frequency Band 2 for standard (top) and short (bottom) conditions. Blue lines and dots represent the TD group, red represents the iASD group, orange represents the FOXP1 group, and green represents the ADNP group. The black line represents the fit line for all groups. Linear regression parameters are presented in Table 15.

Appendix A

Structure Matrix of SAND Sensory Subtype Scores for TD, iASD, and ADNP Groups

	Function	
SAND Scale	1	2
Sensory Seeking	.834*	-.541
Hyporeactivity	.471*	.033
Hyperreactivity	.395	.837*

Note. Pooled within-groups correlations between discriminating variables and standardized canonical discriminant functions. Variables are ordered by absolute size of correlation within function. * denotes the largest absolute correlation between each variable and any discriminant function.

Functions at Group Centroids of SAND Sensory Subtype Scores for TD, iASD, and ADNP Groups

	Function	
Group	1	2
TD	-2.015	-.124
iASD	.509	.234
ADNP	1.273	-.616

Note. Unstandardized canonical discriminant functions are evaluated at group means.

Structure Matrix of SAND Sensory Domain Scores for TD, iASD, and ADNP Groups

	Function	
SAND Scale	1	2
Total Tactile	.884*	-.402
Total Visual	.731*	.376
Total Auditory	.615*	.550

Note. Pooled within-groups correlations between discriminating variables and standardized canonical discriminant functions. Variables are ordered by absolute size of correlation

within function. * denotes the largest absolute correlation between each variable and any discriminant function.

Functions at Group Centroids of SAND Sensory Domain Scores for TD, iASD, and ADNP Groups

	Function	
Group	1	2
TD	-1.996	-.281
iASD	.441	.411
ADNP	1.478	-.992

Note. Unstandardized canonical discriminant functions are evaluated at group means.

Structure Matrix of SAND Sensory Subtype Scores for TD, iASD, and FOXP1 Groups

	Function	
SAND Scale	1	2
Sensory Seeking	.808*	-.584
Hyporeactivity	.443*	.302
Hyperreactivity	.468	.699*

Note. Pooled within-groups correlations between discriminating variables and standardized canonical discriminant functions. Variables are ordered by absolute size of correlation within function. * denotes the largest absolute correlation between each variable and any discriminant function.

Functions at Group Centroids of SAND Sensory Subtype Scores for TD, iASD, and FOXP1 Groups

	Function	
Group	1	2
TD	-1.888	-.028
iASD	.604	.159
FOXP1	.807	-.540

Note. Unstandardized canonical discriminant functions are evaluated at group means.

Structure Matrix of SAND Sensory Domain Scores for TD, iASD, and FOXP1 Groups

	Function	
SAND Scale	1	2
Total Visual	.794*	-.160
Total Auditory	.778*	-.294
Total Tactile	.757*	.643

Note. Pooled within-groups correlations between discriminating variables and standardized canonical discriminant functions. Variables are ordered by absolute size of correlation within function. * denotes the largest absolute correlation between each variable and any discriminant function.

Functions at Group Centroids of SAND Sensory Domain Scores for TD, iASD, and FOXP1 Groups

	Function	
Group	1	2
TD	-1.842	.007
iASD	.620	-.148
FOXP1	.675	.531

Note. Unstandardized canonical discriminant functions are evaluated at group means.

Structure Matrix of SAND Combined Sensory Domain and Subtype Scores for TD, iASD, and FOXP1 Groups

	Function	
SAND Scale	1	2
Visual seeking	.552*	-.075
Auditory hyperreactivity	.519*	.439
Tactile seeking	.504*	-.464
Auditory seeking	.444*	-.279
Tactile hyporeactivity	.373*	-.152
Visual hyporeactivity	.354*	.167
Visual hyperreactivity	.168	.440*
Auditory hyporeactivity	.088	.404*
Tactile hyperreactivity	.167	.177*

Note. Pooled within-groups correlations between discriminating variables and standardized canonical discriminant functions. Variables are ordered by absolute size of correlation within function. * denotes the largest absolute correlation between each variable and any discriminant function.

Functions at Group Centroids of SAND Combined Sensory Domain and Subtype Scores for TD, iASD, and FOXP1 Groups

	Function	
Group	1	2
TD	-2.308	-.037
iASD	.747	.249
FOXP1	.956	-.855

Note. Unstandardized canonical discriminant functions are evaluated at group means.

Structure Matrix of SAND Sensory Subtype Scores for TD, iASD, and PMS Groups

	Function	
SAND Scale	1	2
Hyporeactivity	.798*	.601
Sensory Seeking	-.300	.746*
Hyperreactivity	-.376	.469*

Note. Pooled within-groups correlations between discriminating variables and standardized canonical discriminant functions. Variables are ordered by absolute size of correlation within function. * denotes the largest absolute correlation between each variable and any discriminant function.

Functions at Group Centroids of SAND Sensory Subtype Scores for TD, iASD, and PMS Groups

	Function	
Group	1	2
TD	-.259	-1.800
iASD	-.786	.615
PMS	1.647	.312

Note. Unstandardized canonical discriminant functions are evaluated at group means.

Structure Matrix of SAND Sensory Domain Scores for TD, iASD, and PMS Groups

	Function	
SAND Scale	1	2
Total Visual	.823*	-.385
Total Auditory	.771*	-.122
Total Tactile	.757*	.639

Note. Pooled within-groups correlations between discriminating variables and standardized canonical discriminant functions. Variables are ordered by absolute size of correlation within function. * denotes the largest absolute correlation between each variable and any discriminant function.

Functions at Group Centroids of SAND Sensory Domain Scores for TD, iASD, and PMS Groups

	Function	
Group	1	2
TD	-1.828	-.013
iASD	.551	-.131
PMS	.453	.250

Note. Unstandardized canonical discriminant functions are evaluated at group means.

Structure Matrix of SAND Combined Sensory Domain and Subtype Scores for TD, iASD, and PMS Groups

	Function	
SAND Scale	1	2
Visual seeking	.677*	.032
Auditory hyperreactivity	.630*	.018
Auditory seeking	.391*	.141
Tactile hyperreactivity	.231*	-.025
Visual hyperreactivity	.182*	.094
Visual hyporeactivity	-.017	.850*
Auditory hyporeactivity	-.265	.720*
Tactile hyporeactivity	.015	.694*
Tactile seeking	.328	.354*

Note. Pooled within-groups correlations between discriminating variables and standardized canonical discriminant functions. Variables are ordered by absolute size of correlation within function. * denotes the largest absolute correlation between each variable and any discriminant function.

Functions at Group Centroids of SAND Combined Sensory Domain and Subtype Scores for TD, iASD, and PMS Groups

	Function	
Group	1	2
TD	-1.445	-1.537
iASD	1.207	-.115
PMS	-1.056	1.441

Note. Unstandardized canonical discriminant functions are evaluated at group means.

Appendix B

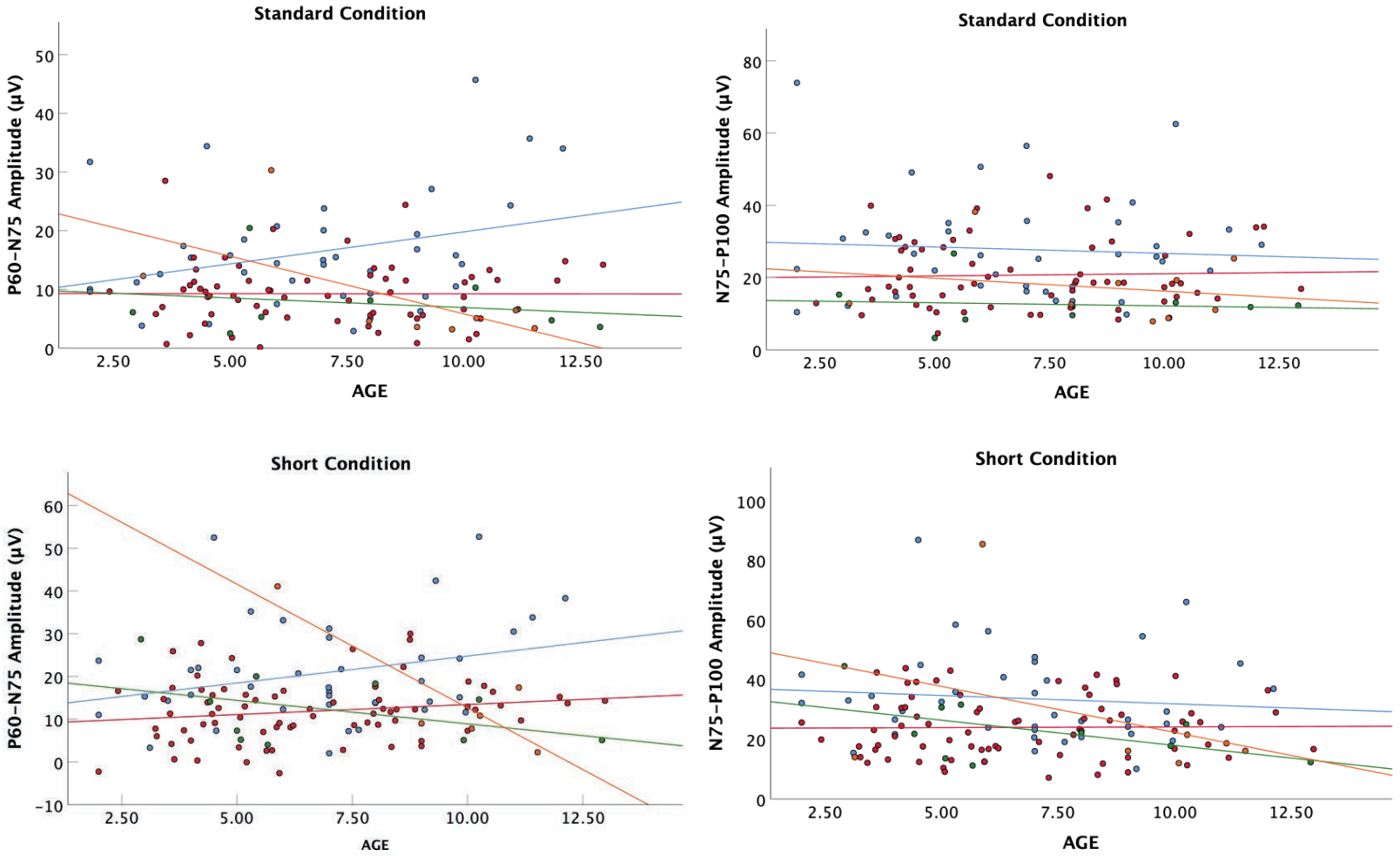

Grouped scatter plots of P_{60}-N_{75} and N_{75}-P_{100} amplitudes by age for TD, iASD, ADNP, and FOXP1 groups for standard (top row) and short (bottom row) conditions. Blue lines and dots represent the TD group, red represents the iASD group, orange represents the FOXP1 group, and green represents the ADNP group.

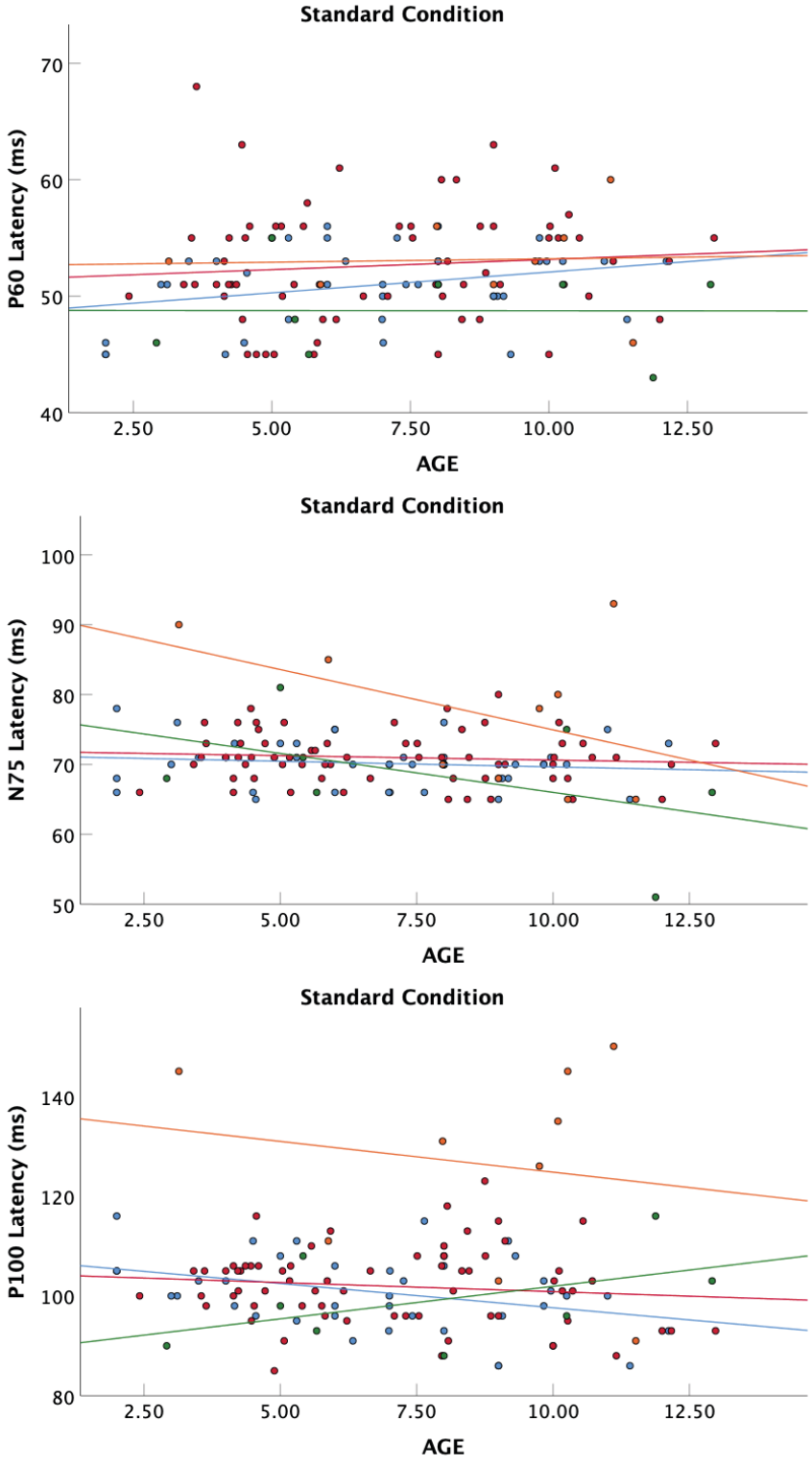

Grouped scatter plots of P_{60}, N_{75}, and P_{100} latency by age for TD, iASD, ADNP, and FOXP1 groups for the standard condition. Blue lines and dots represent the TD group, red represents the iASD group, orange represents the FOXP1 group, and green represents the ADNP group.

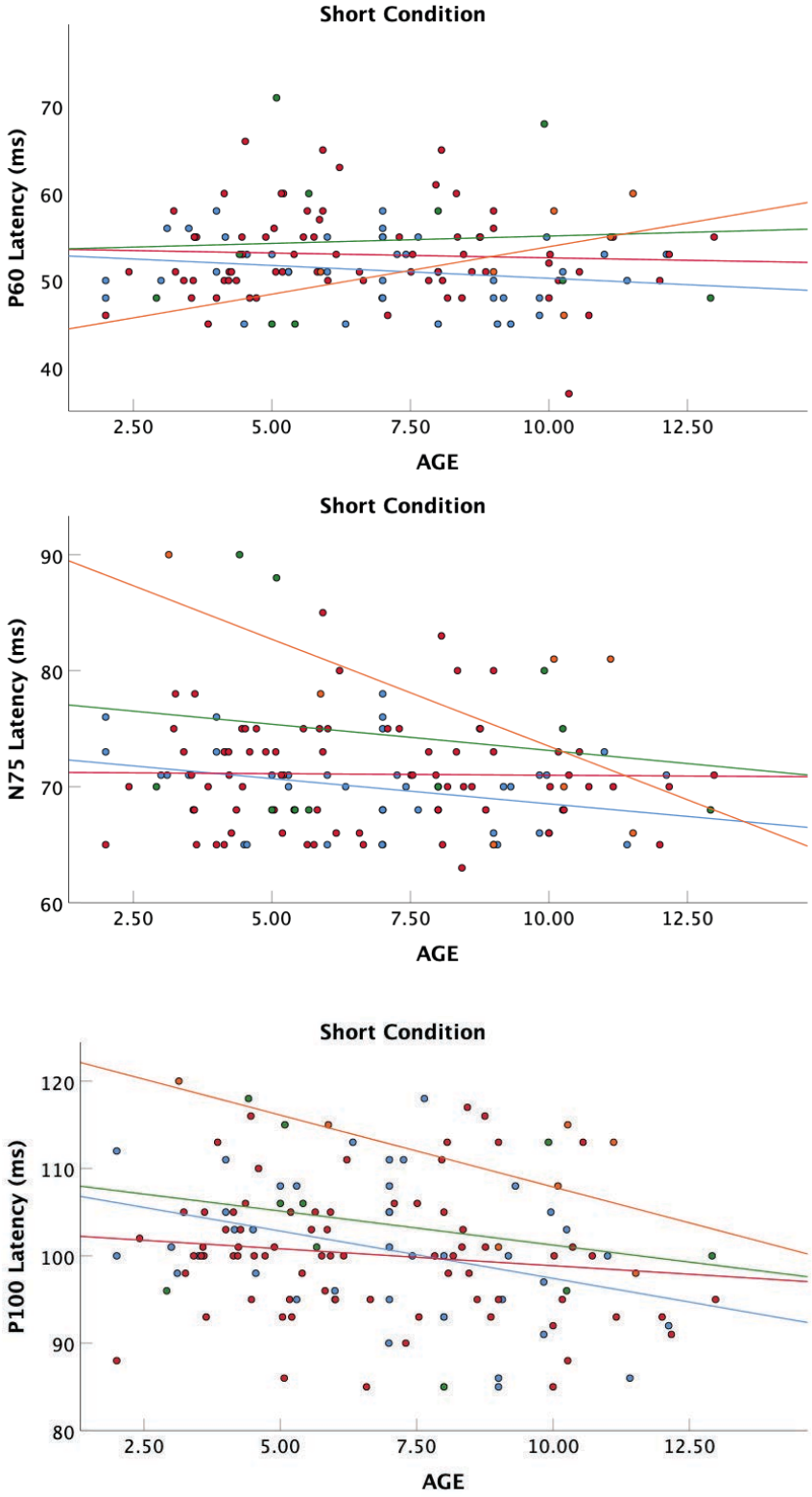

Grouped scatter plots of P_{60}, N_{75}, and P_{100} latency by age for TD, iASD, ADNP, and FOXP1 groups for the short condition. Blue lines and dots represent the TD group, red represents the iASD group, orange represents the FOXP1 group, and green represents the ADNP group.

	Amplitude				Latency					
	Standard		Short		Standard			Short		
	P_{60}-N_{75}	N_{75}-P_{100}	P_{60}-N_{75}	N_{75}-P_{100}	P_{60}	N_{75}	P_{100}	P_{60}	N_{75}	P_{100}
TD										
Slope	1.09	-0.35	1.26	-0.56	0.36	-0.16	-0.97	-0.29	-0.44	-1.08
Intercept	8.90	30.24	12.14	37.48	48.5	71.26	0.01	53.21	72.88	108.00
R^2	.09	.004	.08	.01	.09	.02	.13	.04	.10	.13
iASD										
Slope	-0.005	0.12	0.47	0.05	0.18	-0.13	-0.36	-0.11	71.26	-0.39
Intercept	9.30	19.86	8.72	23.66	51.40	71.89	104.00	53.72	-0.03	103.00
R^2	.000	.001	.03	.000	.01	.01	.02	.003	.000	.02
ADNP										
Slope	-0.33	-0.17	-1.10	-1.69	-0.003	-1.11	1.30	0.17	-0.45	-0.78
Intercept	10.16	13.90	19.89	34.83	48.77	77.14	88.89	53.42	77.65	109.00
R^2	.04	.008	.18	.27	.000	.21	.24	.003	.03	.06
FOXP1										
Slope	-1.97	-0.71	-5.79	-3.08	0.06	-1.73	-1.23	1.09	-1.84	-1.64
Intercept	25.48	23.39	70.53	53.11	52.63	92.21	137.00	42.99	91.93	124.00
R^2	.37	.04	.73	.13	.002	.19	.03	.19	.38	.40

Note. Slopes, intercepts, and R^2 values from bivariate scatter plots of tVEP time-domain measures by age by group.

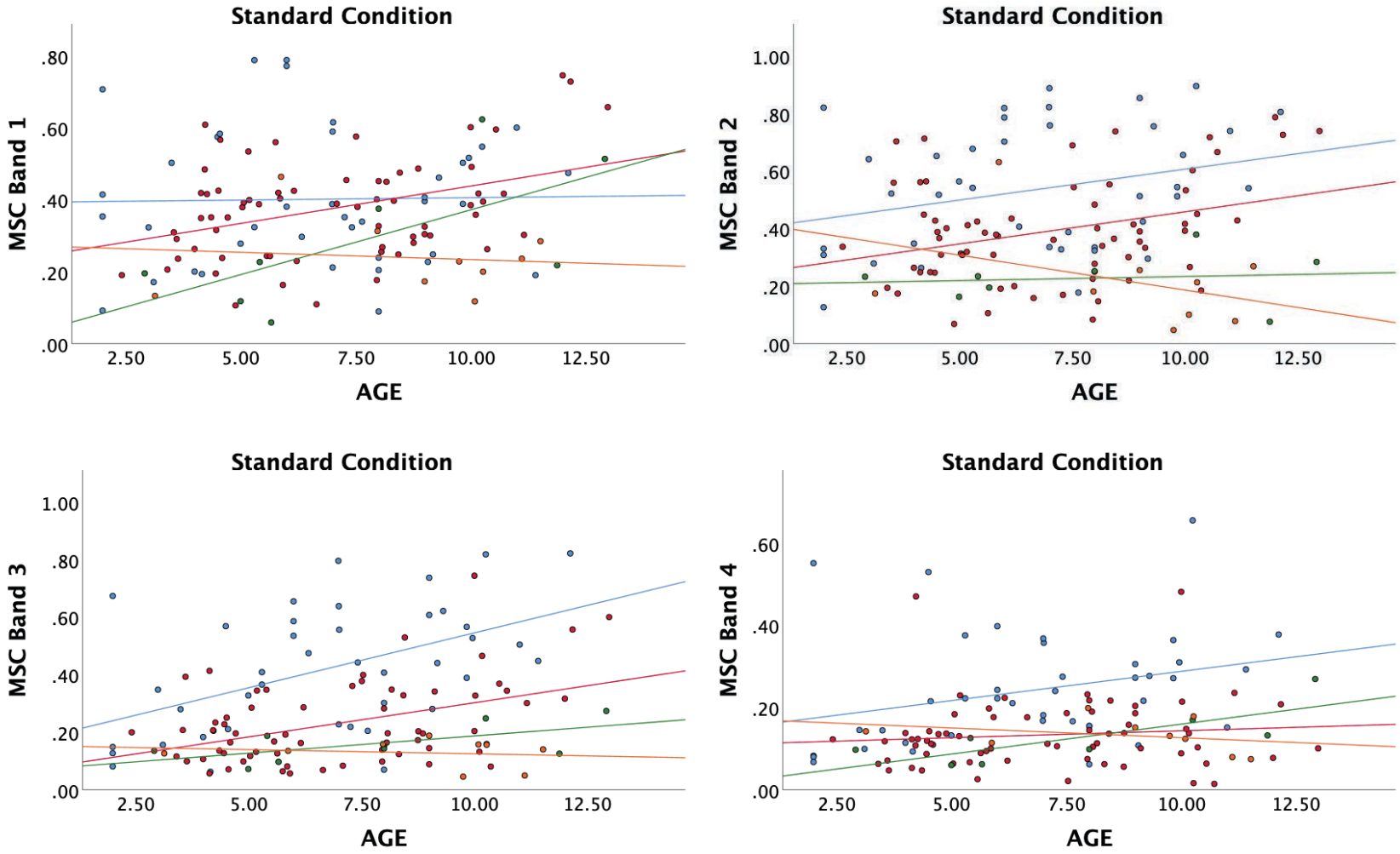

Grouped scatter plots of individual MSC bands by age for TD, iASD, ADNP, and FOXP1 groups for the standard condition. Blue lines and dots represent the TD group, red represents the iASD group, orange represents the FOXP1 group, and green represents the ADNP group.

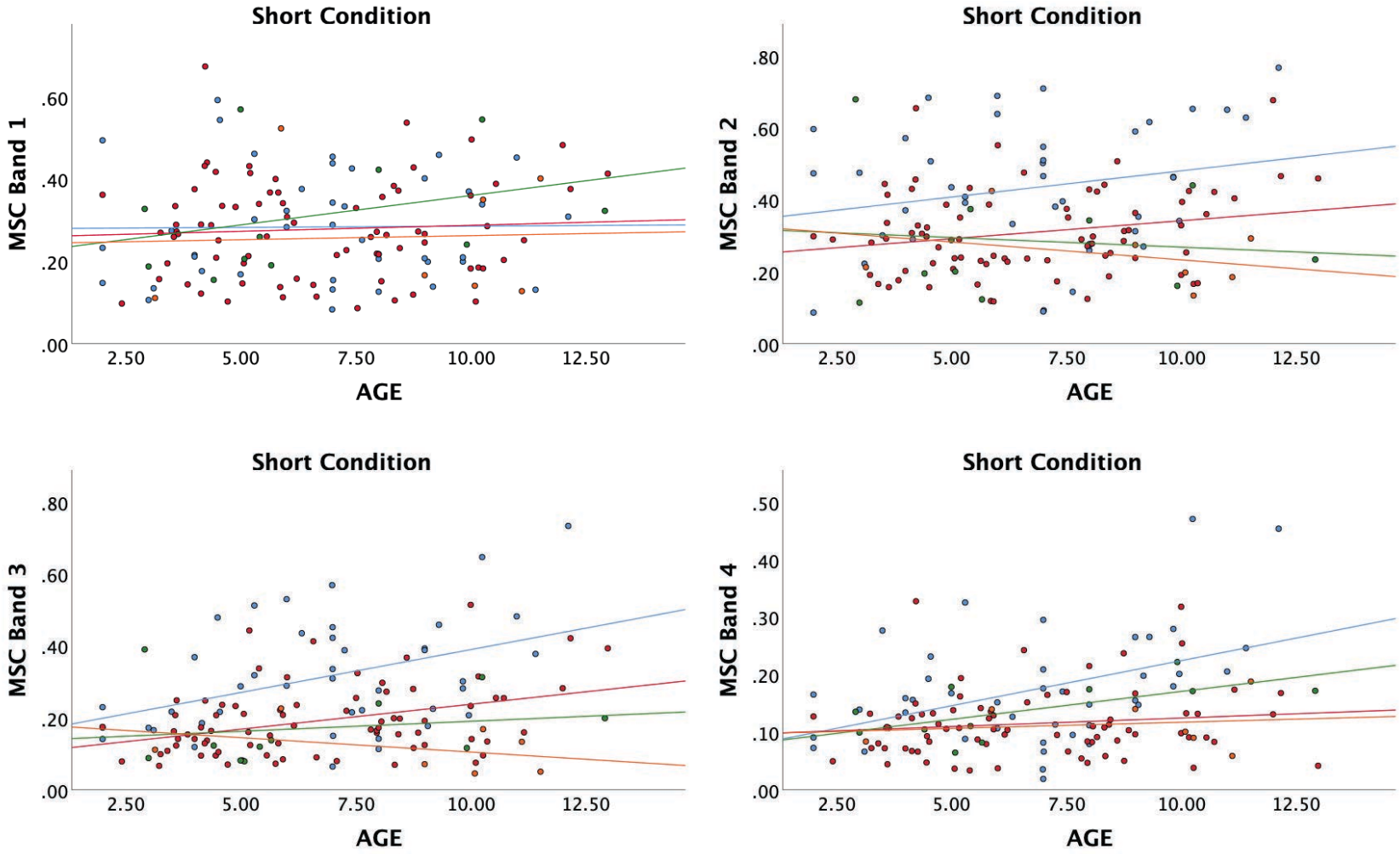

Grouped scatter plots of individual MSC bands by age for TD, iASD, ADNP, and FOXP1 groups for the short condition. Blue lines and dots represent the TD group, red represents the iASD group, orange represents the FOXP1 group, and green represents the ADNP group.

	MSC							
	Standard				Short			
	Band 1	Band 2	Band 3	Band 4	Band 1	Band 2	Band 3	Band 4
TD								
Slope	0.001	0.02	0.04	0.01	0.001	0.01	0.02	0.02
Intercept	0.39	0.39	0.16	0.15	0.28	0.33	0.15	0.07
R^2	.000	.08	.25	.08	.000	0.05	.17	.18
iASD								
Slope	0.02	0.02	0.02	0.003	0.003	0.01	0.01	0.003
Intercept	0.23	0.23	0.07	0.11	0.26	0.24	0.10	0.10
R^2	.15	.10	.18	.01	.004	0.05	.14	0.02
ADNP								
Slope	0.04	0.002	0.01	0.01	0.01	-0.005	0.006	0.01
Intercept	0.01	0.20	0.07	0.01	0.22	0.32	0.14	0.07
R^2	.44	.01	.37	.59	.10	0.01	.03	0.41
FOXP1								
Slope	-0.004	-0.02	-0.003	-0.005	0.002	-0.01	-0.008	0.002
Intercept	0.27	0.43	0.15	0.17	0.24	0.33	0.19	0.10
R^2	.01	.14	.03	.10	.001	.10	.14	0.02

Note. Slopes, intercepts, and R^2 values from bivariate scatter plots of tVEP MSC values by age by group.

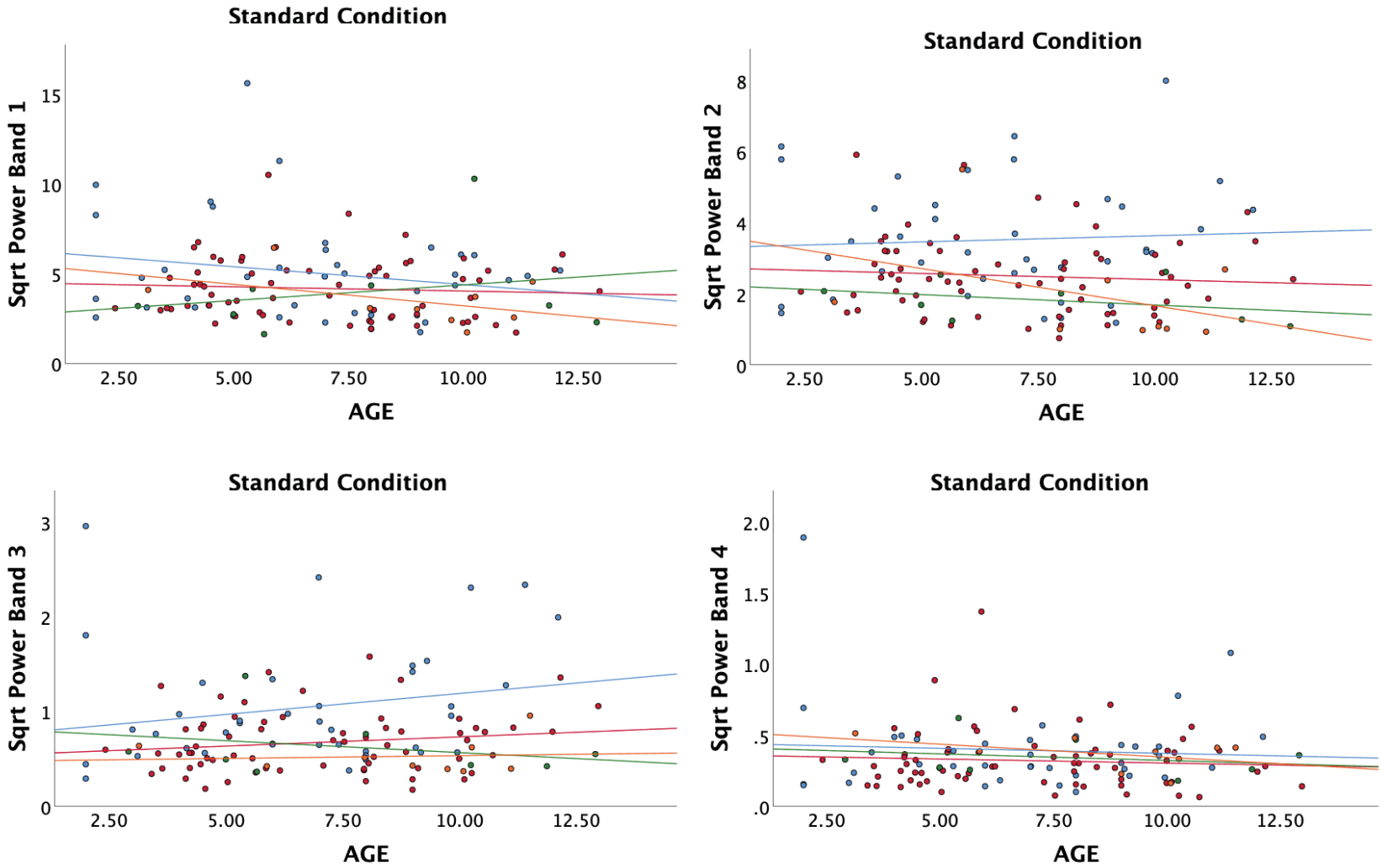

Grouped scatter plots of individual power bands (square root of power) by age for TD, iASD, ADNP, and FOXP1 groups for the standard condition. Blue lines and dots represent the TD group, red represents the iASD group, orange represents the FOXP1 group, and green represents the ADNP group.

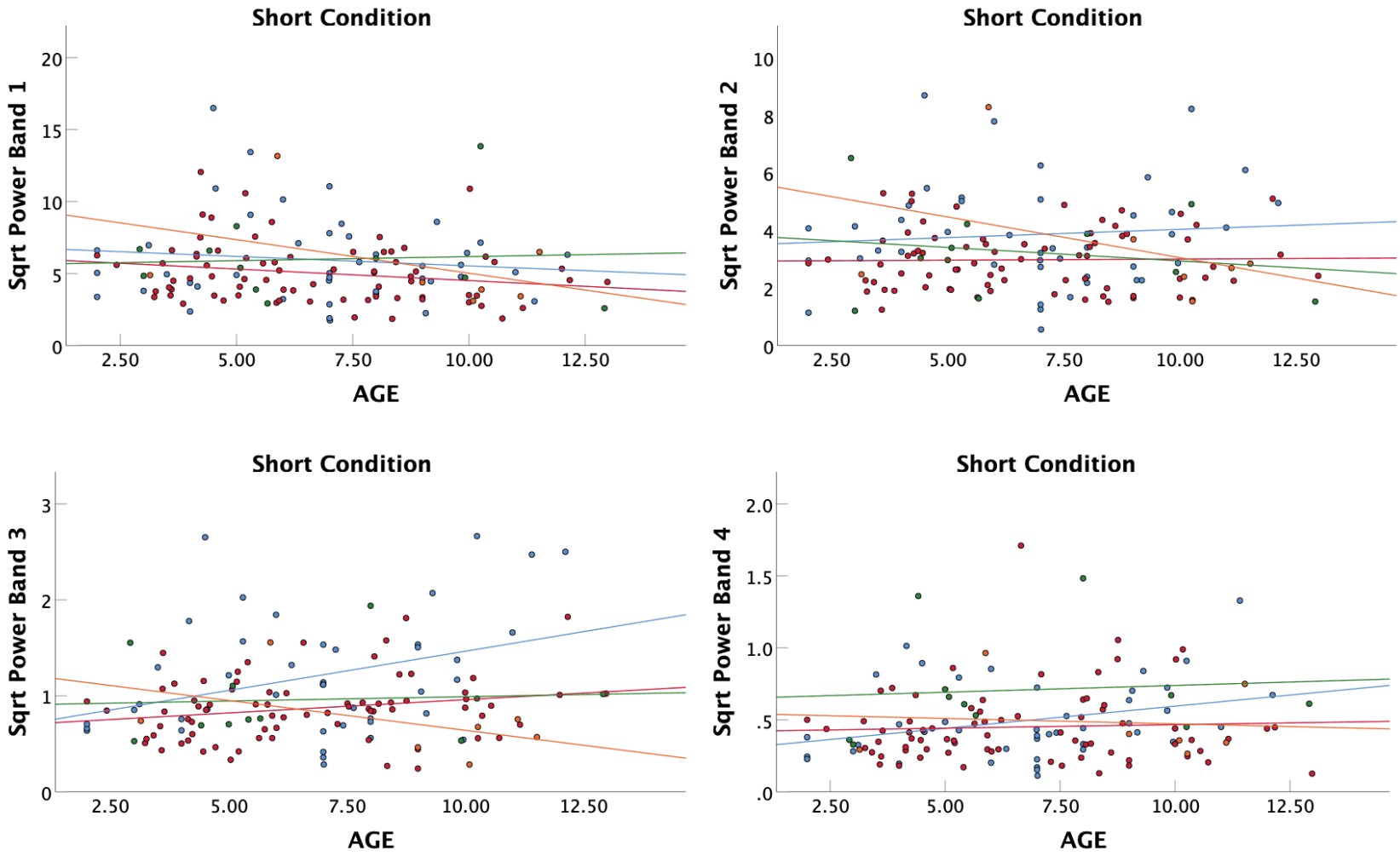

Grouped scatter plots of individual power bands (square root of power) by age for TD, iASD, ADNP, and FOXP1 groups for the short condition. Blue lines and dots represent the TD group, red represents the iASD group, orange represents the FOXP1 group, and green represents the ADNP group.

	Power							
	Standard				Short			
	Band 1	Band 2	Band 3	Band 4	Band 1	Band 2	Band 3	Band 4
TD								
Slope	-0.20	0.03	0.04	-0.007	-0.13	0.06	0.08	0.03
Intercept	6.39	3.28	0.75	0.44	6.85	3.46	0.65	0.29
R^2	.04	.004	.04	.004	.01	.01	.12	.09
iASD								
Slope	-0.05	-0.03	0.02	-0.006	-0.16	0.008	0.03	0.005
Intercept	4.51	2.74	0.54	0.36	6.12	2.92	0.68	0.42
R^2	.005	.01	.03	.005	.04	.000	0.05	.002
ADNP								
Slope	0.17	-0.06	-0.03	-0.009	0.06	-0.09	0.009	0.009
Intercept	2.65	2.27	0.82	0.42	5.61	3.88	0.90	0.64
R^2	.05	.13	.08	.06	.003	.04	.004	.01
FOXP1								
Slope	-0.24	-0.21	0.48	-0.02	-0.47	-0.28	-0.06	-0.008
Intercept	5.61	3.75	0.006	0.53	9.68	5.88	1.26	0.55
R^2	.21	.14	.01	.20	.17	.15	.23	.01

Note. Slopes, intercepts, and R^2 values from grouped bivariate scatter plots of tVEP square root of power values by group by age

Appendix C

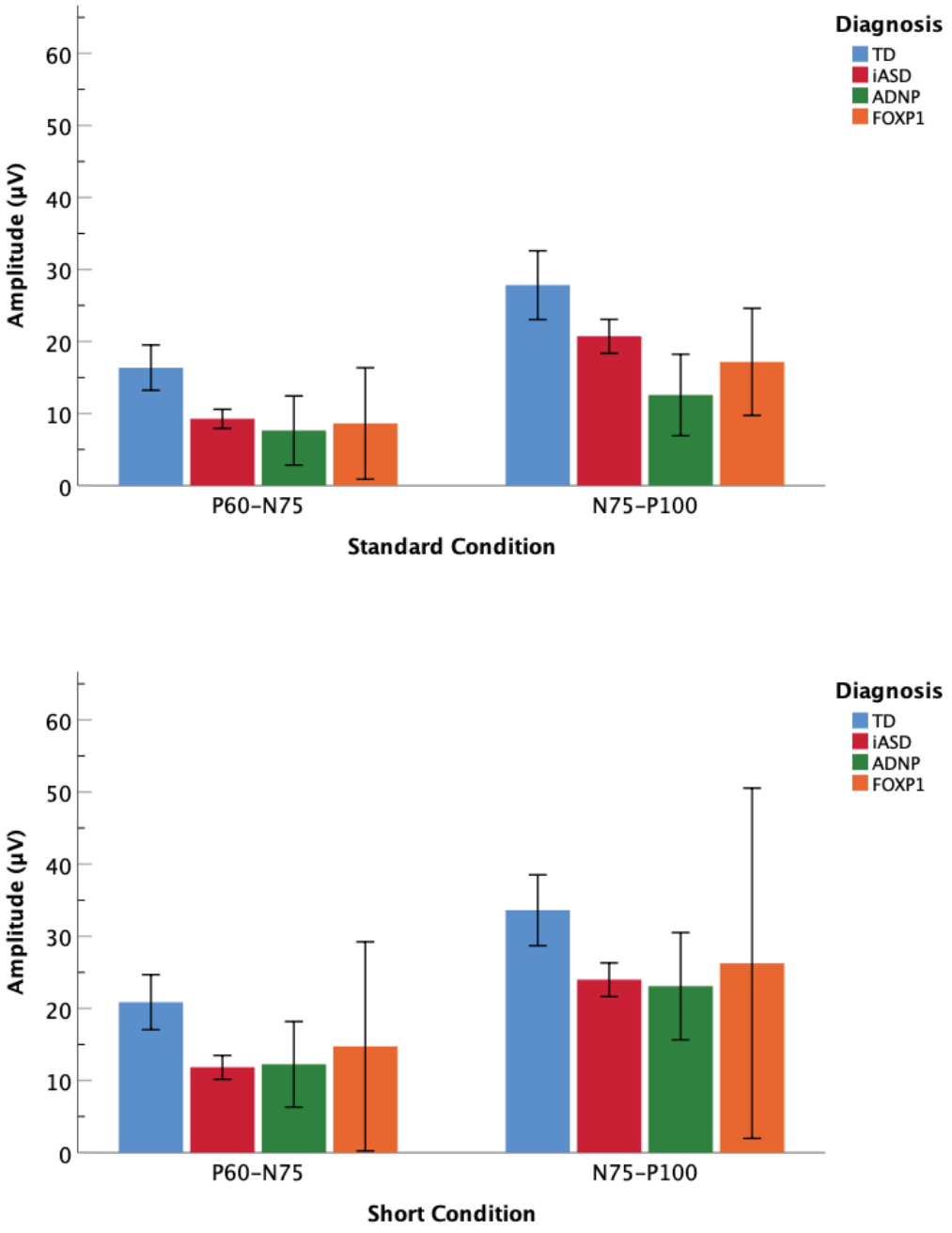

Mean P_{60}-N_{75} and N_{75}-P_{100} amplitudes for TD, iASD, ADNP, and FOXP1 groups for standard and short conditions. Error bars are 95% confidence intervals.

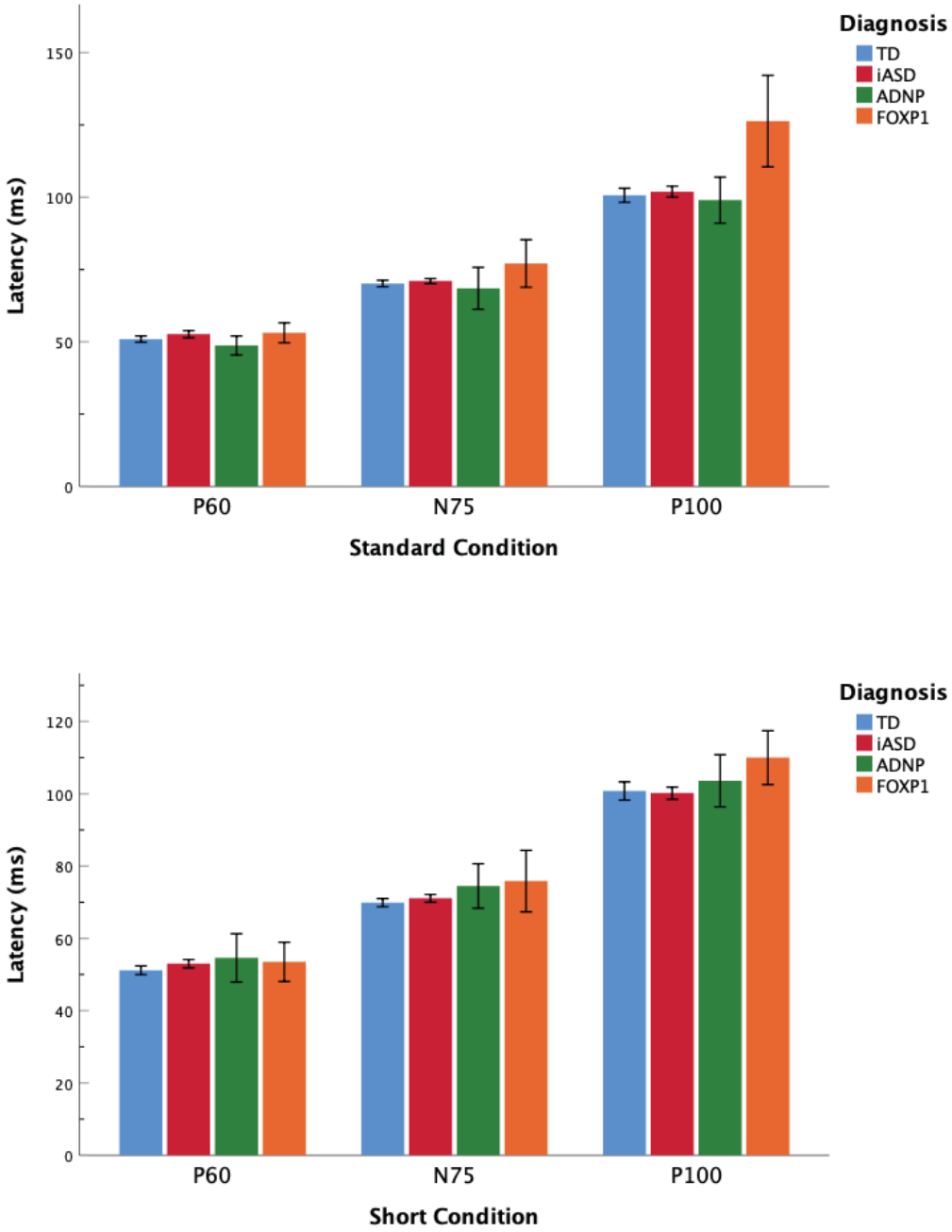

Mean P_{60}, N_{75}, and P_{100} latencies for TD, iASD, ADNP, and FOXP1 groups for standard and short conditions. Error bars are 95% confidence intervals.

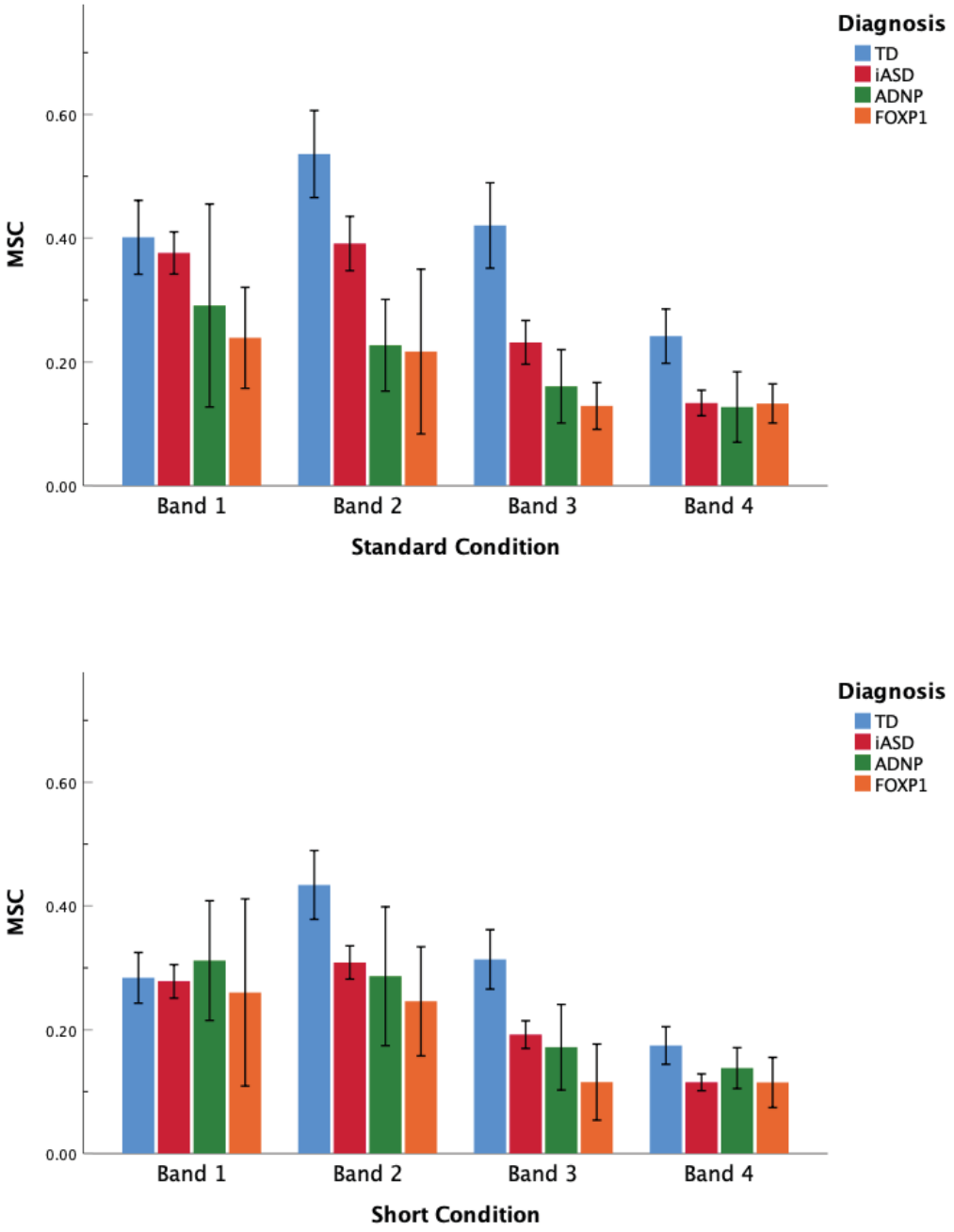

Mean magnitude-squared coherence (MSC) in Frequency Bands 1, 2, 3, and 4 for TD, iASD, ADNP, and FOXP1 groups for standard and short conditions. Error bars are 95% confidence intervals.

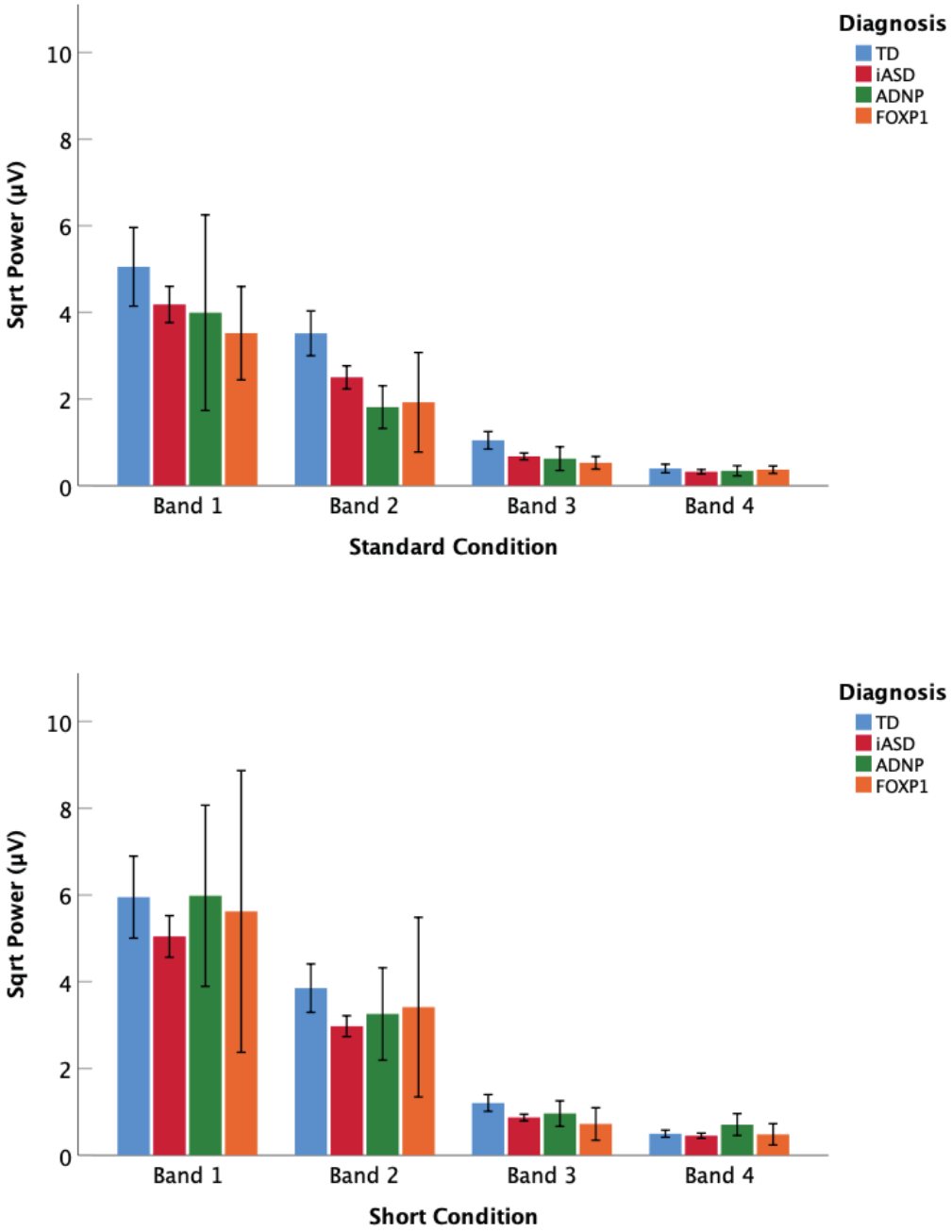

Mean square root of power in Frequency Bands 1, 2, 3, and 4 for TD, iASD, ADNP, and FOXP1 groups for standard and short conditions. Error bars are 95% confidence intervals.